UC Riverside

UC Riverside Electronic Theses and Dissertations

Title
The Evolutionary Developmental Biology of Mucoromycotina

Permalink
https://escholarship.org/uc/item/886741h0

Author
Peña, Jesús Federico

Publication Date
2022

Supplemental Material
https://escholarship.org/uc/item/886741h0#supplemental

Copyright Information
This work is made available under the terms of a Creative Commons Attribution License, availalbe at https://creativecommons.org/licenses/by/4.0/

Peer reviewed|Thesis/dissertation

eScholarship.org Powered by the California Digital Library
University of California

UNIVERSITY OF CALIFORNIA
RIVERSIDE

The Evolutionary Developmental Biology of Mucoromycotina

A Dissertation submitted in partial satisfaction
of the requirements for the degree of

Doctor of Philosophy

in

Microbiology

by

Jesús Federico Peña

June 2022

Dissertation Committee:

- Dr. Jason E. Stajich, Chairperson
- Dr. Katherine Borkovich
- Dr. Patrick Degnan

Copyright by
Jesús Federico Peña
2022

The Dissertation of Jesús Federico Peña is approved:

_____

_____

_____

Committee Chairperson

University of California, Riverside

Acknowledgements

First, I would like to extend my sincere thanks to my advisor Dr. Jason E. Stajich for his support of my academic development and encouragement to pursue the research presented in this dissertation. I also want to thank my committee members, Dr. Katherine Borkovich and Dr. Patrick Degnan for their invaluable feedback. I would also like to extend my sincerest thanks to my mentor Dr. Scott A. Nichols, who first trained me as an evolutionary developmental biologist and who helped increase my confidence in my ability to pursue and complete a PhD. I am also grateful for Dr. Dennis Barrett, who first showed me what it means to be your authentic self in the pursuit of knowledge. I also want to thank Dr. Howard Judelson, Dr. Ian Wheeldon, Dr. Holly Bik, and Dr. Morris Maduro for serving on my qualifying exam committee.

Funding for these projects came from a grant from the National Science Foundation for the Zygomycete Genealogy of Life (ZyGoLife) (#1441715). I would like to specifically thank ZyGoLife collaborators Dr. Robert Roberson and Phakade Shange for their help with microscopy; Dr. Matt Smith and Dr. Nicole Reynolds for providing our lab with mucoromycete mating-type pairs; and Jericho Ortañez who spent the better part of a year extracting DNA from all the zygos - there'd be no genomes without his efforts!

Besides funding, this project would not have been possible without the support and friendship of my lab mates. The original research questions were conceived in a conversation with Dr. Derreck A. Carter-House towards the end of my first year. Without Dr. Carter-House's initial support and informal mentorship, the ideas presented herein

may not have been explored. Similarly, Dr. Nuttapon Pombubpa gave me lots of great advice on navigating the early years of graduate school as well as helpful strategies for writing the dissertation. Thanks, Nat and Derreck!

Tania Kurbessoian and Julia Adams joined the lab a year after me, and I cannot express my gratitude enough for their support. Tania has always been quick to provide feedback on my writing and is invaluable towards keeping the lab running -- Tania, we all owe you our deepest gratitude, you're the lab MVP! For the past year or so, as I approach the end of my grad school experience, Julia has sent me job ads that I might be interested in on a regular basis. Our conversations are often about our career trajectories and they always leave me feeling hopeful -- thanks for all your support, Julia! I also want to thank Sawyer Josmaphilon who brought our lab together as we adventured through distant lands, crawled through dungeons, and faced off against dragons.

I am deeply grateful for my husband, Paul Teten, for his emotional support throughout this process. I could not have completed this without him. I am also thankful for the support from my family back in Denver: Anabel Rodriguez, Leonardo Peña, Litzahaya "Billie" Arcanjo, Zeke Perez and Natalee Elledge, Khalae Adams, Abrehet Gebremedhin, Angelica Ledezma, Ryan Schultz, and Lauren Friesen. I've missed you all so much during my time in grad school but your friendship, love, and support have kept me motivated.

Dedico este trabajo a Anabel Rodriguez - gracias por tu apoyo todos estos años

This dissertation is also dedicated to

my sister, Litzahaya Arcanjo,

my brother, Leonardo Peña,

and

the love of my life, Paul S. Teten

ABSTRACT OF THE DISSERTATION

The Evolutionary Developmental Biology of Mucoromycotina

by

Jesús Federico Peña
Doctor of Philosophy, Graduate Program in Microbiology
University of California, Riverside, June 2022
Dr. Jason E. Stajich, Chairperson

Sexual reproduction and sexual development in fungi is coordinated by single, differentially encoded genes at the mating-type locus. The Mucoromycotina are a subphylum of the Mucoromycota, a group that is sister to the dikarya. Mucoromycetes are capable of asexual and sexual reproduction. Sexual reproduction in this lineage is coordinated by an HMG-domain gene at the mating-type locus. The sexual cycle of *Phycomyces blakesleeanus* involves well characterized cell differentiation events, but less is known about the genetic mechanisms underlying these morphological transitions. Time series transcriptomes were generated for three timepoints during the *P. blakesleeanus* sexual cycle. The differentially expressed genes were correlated with the development of specific sexual structures. In a recapitulation of prior studies, nitrogen starvation genes, the mating-type genes, and carotenoid biosynthetic genes were also differentially expressed. Coexpression clusters of genes were identified and they also correlated with a particular stage during sexual development. Many of the differentially co-expressed genes that were identified are conserved in other fungal species and also play roles in sexual development, suggesting the existence of sexual developmental toolkits. Additionally, phenotypic differences between the two mating-types of *P. blakesleeanus* were observed. The vegetative transcriptomes of each mating-type were characterized and evidence was found for mating-type-biased gene expression.

Mating-type biased gene expression points to a role for the mating-type genes during vegetative growth. Lastly, the evolution of mating-type loci across the subphylum Mucoromycota was explored. A high-throughput strategy for identifying these loci was developed and the resulting analysis identified mating-types in 427 isolates. Support was found for a stepwise assembly of mating-type locus genes akin to the stepwise evolution of sex chromosomes. Furthermore, assessment of the evolution of the individual mating-type genes suggested that SexP may have evolved before SexM and that SexM evolved from SexP.

Table of Contents

Preface: Dinosaurs, Land Whales, and Horse Cousins xii

Chapter 1: Introduction 1

Chapter 2: Mating-type Biased Gene Expression in *Phycomyces blakesleeanus* 16

- Introduction 16
- Results 17
- Discussion 35
- Methods 43

Chapter 3: Mating Transcriptome of *Phycomyces blakesleeanus* 45

- Introduction 45
- Results 47
- Discussion 64
- Methods 69

Chapter 4: Characterization and Evolution of the Mucoromycotina Mating-type Locus 72

- Introduction 72
- Results 74
- Discussion 87
- Methods 92

Chapter 5: Conclusion 95

Figures 100

References 143

Appendix 160

List of Figures

Figure 1.1. Summary of sexual reproduction strategies across kingdom fungi **100**

Figure 2.1. Comparison of (-) and (+) *P. blakesleeanus* mating-types **101**

Figure 2.2. Summary of differential gene expression analysis **105**

Figure 2.3. GO enrichment analysis of differentially expressed genes between mating-types of *P. blakesleeanus* **108**

Figure 3.1. Reproductive cycles of *P. blakesleeanus* and associated structures **110**

Figure 3.2. Gene expression profiles of *Phycomyces blakesleeanus* during mating **111**

Figure 3.3. Expression cluster GO enrichment results **114**

Figure 3.4. Schematic of carotenogenesis and trisporic acid synthesis pathways and expression of associated genes **119**

Figure 3.5. Mating-type locus gene expression **121**

Figure 4.1 General characteristics of mating-type loci and overview of locus identification **125**

Figure 4.2 Locus length by mating-type across the species tree **130**

Figure 4.3 Mating-type locus schematics mapped to a representative species tree **132**

Figure 4.4 Comparison of SexM and SexP gene and protein sequences **134**

Figure 4.5 Tanglegrams of SexP and SexM trees **137**

Figure 4.6 Comparison of branch similarity between the representative species tree and combined SexP-SexM gene trees **140**

List of Tables

Table 2.1. Summary of differential gene expression analysis (FDR<0.05, 2x<|LFC| **21**

Table 2.2. Mating-type biased expression status of light induced genes from Tagua et al. 2020 **27**

Table 2.3. Upregulated single-copy genes in common with light induced genes from Corrochano et al. 2016 **30**

Table 2.4. Downregulated single-copy genes in common with light induced genes from Corrochano et al. 2016 **34**

Table 3.1. Differential gene expression analysis summary **50**

Table 3.2. Cluster Assignments **50**

Table 3.3. Carotenogenesis and TA synthesis genes **62**

Dinosaurs, Land Whales, and Horse Cousins

This story is about molds, yet much like other stories born of biological research, this story does not exist in a vacuum independent of past stories. Like many children, I was intensely interested in dinosaurs and fossils. Learning about extinction at a young age made me curious to learn about how life on Earth has changed over time -- that is, species alive today may not have been present in earlier points of the planet's history. Some years later, following the discovery and description of *Ambulocetus* fossils from Pakistan [1], I was introduced to the idea that life on Earth can change not only through shifts in composition brought on by extinction events, but also through direct changes to the organism's body. This was my introduction to the concept of evolution, as explained to me by my late father, a man of science who lacked support and resources to pursue his own training in biology. While learning about evolution from my father, the description of zebras as the cousins of horses stood out in my mind -- sure these two species are similar in form, but there are obvious differences, so how could these two things be related? And so the stage was set for what has become a lifetime of inquiry and curiosity, beginning with stories about extinct lifeforms, stories about organisms undergoing morphological change over time, and stories on the idea of species relatedness. These early experiences catalyzed my interest in biology and have ultimately culminated in the story told in the pages that follow, a story about molds.

Chapter 1: Introduction

Development in the Light of Evolution

In the closing line of Charles Darwin's *On the Origin of Species*, he remarks on "endless forms most beautiful" in reference to the diversity of life found on Earth [2]. Though traditionally the study of evolution relied on systematics, paleontology, and anatomy and functional morphology, the discovery of DNA reconciled with Mendelian genetics ushered in a new perspective on the mechanisms of evolution. Fields such as genomics, cell biology, and developmental biology, while traditionally the realm of biomedical research, have contributed to evolutionary biology becoming a cross-disciplinary field that has shed light on this natural phenomenon. Despite all this progress, just over a century after Darwin's death, we are only beginning to understand the molecular underpinnings of such diversity of form.

A major step in the field was the discovery of conserved homeobox genes in animals [3]. This discovery introduced a new level of biological organization: single genes were acting as master regulators of development. Mutations to these homeobox genes, when not lethal, resulted in drastic changes to the body plan of *Drosophila* [3]. Homeobox genes have been functionally characterized in various animal models of development [3,4] and homologous sequences have been identified in numerous other animal species including the early diverged ctenophores [5,6] and, to some extent, sponges [7,8]. Discovery of homeobox genes in animals with disparate body plans brings to light the paradox that the development of form, however different, is controlled or regulated by closely related or similar sets of genes [9]. Rather than hindering our understanding of evolution, the ubiquity of conserved regulators of development

transformed the field of developmental biology into a lens for understanding evolutionary change. Indeed, these discoveries and observations have culminated in the interdisciplinary field of evolutionary developmental biology.

Much of evolutionary developmental biology (evo-devo) has focused on model organisms, primarily animals, with a longstanding presence in laboratories [10]. Intense research in these systems has not only given us an understanding of the developmental process, but how those processes, and the molecules driving them, have changed over evolutionary time leading to evolutionary novelty. Evo-devo has given rise to a genetic theory of morphological evolution which states that form evolves from differential expression of conserved genes, driven by mutations in regulatory regions [9]. Changes to regulatory sequences, rather than changes to coding sequences, allows for selection and evolution to tinker with the various steps of development without disrupting the functions of genes participating in the developmental program [9,11]. In this way, development is a series of interacting molecular modules (e.g. morphogenetic fields, pathways, cell lineages) which result in morphological/cytological modules (e.g. limbs, eyes, stem cells, mushroom caps). The process of co-option, or recruitment, is when components of modules are integrated into a seemingly unrelated module. An example of recruitment leading to evolutionary novelty is the elytra of beetles. Elytra are the hardened forewings characteristic of this animal group, and are a result of recruitment of the genetic exoskeletal development module to the module for dorsal wing development [12].

The genes participating in the various modules of development exhibit varying degrees of conservation. For example, the protist *Capsaspora owczarzaki*, a unicellular relative of animals, regulates cell proliferation with the same transcription factors used by

animals during gastrulation despite *C. owczarzaki* not gastrulating [13]. This is a striking example of the property of molecular parsimony, or the conservation of genes and processes in distinct cell types. These conserved sets of genes that are components of developmental programs are frequently conceived of as developmental toolkits which aid in building and patterning the body plan [9,14,15]. Conservation of developmental toolkits and their developmental pathways in distinct organisms highlights the property of deep homology [16]. Many genes and pathways involved in establishing body axes in animals constitute examples of deep homology [17]. Through the study of embryo morphology, the hourglass model of development came to fruition [18]. This model posits that the early and late stages of embryogenesis exhibit divergent morphologies while features of mid-stage embryos, the phylotypic stage, are highly conserved within the respective phylum. This model is supported not only by morphological studies in animals, but also molecular work that has demonstrated transcriptomic similarities, particularly among the deep homologous toolkits, between different species at the phylotypic stage [18–20].

Generally, development in eukaryotes relies on evolutionarily related genes, or orthologues. A notable example are the Hox genes. The various Hox genes observed in the genomes of animals all stem from a single ancestral Hox gene that underwent duplication during the evolution of metazoans [21]. Gene duplication provides an additional mechanism for evolution to act on developmental processes. In a scenario where a developmental transcription factor is duplicated, only one copy will be under evolutionary constraints so as to maintain its normal function [22]. The duplicate is then essentially ignored by natural selection, allowing it to accumulate mutations in their coding or regulatory sequences that may lead to novel functions [11,22].

Eukaryotic Sexual Reproduction

Among eukaryotes, sexual reproduction is a mechanism that divides the burden of maintaining developmental genes safe from deleterious mutations. In many cases, this process kickstarts the developmental process through the union of two haploid parental genomes. This union of haploid genomes in plants and animals is a characteristic of sexual reproduction. In these systems, two distinct cell types, one from each parent and each harboring haploid versions of the parental genomes, undergo cell fusion (fertilization) and karyogamy (fusion of nuclei) to produce a diploid zygote [23–26]. The zygote, now equipped with a full genome, can then begin its developmental program. Sexual reproduction is not a requirement of development, as there are many examples across the domains of life of organisms propagating their species through other forms of reproduction including asexual reproduction in single-celled microbes; clonal parthenogenesis in vertebrates, invertebrates, and plants; and even through laboratory genome manipulation [27–31]. Erasmus Darwin, grandfather of Charles Darwin and an influence on Charles Darwin's ideas on evolution, once referred to sexual reproduction as "the chef d'oeuvre" or masterpiece of nature referencing the biological and energetic investment made by various organisms in order to reproduce the species sexually [32]. Indeed, many organisms have evolved traits that facilitate sexual reproduction such as male and femal phenotypes and specialized structures and behaviors [33–35]. Reasons for the evolution of sexual reproduction in eukaryotes remains an open question. Nevertheless, the combination of two different genomes to generate a new one may have some advantages such as creating novel and possibly advantageous combinations of genes while eliminating undesirable phenotypes [36,37].

The same properties of sexual reproduction that led to Erasmus Darwin's proclamation also present the costs of this mode of reproduction. The energetic investment of asexual reproduction is lower given that mitotic division reproduces an organism in a single step [33]. Despite this, sexual reproduction is widely distributed across eukaryotes [34]. Among the various kingdoms of eukaryotic life, fungi appear to be an outlier when it comes to sexual reproduction. Unlike sex obligate plants and animals, fungi do not produce haploid gametes and by extension lack separate sexes. Most fungi exist as haploids, assuming a diploid state only when undergoing sexual reproduction. Despite not having differentiated sexes, fungi rely on mechanisms that establish cell identity which determine mating compatibility.

Sexual Reproduction in Fungi

Microbial organisms have evolved genetic mechanisms to express sex-specific factors, although in these systems the term mating-type is used in place of sex identity [38]. Efforts to understand sexual development in fungi have largely focused on Ascomycota and Basidiomycota given the tractability of these species as model organisms and their relevance to human health [39]. The dikaryan fungi produce fruiting bodies as part of their sexual cycle to aid in production and dispersion of sexual spores [40,41]. Development of these structures relies on tightly regulated gene expression not only to direct responses to the environment and mating partners, but also to drive the morphological transitions necessary to generate fruiting bodies and spores [42–46]. Although *Saccharomyces cerevisiae* does not make a macroscopic fruiting body, it is a prime example of how cell identity and mating status as well as environmental cues can cause bulk changes in transcription associated with changes in morphology [47,48].

Haploid yeast cells, upon detecting a mating pheromone, will form cell extensions in the direction of the compatible partner [49]. Compatible partners have complementary mating-types, determined by idiomorphic transcription factors. These mating-type genes in yeast regulate mating-type specific gene expression as well as diploid-state specific gene expression [47,48,50]. Gene expression during mating has also been investigated in *Neurospora spp.* and *Chaetomium globosum*. As mating proceeds, changes in morphology correlate with, and often are induced by, changes to gene expression dynamics [42,43]. In *C. globosum* and *N. crassa*, the mating-type genes and environmentally responsive genes exhibit coordinated regulation during mating [42]. This supports the observation that sexual reproduction and harsh environmental conditions are tightly linked in fungi [39,42,51–54]. In fact, the sexual spores of fungi are generally more tolerant of environmental stress than the asexual spores [55]. Frequently, sexual spores are the dispersal mechanism for fungi, so they must be able to survive myriad environmental challenges such as desiccation, long resting phases, or UV irradiation [55,56]. Sexual spores also carry reserve compounds, such as trehalose, which when metabolized, are involved in breaking a dormancy period, signaling to the spore that growth conditions are once again optimal [55,57–59].

As mentioned, research on sexual reproduction in the ascomycetes has uncovered the fact that sexual reproduction is a response to environmental changes [39,42,60]. This feature is facilitated by the facultative nature of sexual reproduction in fungi and helps to address some of the costs of sexual reproduction. That is, since most fungi reproduce asexually, they do not need to constantly invest energy into developing specialized sexual structures or deal with mate attraction [33,40]. Instead, sexual reproduction is limited to scenarios where the fungus is experiencing some form of

environmental assault, such as nutrient limitation [28,42,52,61]. Specifically, the availability of nitrogen determines whether sexual or asexual reproduction is promoted. Nitrogen limitation is a common trigger among dikarya, and even some algae, to induce the sexual state [51,60–66]. Additionally, the meiotic spores of most fungi allow for survival under environmental stress given that they are used for dispersion. Since they function to essentially “evacuate” a harsh environment, meiotic spores have evolved mechanisms to enhance their survival in diverse environments [55,56]. These spores are also packed with reserve nutrients that aid in reactivation once a favorable environment is reached [55,57–59].

The mating-type locus (MAT) is the genetic locus that coordinates sexual development and cell identity in fungi [33,40,67]. In other eukaryotes, expression of a sex determining transcription factor, like the SRY gene of mammals, specifies cell identity and mating compatibility [68]. In mammals, the presence or absence of this gene determines whether the organism will be male or female, respectively. In males, the SRY gene activates a gene expression cascade that contributes to the male phenotype. Without the SRY gene, an alternative gene expression cascade remains active which leads to the female phenotype. Unlike mammals, fungi generally do not have differentiated sexes, and in many cases they lack sex chromosomes. The mating-type genes of fungi confer cell identity and determine whether individuals can mate [33]. In order for sexual reproduction to occur in heterothallic (self-sterile) fungi, the partners must carry divergent alleles, or idiomorphs, at the MAT locus. In homothallic species, strains are capable of self-mating and do not require a sexually compatible partner [33]. Mating polarity describes the number of loci which contribute to mating-type identity. The Basidiomycota generally rely on two unlinked loci, making them a tetrapolar group while

most other fungi are bipolar, relying on only one locus [33]. The content of mating-type loci and the strategies used by fungi to undergo sexual reproduction vary by phyla (**Figure 1.1**).

The gene content of the MAT locus varies across fungal taxa, but typically contains genes which encode transcription factors [33,40,67,69–71]. During sexual reproduction, these transcription factors may interact to regulate expression of genes involved in the sexual cycle while, in some cases, also regulating expression of genes specific to the non-sexual haploid state [69]. The role of mating-type genes has been extensively studied in the ascomycetes, particularly *Saccharomyces cerevisiae* and *Neurospora crassa*. The protein MATα1p of the *S. cerevisiae* mating-type locus acts as a transcriptional co-activator that regulates expression of a subset of genes specific to the MATα haploid strain [69]. During mating, this same gene facilitates synthesis and recognition of mating pheromones [33,69,72]. Unlike the single-celled yeasts, *N. crassa* develops differentiated female sexual structures as well as cells designated male [73]. Genes of the *N. crassa* MAT locus regulate entry into the sexual cycle [74].

In the filamentous Ascomycetes, both mating types, *MAT1-1* and *MAT1-2*, encode an HMG-domain protein [33]. While HMG-domain proteins are missing from the *S. cerevisiae MAT* locus, the *MATα* mating type encodes a protein containing α-box domain, a DNA-binding domain, that is evolutionarily related to the HMG-domain [69]. The HMG-domain proteins in these fungi are involved in regulating mating-type specific genes such as those involved in the synthesis of peptide pheromones and their associated receptors which initiate sexual reproduction [33,48,50]. In the Basidiomycota, there are generally two unlinked regions that determine mating type, making these tetrapolar mating systems [33,40]. In these basidiomycetes, one locus encodes

homeodomain proteins and the other encodes the sex pheromone and its receptors [70]. In some basidiomycetes, particularly those of the genus *Microbotryum*, the two mating-type loci have become linked and exist on a single chromosome [75,76]. Except for the the content of the MAT locus, individuals of these fungal species are generally considered isogenic. However, there is mounting evidence that the mating-type genes of some fungi are not exclusively involved in sexual reproduction, but also contribute to a gene expression dimorphism based on mating-type [44,77–80].

The Understudied Fungi

In contrast to the dikaryan lineages, less is known about the genetic and molecular mechanisms that regulate sex and development in other divergent fungal lineages such as Cryptomycota and Microsporidia, Chytridiomycota, Blastocladiomycota, Zoopagomycota, and Mucoromycota [33]. With the exception of Cryptomycota, sexual reproduction has been observed or inferred in all of these lineages [33,40,81,82]. Indeed, the first reported sexually reproducing fungus was a mucoromycete [83]. These enigmatic groups have distinct life histories and can occupy diverse environmental niches [84]. The Zoopagomycota and Mucoromycota were previously classified as Zygomycota Moreau (1954) based on the production of a zygospore [81,85]. Despite this shared character, Zoopagomycota are typically animal and fungi associated while Mucoromycota are plant-associated [81]. The Mucoromycetes (phylum Mucoromycota, subphylum Mucoromycotina) are an order of filamentous, coenocytic fungi which produce specific structures for asexual and sexual spores [81]. These species have been studied in labs for at least 200 years [83,86]. However, they are not as amenable to genetic transformations as the dikaryan fungi, so they have resisted molecular

investigation of their sexual developmental cycles [86]. Despite this, the mucoromycetes have been the subject of studies concerned with the photo- and gravitropism of the sporangiophore [87–90] and the biosynthesis of industrially-relevant chemicals. For example, the anticancer drug camptothecin has historically been isolated from roots of two tree species, but recently a study described an endophytic Mucoromycete that also produces the drug [91]. Industrial production of β-carotene, an antioxidant and precursor for vitamin A, uses the mucoromycete *Blakeslea trispora* [92–97]. β-carotene is important for the initiation of mating and sexual development in Mucoromycetes, so a deeper understanding of their sexual development would inform future work that seeks to exploit these systems for compound production and drug discovery.

While Mucoromycota may harbor unexplored benefits, some members of this phylum have pathogenic potential. The mucoromycetes are causative agents of mucormycosis, the third most common life-threatening fungal infection in humans [98–100]. In fact, during the ongoing COVID-19 pandemic, COVID-19 associated-mucormycosis emerged as a significant threat to human life with mortality rates of about 49% [100,101]. Sexual reproduction may contribute to the evolution of pathogenicity as it would allow for the spread of anti-fungal resistance and virulence genes [102]. Some members of Mucoromycota such as *Rhizopus spp.*, *Mucor spp.*, and *Gilbertella spp*. are implicated in post-harvest disease of fruits and present an economic threat to agriculture [103,104]. While asexual reproduction may be a faster method for colonizing a host, sexual reproduction would ensure a persistent infection as zygospores are thick-walled dormant propagules [33,92]. The zygospore represents a survival structure, given that in the laboratory the use of nutrient poor media promotes mating [33,99,102]. It is possible that in a case of mucormycosis, treatment with antifungals that

create an adverse environment will promote the formation of zygospores thereby prolonging the infection. Understanding the molecular mechanisms underlying sexual development in Mucoromycota would uncover novel targets of antifungals that could be used in combination with current treatments to reduce the risk of reinfection.

Related to the pathogenic potential of the Mucoromycota fungi is parasitism. Some members of the phylum are mycoparasites [81]. The mycoparasite *Parasitella parasitica* forms a cytoplasmic bridge between itself and its host which allows for the transfer of nuclei. The parasitic interaction is mating-type dependent, where a (+) parasite will infect (-) host and a (-) parasite will infect (+) hosts [105]. It has also been shown that genes involved in the early stages of sexual reproduction are also involved in the parasitism of *P. parasitica* [106]. An important technique in biology is transformation, through the introduction and subsequent integration of foreign DNA. There are efficient transformation methods for the mucoromycetes, but transformants are generally mitotically unstable [86,104]. In understanding the regulators of the sexual cycle, which are shared with parasitism, there may be an opportunity to fine-tune or develop transformation methods for Mucoromycota. The study of sexual development in Mucoromycotina will also expand our understanding of the evolution of sex in Fungi and our knowledge of this diverse phylum. This work will open new avenues to exploit these organisms for biosynthesis of compounds relevant to human health and industry and provide baseline data for discovery of novel antifungal targets.

To address questions about mating-type biased gene expression and gene expression during sexual development, I used the mucoromycete *Phycomyces blakesleeanus* . In the early to mid 20th century, *P. blakesleeanus* was a popular model organism given that its massive single-celled sporangiophore is highly responsive to

light, gravity, and physical obstacles [107]. Phototropism in *P. blakesleeanus* is regulated by white-collar protein homologues MadA and MadB [87,108,109]. Gravitropism evolved in *P. blakesleeanus* following a horizontal gene transfer event from bacteria [110]. Like other mucoromycetes, *P. blakesleeanus* is a coenocytic, filamentous, heterothallic fungus that is capable of both asexual and sexual reproduction [109,111]. Similarly, mating-type identity is determined by idiomorphic genes encoding HMG-box containing proteins [109,112,113]. In the (+) mating-type, the HMG-box gene is called sexP (sex plus) while in the (-) mating-type the gene encodes sexM (sex minus).

Previous work has examined expression of the mating-type locus genes in *P. blakesleeanus* and other mucoromycetes [88,109]. In the closely related *Mucor circinelloides*, the gene *sexM* is not expressed during vegetative growth of the (-) mating-type, in contrast to *sexP* which is expressed [114]. Furthermore, in *M. circinelloides*, the asexual spores are dimorphic where the (-) mating-type spores are consistently larger and more virulent than those of the (+) mating-type [114]. Other evidence for possible dimorphism in the mucoromycetes include the cooperative synthesis of trisporic acid sex pheromones [115,116], mating-type specific Manoilov reactions [117,118], lack of linoleic acid in lipids of the (-) mating-type [119], uniparental inheritance of mitochondria [120], and accumulation of protector carbohydrates in the (+) mating-type of *B. trispora* [118,119]. In chapter 2, following the observation of a phenotypic difference between two compatible mating-types of *P. blakesleeanus*, I explore differences in gene expression during vegetative growth. I hypothesized that differentially expressed genes between the two mating types may point to a molecular dimorphism associated with traits optimized for a particular role during asexual growth. *P. blakesleeanus* may be an ideal model or representative of Mucoromycota in the

context of mating-type biased gene expression given that we know the identities of the mating-type genes, cells are large and recognizable, and previous work has characterized several biochemical and ecological characteristics of this fungus [88,109,121–125].

Furthermore, the sexual cycle of *P. blakesleeanus* has also been characterized morphologically and, to some extent biochemically [40,107,126]. In the presence of a compatible mating partner, hyphae of *P. blakesleeanus* differentiate into zygophores, thickened and highly branched hyphae [107,115,127]. Trisporic acid (TA) is the mucoromycete pheromone and it plays a role in differentiating zygophores [115]. Zygophorogenesis and subsequent “aerialization” in *P. blakesleeanus* are markedly different from zygophorogenesis in other mucoromycetes. While other mucoromycetes generate zygophores from sporangiophores, which are already aerial structures, *P. blakesleeanus* generates zygophores from hyphae that are submerged in the substrate [107]. Zygophores of opposite mating pairs grow towards each other until they make contact and become aerial [107]. Prior to fusion at the cell apices, the zygophores will form progametangia, a ring-like structure. The onset of cell fusion gives rise to gametangia, 3-D multicellular structures with adventitious septa that delimit the nascent zygospore. At this point, the zygophores act as tong-like suspensor cells. As the zygospore develops, thorn-like appendages appear on the suspensor cells at sites closest to the zygospore [107]. The mature zygospore then enters a period of dormancy determined in part by the degree to which the parents are isogenic [128]. In chapter 3, I present one of the first time-course transcriptomes of the *P. blakesleeanus* sexual cycle. By exploring the global transcriptomic landscape of *P. blakesleeanus* mating, we can

begin to identify candidate developmental toolkits that are associated with the serial morphological transitions characteristic of the mucoromycete sexual cycle.

As mentioned previously, the mating-type genes confer cell identity that determines mating compatibility. The mating-type locus establishes cell identity and coordinates sexual reproduction and development not unlike the SRY genes of mammals [33,40,67]. Genes found at the mating-type locus vary across the fungal kingdom, but in most cases these genes play a direct role in regulating mating-type specialization during vegetative growth and also regulate sexual developmental processes [77–79,129]. The genomes of individual fungal species which are considered to be distinct mating-types will differ only by the content of their mating-type locus. Not all mucoromycetes have had their mating-type locus identified or characterized to the degree of dikarya [41,113,130–132]. The few species that have been examined, however, reveal that the locus is generally syntenic within the subphylum Mucoromycotina and includes either a *sexP* or *sexM* gene flanked by a triose-phosphate transporter gene (*tptA*) and an RNA helicase gene (*rnhA*) [41]. High-throughput attempts to characterize the mating-type locus of mucoromycetes have been limited by the availability of genomes for these understudied groups as well as by computational approaches [131]. In chapter 4, I present the results of a high-throughput mucoromycete mating-type identification pipeline. I hypothesized that locus organization would be conserved within the subphylum Mucoromycotina, and that each mating-type gene would have distinct evolutionary trajectories, due to the various differences between some mucoromycete mating-types [114,120,133]. The study of sexual development in Mucoromycotina will expand our understanding of the evolution of sex in fungi and increase our knowledge of this diverse group. This work may open new avenues to

exploit these organisms for biosynthesis of compounds relevant to human health and industry and provide baseline data for discovery of novel antifungal targets.

Chapter 2: Mating-type Biased Gene Expression in *Phycomyces blakesleeanus*

Introduction

There is mounting evidence that the mating-type genes of some fungi are not exclusively involved in sexual reproduction, but also contribute to a dimorphism based on mating-type biased differential gene expression [44,77–80]. In the mucoromycetes, differential regulation of the mating-type genes during asexual and sexual development points to the possibility of a similar molecular dimorphism underlying vegetative development. An example of dimorphism in the Mucoromycotina is the pathogenicity of *M. circinelloides* where the (+) mating-type is more virulent than the (-) mating-type [114]. The mating-type of plant-associated fungi, like the arbuscular mycorrhiza *Rhizophagus irregularis* (Glomeromycotina), may also contribute to successful symbioses. Indeed, in coinocculation experiments, it appears that the host plant genotype influences growth rates of this AM fungus through an unknown mating-type specific manner [134]. The mating-type genes of AM fungi continue to be explored, however, *P. blakesleeanus* may be a suitable model for the phylum Mucoromycota given its cell size, ease of laboratory maintenance, and the fact that the mating-type genes in this species are characterized.

Understanding the basis of mating-type biased gene expression in *P. blakesleeanus* can reveal more about how mating-types have evolved through additional insight about possible ecological roles. Furthermore, many mucoromycetes are promising sources of compounds relevant to human health, particularly the carotenoids [94,118]. *B. trispora* has been used in the industrial synthesis of β-carotene and lycopene [93,118,135]. While co-culturing of (+) and (-) mating-types increases the yield

of these compounds, the process can be simplified by treating only the (-) *B. trispora* strain with trisporic acids or inhibitors of acetyl-CoA synthesis [118]. This observation suggests that one mating-type of *B. trispora* more readily produces carotenoids and responds to mating signals.

Through working with *P. blakesleeanus*, I observed a color difference between the two mating-types: the (-) mating-type accumulates more yellow pigment than the (+). Here, I show evidence for a gene expression dimorphism between the two mating-types of *P. blakesleeanus*. A difference in phenotype combined with the observation of differentially expressed genes between the two mating-types suggests that even prior to sexual reproduction, each mating-type exhibits a degree of specialization. I also found a subset of differentially expressed genes which were previously shown to be light-responsive genes. The present work is a first step towards understanding the basis for mating-type biased gene expression in an organism that lacks differentiated sex chromosomes and is considered an early-diverged fungus.

Results

Phenotypic Differences and Orthology

There are visible morphological differences in colonies of (+) and (-) mating-types of *P. blakesleeanus* when grown on rich media under a 12-hour light cycle. The (-) mating-type develops deep yellow to green sporangiophores whereas the (+) mating-type appears light yellow to white; similar phenotypes are observed when grown on nutrient limited media (**Figure 2.1A**). The phenotypic differences are observable even

when colonies are in the dark. The lack of light reduces the amount of sporangiophores that develop, but mycelia are still distinguishable based on pigment accumulation.

To test if gene content differences in the individual strains could be attributed to these visible differences, I performed OrthoFinder analysis with the predicted proteomes of *P. blakesleeanus* strains NRRL 1555 (minus mating-type) and UBC21 (plus mating-type). The (-) strain has 16528 predicted genes compared to 12840 genes in the (+) strain (**Figure 2.1B**). To ensure the differences in quality of genome assembly or annotation were not a source of significant error, we used the BUSCO tool and the mucoromycota_odb10 marker set (1614 orthologs) to compare protein content and found 96.8% completeness for UBC21 and 93.5% for NRRL 1555 (**Figure 2.1C**).

The OrthoFinder analysis found that in total, 9247 genes were single-copy orthologs between the two strain genomes, corresponding to 56% of all (-) strain genes and 72% of all (+) strain genes (**Table A.2.2**). More broadly, the comparison showed that 70% of the predicted genes in the (-) strain had orthologues,of varying copy numbers, in the (+) mating-type (**Figure 2.1B; Table A.2.1**). In contrast, approximately 88% of genes in the (+) mating-type had orthologues in the (-) mating-type (**Figure 2.1B**). For comparison, analysis between the two homothallic mating strains of *Neurospora tetrasperma* found that the two mating types had a total of 9893 genes that were single-copy orthologues. These single-copy orthologs corresponded to 95% of the Mat **A** genome and 88% of the Mat **a** genome (**Table A.2.2**). Regardless of copy number, 91% of the Mat **a** genome had orthologues in Mat **A**; 97% of Mat **A** genes had orthologues in Mat **a** (**Figure 2.1B; Table A.2.1**).

The 4939 genes categorized as (-) mating-type specific (**Figure 2.1B**) can be subdivided based on whether or not the gene has a predicted function assigned to the

protein product in FungiDB. Of these genes, 408 had annotated products while the remaining 4531 were unspecified products or uncharacterized conserved proteins (**Figure 2.1D; Table A.2.3**). The (+) mating-type had fewer genes that lacked an orthologue in the (-) mating-type (**Figure 2.1B**). Of these 1491 (+) mating-type specific genes, only 165 were characterized as a particular product (**Figure 2.1E; Table A.2.3**). The remaining 1325 genes were categorized as expressed proteins, uncharacterized, or hypothetical proteins (**Figure 2.1E**). These mating-type specific genes may not reflect an actual heterogenic situation, given that average nucleotide identity between the two genomes is 99.5% (**Table A.2.4**). A difference in genome assembly was also detected between the two genomes, where multiple (-) mating-type scaffolds mapped to a single (+) mating-type scaffold (**Table A.2.4**). Furthermore, these functional assignments are limited by the relative paucity of genetic and molecular or cellular studies in *P. blakesleeanus* as only 42% of the NRRL 1555 genes have a functional assignment.

Differential Gene Expression Analysis

To examine if gene expression differences characterize each mating-type, we used RNAseq to profile strains after 3 days of growth. Triplicate biological replicates from the (-) and (+) mating-types were analyzed using the *P. blakesleeanus* NRRL 1555 genome as a reference since the average nucleotide identity between NRRL 1555 and UBC21 is 99.5% (**Table A.2.4**). The pairwise expression comparison found a total of 2002 differentially expressed genes (FDR<0.05, $2x<|L_2FC|$) between mating types. Of these, 578 were upregulated in (+) and 1424 were downregulated in (+). As previously noted, the (-) *P. blakesleeanus* genome has 16,528 predicted genes, but only 10,220 had non-zero counts (i.e. were expressed) in this analysis. While the upregulated genes

represented 3.5% of the genome, they accounted for 5.66% of all expressed genes. In contrast, the downregulated genes represented 8.62% of the genome and 13.93% of all expressed genes (**Table 2.1**; **Table A.2.6, Table A.2.7**).

Principal component analysis showed that 75.8% of the transcript expression variation can be attributed to mating-type, and replicates cluster together along PC1 (**Figure 2.2A**). The replicates of the (-) mating-type also clustered together along PC2, which accounted for 11.3% of variance (**Figure 2.2A**). The (+) mating-type replicates displayed more variance along PC2 compared to the (-) mating-type replicates, but because they clustered along PC1, it was not removed from the analysis. Hierarchical clustering using the Spearman correlation also resulted in replicates forming clusters distinguished by mating-type (**Figure 2.2B**). Similarly, hierarchical clustering of genes by Pearson correlation captured the patterns of up- and downregulated genes in the analysis (**Figure 2.2B**). The (+) mating-type replicate that did not cluster along PC2 is represented by the column on the far right in the heatmap (**Figure 2.2B**).

Lastly, I looked at the proportion of differentially expressed genes that corresponded to the orthologues that were identified with OrthoFinder. Of the 11589 orthologues from the (-) mating-type that corresponded to the 11349 genes of the (+) mating-type, only 1570 were differentially expressed (FDR<0.05, $2x<|L_2FC|$; **Figure 2.2C**). Among these, 445 genes were upregulated while 1125 genes were downregulated. A subset of 1128 orthologous genes were single-copy orthologues (**Figure 2.2C**, orange points). A total of 312 single-copy orthologues were upregulated, while 816 were downregulated. The subset of genes which lacked orthologues in the complementary mating-type were not considered in this analysis, but all were generally uncharacterized or hypothetical proteins (**Table A.2.3**).

Table 2.1. Summary of differential gene expression analysis (FDR<0.05, 2x<|LFC|)

	Count	Percent of Expressed Genes	Percent of Genome	(+)/(-) Orthologues	Single-copy orthologues
total DGE	2,002	19.6%	12.1%	1,570	1,128
LFC > 0	578	5.7%	3.5%	445	312
LFC <0	1,424	13.9%	8.6%	1,125	816
All genes	16,529				
Non-zero count genes	10,220				
Zero-count genes	6,309				

Functional Characterization

I performed gene ontology enrichment analysis on the differentially expressed genes using the Biological Process Ontology. For this analysis, we included only genes with an absolute log2 fold change greater than two and a false discovery rate less than 5%; this limited the pool of genes to 578 total upregulated genes and 1424 total downregulated genes. This analysis is limited by the fact that only 25% (4227/16528) of the *P. blakesleeanus* genome was assigned a GO annotation in FungiDB. Of the 2002 differentially expressed genes that I identified, only 566 had a GO annotation. With this in mind, I identified the top 100 enriched GO terms for up- and downregulated genes (total of 200 enriched terms) using the elimination test in the R package topGO [136]. The enriched GO terms were processed with Revigo [137] to eliminate redundant GO terms based on semantic similarity. Once redundant terms were removed, I adjusted p-values using the Bonferroni-Hochberg method and I applied an adjusted p-value cutoff of 0.05. This resulted in 19 enriched GO terms associated with upregulated genes and 9 enriched GO terms associated with downregulated genes (**Figure 2.3A; Table A.2.9**).

Two GO terms were significantly enriched in both the upregulated and downregulated gene sets and accounted for the greatest share of genes. The first term was Transmembrane transport (GO:0055085) (**Figure 2.3A**). This duplicate term was enriched by 45 upregulated genes and 57 downregulated genes (**Figure 2.3A**). Despite being differentially regulated, 17 upregulated genes associated with transmembrane transport corresponded to 12 paralogues in the downregulated set (**Table A.2.10**). Among these paralogoue sets linked to Transmembrane transport, there were two predicted sexual differentiation process protein ISP4, one which was upregulated and another that was downregulated (**Table A.2.10**). Two additional predicted ISP4 genes were part of the upregulated genes and neither was a paralogue of the previously mentioned ISP4 genes with divergent expression status (**Table A.2.10**). Other paralogous genes were predicted to encode various ABC superfamily transporters, permeases of the major facilitator superfamily, and ion-nucleoside transporters (**Table A.2.10**). Carbohydrate metabolic process (GO:0005975) was also enriched in both sets of differentially regulated genes (**Figure 2.3A**). In the upregulated set, it accounted for 35 genes whereas in the downregulated set it was associated with 36 genes (**Figure 2.3A**). Seven of the upregulated genes corresponded to nine paralogues in the downregulated set (**Table A.2.10)**. The paralogous genes are predicted to encode dehydrogenases, reductases, and kinases (**Table A.2.10**). There were some unspecified products as well, but their ortholog group assigned by FungiDB/OrthoMCL-DB groups them with two different acetylglucosaminyltransferases (**Table A.2.10**).

As previously mentioned, only 566 differentially expressed genes had an assigned GO annotation. Of these, only 121 upregulated genes and 106 downregulated genes were associated with enriched GO terms (**Table A.2.9**). Within each GO term, the

percentage of genes which were single-copy multi-copy orthologues between (+) and (-) strains varied (**Figure 2.3B, 2.3C**); I also found a small subset of (-)specific genes among the upregulated genes. A total of 73 single-copy orthologues were associated with upregulated GO terms and 78 were associated with downregulated GO terms. The upregulated Transmembrane transport and Carbohydrate metabolic process both had similar proportions of single-copy orthologues to multi-copy orthologues, with single-copy orthologues making up a greater portion of the associated genes: 62% single-copy Transmembrane transport and 65% single-copy Carbohydrate metabolic process (**Figure 2.3B**). The downregulated versions of these two terms had different proportions to each other, with single-copy orthologues accounting for ~65% of transmembrane transport genes while single-copy orthologues associated with carbohydrate metabolic process accounted for 86% of associated genes (**Figure 2.3C**). The only term associated with (-)specific genes was proteolysis, where two genes (10.5%) out of 19 were (-)specific (i.e. lacked orthologues in the + mating-type). One of these genes was predicted to be beta-1, 6-N-acetyl glucosaminyl transferase with a WSC domain and the other was unspecified, though it has homology to Retrotransposon TYA Gag of *S. cerevisiae* (FungiDB).

There were five enriched terms exclusively associated with upregulated single-copy orthologues between (+) and (-) strains (**Figure 2.3B**). The GO term de novo IMP biosynthetic process was assigned to four differentially expressed genes which were all single-copy orthologues between the two mating-types. These genes are homologues of ADE2, ADE4, and ADE16/17 of *S. cerevisiae* (FungiDB). In yeast, these genes are involved in the synthesis of IMP, a purine precursor [138]. Mutations to these genes cause adenine deficiencies which result in *S. cerevisiae* colonies with red

pigmentation. Although the *P. blakesleeanus* orthologues are differentially expressed, they represent only the first, sixth, and ninth steps of the 10-step IMP synthesis pathway. Branched-chain amino acid biosynthetic process was another enriched term associated with single-copy (+)/(-) orthologues. The three genes associated with this term have homologues in yeast which are involved in three non-sequential steps of isoleucine biosynthesis; homologues of other genes in this pathway were not differentially expressed. Pectin catabolic process and galacturonan metabolic process were two other terms linked to single-copy orthologues between the mating-types (**Figure 2.3B**). Both terms were associated with the same two genes which are homologues of *N. crassa* pectin methylesterases (FungiDB). The last term exclusively associated with single-copy orthologues was galactose metabolic process (**Figure 2.3B**). These genes encode homologues of *S. cerevisiae* GAL1 and GAL7 which are components of the galactose degradation pathway. Based on these terms associated with single-copy (+)/(-) orthologues, the (+) mating-type has increased expression of genes which contribute to amino acid and purine synthesis, homeostasis, and general metabolism.

In contrast, only two enriched GO terms were exclusively linked to downregulated single-copy orthologues (**Figure 2.3C**). One of these terms was (1->3)-beta-D-glucan biosynthetic process, and it was associated with three genes. All three genes are predicted 1,3-beta-glucan synthases. While these three genes are single-copy between the two mating-types, all three genes have homology to FKS1,GSC2, and FKS3 in *S. cerevisiae* (FungiDB). These three genes were also homologous to bgs1/2/3/4 of *Schizosaccharomyces pombe* (FungiDB). In *S. pombe*, bgs1 is involved in septum formation, bgs2 plays a role in ascospore wall synthesis, and bgs3 and 4 are involved in apical wall synthesis [139]. The other GO term associated with downregulated

single-copy orthologues was carotenoid biosynthetic process (**Figure 2.3C**). Only two genes were associated with this term and they encode either *carRA* (a bifunctional phytoene synthase/lycopene cyclase gene) and *carB* (a predicted phytoene desaturase). Other work has shown that these genes are involved in the early steps of carotene synthesis in response to light or mating [123]. As stated earlier, the (+) mating-type appears light yellow to white and with less pigmentation overall when compared to the (-) mating-type (**Figure 2.1A**).

Carotene Biosynthesis and Light-regulated Genes

As previously mentioned, mucoromycete carotenogenesis is stimulated by light or sexual reproduction. Given the difference in color between the two mating-types and the downregulated enrichment of the GO term Carotenoid biosynthetic process, the (-) mating-type may have a lower threshold for activating this biosynthetic process. This result is surprising given that RNA was isolated from strains that were grown in the dark and lacked mating signals. When considering genes involved in carotene biosynthesis (including *carRA* and *carB*), I found that 18 of 22 (identified in [124]) were differentially expressed. Five of these were upregulated in the (+) mating-type and included *carS* (carotenoid oxygenase), an allantoate permease, *ggsb* (GGPP synthase), a secreted CotH spore-coat protein domain, and a monooxygenase involved in ubiquinone biosynthesis (**Table 2.2**). The 13 downregulated genes had greater absolute log2 fold changes than the upregulated genes, and a majority of these were also considered light-induced genes by [124]; there were no upregulated light-induced carotenogenic genes. A paralogue of the *P. blakesleeanus* WC-2 homolog, *wctD*, was among the downregulated genes. The downregulated light-induced carotenogenic genes included

hspA (Hsp100 homolog), *hogA* (MAPK), *cryA* (cryptochrome), *hemH* (ferrochelatase involved in heme biosynthesis), Acyl-CoA oxidase/dehydrogenase, an aldo/keto reductase, *gldA* (NAD-dependent glycerol-3-phosphate dehydrogenase), and *pdcA* (pyruvate decarboxylase) as well as *carRA*. Light-independent downregulated genes in this set included a beta-lactamase and Acyl-CoA synthetase. The genes encoding carotenoid regulatory proteins (*crgA-D* from [124]) were not differentially expressed between the mating-types.

Table 2.2. Mating-type biased expression status of light induced genes from [124]

Gene ID	Symbol	Product Description	Light Induced	Log2 Fold Change	Status
PHYBL_20510T0		Allantoate permease		2.14623003	Upregulated
PHYBL_77204T0		Secreted CotH spore-coat protein domain-containing protein		1.47493396	Upregulated
PHYBL_80493T0		Monooxygenase involved in ubiquinone biosynthesis		1.10091243	Upregulated
PHYBL_183749T0	*carS*	Carotenoid oxygenase		2.46551037	Upregulated
PHYBL_183831T0	*ggsB*	GGPP synthase		1.96278242	Upregulated
PHYBL_128779T0		Acyl-CoA oxidase/dehydrogenase	Y	-1.3711599	Downregulated
PHYBL_85761T0	*cryA*	Cryptochrome	Y	-1.287355	Downregulated
PHYBL_179972T0	*hemH*	Ferrochelatase	Y	-1.1855803	Downregulated
PHYBL_30672T0	*gldA*	NAD-dependent glycerol-3-phosphate dehydrogenase	Y	-3.3046984	Downregulated
PHYBL_112379T0	*hogA*	Mitogen-activated protein kinase	Y	-1.0022884	Downregulated
PHYBL_85757T0	*wctD*	White collar protein	Y	-2.5301867	Downregulated
PHYBL_116342T0		Beta-lactamase		-1.0270255	Downregulated
PHYBL_180269T0	*pdcA*	Pyruvate decarboxylase	Y	-4.7549781	Downregulated
PHYBL_35373T0		Acyl-CoA synthetase		-1.4781642	Downregulated
PHYBL_186020T0		Aldo/keto reductase	Y	-2.1015688	Downregulated
PHYBL_180114T0	*carRA*	Lycopene cyclase and phytoene synthase	Y	-1.4375894	Downregulated
PHYBL_37852T0	*carB*	Phytoene dehydrogenase		-1.6666612	Downregulated
PHYBL_29012T0	*hspA*	Heat-shock protein (Hsp100)	Y	-1.6369514	Downregulated
PHYBL_179746T0	*crgC*	Ubiquitin ligase	-	-	Non-DE
PHYBL_85770T0	*crgC/D*	Ubiquitin ligase	-	-	Non-DE
PHYBL_137151T0	*crgA*	Ubiquitin ligase	-	-	Non-DE
PHYBL_33844T0	*crgA/B*	Ubiquitin ligase	-	-	Non-DE

Other work has identified sets of light-induced genes expressed in mycelia or sporangiophores that are not necessarily related to carotene biosynthesis [109]. Of the genes that were differentially expressed between the two mating-types, 309 were also differentially expressed in mycelia exposed to light (**Table A.2.11**); 224 of them were single-copy orthologues between the two mating-types, and the remainder of this section focuses only on these single-copy mating-type orthologues. The expression status of these 224 genes did not not always track their expression status in the light-induction experiment. That is, while 73 of 224 genes were upregulated in the mating-type comparison (present work), these same genes were either upregulated or downregulated in light-exposed mycelia from [109]. Genes with divergent expression between this study and the work of Corrochano and colleagues [109] were not explored as deeply because it is not clear whether these genes are responding to light exposure or mating-type and genetic background, since this work relies on cultures grown in the dark only. To fully determine if these genes with divergent expression status are responding to light or mating-type and genetic background, this experiment would need to be repeated with cultures grown or exposed to light before RNA is isolated. When the divergent expression genes are removed, the 224 single-copy differentially expressed orthologues are reduced to 59 differentially expressed genes (**Table 2.3, Table 2.4**).

Of the 73 upregulated single-copy (+)/(-) orthologues, 31 were in common with the upregulated genes from light-exposed mycelia (**Table 2.3**). These 31 genes included components of carbon assimilation/aerobic respiration including alpha subunit of succinyl-CoA synthetase, monocarboxylate permease, glycolate oxidase, galactokinase, and sorbitol dehydrogenase. The beta subunit of succinyl-CoA synthase was upregulated in the (+) mating-type but downregulated in response to light. The beta

subunit of casein kinase II, a pseudouridine synthase, and an ATP-dependent RNA helicase homologous to MSS116p were also among the upregulated genes. In yeast, MSS116p is important for mitochondrial transcription [140]. Pseudouridine synthase is involved in post-transcriptional modification [141], whereas casein kinase II has diverse roles in cell growth and proliferation, acting on transcription factors and RNA polymerases [142]. All three of these genes were upregulated in response to light [109]. I previously noted the presence of geranylgeranyl pyrophosphate synthase (GGPPS) among the upregulated carotenogenic genes. This enzyme is responsible for generating geranylgeranyl diphosphate, a precursor molecule for various compounds including carotenoids [125,143]. In light exposure experiments [109], this gene was downregulated in mycelia, but was upregulated in the (+) mating-type relative to the (-) mating-type. However, as previously mentioned, whether mating-type and genetic background or light exposure regulate this gene may not be clearly discerned with the present data.

Table 2.3. Upregulated single-copy genes in common with light induced genes from [109]

Gene ID	Product description	OrthologGroup. MCL	OrthoMCL keywords
PHYBL_17957T0	Acyl-CoA synthetase	OG6_100107	unknown; source; uniProtKB/TrEMBL;Acc; ligase
PHYBL_99197T0	Amino acid transporter protein	OG6_100459	aa_trans domain containing protein; source; uniProtKB/TrEMBL;Acc; amino acid; unknown; amino acid...
PHYBL_88105T0	ATP-dependent RNA helicase pitchoune	OG6_105578	helicase; unknown; source; uniProtKB/TrEMBL;Acc; RNA helicase
PHYBL_148963T0	Ca2+-dependent lipid-binding protein CLB1/vesicle protein vp115/Granuphilin A, contains C2 domain	OG6_100476	unknown; source; uniProtKB/TrEMBL;Acc
PHYBL_106612T0	Casein kinase II, beta subunit	OG6_100687	kinase; casein kinase; ii; casein kinase ii; casein kinase ii subunit; casein kinase ii subunit b...
PHYBL_130479T0	Cysteine desulfurase NFS1	OG6_102710	domain containing protein; aminotran_5 domain containing protein; source; uniProtKB/TrEMBL;Acc; u...
PHYBL_75851T0	Cytochrome P450 CYP2 subfamily	OG6_585402	cyp5209 protein; source; uniProtKB/TrEMBL;Acc; unknown
PHYBL_155813T0	Fumarate reductase, flavoprotein subunit	OG6_104311	source; uniProtKB/TrEMBL;Acc; domain containing protein; binding; unknown; binding domain; bindin...
PHYBL_74616T0	Galactokinase	OG6_102769	galactokinase; source; uniProtKB/TrEMBL;Acc; unknown
PHYBL_107982T0	Glycolate oxidase	OG6_100930	dehydrogenase; source; domain containing protein; fmn; fmn hydroxy acid dehydrogenase domain cont...
PHYBL_179228T0	Hydrolytic enzymes of the alpha/beta hydrolase fold	OG6_100644	unknown; serine; source; uniProtKB/TrEMBL;Acc
PHYBL_115910T0	Inorganic phosphate transporter	OG6_112813	mfs domain containing protein; source; uniProtKB/TrEMBL;Acc
PHYBL_128711T0	Kelch repeat-containing proteins	OG6_112507	source; uniProtKB/TrEMBL;Acc; unknown; containing; containing protein; domain containing protein;...
PHYBL_22222T0	Monocarboxylate transporter	OG6_100246	mfs; source; domain containing protein; mfs domain containing protein; uniProtKB/TrEMBL;Acc; unknown
PHYBL_98007T0	Pattern-formation protein/guanine nucleotide exchange factor	OG6_135291	sec7 domain containing protein; source; uniProtKB/TrEMBL;Acc

PHYBL_188721T0	Predicted FAD-dependent oxidoreductase	OG6_101318	domain containing protein; dao domain containing protein; source; uniProtKB/TrEMBL;Acc
PHYBL_121915T0	Predicted transporter (major facilitator superfamily)	OG6_220691	mfs domain containing protein; source; uniProtKB/TrEMBL;Acc
PHYBL_134414T0	Pseudouridine synthase	OG6_100327	source; uniProtKB/TrEMBL;Acc; domain containing protein
PHYBL_118095T0	Pyruvate dehydrogenase E1, alpha subunit	OG6_100754	dehydrogenase; pyruvate dehydrogenase; E1; pyruvate dehydrogenase E1; E1 component; pyruvate dehy...
PHYBL_158271T0	Sorbitol dehydrogenase	OG6_100349	source; uniProtKB/TrEMBL;Acc; containing; domain containing protein; pks_er domain containing pro...
PHYBL_28725T0	Succinyl-CoA synthetase, alpha subunit	OG6_100834	ligase; subunit alpha; succinate--CoA ligase; mitochondrial; ADP-forming; source; uniProtKB/TrEMB...
PHYBL_115226T0	Transcription factor of the Forkhead/HNF3 family	OG6_149140	fork-head domain containing protein; source; uniProtKB/TrEMBL;Acc; hypothetical protein
PHYBL_181839T0	unspecified product	OG6_100979	source; unknown; uniProtKB/TrEMBL;Acc; synthase; dihydrodipicolinate
PHYBL_28643T0	unspecified product	OG6_101919	source; pnp_udp_1 domain containing protein; phosphorylase; uniProtKB/TrEMBL;Acc; uridine; uridin...
PHYBL_148565T0	unspecified product	OG6_112049	permease; L-lactate permease; unknown
PHYBL_180349T0	unspecified product	OG6_177358	unknown; hypothetical protein
PHYBL_131986T0	unspecified product	OG6_103201	domain containing; domain containing protein; peptidase; M20 domain containing; peptidase M20 dom...
PHYBL_157006T0	unspecified product	OG6_141494	unknown; hypothetical protein
PHYBL_89330T0	unspecified product	OG6_116164	source; uniProtKB/TrEMBL;Acc; nodB homology domain containing protein
PHYBL_181097T0	unspecified product	OG6_101105	source; isomerase; uniProtKB/TrEMBL;Acc; ribose-5-phosphate isomerase; D-ribose-5-phosphate ketol...
PHYBL_168308T0	unspecified product	OG6_103201	domain containing; domain containing protein; peptidase; M20 domain containing; peptidase M20 dom...

Single-copy genes that were downregulated in the (+) mating-type had similar patterns as the upregulated genes when compared to gene expression in light exposed mycelia (i.e. though downregulated between mating-types, light treatment response varies; **Table A.2.11**). In total, there were 123 genes which were downregulated in the present work and were differentially expressed in Corrochano and colleagues' (2016) light exposure experiments (**Table A.2.11**). Only 28 of these genes were downregulated in both studies (**Table 2.4**). Six of these genes were assigned a product description (on FungiDB), and the remaining 22 were all unspecified products. One of the predicted genes was a beta β-carotene 15,15'-dioxygenase. The only fungi with orthologues of this gene were Mucoromycetes [144]. In metazoans, this gene cleaves β-carotene into two molecules of retinal [145]. A carboxylesterase with an alpha/beta hydrolase domain and a fatty acyl-CoA elongase. The fatty acyl-CoA elongase has homology to *S. cerevisiae* ELO3, which is involved in sphingolipid biosynthesis (FungiDB orthology)[146]. In yeast, ELO3p is involved in trafficking GPI-anchored proteins via complex sphingolipid [147]. A protein with a GNAT domain was also among the six predicted genes with a functional assignment in FungiDB. This gene had homology to GNA1 of yeast, which plays key roles in the cell cycle. Notably, yeast cells deficient in GNA1p will swell and lyse as well as form chains of cells [148]. The last two proteins with functional assignments were a kinesin-like protein and a zinc finger protein with homology to MLP/LIM regulatory proteins. The kinesin-like protein lacked orthologues in other fungi except for *R. delemar* on FungiDB. Orthologues of MLP/LIM domain proteins were found to be important for regulation of cell wall biogenesis in *Magnaporthe oryzae* [149].

The other 22 downregulated genes were unspecified products, so to make predictions about their functions, I queried OrthoMCL DB using orthogroups assigned by

FungiDB (**Table 2.4**; **Table A.2.11**). One of these genes had an squalene/phytoene synthase domain, implicating it as yet another gene involved in pathways upstream of carotenoid synthesis. Three other unspecified genes with inferred functions were a homologue of *N. crassa* ribose phosphate isomerase-1, a protein with homology to the Tom5 subunit of the mitochondrial outer membrane translocase complex, and a protein with NTR2 and LtrA domains (**Table 2.4**). RPI-1 is involved in the pentose phosphate pathway which regulates cellular redox homeostasis. The Tom5 subunit is required for importing proteins into the mitochondria [150]. The LtrA domain has been studied in bacteria, and is part of a protein required for growth at low temperatures [151]. The yeast NTR2 protein is involved in spliceosome disassembly [152,153]. While not part of the light-induced set, a homologue of yeast SSP382 was also downregulated, though its log2 Fold Change did not meet the significance cutoff. In yeast, the proteins NTR2 and SSP382 form a trimer with PRP43, a DEAH-box RNA helicase, to regulate spliceosome disassembly [153]. The orthogroups of 18 downregulated genes were less informative and the protein sequences lacked PFAM domains (**Table 2.4**).

Table 2.4. Downregulated single-copy genes in common with light induced genes from [109]

Gene ID	Product description	OrthologGroup	OrthoMCL keywords
PHYBL_181537T0	Beta, beta-carotene 15,15'-dioxygenase and related enzymes	OG6_587927	unknown
PHYBL_144872T0	Carboxylesterase and related proteins	OG6_103562	domain containing protein; abhydrolase_3 domain containing protein; source; uniProtKB/TrEMBL;Acc;...
PHYBL_177105T0	Fatty acyl-CoA elongase/Polyunsaturated fatty acid specific elongation enzyme	OG6_100813	fatty; elongation; fatty acids; fatty acids protein; source; uniProtKB/TrEMBL;Acc; unknown; long ...
PHYBL_127304T0	Glucosamine-phosphate N-acetyltransferase	OG6_102114	N-acetyltransferase; 6-phosphate; glucosamine 6-phosphate N-acetyltransferase; source; uniProtKB/...
PHYBL_182836T0	Kinesin-like protein	OG6_178085	unknown; hypothetical protein
PHYBL_159404T0	Regulatory protein MLP and related LIM proteins	OG6_104400	LIM; cysteine; glycine rich; glycine rich protein; source; muscle; muscle LIM protein
PHYBL_58805T0	unspecified product	OG6_585800	unknown
PHYBL_178854T0	unspecified product	NA	NA
PHYBL_75728T0	unspecified product	NA	NA
PHYBL_150839T0	unspecified product	OG6_181279	unknown
PHYBL_79632T0	unspecified product	OG6_585869	unknown
PHYBL_159665T0	unspecified product	NA	NA
PHYBL_151839T0	unspecified product	NA	NA
PHYBL_77887T0	unspecified product	OG6_157827	unknown; uncharacterized protein
PHYBL_163749T0	unspecified product	OG6_181272	unknown; hypothetical protein
PHYBL_153170T0	unspecified product	OG6_141494	unknown; hypothetical protein
PHYBL_142539T0	unspecified product	OG6_220803	unknown
PHYBL_170975T0	unspecified product	NA	NA
PHYBL_178991T0	unspecified product	NA	NA
PHYBL_171214T0	unspecified product	OG6_585550	unknown
PHYBL_62285T0	unspecified product	OG6_173372	unknown; hypothetical protein
PHYBL_68687T0	unspecified product	OG6_161780	unknown; hypothetical protein
PHYBL_60641T0	unspecified product	OG6_205388	unknown; hypothetical protein; phytoene synthase/Lycopene cyclase; source; uniProtKB/TrEMBL;Acc
PHYBL_71912T0	unspecified product	OG6_380243	unknown
PHYBL_159977T0	unspecified product	OG6_132845	unknown
PHYBL_182745T0	unspecified product	OG6_104687	isomerase; ribose; source; uniProtKB/TrEMBL;Acc; ribose 5-phosphate; ribose 5-phosphate isomerase...
PHYBL_66456T0	unspecified product	OG6_125900	unknown
PHYBL_148686T0	unspecified product	NA	NA

Discussion

The mating-types of the mucoromycete *P. blakesleeanus* have different contributions to the sexual cycle. The offspring of a *P. blakesleeanus* cross inherit mitochondria only from the (+) mating-type [120]. Additionally, the synthesis of trisporic acid hormone is cooperative, and each partner processes and exchanges different precursors [116,127]. When mating-types were grown separately, I observed a difference in phenotype, where the (-) mating-type appeared to accumulate more yellow pigment in its mycelia than the (+) mating-type, which appeared to be whiter. This difference in phenotype was observed despite growth conditions being kept the same for both cultures. A phenotypic difference in an organism that has differential roles during sexual reproduction could suggest that each mating-type has distinct, specialized non-mating roles. Indeed, the OrthoFinder analysis suggested that there are some differences in the genome between the two mating-types but genome comparisons found that the mating-types share, on average, ~99% nucleotide identity. The BUSCO analysis suggested the genomes are also complete and comparable. This observation was consistent with other systems, such as *N. tetrasperma*, where a portion of the genome between the two mating-types did not have orthologues in the partner. One limitation of this study, however, is that differences between the two mating-types of *P. blakesleeanus* may not be due solely to the mating-type gene and could be ascribed to the genetic background of each strain.

Even with this caveat, differential gene expression analyses found approximately 12% of genes to be differentially expressed between the two *P. blakesleeanus* mating-types. This proportion is only slightly higher than expression differences between mating-types of the anther smut fungus *Microbotryum lychnidis-dioicae* [80]. The

observation that similar proportions of genomes are differentially expressed in other fungal groups further suggests that mating-type biased gene expression is a conserved feature among fungi. In *P. blakesleeanus*, a greater proportion of the differentially expressed genes were downregulated in the (+) mating-type. Previous studies have suggested that the mating-type gene, *sexP*, of the (+) strain is constitutively expressed, whereas *sexM* of the (-) mating-type is only expressed during sexual reproduction [126]. Taken together, there is the potential that SexP, in its role as a transcription factor, may be involved in repressing expression of a subset of genes. This idea requires further testing through a comparison of gene expression in *P. blakesleeanus* mutants such as those that are heterozygous for the mating-type genes [112]. If the SexP transcription factor can act as a repressor, then I would expect these intersexual strains to have a transcriptome profile more similar to that of a strain undergoing mating despite growing in conditions that favor vegetative growth. My work also found differentially expressed genes that lacked clear orthologues in the opposite mating-type. While these "mating-type specific" genes were generally excluded from our analyses, future work should use targeted gene expression approaches to investigate the status of these genes in both mating-types of *P. blakesleeanus* and other mucoromycetes.

The observed phenotypic differences were hypothesized to be a result of accumulation of yellow pigment. Gene ontology enrichment found that genes related to carotenoid biosynthesis were downregulated in the (+) mating-type. Although only two genes related to this process had this GO annotation, they represent the genes involved in the early steps of carotenogenesis [125]. Expression of the genes *carRA* and *carB* is stimulated by light or mating. The colonies used in this study were grown in the dark and kept separate from compatible mating partners. Under these conditions, neither of the

carotenogenic genes were expected to be differentially expressed between the two mating-types -- the lack of stimuli would mean lower but comparable counts. Downregulation of these genes in the (+) mating-type offers a possible explanation for its paler/whiter appearance when compared to (-). Notably, the gene *carS*, which encodes a carotenoid oxygenase, was upregulated in (+). This carotenoid oxygenase is required for cleavage of β-carotene [154]. In contrast, a gene encoding beta β-carotene 15,15'-dioxygenase was downregulated in (+). β-carotene cleavage products are precursors of the mating pheromone, which is cooperatively synthesized in the early stages of sexual reproduction. The gene *carS* also has a role in negative regulation of β-carotene synthesis. In *carS* mutants, β-carotene content is increased [154]. The pale/white appearance of the (+) mating-type could be partially due to the action of *carS* preventing accumulation of β-carotene. An accumulation of β-carotene in the (-) mating-type, under vegetative growth (so the *sexM* gene is not expressed), could serve as a way to prime strains to respond to the earliest signals for sexual reproduction from the (+) mating-type. The identity of these signals remains an open question. Additionally, since carotenoid biosynthesis is being downregulated, I would expect that the carotenoid regulatory proteins would also be differentially expressed, but this was not the case. These regulatory proteins are also not differentially expressed when exposed to light [124] so it is possible that they are constitutively expressed in both mating-types regardless of environmental stimuli. Upstream of carotenoid biosynthesis is the pathway that generates geranylgeranyl pyrophosphate. Among the upregulated genes, I also found a predicted GGPP synthase gene.

Other enriched GO terms which were related to color or pigmentation in other fungi included *de novo* IMP biosynthetic process. The genes with this GO annotation

that were upregulated were homologous to genes involved in generating adenine in yeast. In adenine auxotrophs, the resulting adenine deficiency is associated with red colonies [138]. The red color of adenine auxotroph colonies comes from oxidized ribosylaminoimidazole, this compound is not structurally related to carotenoids or terpenoids [138]. Furthermore, no red pigment appears to accumulate in the (-) mating-type. However, the upregulation of these genes suggests that the (+) mating-type is able to invest in *de novo* synthesis of purines. Where the (-) strain may prioritize a β-carotene priming, readying it to respond to possible mating signals if conditions change, the (+) mating-type prioritizes pathways that may prepare it for DNA synthesis and cell division during vegetative growth. Another term enriched by upregulated genes in the (+) mating type was synthesis of branched chain amino acids. Mucoromycetes, like *Blakeslea trispora*, are organisms of interest to produce compounds relevant to human health, one of these being β-carotene [93,94,118]. While the (+) *P. blakesleeanus* may not be the most carotenogenic strain, the finding that BCAA biosynthesis is enriched may offer an alternative source for synthesis of BCAAs, specifically isoleucine, for nutritional supplements. Previous research has found that ingesting isoleucine stimulates glucose uptake from the blood [155]. However, further work is needed to determine whether *P. blakesleeanus* is a viable source of these compounds.

Other downregulated GO terms included 1->3-beta-D-glucan biosynthetic process. The genes associated with this term were homologues of genes involved in septum formation during cell growth, spore wall synthesis, and synthesis of apical wall in yeasts. This finding presents a possible contradictory scenario in which the (+) mating-type is generating nucleotide precursors, potentially for use in DNA synthesis, but the related processes of cell growth and cell wall synthesis are downregulated. Other

genes involved in cell growth, cell wall synthesis, or the cell cycle, were also downregulated; these genes included a fatty acyl-CoA elongase, a GNAT domain protein, and a homologue of MLP/LIM regulatory proteins. Treating both mating-types of *P. blakesleeanus* with BrdU stain would identify proliferating nuclei in the (+) mating-type. This would begin to answer the question of whether the nucleotide precursors are actually being used in DNA synthesis at higher rates in the (+) mating-type relative to the (-) mating-type.

The GO terms Transmembrane transport and Carbohydrate metabolic process were enriched among upregulated and downregulated genes. Subsets of genes associated with these two terms were paralogous. One set of paralogues associated with transmembrane transport were homologues of a *S. pombe* gene encoding the sexual differentiation protein ISP4. Two of these paralogues had divergent expression status -- one was upregulated and the other downregulated. Two additional homologues of ISP4 were detected among upregulated genes, and neither was paralogous to the divergently expressed ISP4 genes. In *S. pombe*, isp4 encodes an oligopeptide transporter that is upregulated by nitrogen starvation and induces meiosis [63,156]. Since the strains used in my study were grown on limited media, these genes may indicate a response to nitrogen starvation and the conservation of the link between nitrogen-starvation and, broadly, sexual reproduction. However, no homologues of genes dedicated to meiosis were differentially expressed except for two downregulated homologues of Msh4 and Msh5. Meiosis in *P. blakesleeanus* remains an open question despite evidence for recombination [88]. Two explanations for the observed recombination are that *P. blakesleeanus* nuclei undergo meiosis in the zygospore or *P. blakesleeanus* has high rates of mitotic recombination. The former is supported by

previous genetic linkage analyses [88]. My data add to this understanding through the observation that meiotic genes are not differentially expressed during vegetative growth, and the two which are DE are downregulated -- it is not likely that *P. blakesleeanus* has high rates of mitotic recombination.

Sexual reproduction, phototropism, and carotenogenesis are processes that in *P. blakesleeanus* are closely associated. Mating and light stimulate carotene biosynthesis. Carotene biosynthesis is required for biosynthesis of trisporic acid mating pheromone. Light also inhibits sexual reproduction. In my work, neither mating type was exposed to a compatible mating partner at the time of RNA isolation, nor were they exposed to light for longer than 15 seconds during tissue isolation and flash freezing. Despite the lack of light exposure, there was a subset of genes which have previously been shown to respond to light which were also differentially expressed in the present work. I focused exploration of these genes on those with matching expression statuses between the present work and the light-induction work by Corrochano et al (2016). Genes upregulated in the (+) mating-type which were also upregulated in response to light were broadly related to carbon assimilation. Upregulation of an ATP-dependent RNA helicase homologous to a *S. cerevisiae* gene important for mitochondrial transcription was also observed. Uniparental inheritance of these organelles in *P. blakesleeanus* has been previously reported to occur, with the (+) parent passing on the organelles [120]. The gametes of organisms like animals differ in size, and cytoplasmic size differences contribute to the uniparental inheritance of mitochondria, where the larger gamete (typically the oocyte) contributes the majority of mitochondria. However, like other mucoromycetes and most fungi, *P. blakesleeanus* does not have different sized gametes so the mechanism of uniparental inheritance relies on degradation of the (-) parent's

mitochondrial genome [120]. Given that the mitochondrial transcription gene as well as aerobic respiration genes are upregulated in the (+) mating-type, one of the mechanisms that selects the (+) parent mitochondria may involve activity. That is, because the mitochondria of the (+) parent are more active, they are protected from degradation whereas the less active (-) parent mitochondria might resemble aging mitochondria and are marked for mitophagy.

One gene which was downregulated by light [109] and downregulated in the (+) mating type was a homologue of *N. crassa* RPI-1, which shares homology with Tom5 of *S. cerevisiae*. Tom5 is important for maintaining the stability of the TOM complex at higher temperatures [157]. A gene encoding a protein with a LtrA domain was also downregulated. In bacteria, LtrA domains help cells grow at low temperatures [151]. The downregulation of these two genes, one that stabilizes a protein complex at high temperatures and one that plays a role in microbes' ability to grow at low temperatures, hints at a scenario where each mating-type may have differential responses to temperature. Follow up experiments should compare the growth of mating-types with varied temperature conditions.

Genes that were found downregulated in the (+) mating-type which were also downregulated in response to light from [109] were mostly unspecified or uncharacterized products with the exception of six genes. One of these is the beta β-carotene 15, 15'-dioxygenase mentioned previously. This dioxygenase was only conserved in other Mucoromycetes according to FungiDB. The metazoan homologue of this gene is used to generate retinal from β-carotene. Given that this gene is downregulated by light and by vegetative growth, it may be involved in later steps of mating pheromone synthesis. A carboxylesterase was also downregulated in the (+)

mating-type. Carboxylesterases with hydrolytic domains are able to detoxify environmental substances and in some cases degrade plant cell walls to release ferulic acid, a compound important for production of food [158–160]. Because this carboxylesterase is downregulated in the (+) mating-type, it may be slightly more abundant in the (-) mating-type. In order to establish differential carboxylesterase use, however, each mating-type would need to be grown on media supplemented with tributyrin. In this scenario, the (-) mating-type would degrade tributyrin and a halo would appear in the media surrounding the colony. The downregulation of genes that contribute to production of yet another antioxidant molecule begins to paint a picture in which the (+) mating-type may be more susceptible to reactive oxygen species than the (-) mating-type. However, the possibility of more active mitochondria in the (+) mating-type would resolve the issue of ROS accumulation.

Here, I presented an exploration of the transcriptomic differences between the two mating-types of *P. blakesleeanus*. While I observed ~12% of genes in the genome to be differentially expressed, the work is limited by the conditions that were tested as well as the availability of genomics resources for this organism. Follow up work should include additional comparisons where the strains are grown on different media. The transcriptomes discussed here only accounted for nutrient-limited media. An additional comparison of gene expression between the wildtype strains and mutagenized strains would also add another level of understanding to the differences between mating-types. As genomic resources for the mucoromycetes improve, SNP discovery between available mating-types should also be pursued. Similarly, more complete genomes would also help identify genomic decay or divergence and other evolutionary strata among genes that were differentially expressed between the two mating-types.

Methods

Growth, culture conditions, and Orthologue Identification

Strains of *P. blakesleeanus* were obtained from culture collections: UBC21 (+) was from the Fungal Genetics Stock Center and NRRL 1555 (-) was from the Agricultural Research Service Culture Collection (NRRL). The mating-types were grown on malt and yeast extract agar at 23C under a 12-hour light cycle. Phenotypic differences were observed after one week on both MEYE media and ½ cornmeal agar. For RNA isolation, asexual spores were isolated from each mating type and suspended in 500ul of 0.01% tween-20. Suspended spores were centrifuged in a tabletop centrifuge for 30s. The tween-20 was decanted and replaced with sterile water. Strains were cultured on half-strength cornmeal agar at 23C and kept in the dark. Each plate had eight inoculation sites. Each sample had 3 replicates made up of 3 pooled plates for a total nine cultures per mating-type.

OrthoFinder [161] was used to identify orthologues between the two mating types of *P. blakesleeanus*. *P. blakesleeanus* NRRL1555 (GCA_001638985.2) predicted proteins were used as the (-) mating-type while *P. blakesleeanus* UBC21 predicted proteins were used as the (+) mating-type [88]. *N. tetrasperma* sequences were obtained from JGI (FGSC 2508 mat A and FGSC 2509 mat a) [162]. Genome completeness between UBC21 and NRRL1555 was assessed using the BUSCO tool and the mucoromycota_odb10 marker set [163]. Average nucleotide identity between the *P. blakesleeanus* genomes was assessed with FastANI [164]. Whole-genome scaffold comparisons were done with RagTag [165]. The scripts and workflow for these analysis are available in https://github.com/stajichlab/EvoDevo_of_Mucoromycotina.

RNA isolation and sequencing

RNA was isolated from 1cm of leading edge pre-mating mycelia of both mating-types. Mycelial tissue was cut from the substrate in the dark with a sterilized razor blade treated with RNAseZAP (Sigma-Aldrich) and immediately frozen in liquid nitrogen. Myclelia were homogenized with sterilized mortar and pestle that were also treated with RNAseZAP. RNA was isolated with TRIzol reagent (Thermo Fisher Scientific) following the manufacturer's protocol for tissues. Samples were submitted for paired-end illumina sequencing at Novogene.

Differential gene expression analysis and expression profiling

Reads were quantified with kallisto and differential expression analysis was done with DESeq2 following a workflow for pairwise comparison [166,167]. We used the genome of *P. blakesleeanus* NRRL 1555 (GCA_001638985.2) for kallisto indexing. Adjusted p-values were used to determine differentially expressed genes, with a cutoff less than or equal to 0.05. An absolute Log2 fold-change greater than 2 was also used to identify differentially expressed genes. Plots were produced with ggplot2 [168] and heatmaps were produced with the R package Pheatmap [169].

GO Enrichment Analysis

GO enrichment analysis was performed with the TopGO package in R [136]. GO association files for NRRL1555 were obtained from FungiDB. Following enrichment analysis, GO IDs and corresponding p-values were processed with Revigo [137]. Once redundant terms were removed, the p-values were adjusted using BH method, and a cut-off of adj. P-value≤0.05 was applied.

Chapter 3: Mating Transcriptome of *Phycomyces blakesleeanus*

Introduction

Investigation of the dikaryan fungi has enabled the discovery of genes that are important for sexual reproduction and development in these model organisms, however, less is known about the genetic and molecular mechanisms and environmental conditions that regulate sex and development in other divergent fungal lineages such as Cryptomycota and Microsporidia, Chytridiomycota, Blastocladiomycota, Zoopagomycota, and Mucoromycota [33]. In this study, I focus on *Phycomyces blakesleeanus,* a heterothallic mucoromycete notable for its large, phototropic and gravitropic sporangiophores [88,110,170].

Sexual reproduction in *P. blakesleeanus* has been characterized in the context of cell morphology, timing, and, to some extent, biochemistry [88,107]. Like other heterothallic mucoromycetes, successful sexual reproduction relies on the presence of a compatible mating partner, as determined by one of two idiomorphic HMG-box domain genes: *sexP* or *sexM* [88,171]. These transcription factors are homologous to the human male sex determining gene *SRY*, the α-box domain of Matα1p of *Saccharomyces cerevisiae*, and the MAT1-1/MAT1-2 proteins of other ascomycetes [33,69,88,171]. Genes of the mating-type loci of *N. crassa* and *C. globosum* have been shown to participate in sexual development [33,40,42]. In *S. cerevisiae*, the mating-type genes regulate expression of genes specific to either the haploid state or diploid state [49]. Similarly, in *P. blakesleeanus*, the mating-type genes are upregulated during mating, and

SexM translocates to the nucleus, suggesting that it plays a role in coordinating gene expression during mating [126].

Gene expression analyses with respect to the sexual cycle have relied on gene candidate approaches [123–125,154,172]. The carotene synthesis pathway in *P. blakesleeeanus* has been extensively studied in this context. Carotenogenesis is stimulated by light and mating [154,173]. During the sexual cycle, β-carotene is produced and cleaved to generate the trisporic acid (TA) pheromone [125,154,174]. Light induced carotene production is mediated by the MadA MadB complex -- a complex that is homologous to the white-collar complex in *Neurospora crassa* [87]. Additionally, functional studies have identified the enzymes involved in TA synthesis in related mucoromycetes [133,175].

Here, I use RNA sequencing to explore the global transcriptional landscape at three time points during the sexual cycle of *P. blakesleeanus*. I hypothesized that there would be subsets of differentially expressed genes that correspond to stages of mating linked to specific morphological and physiological changes. Additionally, I hypothesized that the subsets of genes would be enriched with conserved developmental and metabolic genes, in particular those involved in nitrogen starvation as crosses were done on nitrogen-limited media and this is a conserved trigger of sexual reproduction in other fungi. I also explored pathways known to be involved in the sexual cycle of *P. blakesleeanus*, like biosynthesis of β-carotene [125,174,176] and trisporic acid biosynthesis [133,175,177,178]. Lastly, I looked at the expression dynamics of the mating-type locus genes. Our analyses present the first comprehensive view of gene expression that drives the sexual cycle and the associated morphological changes in a mucoromycete.

Results

Characterization of Sexual Cycle Stages

P. blakesleeanus readily reproduces asexually (**Figure 3.1A**), but transitions to sexual reproduction in the presence of a compatible mating partner (**Figure 3.1B**). I observed semi-synchronous sexual development in our *P. blakesleeanus* crosses. These crosses produced pigmented, dormant zygospores over the course of eight days following serial morphological transformations. Spores germinated 24 hours after inoculation. At 48-72 hours after inoculation I noted the presence of zygophores within the substrate (**Figure 3.1C**). After 4 days, the zygophores became aerial structures with coralloid swelling apparent at the base (**Figure 3.1D**). In some cases, cells had started forming progametangia, a ring-like structure in which each half is formed by one of the zygophores (**Figure 3.1E**). Given that both aerial zygophores and progametangia are not cells undergoing fusion, both structures were pooled for quantification (**Figure A.3.1**). Progametangia were among the predominant structures at 4 days post inoculation, though some had already transitioned into gametangia. Developmentally, this stage represents the point where the two partners are interacting and tissues are functionally specialized, but most interacting cells have yet to undergo cell or nuclear fusion.

At 6 days post inoculation I observed an increase in gametangia relative to progametangia and aerial zygophores. It is during this stage that I see the appearance of adventitious septa in the suspensor cells (**Figure 3.1F, arrowheads**). At this stage, the cells are undergoing fusion, though different cells may be at different points in the process. In addition, there are small populations of progamentagia and zygospores at this stage. Based on these observations, I selected three timepoints to sample: before

crossing (both mating types, 3 dpi), preceding cell fusion (pre-fusion, 4 dpi), and post fusion of interacting cells (post-fusion, 6 dpi). The Before Crossing time point represents vegetative growth as neither strain was interacting with a mating partner. The two subsequent timepoints were associated with a mating reaction.

Differential Gene Expression Across Sexual Development

Our analysis detected 6,563 differentially expressed transcripts (FDR<0.01), which correspond to 39.7% of total genes and 45% of total expressed genes (**Table 3.1**). An additional 1,954 genes were non-expressed (i.e. had 0 read counts) and 95% of these were unspecified products (**Table A.3.2**, **Table A.3.3**). Principal component analysis also found that differences in expression were likely a result of the developmental stage at which RNA was isolated (**Figure A.3.2**). To determine expression profiles, I clustered genes by expression and developmental stage using hierarchical clustering (**Figure 3.2A**) and k-means clustering (**Figure 3.2B-E**). Hierarchical clustering of genes resulted in 4 broad subpatterns (**Figure 3.2A, Figure A.3.3, Figure A.3.4**). By hierarchical clustering, the four expression profiles were 1) highest expression before cross (BC), 2) highest expression BC and post-fusion, 3) highest expression at pre-fusion, and 4) highest expression post-fusion (**Figure A.3.4**). Biological replicates of each stage also clustered together (**Figure 3.2A**). Gene expression appeared consistent amongst the replicates but distinct from the other stages (**Figure 3.2A, Figure A.3.2**). To further profile expression, I performed k-means clustering using two different values of K. First, I used K=3, as this was the optimal value of K as suggested by the silhouette score and gap statistic methods (**Figure A.3.5**). I also used K=4, given that there are 4 subpatterns visible in the hierarchical clustering

heatmap; this value was also supported by the within-cluster sums of squares statistic [179](**Figure A.3.4**, **Figure A.3.5**).

With K=4, differentially expressed genes are clustered into four distinct clusters (**Figure 3.2B-E ; Figure A.3.6**). Three of these clusters contain genes with their highest expression at one particular stage of development, either before crossing, pre-fusion, or post-fusion (**Figure 3.2B,D,E**). The fourth expression cluster contains genes which have comparable high expression levels before crossing and during the pre-fusion stage (**Figure 3.2C**). Genes assigned to the Before Crossing expression (BCx) cluster (**Figure 3.2B**) have the highest expression before mating starts, and reduced expression at the pre-cell fusion stage followed by a slight increase at the post-cell fusion stage. Members of the Early expression (EAx) cluster (**Figure 3.2C**) have comparable high expression before crossing and at pre-fusion stages but reduced expression at the post-fusion stage; this is the only cluster with high expression at two stages. The EAx cluster is lost when K=3, and the member genes are forced into the other clusters which reduces the consistency of assignments between hierarchical clustering and k-means clustering (**Figure A.3.7**). The cluster membership assigned to a gene from either hierarchical or k-means approaches, where K=4, were largely consistent for BCx (1400 genes overlap), EAx (990 genes overlap), PEx (770 genes overlap), and POx (1600 genes overlap) (**Figure A.3.7**). Genes that are grouped into the Pre-fusion expression (PEx) cluster (**Figure 3.2D**) have increased expression prior to fusion of zygophores and reduced expression before crossing and at post-fusion stages. Lastly, the Post-fusion expression (POx) cluster (**Figure 3.2E**) is characterized by genes with reduced expression before crossing and at pre-fusion stages, but increased expression post-fusion.

Pearson correlation scores were calculated for genes in each cluster to assess how well they corresponded to the cluster centroid (**Figure 3.2B-E**, **Figure A.3.8**). In general, more than 50% of DEGs in each cluster had a Pearson correlation score above the average (**Figure A.3.8**). Furthermore, the differentially expressed genes were more or less evenly distributed among the four expression clusters (**Table 3.2**). The clusters EAx and PEx each contained ~24.4% of all differentially expressed genes. The POx cluster had the highest proportion of differentially expressed genes (27.2%) and BCx had the lowest (23.9%) (**Table 3.2**). In terms of genome representation, all clusters represented between 9.5-10.8% of predicted genes (**Table 3.2**).

Table 3.1. Differential gene expression analysis summary

	Total	Non-zero counts	DE (FDR<0.01)
Gene count	16,528	14,574	6,563
% of genome	100%	88.2%	39.7%

Table 3.2. Cluster Assignments

Cluster	Stage	Gene Count	% of DE genes	% of Genome	% of genes with GO annotation
BCx	Before cross	1,569	23.9	9.5	3.8
EAx	Transition	1,601	24.4	9.7	2.4
PEx	Pre-fusion	1,607	24.5	9.7	1.8
POx	Post-fusion	1,786	27.2	10.8	3.0

Functional Enrichment of Expression Clusters

To explore the possible functions of co-expressed genes, I performed gene ontology enrichment analyses on each expression cluster. One limitation of this analysis is the dearth of genomic resources for *P. blakesleeanus*. As a result, not every gene assigned to a cluster had a GO annotation (**Table 3.2**). The BCx cluster had the least

amount of enriched terms, with a total of 14 (**Figure 3.3A**; **Table A.3.4**). In contrast, the EAx cluster had 23 enriched terms, making the cluster with the most terms (**Figure 3.3B**; **Table A.3.4**). The PEx cluster had 17 enriched terms (**Figure 3.3C**; **Table A.3.4**) and the POx cluster had 18 enriched terms (**Figure 3.3D**; **Table A.3.4**). The GO term Transmembrane transport (GO:0055085) was enriched in both BCx and EAx clusters (**Figure 3.3A,2.3B**). Since not all genes in the P. blakesleeanus genomes had a GO annotation, subsets of differentially expressed genes within each cluster contributed to term enrichment. A total of 252 genes were associated with enriched GO terms in the BCx cluster, corresponding to 3.84% of all differentially expressed genes. The BCx cluster, consequently, had the most genes associated with the enrichment analysis, followed by POx (199 genes), EAx (158 genes), and PEx (115 genes). Additionally, some genes had multiple GO annotations and contributed to enrichment of multiple terms. Even after processing the enriched terms with Revigo [137], some related terms were not eliminated (**Table A.3.4)**. Some of these related terms also shared subsets of genes. I evaluated the degree of overlapping genes between these enriched GO terms and identified “meta” categories (**Figure A.3.9**).

The BCx cluster had three GO terms with exclusively-associated genes: Translation (GO:0006412), Cellular respiration (GO:0045333), and Protein kinase C-activating G protein-coupled receptor signaling pathway (GO:0007205). The other 11 terms had varying degrees of shared genes and constituted three meta categories and an additional four exclusive categories (i.e. the complement of genes that are associated with a GO term that shares genes with another GO term). Translation (GO:0006412) was the term associated with the most genes in this cluster (**Figure 3.3A**). In general, the Translation (GO:0006412) genes were predicted to be ribosomal proteins and

translation elongation factors. Some of these genes were mitochondrial specific, such as an asparaginyl-tRNA synthetase (PHYBL_107910) and mitochondrial translation elongation factor TU (PHYBL_121375). Cellular respiration (GO:0045333) and Protein kinase C-activating G protein-coupled receptor signaling pathway (GO:0007205) did not have genes that overlapped with other enriched terms in the BCx cluster. Cellular respiration was associated with 10 genes encoding various dehydrogenases, oxidoreductases, members of the aconitase superfamily, and a citrate synthase. Only two genes were associated with Protein kinase C-activating G protein-coupled receptor signaling pathway. These two genes are predicted to encode a polyadenylation factor 1 complex subunit (PHYBL_175731) and a diacylglycerol kinase (PHYBL_77550).

Transmembrane transport (GO:0055085) was also enriched in the BCx cluster (**Figure 3.3A**) and shared genes with three other enriched terms: Organic acid transport (GO:0015849), Amino acid transport (GO:0006865), and ATP synthesis coupled proton transport (GO:0015986) (**Figure A.3.9**). A total of 83 genes were associated with Transmembrane transport (GO:0055085), and included all genes linked to ATP synthesis coupled proton transport (GO:0015986). While Transmembrane transport and Organic acid transport each had a subset of exclusively associated genes, the four GO terms constituted the transmembrane transport meta category. Among these sets I observed amino acid transporters, ion transporters, mitochondrial transporters, permeases of the major facilitator superfamily, ATPases, mitochondrial carrier proteins, SLC26 family transporters, mitochondrial membrane translocases, and xanthine/uracil transporters. There were also two genes which were not paralogues of each other but were both orthologous to sexual differentiation process protein ISP4 (PHYBL_142208, PHYBL_181527). I additionally found an ammonia permease (PHYBL_120982) which is

orthologous to MEP1 and MEP2 in *N. crassa*. A single gene was shared between Transmembrane transport and Organic acid transport which was predicted to encode an ABC superfamily transporter involved in peroxisome organization and biogenesis (PHYBL_135582).

The next term in the BCx cluster with a large portion of genes was Carbohydrate metabolic process (GO:0005975), a total of 46 genes enriched this term (**Figure 3.3A**). This term also constituted the carbohydrate metabolism meta category and shared genes with Polysaccharide metabolic process (GO:0005976), Cellular polysaccharide metabolic process (GO:0044264), Amino sugar catabolic process (GO:0046348), and Oligosaccharide biosynthetic process (GO:0009312). Among these genes I found four chitinases (PHYBL_101903, PHYBL_56514, PHYBL_70372, PHYBL_98039) and three trehalose-6-phosphate synthase components (PHYBL_119756, PHYBL_38457, PHYBL_96516).

In the EAx cluster, the GO term with the most genes was Transmembrane transport (GO:0055085) (**Figure 3.3B**). Nine of these genes contributed to a transmembrane transport meta category that included the terms Calcium ion transport/transmembrane transport (GO:0006816/GO:0070588), ammonium transport/transmembrane transport (GO:0015696/GO:0072488), and Protein targeting to ER (GO:0045047) (**Figure A.3.9**). Some of the genes associated with transmembrane transport included four orthologues of sexual differentiation process protein ISP4 (PHYBL_105117, PHYBL_128566, PHYBL_121598, PHYBL_118039, PHYBL_117953). The ISP4 orthologues in the EAx cluster were divided into two sets of paralogous sequences in which PHYBL_105117 and PHYBL_128566 as well as PHYBL_142208 (of the BCx cluster) are paralogues. The second set of ISP4 paralogues includes

PHYBL_121598, PHYBL_118039, and PHYBL_117953, all of which are in the EAx cluster; notably, the second ISP4 orthologue (PHYBL_181527) of the BCx cluster lacked paralogues in the genome. I also found three ammonia permeases (PHYBL_121806, PHYBL_107857, PHYBL_155435) that were paralogous to each other and an ammonia permease that was observed in the BCx cluster (PHYBL_120982).

Microtubule-based process (GO:0007017) was enriched by 15 genes which were not shared with any of the other enriched GO terms of the EAx cluster (**Figure 3.3B**). These genes included various kinesins, tubulins, dynein chains, spindle associated proteins, and inhibitors of motor proteins. Among the tubulins, I found two beta tubulins (PHYBL_124605, PHYBL182106) and gamma tubulin (PHYBL_136269). An orthologue of *N. crassa* SPC97 (PHYBL_154555) was also observed in this subset of genes. The kinesin-like genes associated with this enriched GO term were categorized into three different orthogroups (by orthoMCL DB). The first group included three orthologous kinesin-like proteins (PHYBL_135717, PHYBL_95993, PHYBL_95995). This group is most similar to proteins containing a G3P dehydrogenase domain (orthoMCL DB). The second group of kinesins also included three orthologous genes (PHYBL_29641, PHYBL_108310, PHYBL_155510) which lacked the G3P dehydrogenase domain. The last category of kinesin-like proteins included the gene PHYBL_36914, which is orthologous to a kinesin of the KAR3 subfamily. Four other genes were predicted to be involved in dynein dynamics. This category included a dynein light intermediate chain (PHYBL_163567). Additionally, I observed an orthologue of dynein-associated protein Roadblock (PHYBL_164333) as well as a putative dynamitin (PHYBL_187262) and an orthologue of ASE1 (PHYBL_16656).

There were two meta categories in the EAx cluster related to sulfur metabolism. The first was comprised of genes exclusive to and shared between the terms Glutathione metabolic process (GO:0006749), Cellular modified amino acid catabolic process (GO:0042219), Peptide catabolic process (GO:0043171), Sulfur compound catabolic process (GO:0044273), and Glutathione catabolic process (GO:0006751) (**Figure A.3.9**). Genes associated with these terms included a glutamate-cysteine ligase regulatory subunit (PHYBL_143503), glutathione synthetase (PHYBL_181285), and pyridine nucleotide-disulphide oxidoreductase (PHYBL_125895); this oxidoreductase is orthologous to glutathione reductase of *N. crassa* and *S. cerevisiae*. The three genes in common between glutathione metabolic process and the other, aforementioned terms are predicted to encode a metalloexopeptidase (PHYBL_96544) and two gamma-glutamyltransferases (PHYBL_137033, PHYBL_154572). The metalloexopeptidase is homologous to the glutamine amidotransferase DUG2p subunit of *S. cerevisiae*. Notably, a DUG3p orthologue (PHYBL_132671) was not differentially expressed **(Table A.3.2)**. The second meta category was composed of the terms Hydrogen sulfide biosynthetic process (GO:0070814) and Hydrogen sulfide metabolic process (GO:0070813). The three genes associated with these terms were predicted to encode phosphoadenosine phosphosulfate reductase (thioredoxin, PHYBL_136440), sulfite reductase (ferredoxin, PHYBL_178590), and ATP sulfurylase (PHYBL_30373). Although not associated with an EAx enriched GO term, two genes encoding proteins with basic leucine zipper domains are members of this expression cluster (PHYBL_170697, PHYBL_171357). Similarly, the gene encoding octin (PHYBL_68111) is also in this cluster but not associated with an enriched GO term.

The PEx cluster enriched GO terms with the greatest portion of genes were Cell communication (GO:0007154), Signal transduction (GO:0007165), and Signaling (GO:0023052) (**Figure 3.3C**). There were 45 shared genes associated with these three terms, and nine of them were shared with the terms G protein-coupled receptor signaling pathway (GO:0007186) and one was shared with protein geranylgeranylation (**Figure A.3.9**). Four paralogues predicted to encode G-protein alpha subunits (PHYBL_14598, PHYBL_25132, PHYBL_74312, PHYBL_74741) were part of this set. An unspecified product (PHYBL_160687) was orthologous to STE18 of *S. cerevisiae*. The last three genes shared with G protein-coupled signaling pathway term lacked orthologues in non-mucoromycete filamentous fungi and included a predicted GABA-B ion channel receptor subunit (PHYBL_187578) and a G-protein alpha subunit (PHYBL_80143) that were only observed in other mucoromycetes; the third gene was predicted to encode a glutamate-gated metabotropic ion channel receptor subunit (PHYBL_71184). The one gene shared between Cell communication (GO:0007154), Signal transduction (GO:0007165), Signaling (GO:0023052), and Protein geranylgeranylation (GO:0018344) was predicted to encode a GDP dissociation inhibitor (PHYBL_180189) orthologous to MRS6 of *S. cerevisiae*, an accessory subunit of the type II geranylgeranyl transferase. Protein geranylgeranylation had two additional genes that were exclusive to this term (**Figure A.3.9**). These two genes are predicted to encode alpha (PHYBL_166315) and beta (PHYBL_119718) subunits of a protein geranylgeranyltransferase type II. Lastly, among the 36 genes that were exclusive to cell communication, signal transduction, and signaling I observed two paralogues predicted to encode phospholipase D1 (PHYBL_132024, PHYBL_111269), two paralogues predicted to encode CDC24 (PHYBL_10626, PHYBL_96834), a regulatory subunit of serine/threonine protein

phosphatase (PHYBL_112385), calcineurin-mediated signaling pathway inhibitor (PHYBL_167057), and a gene predicted to encode Cdc42-interacting protein CIP4 (PHYBL_171952). Other genes exclusively associated with these terms included various Ras-related GTPase proteins, Ras GTPase activating proteins, Rho type small GTPases, G protein signaling regulators, IQGAP family proteins, sensory transduction histidine kinase, a Rap1GAP orthologue, and a Sec7 orthologue. Two orthologues of *ste-20* (PHYBL_158973, PHYBL_114945) were also part of the PEx cluster, but not associated with a GO term.

Lastly, there were two PEx enriched GO terms of particular interest: Isoprenoid biosynthetic process (GO:0008299) and Membrane fusion (GO:0061205). The isoprenoid genes included previously described genes *carRA* (PHYBL_180114), *carB* (PHYBL_37852), *ggsA* (PHYBL_183831), and HMG-CoA synthase (PHYBL_126185). Other genes encoded other enzymes involved in isoprenoid synthesis: polyprenyl synthetase (PHYBL_109964), mevalonate pyrophosphate decarboxylase (PHYBL_115639), mevalonate kinase (PHYBL_89956), and an unspecified product (PHYBL_70887) with orthologues in other mucoromycetes, a chytrid, and an ergot fungus (FungiDB). Membrane fusion was enriched by two genes considered unspecified products. When transformed by orthology on FungiDB, however, I found that one of these genes is orthologous to the yeast karyogamy gene KAR5 (PHYBL_168862). The other is an orthologue of *N. crassa* and *S. cerevisiae* pheromone-regulated protein PRM1 (PHYBL_175308).

Finally, in the POx cluster, the majority of genes were associated with the term Organonitrogen compound biosynthetic process (GO:1901566) (**Figure 3.3D**). This term shared 43 genes with nine other terms, comprising a meta category largely related to

amino acid synthesis and translation (**Figure A.3.9**). In this category, I found three paralogous dolichyl-phosphate-mannose:protein O-mannosyl transferases (PHYBL_144376, PHYBL_74350, PHYBL_86467) which are orthologues of PMT1 of *S. cerevisiae*. I also observed a chitin synthase/hyaluronan synthase (PHYBL_24510). there were two terms related to lipid metabolism. The terms lipid metabolic process (GO:0006629) and phospholipid biosynthetic process (GO:0008654) were enriched by 48 and 15 genes, respectively. They shared 13 genes in common and among them was an orthologue of phosholipase D (PHYBL_59406). I also observed an orthologue of TAM41 (PHYBL_181116) and SLC1 (PHYBL_137570) in this set. Of the 48 genes associated with lipid metabolic process, only 23 were exclusively associated with the term (**Figure A.3.9**). One of these genes encodes another phospholipase (PHYBL_76183). Other lipases in this cluster and exclusively associated with this term included two non-paralogous predicted lipases (PHYBL_115329, PHYBL_158216), paralogous lipases/calmodulin-binding heat-shock proteins (PHYBL_71344, PHYBL_65786), and a third lipase/calmodulin-binding heat-shock protein (PHYBL_148903) that was specific to other mucoromycetes. Two genes were related to sterol metabolism, including an orthologue of ERG1 (PHYBL_136751), sterol O-acyltransferase (PHYBL_108349) and sterol reductase (PHYBL_178057). Other genes included a predicted ceramidase (PHYBL_156648), lecithin:cholesterol acyltransferase/acyl-ceramide synthase (PHYBL_127956), sphingolipid hydroxylase (PHYBL_20543), and delta-8 sphingolipid desaturase (PHYBL_15434). Acyl-CoA synthetase (PHYBL_128652), Acyl-CoA reductase (PHYBL_77188), and 3-hydroxyacyl-CoA dehydrogenase (PHYBL_154765) were also among these genes. An orthologue of *S. cerevisiae* MSS4 (PHYBL_87373) was present in this set as well. Five

genes were considered unspecified or uncharacterized products, but two had homology to fatty acid desaturases (PHYBL_120546, PHYBL_155437), an uncharacterized conserved protein which was an orthologue of sei1 (PHYBL_179334), a phosphodiesterase (PHYBL_99878), and a *P. blakesleeanus* specific gene (PHYBL_72696) with PHD and BROMO domains.

Lastly, the term Lipid modification (GO:0030258) was enriched by 7 genes, all of which were shared with the term lipid metabolic process. Among them were three genes (PHYBL_124248, PHYBL_155727, PHYBL_38190) with predicted roles in peroxisome function. PHYBL_124248 is orthologous to a peroxisomal dehydratase in *N. crassa* (NCU08828, NCU09138). PHYBL_155727 and PHYBL_38190 encode peroxisomal Acyl-CoA oxidases. The terms Carbohydrate biosynthetic process (GO:0016051) was associated with 9 genes. Among them were orthologues of *N. crassa* trehalose phosphate synthase *tps-1* (PHYBL_96413), trehalose phosphatase *tps-2* (PHYBL_96533, PHYBL_183480). An orthologue (PHYBL_123073) of the *N. crassa* neutral trehalase *tre-2* was also present in this cluster. All genes discussed in this section are summarized in **Table A.3.5**.

Carotenogenesis and Pheromone Synthesis

Genes implicated in mucoromycete carotenogenesis were overrepresented in the PEx cluster (**Figure 3.3D**,**Table A.3.4**). As mentioned, carotene synthesis is stimulated by light or by mating [125,174]. Carotene synthesis and TA synthesis pathways are summarized in **Figure 3.4A**. Light induced carotene production is mediated by the MadA MadB complex -- a complex that is homologous to the white-collar complex in *N. crassa* [87]. There are three copies of *madA* (*madA, wcoA, wcoB*) and four copies of *madB*

(*madB, wctB-D*) in *P. blakesleeanus* [87]. Only *wctD* (PHYBL_85757) was differentially expressed (**Figure 3.4B,C)**. No other copies of these genes were detected as differentially expressed, in line with previous work suggesting that the complex is constitutively available but induces carotenogenesis only when stimulated by blue light [87]. Despite the MadA MadB complex not being differentially expressed, I identified 11 differentially expressed genes involved in carotenogenesis and TA synthesis (**Table 3.3)**.

The genes *carRA* and *carB* play a role in synthesizing β-carotene in response to light or mating [123,125,180]. Both *carRA* and *carB* are differentially expressed (FDR<1%) and are members of the PEx cluster (**Figure 3.2D**). Once β-carotene is synthesized, it must be cleaved to generate trisporic acid precursors. The *carS* gene encodes a carotenoid oxygenase involved in the initial cleavage of β-carotene and is also a negative regulator of carotenogenesis [125,174,178]. Like the other two carotenogenesis genes, it is part of the PEx cluster, but its relative expression was lower than *carRA* and *carB* (**Figure 3.4D**). Following the pre-fusion stage, these three carotene synthesis genes exhibited reduced expression (**Figure 3.4D**).

As previously mentioned, the β-carotene cleavage products feed into the pheromone synthesis pathway (**Figure 3.4A**). The gene *acaA* (PHYBL_143867) is a carotene oxygenase involved in cleaving β-carotene and links carotenogenesis to pheromone synthesis (**Figure 3.4A,D**) [154,178]. The two mating types produce 4-dihydrotrisporin by distinct mechanisms prior to exporting and exchanging the trisporic acid precursors between partners [116,133,154]. Two genes, *tsp1* and *tsp2*, have been identified in *M. mucedo* that are involved in TA synthesis. The gene *tsp1* encodes a 4-dimethyl trisporate dehydrogenase (TSP1) and is actively transcribed in both mating-types of *M. mucedo*, but it is only active in the (-) mating-type. The gene *tsp2*

encodes a 4-dihydrotrisporin dehydrogenase which is also only active in the (-) mating-type of *M. mucedo [133].* The enzymes act at different points in the TA synthesis pathway, where TSP2 preferentially converts 4-dihydrotrisporin to trisporin, which is exported from the (-) mating-type to the (+) mating-type (**Figure 3.4A**). Similarly, TSP1 preferentially converts 4-dihydromethyl trisporate exported by the (+) mating-type to methyl trisporate in the (-) mating-type. TSP1 has a single orthologue in *P. blakesleeanus*, in contrast to TSP2 which has four orthologues. For ease of reference, I will refer to the orthologue of *tsp1* as *taoA* and the orthologues of *tsp2* as *tatA* through *tatD* (**Table 3.3**) [87,108,181]. Although the five orthologues are differentially expressed, only three have expression profiles associated with a sexual stage, either the EAx cluster or the PEx cluster, while *tatC* and *tatD* are associated with the BCx cluster (**Table 3.3**, **Figure 3.4A, 3.4E**).

Table 3.3. Carotenogenesis and TA synthesis genes

Gene ID	symbol	product	Cluster
PHYBL_85757	*wctD*	wc-2 homologue (GATA-4/5/6 transcription factors)	BCx
PHYBL_124486	*tatC*	4-dihydrotrisporin dehydrogenase	BCx
PHYBL_118385	*tatD*	4-dihydrotrisporin dehydrogenase	BCx
PHYBL_124728	*taoA*	4-dimethyl trisporate dehydrogenase	EAx
PHYBL_168867	*tatA*	4-dihydrotrisporin dehydrogenase	EAx
PHYBL_75000	*hmgR*	HMG-CoA reductase	EAx
PHYBL_21973	*tatB*	4-dihydrotrisporin dehydrogenase	PEx
PHYBL_37852	*carB*	Phytoene desaturase	PEx
PHYBL_180114	*carRA*	Bifunctional lycopene cyclase/phytoene synthetase	PEx
PHYBL_143867	*acaA*	Carotenoid oxygenase	PEx
PHYBL_183749	*carS*	carotenoid oxygenase	PEx
PHYBL_184132	*madA*	wc-1 homologue (K+-channel ERG and related proteins, contain PAS/PAC sensor domain)	NA
PHYBL_77612	*wcoA*	wc-1 homologue (K+-channel ERG and related proteins, contain PAS/PAC sensor domain)	NA
PHYBL_76314	*wcoB*	wc-1 homologue (K+-channel ERG and related proteins, contain PAS/PAC sensor domain)	NA
PHYBL_77137	*madB*	wc-2 homologue (GATA-4/5/6 transcription factors)	NA
PHYBL_179643	*wctB*	wc-2 homologue (GATA-4/5/6 transcription factors)	NA
PHYBL_65293	*wctC*	wc-2 homologue (GATA-4/5/6 transcription factors)	NA

Mating-type locus gene expression

In other filamentous fungi, the genes of mating-type loci are expressed during the sexual cycle and participate regulating sexual development genes [39,42]. In *M. mucedo*, expression of the mating-type genes are thought to be regulated by TA [182]. The mating-type genes are flanked by an RNA helicase gene (*rnhA*) and a triose phosphate transporter gene (*tptA*) (**Figure 3.5A**) [171]. Both *sexM* (**Figure 3.5B**) and *sexP* (**Figure 3.5C**) are differentially expressed and cluster with other genes in the PEx cluster. In neither mating-type were the genes *rnhA* and *tptA* differentially expressed, but whether the proteins are constitutively available remains to be elucidated. The *rnhB* gene in the (-) mating-type, however, is differentially expressed and is part of the POx cluster (**Figure 3.5B**). Downstream of *tptA*, I observed two additional syntenic genes which were not differentially expressed: a predicted mannuronate-specific alginate lyase (referred to as AlgA) and a predicted beta-1,6-N-acetylglucosaminyltransferase (referred to as GcnT) (**Figure 3.5A**).

The *rnhB* gene in the (-) mating-type is approximately 1.5kb upstream of *rnhA* (**Figure 3.5A**). This predicted gene is not present in the (+) mating-type and it encodes a predicted protein that is 227 amino acids in length, smaller than the neighboring (-)*rnhA* which is 649 amino acids [144]. The predicted RnhA protein from the (+) mating type is 1290 amino acids in length. The shorter RNA helicase protein in the (-) mating type aligns with the C-terminal portion of (+)RnhA, whereas (-)RnhA aligns with the N-terminal portion (**Figure 3.5D** ; **Figure A.3.20**). There was a 411 amino acid gap in the alignment corresponding to the 1.5 kb nucleotide gap between (-)*rnhA* and *rnhB* (**Figure 3.5D**). Notably, *rnhb* is differentially expressed and is a member of the POx cluster (**Figure 3.2E, Figure 3.5B**).

Discussion

In this study, I profiled gene expression during the sexual cycle of *P. blakeleeanus*. I identified four clusters of genes with similar expression patterns. Each expression pattern is associated with a particular stage of mating. GO enrichment analyses of the four expression profiles suggests a dynamic transcriptional landscape. Our data also supports previous work that identified mating-induced carotene and trisporic acid synthesis. I also showed that the genes flanking the mating-type genes, though syntenic, are not differentially expressed with the exception of a short RNA helicase gene in the (-) mating-type; however, this may be an artifact of the genome assembly given that both RNA helicases in the (-) mating-type align with distinct regions of the the (+) mating-type RNA helicase, despite divergent expression. The mating-type genes *sexP* and *sexM* are differentially expressed and have highest relative expression during the pre-fusion stage. Like their counterparts in Ascomycetes, these genes encode transcription factors which may regulate expression of other PEx cluster genes (i.e. those involved in carotenogenesis, TA synthesis, and genes required for polarized hyphal growth, morphogenesis, and fusion). I found a number of genes orthologous to genes induced by nitrogen starvation in the earlier stages of mating, supporting the idea of mating as a response to nutrient limitation [61,62,183].

GO terms related to nitrogen compound metabolism were enriched in BCx and POx clusters. Despite these GO terms being enriched in only two clusters, genes associated with nitrogen metabolism were observed in all four expression clusters. These genes are orthologues of *N. crassa gln-1/gln-2*, *nit-2*, *nit-4*, and *nit-3*. An active *gln-1/2* orthologue (PHYBL_106758) in this cluster suggests that *P. blakesleeanus* has a conserved mechanism for regulating nitrogen catabolite repression [184–187]. This is

not surprising given that these crosses were cultured on nutrient poor media and nitrogen starvation is a common trigger of sexual reproduction in fungi. Glutamine synthetase is a positive regulator of *nit-2* in *N. crassa* [188], and similarly *nit-2* is a positive regulator of *nit-4 [188,189]*. In turn, *nit-4* regulates expression of nitrate and nitrite reductases, *nit*-3 and *nit-6* respectively, in *N. crassa [189]*. While I did not find an orthologue of *nit-6*, the other genes in this nitrogen assimilation pathway were all present in both BCx and EAx clusters. The PEx cluster is only associated with orthologues of *nit-4* and *nit-3*, while the POx cluster was only associated with a *nit-2* orthologue. I hypothesize that as mating proceeds, there is a shift away from primary metabolic processes so that energy is invested into processes needed for sexual reproduction, such as signalling and differentiation. The *nit-4* and *nit-3* orthologues that were members of the PEx cluster may represent a *nit-2*-independent mechanism of nitrate assimilation that is specific to differentiated cells involved in mating. The nit-2 orthologue that I observed in the POx cluster was not associated with an enriched GO term, but since it is a major regulator of nitrogen catabolism, it may play an indirect role in amino acid metabolism during the later stage of mating.

The terms localization, transport, and glutathione metabolism were only enriched in the EAx cluster. The genes associated with localization and transport include orthologues of ISP4, which in other systems is upregulated by nitrogen starvation and is important for sexual morphogenesis in ascomycetes [51,156]. Other genes associated with the localization and transport GO terms have roles in morphogenesis and nitrogen metabolism, such as the ammonia permease orthologous to the *tam-1/2/4* proteins of *N. crassa*. Other genes that may be contributing to a morphological transition include two trisporic acid synthesis enzymes and octin. Co-expression of the exocyst complex and

SNARE complex along with the TA synthesis enzymes, *taoA* and *tatA*, may indicate a possible mechanism for the export of TA intermediates between the mating pairs leading to differentiation of hyphae to zygophores. Because zygophores of *P. blakesleeanus* dive within the substrate, I likely did not recover any of these cell types in our experiment. However, because the gene that encodes OCTIN is a member of this cluster and the sampled tissue lacked asexual sporangiophores, I posit that OCTIN has an additional role in generating aerial zygophores.

Glutathione metabolism and oxidation-reduction processes were also enriched in the EAx cluster. Oxidation-reduction process harbors a suite of genes that, in *N. crassa*, play key roles in sulfur assimilation [190]. This pathway generates cysteine, which is a key component of glutathione. The sulfur assimilation genes are co-expressed with glutathione biosynthetic and catabolic genes. This points to a deviation from homeostatic levels of glutathione, which is associated with the presence of reactive oxygen species. In other eukaryotes, regulation of ROS is involved in cell differentiation [191–193]. Additionally, in *Aspergillus nidulans*, the redox state of cells contributes to whether or not sexual reproduction occurs. *A. nidulans* mutants deficient in a thioredoxin system do not form sexual structures unless given reduced glutathione [60]. The presence of exocyst complex subunit genes and SNARE complex genes along with components of nitrogen, sulfur, and ROS metabolic pathways in this cluster supports the idea that polarized growth and morphogenesis define the EAx cluster. Because these genes are shared between two distinct stages, I hypothesize that they represent components involved in the transition from vegetative growth to sexual development.

Morphogenic genes are not limited to the EAx cluster set. The PEx and POx clusters are associated with a single stage of sexual reproduction and subsequently

linked to the presence of specific sexual structures. Notably, the expression of the mating-type genes, carotenogenic genes, and a copy of the *tsp2* orthologue, *tatB*, were highest at this stage, in agreement with previous work [125,126,133,154,177]. Previously uncharacterized orthologues of PLD1, CDC24, and Bzz1p/CIP4 were also members of the PEx cluster. These three genes may be responding to increased levels of TA in conjunction with the transcription factor activity of the mating-type genes. One possible scenario is that PLD1 is involved in mediating the response to TA, since PLD1 in yeast is responsible for pheromone sensing and pheromone induced morphogenesis [52]. In other filamentous fungi, PLD1 and phosphatidic acid are involved in cell-cell fusion [194], so its relatively high expression at the pre-fusion stage suggests a role in mediating fusion between the two parent zygophores. CDC24 and Ste-20 are involved in polarized growth [195,196], Bzz1p/CIP4 is required for endocytosis, motility, cell polarity, and cytokinesis [197−199]. Taken together I hypothesize that TA and the mating-type genes induce expression of these morphogenic genes to guide the transition from pre-fused cells towards fusion.

As progametangia develop into gametangia and then zygospores, the number of enriched GO terms increases and shifts towards metabolic and biosynthetic processes. Notably, the term with the highest enrichment was arginine biosynthetic process. Arginine has various roles in cells including urea and nitric oxide biosynthesis [200], induction of filamentation in response to stress [201], and aids in conidial germination and sexual reproduction and development [202,203]. Mutations of *arg-12* in other filamentous fungi leads to the production of immature fruiting bodies [203]. These represent another set of potential morphogenic genes that are specifically involved in the

later stages of the sexual cycle of *P. blakesleeanus*, pointing to the importance of amino acid derivatives in coordinating development of the zygospore.

One of the features of the post-fusion stage is the presence of adventitious septa. The chitin synthases that were identified in the POx cluster are orthologous to those that localize to the spitzenkorper and to developing septa of *N. crassa*. While *P. blakesleeanus* does not produce a spitzenkorper proper, it does have an apical vesicle crescent which may function similarly [204,205]. These chitin synthases likely play a role in deposition of the adventitious septa that separate the developing zygospore from the parental cells. I also observed genes with predicted roles in peroxisome function. In other filamentous fungi, the peroxisome is important for formation of fruiting bodies and development of meiotic spores. They also play a role in regulating progression of the meiotic cycle [206]. These genes were co-expressed with trehalose biosynthetic genes. Trehalose is associated with dormancy in fungi, where it accumulates within spores and is catabolized by trehalases to break dormancy [59,207]. The peroxisome of *P. blakesleeanus* may be directly involved in mobilizing reserve compounds as it enters dormancy. Related to these processes is an orthologue of *cdc1*. In yeast, CDC1p is involved in recombination and organelle inheritance [208,209] as well as facilitating the integration of GPI anchored proteins into the cell wall [210]. Neutral trehalases in fungi have a GPI anchoring domain [211], so in addition to potential roles in regulating the cell cycle, the *cdc1* orthologue may also contribute to sequestering enzymes that will eventually aid in breaking the zygospore dormancy period. I also hypothesize that it plays a key role in the thickening of the zygospore cell wall, since mutations to this gene in yeast can also lead to fragile cell walls [211].

Although functional studies and finer coarse time-series of development will be necessary to implicate the function of these genes in the sexual cycle of *P. blakesleeanus*, I have identified broad patterns of gene expression. I have shown that while *P. blakeleeanus* undergoes unique morphological changes during sexual reproduction compared to the dikaryan fungi, many of the genes associated with particular stages have orthologues in other systems with conserved functions during mating. Additionally, these orthologues have varying copy numbers in *P. blakesleeanus,* and in some cases different copies are associated with different stages of sexual development and presents a scenario in which *P. blakesleeanus* paralogues are each specialized to respond to a particular stimulus.

Methods

Culturing conditions, crosses, and microscopy

Strains of *P. blakesleeanus* were obtained from the Agricultural Research Service Culture Collection (NRRL 1555, (-) mating-type) and the Fungal Genetics Stock Center (UBC21, (+) mating-type). The mating-types were grown on malt and yeast extract agar at 23C under a 12-hour light cycle. Asexual spores were isolated from each mating type and suspended in 500ul of 0.01% tween-20. Suspended spores were centrifuged in a tabletop centrifuge for 30s. The tween-20 was decanted and replaced with sterile water. Strains were co-cultured on half-strength cornmeal agar at 23C and kept in the dark. Each plate had eight inoculation sites with alternating mating-type. Each sample had 3 replicates made up of 3 pooled plates for a total nine cultures per time point. Crosses for structures shown in figure 3.1C,D,F,G were set up in the same way as the RNA isolation crosses with the exception that spores were added to a culture slide.

Culture slides consisted of a microscope slide with a thin layer of ½ cornmeal agar. Mating-types were placed at opposite ends of the slide and their development was documented daily for 6 days after inoculation. Images in figure 3.1E,H were taken with a dissecting scope from strains crossed on ½ CMA plates.

RNA isolation and sequencing

RNA was isolated from 1cm of leading edge pre-mating mycelia of both mating types and from mated mycelia within a 1cm boundary centered along the line of mating interaction. Mycelial and sexual tissues were cut from the substrate in the dark with a sterilized razor blade treated with RNAseZAP (Sigma-Aldrich) and immediately frozen in liquid nitrogen. Tissues were homogenized with sterilized mortar and pestle that were also treated with RNAseZAP. RNA was isolated with TRIzol reagent (Thermo Fisher Scientific) following the manufacturer's protocol for tissues. Samples were submitted for paired-end illumina sequencing at Novogene.

Differential gene expression analysis and expression profiling

Reads were quantified with kallisto and differential expression analysis was done with DESeq2 [166,167]. I used the genome of *P. blakesleeanus* NRRL 1555 (GCA_001638985.2) for indexing. The likelihood ratio test was used to compare differences among all samples across time (adjusted P-value<0.01). Hierarchical clustering and K-means clustering were done in R. For k-means clustering, the value of K was optimized with the package NbClust [179], and K-means clusters were calculated based on the optimal K and hierarchical cluster data. Counts were Z scaled for plots showing cluster-wide expression. Plots of specific genes or groups of genes use

regularized log transformed count data. Plots were produced with ggplot2 [168] and heatmaps were produced with the R package Pheatmap [169].

GO enrichment analysis and function prediction

GO enrichment analysis was performed with the TopGO package in R [136]. GO association files for NRRL1555 were obtained from FungiDB. Following enrichment analysis, GO IDs and corresponding p-values were processed with Revigo [137]. Once redundant terms were removed, the p-values were adjusted using BH method, and a cut-off of adj. P-value≤0.05 was applied.

Orthology Inference

Orthologous proteins between *P. blakesleeanus* NRRL1555 (GCA_001638985.2) and *N. crassa* OR74A (GCA_000182925.2), *S. cerevisiae S288C* (GCA_000146045.2), *S. macroscpora* k-hell (GCA_000182805.2), *F. graminearum* PH-1 (GCA_900044135.1), *M. mucedo* NRRL 3635 (JGI), *B. trispora* NRRL 2456 (JGI), *S. vasiformis* B4078 (JGI), and *E. cuniculi* EcunIII-L (GCA_001078035.1) were inferred with FungiDB by uploading *P. blakesleeanus* gene IDs and transforming by orthologues [144]. For mating-type locus comparisons, I used the genome of *P. blakesleeanus* UBC21 produced by the US Department of Energy Joint Genome Institute (http://www.jgi.doe.gov/) in collaboration with the user community.

Sequence analysis

Predicted protein sequences of the mating-type locus RNA helicases (RnhA: PHYBL_87354, RnhB: PHYBL_157139) in *P. blakesleeanus* NRRL 1555 were obtained from FungiDB [144]. Alignments were done with clustal [212].

Chapter 4: Characterization and Evolution of the Mucoromycotina Mating-type Locus

Introduction

Genes found at the mating-type locus vary across the fungal kingdom, but in most cases these genes play a direct role in regulating mating-type specialization during vegetative growth and also regulate sexual developmental processes[77–79,129]. The genomes of individual fungal species which are considered distinct mating-types will differ only by the content of their mating-type locus (*MAT* locus). While the *MAT* loci of the diakryan lineages have been extensively studied, fewer studies have explored the mechanisms of mating-type determination in non-dikaryan fungi such as the flagellated fungi (chytrids and Blastocladiomycetes), Zoopagomycetes, or mucoromycetes. The mating-type locus of phylum Mucoromycota is an example of a bipolar mating system where mating types are distinguished from each other by a single differentially encoded gene [67,88,113]. The mucoromycete mating-type genes encode HMG-box domain proteins. In Mendelian genetic analyses, the two loci segregate independently in heterothallic species [88,121,171][33,41,67,130]. The mucoromycete mating-type locus has been examined in a handful of species, with particular focus on the subphylum Mucoromycotina [41,130]. Examined species include *Phycomyces* spp., *Mucor* spp., *Rhizopus* spp., *Blakeslea trispora*, and *S. megalocarpus* [41,113,132]. The organization of the mating type locus in these species is generally conserved, where the HMG-domain coding genes are flanked by a triose phosphate transporter gene (*tptA*)

and an RNA helicase gene (*rnhA*) [41]. A similar arrangement of the mating-type locus is observed in Microsporidia, but there is weak support for the orthology of the *tptA* and *rnhA* genes [213]. Thus it is not clear whether the MAT loci of Microsporidia and Mucoromycetes are an example of convergent evolution or an ancestral trait lost in other fungal lineages.

Prior studies have found that expression of *sexP* and *sexM* may be regulated by trisporic acids, the sex pheromone of Mucoromycetes [182]. The mating-type genes are differentially expressed, where *sexP* is expressed during vegetative growth and *sexM* is only expressed during sexual reproduction [67,113,173,182]. Factors such as light and carotenoid accumulation also regulate expression of *sexP* [214]. Additionally, unlike some Ascomycetes in which the MAT proteins dimerize to regulate expression of sexual reproduction genes, SexP and SexM may act independently [173]. Detailed genetic and molecular study of these genes and their loci has been hindered by the fact that the mucoromycetes are not especially amenable to genetic manipulation [33,86].

Initial attempts to identify mating-type loci in diverse fungal groups were hampered by the paucity of available genomes. However, recent sequencing efforts have recovered genomes of early-diverging fungi like the Mucoromycota [81]. Prior to the availability of these genomes, high-throughput attempts to identify and describe these mating-type loci relied on BLAST searches against a set of 23 mucoromycete species [131]. It is unclear if this previous study used reciprocal BLAST to identify orthologous mating-type locus genes or translated searches against a whole genome (tBLASTn) [131]. Despite these limitations, that study found support for synteny at the mucoromycete mating-type locus except for the *Lichtheimia spp*. [131]. The work also

found that gene content of the mating-type locus varied to some extent between different species, between mating-types, and within homothallic species [131].

Here, I sought to investigate the conservation of the mating-type locus in a larger set of mucoromycetes using multiple sequence comparison tools. Candidate loci were identified within the genome using protein queries. Candidate scaffolds were processed to predict protein sequences, then HMMer was used to verify predicted protein sequence identity. Assessing the conservation of gene order will help address the origins of the mating-type locus in the subphylum Mucoromycotina and lay the foundation for further investigating the mechanisms of mating-type determination in diverse species of the Mucoromycotina. More broadly, studying how mating-type loci evolved can inform broader dynamics of the evolution of sex determination and cell identity, the evolution of gene regulation, and evolution of intraspecies cell communication and signaling.

Results

Identification of Candidate Mating-Type Loci

Previous work on Mucoromycetes describes the organization of the mating-type locus for a handful of species including *P. blakesleeanus* and *R. oryzae*. In each case, the mating-type gene is flanked by genes encoding RNA helicase (*rnhA*) and a triose-phosphate transporter (*tptA*; **Figure 4.1A**). In contrast to *P. blakesleeanus*, *R. oryzae* and other members of the *Rhizopus* species complex harbor two additional genes near the locus: a glutathione reductase (*glrA*) and BTB-domain containing protein (*arbA*) [130,132]. Using the predicted protein sequences of these five genes, I identified candidate mating-type loci in 427 different isolates of the subphylum Mucoromycotina

(**Table A.4.1**). These isolates correspond to 138 unique species, representing 36 genera (**Figure 4.1B**). The genus *Amylomyces* was included with *Rhizopus*, as previous studies support that these genera are synonymous [215]. Similarly, two species of *Zygorhynchus* (*Z. exponens* and *Z. megalocarpus*) were grouped with *Mucor* [216]; genus or species synonyms are summarized in **Table A.4.1**. The genera *Rhizopus* and *Mucor* also harbored the most species compared to others (**Figure 4.1B**). The distribution of mating-types among these isolate-rich genera was nearly equal, with *Rhizopus* having 12 (-) species and 16 (+) species (**Figure 4.1B**). Among the genera that represented fewer species in which both mating-types were found, the ratio of (+) and (-) mating-types generally followed a similar pattern as with *Rhizopus* and *Mucor*, nearly equal numbers of both mating-types at the genus level (**Figure 4.1B**). *Phycomyces*, *Fennellomyces*, *Thamnostylum*, and *Pilaira* represented six or less isolates and the distribution of mating-types among them were skewed (**Figure 4.1B**). These skewed genera, where one mating-type was overrepresented, typically accounted for isolates of the same species. When plotting the distribution of mating-types across the different species of the *Rhizopus* and *Mucor* genera, I observed a similar pattern of overrepresentation (**Figure 4.1B'**) -- generally, more (+) mating-type isolates were observed among distinct species.

The percent identities of hits recovered by translated searches varied. Based on the distribution of percent identities, there was no difference between light coverage genomes (LCG) and reference genomes (REF) (**Figure 4.1C**). Relative to the mating-type genes (*sexP* and *sexM*), the flanking genes tended to have higher percent identity to the query protein (**Figure 4.1C**). The *arbA* gene was only observed in *Rhizopus* and *Syzygites* and since the query proteins were from *Rhizopus* species, the

percent identities were much higher compared to the other flank genes (**Figure 4.1C**). Additionally, following verification with HMMer, I found that the HMMer supported flank genes had higher percent identities in the translated search than hits in other parts of the genome (**Figure 4.1C**). These non-mating-type locus hits were removed at various steps in the analysis and do not contribute to the count of 427 isolates that were mating-typed. The HMMer-verified mating-type genes had on average higher percent identities than their unverified counterparts (**Figure 4.1C**). Surprisingly, there was no significant difference in percent identity between HMMer-supported and unverified *sexM* or *sexP* genes among the set of reference genomes (**Figure 4.1C**). A possible explanation for this is that the HMG-box is a domain that is not exclusive to the mating-type genes so the set of HMMer unverified HMG-box genes may represent other transcription factors in the genome.

While other research has demonstrated that the mucoromycete mating-type locus contains at least three syntenic genes (*rnhA*, *tptA*, and *sexM* or *sexP*), my analysis found some variation in gene content. The analysis identified 10 distinct variations of the locus (**Table 4.1**). The most common variant included an HMG-box gene flanked by *rnhA* and *tptA* with *glrA* in the vicinity of the locus (**Table 4.1**). This variant was also the most widely distributed among genera, but *Mucor spp.* made up the majority of species with this variant (**Figure 4.1D**). The next most common and widely distributed locus variant did not include any of the known flanking genes, that is, among 12 genera only the HMG-box domain gene was found (**Figure 4.1D**; **Table 4.1**). This does not preclude the existence of alternative flanking genes in genera where this variant represents the majority of species. With the exception of *Rhizopus* and *Mucor*, each genera was associated with at most four different variants total (**Figure 4.1D**). When I separate locus

variants and genera by the type of genome (light-coverage vs reference), the reference genomes have fewer variants per genus and the most widely distributed variant locus had only *rnhA* and an HMG-box gene (**Figure 4.1D**). The reference genomes of *Rhizopus* and *Mucor* species exhibited a wider variety of locus variants than other genera (**Figure 4.1D**).

Characteristics of Candidate Loci

In addition to variations in gene content of candidate loci, I also observed differences in the length of the locus. Here, length is defined as the number of nucleotides from the start of the first gene of the locus to the end of the last gene; this conception of length includes intergenic regions. Locus length and mating-type were mapped against a pruned species tree (**Figure 4.2**). Six isolates had locus lengths greater than 50kb, so they were not plotted. These include *Rhizopus delemar* (IGS99-880), *Cunninghamella bertholletiae* (B7461), *C. elegans* (B9769), *Fennellomyces sp.* (T-0311), *Syncephalastrum verruculosum* (RSA 2127), and *Blakeslea trispora* (NRRL 2456). Besides the six outliers, the length of the loci did not vary considerably between isolates of the same genera (**Figure 4.2**). Species in the *Rhizopus oryzae* complex were primarily identified as (+) mating-types, and the few (-) mating-types had slightly shorter mating-type loci by comparison (**Figure 4.2**). The *Rhizopus stolonifer* complex, which was sister to the *R. oryzae* clade and includes *Amylomyces rouxii*, *Sporodiniella umbellata*, and *Syzygites sp.*, had slightly more (-) mating-type representatives than (+) mating-types (**Figure 4.2**). Given that these loci had less consistent gene content, the locus sizes varied between isolates. However, where gene content was comparable between two mating-types of the same species, I again observed the (-) mating-type

locus as slightly shorter than the (+) counterpart. In the case of *Syzygites sp.* (MES 3091), the species is known to be homothallic and this analysis detected two mating-type loci with distinct gene content. In *Syzygites sp.*, the gene encoding SexM was near genes that encoded ArbA and RnhA, while SexP was on a scaffold that contained *glrA* (**Table A.4.1**, **Figure A.4.2**). Despite the (-) locus of *Syzygites sp.* having more genes than the (+) locus, it was shorter by ~16kb (**Figure 4.2**). A third *Rhizopus* species complex was sister to the aforementioned clades, and included species like *R. microsporus*, *R. chinensis*, and *R. circinans*, among some *Rhizopus* spp (**Figure 4.2**). *R. circinans* isolates had longer mating-type loci than other members of this clade which were generally similar in size (**Figure 4.2**); notably, the (+) locus of *R. circinans* was longer than the (-) isolates (**Table A.4.1**).

Outside the *Rhizopus* species clades there were six paraphyletic groups that predominantly represented *Mucor spp.* but other non-Mucor species were also among these clades (**Figure 4.2**). The first of the *Mucor* complexes which was sister to the *Rhizopus* complex was majority *M. racemosus* isolates of (-) mating-type of comparable length; in contrast, the one (+) isolate with a locus with similar gene content was roughly 7kb longer (**Figure 4.2**). The other (+) isolates of *M. racemosus* had much shorter loci composed only of *sexP* and *tptA*. In the M. racemosus isolate NRRL A-19185, I detected two different mating-type genes on separate scaffolds: the (+) locus contained only *tptA* and *sexP* while the (-) locus had *sexM* and *rnhA* (**Figure 4.2**, **Table A.4.1**,**Figure A.4.2**). The next Mucor complex represented *M. genevensis, M. philippovi,* and *M. globosus*. This clade was majority (+) mating-type with highly variable lengths (**Figure 4.2**). The third clade of the *Mucor* complex had a majority of *Mucor* species but also contained *Chaetocladium, Thamnostylum, Actinomucor, Circinomucor,* and *Ellisomyces* (**Figure**

4.2). With the exception of *C. brefeldii* (NRRL 1350) and a single *M. circinelloides* isolate (NRRL A-25893), the loci were comparable in length and gene content (**Figure 4.2**, **Table A.4.1**). The Mucor complex that included *Pilaira spp., Zygorhynchus* (and synonymous *Mucors), Rhizomucor,* and various *Mucor spp.* had highly variable locus lengths (**Figure 4.2**). The *Pilaira* species were all of the (-) mating-type, and their corresponding loci had very different lengths. *Z. heterogamus* and *M. heterosporus* (synonymous: *Z. heterosporus*) are known to be homothallic and this analysis detected two different size loci containing one of the two mating-type genes (**Figure 4.2**, **Table A.4.1**). The fifth Mucor complex only included three species: *M. laxorrhizus*, *Actinomucor elegans*, and *Circinella simplex* (**Figure 4.2**).The mating-type loci of *A. elegans* and *C simplex* were of comparable length, although *C. simplex* had a slightly longer locus. The last (earliest-diverged) of the Mucor complexes included *B. trispora, Benjaminiella youngii, Circinella muscae, Poitrasia circinans*, and various *Mucor* species (**Figure 4.2**). The mating-type locus of *B. trispora* was (+) and stood as an outlier in terms of length, being composed of 88.6kb (**Table A.4.1**). The remaining (+) loci of species in this complex were majority *Mucor* species as well as *P. circinans*. These loci were generally comparable by length (**Figure 4.2**). *B. youngii* and *C. muscae* were both (-) mating-types, their loci harbored only *sexM* and *rnhA* (**Figure 4.2**, **Table A.4.1**, **Figure A.4.2**).

Another four paraphyletic clades made up the “early-diverged” lineages of the Mucoromycotina. The first, which was sister to the Mucor complex, included *Mycotypha microspora, Cokeromyces recurvatus,* and *Backusella spp.* (**Figure 4.2**). All *Mycotypha* isolates were (-) and, along with *C. recurvatus*, had loci which harbored only *rnhA* and *sexM* (**Table A.4.1**, **Figure A.4.2**). Unlike the other *Backusella* species, *B. lamprospora*

lacked any of the known flanking genes, so its locus was much smaller (**Figure 4.2**, **Figure A.4.2**). Only *B. dispersa* was (-) mating-type among this genus, and its locus was slightly shorter than its (+) relatives (**Figure 4.2**). The next complex predominantly represented *Cunninghamella spp.*, *Absidia spp*., and *Gongronella butleri* (**Figure 4.2**). Among the *Cunninghamella* species, I observed a similar length pattern as with *Rhizopus*: (+) loci were generally longer than (-). This was also the case for the *Absidia* species (**Figure 4.2**). The (+) loci of all three *G. butleri* isolates were close in size as well (**Figure 4.2**). The next complex include *Phycomyces spp., Apophysomyces spp., Saksenaea oblongisporus*, and *Rhizomucor pusillus* (**Figure 4.2**). The *P. blakesleeanus* isolates also followed the *Rhizopus* pattern (shorter (-) loci). The other species and isolates only represented a single mating-type, and species of the same genera had comparable lengths of loci. *Rhizomucor pusillus* and a *Phycomyces sp.* isolate had loci of the same size (**Figure 4.2**).

The last of the early-diverged species complexes could be subdivided into four paraphyletic clades. The most derived of these included *Circinella spp*., *Fennellomyces spp*., *Thamnostylum spp*., and *Helicostylum*. All species in this group were (-) mating-types (**Figure 4.2**). The *Circinella* species had mating loci of the same length. *Fennellomyces* and *Thamnostylum* species had more variable lengths, but were generally longer than the *Circinella* species even though their loci contained only *sexM* and *rnhA* (**Figure 4.2**, **Table A.4.1**, **Figure A.4.2**). The single *Helicostylum* isolate had both mating-type genes on different scaffolds and may represent a homothallic species, however there were none of the expected neighboring genes to distinguish the loci (**Figure 4.2**, **TABLE A.4.1**, **Figure A.4.2**). The sister of the *Circinella-Fennellomyces-Thamnostylum* complex included *Lichtheimia* spp. and

Dichotomocladium spp. All of these species featured loci that lacked any of the expected flanking genes so they were only as long as the gene encoding the mating-type gene (**Figure 4.2**, **Figure A.4.2**). Similarly, the third subdivision of the early-diverged complexes, which represented *Rhizomucor pusillus* and *Rhizomucor miehei*, also featured mating-type genes that were not flanked by the expected genes (**Figure 4.2**, **Figure A.4.2**). The final subdivision included *Syncephalastrum verruculosum* and *S. racemosum*, both of which were (-) strains. Despite having the same gene content (*rnhA* and *sexM*), the locus of *S. racemosum* was longer (**Figure 4.2**, **Figure A.4.2**).

The last two branches, and the earliest diverged, of the phylogeny represented *Lentamyces zychae* and *Umbelopsis ramanniana* (**Figure 4.2**). The locus of *L. zychae* was comparable to the loci of the *Syncephalastrum spp*. in terms of general gene content and size (**Figure 4.2**, **Figure A.4.2**). In contrast, *U. ramanniana* resembled other early diverged groups in that it lacked the expected flanking genes. While there were some clade-specific patterns of mating-type locus length, it was less clear whether speciation contributed to the size of the loci. Additionally, longer loci did not always correlate with increased gene content. To address whether loci were compressed, I calculated the percentage of intergenic space within the locus and mapped it to a species tree (**Figure A.4.3**). While *Rhizopus* species generally had more genes in their mating-type locus, they had a lower proportion of intergenic space compared to the *Mucor* complexes which had fewer genes in the mating-type locus (**Figure A.4.3**).

Synteny

Next, I investigated whether locus organization was conserved. Specifically, I evaluated gene order and orientation, rather than gene content exclusively as in the

previous sections. Using representative species that had the best support from the translated searches and HMMer verification step, I mapped schematics of mating-type loci to a species phylogeny (**Figure 4.3**). As noted earlier, only *Rhizopus* species contained the gene encoding ArbA. Among *R. oryzae* and *R. delemar*, the orientation or location of this gene varied by mating-type. In *R. delemar*, the (-) mating-type locus featured an *arbA* gene that was upstream of *tptA* and divergently oriented with respect to *sexM* (**Figure 4.3**). In contrast, the (+) *R. delemar arbA* gene was flanked by *tptA* and *sexP* and was also co-oriented with both of these flanks (**Figure 4.3**). *R. oryzae* and *R. circinans* followed the same pattern. Notably, *R. stolonifer* lacked *tptA*, and the *arbA* gene in both mating-types was syntenic (**Figure 4.3**). *R. microsporus*, and other species represented by its particular clade, were the only *Rhizopus* species that lacked *arbA*. Furthermore, all *Rhizopus* representative mating-type loci featured the *rnhA* gene co-oriented with the mating-type gene and was always found between the mating-type gene and divergently oriented *glrA* (**Figure 4.3**).

The two mating-types of *Mucor racemosus* differed in intergenic space between the mating-type gene and the flanking genes. The *rnhA* gene in *M. racemosus* (-) was much closer to *sexM* than its counterpart in the (+) locus (**Figure 4.3**). Sister to these two isolates was *Mucor globosus*, a candidate homothallic species (**Figure 4.3**). The (+) locus of *M. globosus* had similar structure to (+) *M. racemosus*, but its (-) locus, which was on a different scaffold, was notably different. In the (-) *M. globosus* locus, *sexM* was flanked by *tptA* and *rnhA*, with *glrA* downstream of the gene cluster. These two loci had *tptA* in common, and in both cases, the gene was divergently oriented relative to the sex gene (**Figure 4.3**). Two other candidate homothallic species also had distinct locus arrangements. These included *M. heterosporus* and *S. verruculosum*. The (+) locus of

M. heterosporus contained more genes and resembled the organization of other loci more than its (-) locus; where *sexM* was found upstream of *rnhA* (**Figure 4.3**). Similarly, *S. verruculosum* (-) locus only featured a divergently oriented *rnhA*, whereas its (+) locus had a *glrA* instead. No other expected flank genes were detected among the remaining candidate homothallic species.

Generally, species of the genus *Mucor* tended to have very similar mating-type loci regardless of mating-type gene. Indeed, except for the sex genes, the mating-type loci of *M. circinelloides* were virtually identical in terms of gene organization, orientation, and scale (**Figure 4.3**). There were some cases where a locus resembled that of a homothallic *Mucor*, for example *M. hiemalis* and *M. heterosporus* had nearly identical (+) mating-loci (**Figure 4.3**). The species *B. youngii*, *C. muscae*, and *C. recurvatus* formed the clade that was sister to the *Mucor* paraphyletic complex, and their mating-type loci were also highly similar (**Figure 4.3**). In fact, among many of these early-diverged groups of Mucoromycotina, mating-type loci did not differ as much within species as was observed in *Mucor* and *Rhizopus*. One exception to this was *P. blakesleeanus*, in which *sexP* is co-oriented with *rnhA* and *sexM* is divergently oriented (**Figure 4.3**); this observation has been previously reported in other studies [86,113,130]. The remaining early-diverged groups generally had less of the predicted genes at their loci, making *P. blakesleeanus* one of the earliest groups in which we observe the sex gene flanked by *rnhA* and *tptA* (**Figure 4.3**). This does not preclude the presence of some of the flanking genes, as *Thamnostylum spp., Circinella angarensis*, *Syncephalastrum spp.*, and *Lentamyces zychae* all had an *rnhA* gene somewhere near the sex gene (**Figure 4.3**). The outgroup species was *Umbelopsis ramanniana*, and its mating-type locus lacked the expected flank genes as well.

Based on this coarse view of the Mucoromycotina species, there are a few trends that stand out. First, homothallism does not appear restricted to particular groups, as even in this pruned species tree, there are examples distributed among three different clades (**Figure 4.3**). However, this analysis may not reliably identify true homothallic strains given that other *Zygorhynchus* species only had strong support for one mating-type gene (**Table A.4.1**). The second pattern concerns the expansion of the mating-type locus through the recruitment of other genes. This is especially true of the *Rhizopus clades*, which feature additional genes in the neighborhood of the sex genes and which are organized in a mating-type specific manner (**Figure 4.3**). Additionally, in the lineages that come after the P. blakesleeanus clade, the rnhA gene is generally co-oriented with the sex gene (**Figure 4.3**). Where they co-occurred, rnhA and glrA were generally divergently oriented and always on the same side of the locus.

Evolution of SexP and SexM

The mating-type loci identified here varied in gene content, length, and organization. Given that this analysis targeted the mating-type genes, it followed that they were a consistent feature among all queried species. In terms of DNA sequence length, the *sexP* genes were generally longer than *sexM*, and *sexM* had less consistent sizes across all species (**Figure 4.4A**, **Figure A.4.4**). The predicted protein length generally correlated with nucleic acid length (**Figure 4.4A**, **Figure A.4.4**). For the most part, the protein lengths were comparable but length had no clear phylogenetic pattern. These predicted proteins were used to generate a midpoint-rooted tree (**Figure 4.4B**) as well as an unrooted tree (**Figure 4.4C**). The midpoint rooted tree was divided into two large clades, each of which represented either SexP or SexM proteins from all 475

queried isolates. Locus gene content (**Table A.4.1**) was mapped to both gene trees. When considering the midpoint rooted tree (**Figure 4.4B**), the clades generally represented the same locus content despite being composed of distinct species or isolates. The mating-type genes of *Rhizopus spp*., which shared the locus with *arbA*, (green leaves, **Figure 4.4B**) also clustered separately from each other based on mating-type.

The unrooted phylogeny (**Figure 4.4C**) exhibited a similar distribution of clades. In contrast to the midpoint root tree, the unrooted gene did not form two large, discrete clusters; however, the tree could still be divided into two hemispheres and each contained clades representing a single one of the two mating-type genes (**Figure 4.4C**). Despite the absence of two large caldes, within the subclades, I observed a very similar pattern of clustering based on the gene's locus gene content. This is again especially evident when considering the expanded loci of *Rhizopus* spp. that contained an *arbA* gene (green leaves, **Figure 4.4B**). The midpoint rooted tree may coerce the distinct clustering of the two mating-type genes. Since the unrooted tree has a similar topology to the midpoint rooted tree, the protein sequences of the mating-type genes may be diverged enough to be phylogenetically informative. The most likely explanation for these patterns is that the mating-type genes have evolved with speciation events. To investigate this phenomenon, I used the representative species tree (**Figure 4.3**) to generate tanglegrams (**Figure 4.5**). When the SexP gene tree is tangled with the representative species tree, there were fewer cross-links, which may suggest higher similarity between the two trees (**Figure 4.5A**). This contrasts with the SexM tanglegram, where there were more crosslinks, suggesting branching order between the two trees is incongruent (**Figure 4.5B**).

An alternative approach to assess similarity between the species tree and the mating-type gene trees was to process the phylogenies with phylo.io [217]. Rather than linking tips as in the tanglegrams, it calculates degree of similarity using a Jaccard index variation, which allows for identification of equivalent nodes and taxa. Branches are also colored by similarity (**Figure 4.6**). The species tree was rooted with *U. rammanniana* as before (**Figure 4.6A**). Rather than comparing individual SexP and SexM gene trees as in the tanglegrams (**Figure 4.5**), the unrooted combined SexP-SexM trees (**Figure 4.4C**) were trimmed to include only the taxa shown in the representative species tree (**Figure 4.6B, 4.6C**). As would be expected, the different mating-types of the various species form clades (**Figure 4.6A**). When comparing the branching order to the unrooted SexP-SexM phylogeny, however, any species designated as (-) mating-type seems to be more derived relative to the (+) mating-types (**Figure 4.6B**). The node in the species tree in which the *P. blakesleeanus* lineage splits is denoted with a red square and an asterisk (**Figure 4.6A**). Phylo.io identified an equivalent node in the unrooted tree, where it marks the beginning of the SexM clade (**Figure 4.6B**). Furthermore, the presence of light-colored branches in the unrooted tree indicated very low similarity between the species tree and the gene tree (**Figure 4.6B**). To test if the unrooted tree could be coerced to match the branching order of the species tree, the *U. ramanniana* SexM protein was set as the outgroup in a rooted SexP-SexM tree (**Figure 4.6C**). The topology of the tree changed such that there were two major clades each representing one of the mating-type genes. Within each of these clades, the branching order and subclades resembled the species tree more closely; however, the branch colors did not change as much (**Figure 4.6C**).

Discussion

Here, I identified the mating-type loci of 427 isolates of Mucoromycotina, representing 138 unique species. After identifying the genomic locus, the sequences were used to predict proteins which were further assessed with Hidden Markov Models. This approach was generally robust, given that identity of the DNA sequence to the proteins of *P. blakesleeanus* were significantly higher in the HMMer-verified proteins compared to those that were off-target hits. This relationship was not significant for the actual mating-type genes, but was observed in the genes that flank them. This facilitated identification by using the flanking genes (*rnhA, arbA, glrA, tptA*) as genomic landmarks. However, not every species had these specific flanking genes. Previous studies that have attempted large-scale identification of this locus with different approaches also uncovered this gene content variability, especially in the clade that includes species of *Lichtheimia* [131]. At the genus level, there was no clear phylogenetic distribution of the 10 locus variants, given that variations existed at the species level. However, by considering the distribution of the variants within a genus, we can hypothesize about a consensus locus for the genus. One caveat, though, is that species that have been assigned to a particular genus may not actually belong to the genus. That is, some species may be misidentified in culture collections, and when shown in the species phylogeny, may not actually end up in a clade with other species of the same name.

One way to attempt to address these discrepancies was to measure the length of the mating-type loci across all sampled species. The lengths would serve as a proxy for gene content, meaning that if a locus had more genes, then it would be longer. Additionally, species of the same genus should have similar mating-type locus lengths if they were the same mating-type. Locus lengths were variable across the species tree,

and within-genus lengths were generally consistent. One species of *Rhizomucor pusillus* was part of the same clade as some *Phycomyces spp.* isolates. A separate clade of *R. pusillus* was identified as more basal relative to the *Phycomyces* clade. The locus lengths of these two *R. pusillus* isolates differed. The *R. pusillus* isolate that clustered with *Phycomcyes spp.* had a locus of a length comparable to the various *Phycomyces* species. Given this observation along with the fact that it does not cluster with the other isolates of the same name, it is likely that this *R. pusillus* isolate was misidentified and is actually a species of *Phycomyces*. It is possible that the lengths of loci may provide clues about taxonomic organization, but further study is warranted as this is speculation. Locus length was not a reliable indicator of gene content. If this were the case, then the *Rhizopus* species complex would feature the longest loci. However, the majority of other species with fewer flanking genes were comparable to the *Rhizopus* species, and 36 other species had much longer loci. Indeed, the mating-type locus of the *R. pusillus* isolate in the *Phycomyces* clade exceeded the length of *Rhizopus* loci by about 2kb. This pattern could be explained by reduced intergenic distances in the *Rhizopus* clades.

When to-scale schematics of the mating-type locus were mapped to a pruned species tree, it becomes evident that the *Rhizopus* species, while having more genes associated with the mating-type locus, the locus itself is compacted when compared to non-Rhizopus groups. In general, the greatest distances between genes were observed in Mucor species where a *glrA* gene was detected. Unlike Rhizopus, where *glrA* was relatively closer to the genes of the mating-type loci, among the Mucors *glrA* was much further away from the locus. Although in Chapter 3, I did not find evidence for differential expression of the flanking genes in *P. blakesleeanus*, I did find enrichment of glutathione metabolic processes associated with the transition from vegetative growth to sexual

reproduction. Additionally, reduced glutathione has been shown to influence whether *Aspergillus nidulans* can begin sexual reproduction [60]. Taken together, it is possible that Rhizopus species are especially sensitive to cellular redox state during sexual reproduction, so their mating-type loci have recruited *glrA* so that it is co-expressed with the mating-type genes during sexual reproduction. Future work on sexual development that focuses on *Rhizopus* species should make use of lanthionine thioether, a non-reducible analogue of glutathione [218]. Unlike *P. blakesleeanus*, Rhizopus sexual reproduction is entirely aerial, with zygophores developing from aerial hyphae [219]. If mating-types of a *Rhizopus* species are crossed on media supplemented with non-reducible sulfur compounds I hypothesize sexual reproduction would not be observed. By extension, if gene expression studies were performed on *Rhizopus* crosses, then the *glrA* of the mating-type locus would exhibit increased expression as the strains transition from vegetative growth to sexual reproduction, much like *P. blakesleeanus*. Since the distance between *glrA* and the bulk of the mating-type locus in *Mucor* spp. Is large and because these lineages are paraphyletic, they could represent transitional species where *glrA* is being recruited to the locus.

Another pattern related to the recruitment of genes to the locus is the observation that the *Phycomyces* clade is the earliest branching lineage where I observed the first 3-gene assembly of the mating-type locus. Lineages that diverged prior to the *Phycomyces* clade tended to either completely lack the four flanking genes targeted here, or they only had *rnhA* near the mating-type gene. Furthermore, the subsequent branching events that come after divergence of the *Phycomyces* clade coincide with the detection of *glrA* in the vicinity of the mating-type locus. Taken together, these data suggest a stepwise assembly of the mating-type locus alongside reduction of intergenic

space. This may also support the hypothesis that the mating-type loci of mucoromycetes and microsporidia are an example of convergent evolution [213], since here there is evidence of the locus evolving within Mucoromycotina.

The inclusion of *arbA* in the *Rhizopus* loci points to an additional *Rhizopus* innovation. The gene encodes a protein with BTB/ankyrin/RCC1 domains and its orientation matches what has been previously reported [132]. Since it is co-oriented with *sexP*, the constitutively active mating-type gene, there is the possibility that it is involved in the mating reaction of (+) mating-types. The presence of ankyrin in the *arbA* gene also points to a role in linking membrane proteins to the cytoskeleton [220]. The orthologues of this gene on FungiDB do not include the RCC1 domain, and instead suggest that this protein is involved in mediating interactions with ubiquitin and its substrate [144]. The *P. blakesleeanus* orthologue of *arbA* (PHYBL_149462), was also differentially expressed in chapter 3 and was coregulated with genes in the transition from vegetative to sexual development. In mice, a protein containing both BTB and RCC1 domains localizes to the acrosome of sperm cells. The acrosome facilitates fusion with oocytes during fertilization, and the mouse RC/BTB2 protein is thought to be involved in trafficking proteins to the acrosome during spermiogenesis [221]. I speculate about the possibility of ArbA functioning to recruit digestive enzymes to the progametangia preceding cell fusion during sexual development.

The mating-type locus appears to have evolved as a unit that follows speciation within the subphylum. Focusing just on the representative species, I observed that each mating-type gene is variable in length at the DNA level and the protein level. The SexP DNA sequence was generally longer than the SeM sequence. The protein sequences appeared less variable between mating-types of the same species, but overall SexP was

still longer. In *P. blakesleeanus*, the *sexP* locus is longer due to the presence of small repetitive elements [113]. These repetitive elements are direct repeats and mitotic recombination is believed to be capable of deleting large regions of the locus which would lead to sterility [113]. While I did not probe the *sexP* sequences for repetitive elements, the fact that *sexP* of other species is consistently longer than the *sexM* counterpart suggests that these repetitive elements may exist in all *sexP* DNA sequences. Further study is needed to identify the presence of these repetitive elements in other Mucoromycotina lineages. Additionally, population genetics approaches would help to identify if recombination is arrested at the mating-type loci.

After aligning the protein sequences of both SexP and SexM, the resulting trees had two large clades encompassing one or the other mating-type gene. The midpoint rooted tree was essentially coerced into generating the two clades, but when compared to an unrooted tree, a very similar, though not exact, distribution is observed. This suggests that the protein sequences are diverged enough as to be able to be distinguishable. In both of these trees, the mating-type proteins seem to cluster by species after they cluster by sequence similarity. Separating the unrooted gene tree into individual gene trees for each mating-type gene allowed me to compare tree congruence between the gene trees and the species tree. Tanglegrams pointed at differences between the gene trees and the representative species tree. Notably, the SexM tree exhibited a higher number of tip links which are generally interpreted as a higher level of tree incongruence. Certainly when the various clades are compared visually, their position in the gene tree does not seem to match the position in the species tree. One example is the *Rhizopus* clade, which in the species tree is the most derived clade, that is, it is nested within other clades. However, the *Rhizopus* clade in the SexM tree is

sister to a group which diverged earlier in the species tree. A different comparison of the trees highlighted differences in branching order. Rather than using the individual SexP or SexM trees, the unrooted combined tree was compared to the species tree. The unrooted gene tree seemed to match the topology of the species tree when looking at one or the other mating-type clades. However, the clade composed of SexM species appeared to be nested within the SexP tree. This could mean that SexP resembles the ancestral mating-type gene and that SexM evolved from SexP. Certainly the fact that each of these genes experiences differential regulation and expression points to distinct evolutionary constraints. SexP localities to mitochondria and the cytoplasm whereas SexM, which is expressed only during mating and localizes to nuclei [120,173]. Additionally, prior to sequencing technology, mating-types were identified by crossing isolates with a tester strain, often of a different species. Tester strains and the unknown mating-type strains could initiate sexual reproduction, but the mating reactions are not completed. This cross-reactivity could be dependent on SexP acting as the master regulator of initiation of sexual reproduction, whereas SexM would only be activated if the mating was between members of the same species.

Methods

Locus Identification

Translated searches with tfastx [222] were performed using protein sequences of RnhA (JGI: PhyblUBC21 1878835), SexP (GenBank: ABX27912.1), SexM (GenBank: ABX27909.1), and TptA (GenBank: ABX27908.1) from *P. blakesleeanus* as well as GlrA (GenBank: CEG66502.1) from *Rhizopus microsporus* and ArbA (GenBank: AWD37088.1) from *R. stolonifer*. Scaffolds with a hit for SexP or SexM were subsetted to

include the candidate locus plus 100 bp on either end using bedtools [223]. Species where SexP or SexM were not detected were not included in later steps of the analysis. Species that had a sex gene were further analyzed by exonerate [224] in order to predict protein sequences of candidate locus genes. Exonerate produced DNA coding sequences which were translated by emboss [225]. After obtaining protein sequences of candidate loci, those with the lowest e-values in the tfastx search and the highest percent identities were used to build HMMer profiles of the locus. HMMer was run on the exonerate predicted proteins to verify the identities of these candidates. Loci that were supported by all three search strategies were considered putative candidates and used for the characterization analyses presented here. Where multiple strains of the same species were available, the loci variants were inspected and consensus loci were determined based on frequency of locus variant within species (compare evolutionarily related species to each other and if a strain's locus is very different from sister taxa, it was flagged and removed from main analysis). Plots of locus distribution among genera and locus length were generated with ggplot2. The implementation of this workflow can be accessed in https://github.com/stajichlab/EvoDevo_of_Mucoromycotina.

Phylogenetic analyses

The species tree was generated by J. Stajich. For gene trees, the exonerate predicted HMMer verified SexP and SexM proteins were aligned with muscle [226] then refined using the -refine option on the initial alignment. All trees presented here were generated with FastTree [227]. Tanglegrams were generated with phytools [228]. Analyses of tree topology were done with phylo.io [217]. Selection of representative species for the representative species trees was based on the distribution of mating types within genera of the species tree, the prevalence of locus variants, and support from manual inspection

of hits. The R packages ape and ggtree were used to manipulate phylogenies and plot them alongside other data [229,230]. The phylogenetic tree with locus arrangements was generated with ggplot2. R scripts are also available in the repository https://github.com/stajichlab/EvoDevo_of_Mucoromycotina.

Chapter 5: Conclusion

In this dissertation, I presented work that begins to address the molecular mechanisms involved in sexual reproduction in fungi of the subphylum Mucoromycotina. By profiling the transcriptome of *P. blakesleeanus*, I identified differentially expressed genes that correlated with differentiated cell types during vegetative growth and sexual reproduction. Some of the differentially expressed genes had been characterized in other work, which lends support to the design of this experiment. The presence of nitrogen starvation response genes, while unsurprising giving culturing conditions, also supports the idea of deep homology in fungi. That is, not only does nitrogen limitation trigger sexual reproduction in diverse fungal groups, but some of the genes involved in this response are also conserved in early-diverging lineages. Follow up studies should test the effect of diverse nitrogen sources on both vegetative growth and sexual reproduction in *P. blakesleeanus*.

Genes associated with the transition from vegetative growth to sexual reproduction, in particular glutathione metabolic genes, are also conserved in other fungal species and play a role in transitioning into the sexual development state. Once mating-types have transitioned to sexual interactions, a different suite of genes are coexpressed with the mating-type genes. Orthologues of phospholipase D1, which is involved in pheromone detection and plays a role in mediating fusion between hyphae, as well as CDC24 and Ste-20, which imbue polarity, are highly expressed during the initial stages of interaction between the *P. blakesleeanus* mating-types. This presents a scenario in which trisporic acids and the mating-type genes mediate fusion of progametangia. As gametangia become suspensor cells and the zygospore is formed,

there is increased expression of genes involved in chitin synthesis, trehalose synthesis, and peroxisome organization. The presence of these genes helps to explain how zygospores enter dormancy after they mature. Furthermore, an orthologue of CDC1p may have roles in recombination, anchoring trehalases to the cell wall, and guiding inheritance of organelles. The precise roles of these genes during the mucoromycete sexual cycle remain an open question.

The transition from asexual development to sexual reproduction in *P. blakesleeanus* is characterized by cell differentiation in response to a nearby compatible mating partner. Observing zygophores, the first differentiated cells of the sexual cycle, requires the use of culture slides - a microscope slide with a thin layer of agar or gelatin gelled medium. In combination with time-lapse microscopy, culture slides would aid in direct observation of the differentiation process while providing temporal and spatial metrics related to this transformation. Other sexual development morphological transitions could also be documented, but the subsequent structures are 3-dimensional and would require frequent focus adjustments. In order to identify genes involved in the first differentiation, it will be important to characterize the timing of this change.

The presence of CDC1p at the later stage of sexual development was particularly striking given its possible role in organelle inheritance. The mating-types of *P. blakesleeanus* have been shown to exhibit distinct functions with respect to sexual reproduction. Notably, each mating-type produces distinct precursors to the mating pheromone which are exchanged between partners to convert them to trisporic acid. Furthermore, mitochondrial inheritance is uniparental and determined by mating-type. Combined with the additional observation that *sexP* is always expressed while *sexM* is only expressed during sexual reproduction, I hypothesized that even under vegetative

growth, the mating-type genes may play a role in regulating non-sexual genes. That is, each mating-type may have specialized roles outside of sexual reproduction that is determined by the SexP master regulator. Other specializations downstream of the mating-type gene could relate to mating priming of the (-) strain by the accumulation of β-carotene to rapidly respond when in proximity to a compatible mating-partner. While the (+) strain has SexP being expressed, it downregulates production of β-carotene but upregulates genes involved in *de novo* purine synthesis and branched chain amino acid synthesis to set up the machinery for DNA synthesis and cell division. One way to test for proliferation is to treat each mating-type strain with BrdU and measure fluorescence as a proxy for DNA synthesis. Higher fluorescence in the (+) mating-type would indicate a higher rate of DNA synthesis and support the idea that these strains prioritize different biosynthetic processes. In future work, environmental cues should also be tested to determine the role of mating-type on ecological roles. Much of the literature on *P. blaeksleeanus* focuses on its phototrophic responses, including more study of genes induced or repressed between the two mating-types in the absence of light will provide additional understanding in innate differences in gene expression wiring in strains of different mating types. This study would also be enhanced by population genetics studies to compare allelic variation between multiple mating-types as not all strains undergo rapid mating even in the presence of compatible partners.

While behavior of the *P. blakesleeanus* sporangiophore has been the subject of sensory biology studies, other work seeking to elucidate differences in mating-types should consider the behavior of mycelia. Vegetative hyphae of *R. stolonifer* exhibit branching exploratory behavior when grown in microfluidic chamber mazes [231]. The strain used in the Fungal Olympics study was identified as a (+) mating-type in chapter

4. Since *P. blakesleeanus* mating-types appear to be optimized for a particular form of growth, it is possible that a comparison of their hyphal exploratory habits could uncover another dimorphic trait. I hypothesize that since the (+) mating-type has upregulated sets of genes that promote vegetative growth, that it would exhibit a higher degree of branching exploration than the (-) mating-type. Another behavioral trait that can be tested in the context of sexual reproduction is gravitropsim. In chapter 3, I detected the gene encoding OCTIN as differentially expressed and associated with the stage of mating where I first observed aerial sexual structures. A simple assay to explore the effect of gravity on the generation of aerial zygophores and subsequent structures would be to cross strains on plates that are turned upside down or sideways at around 2 days post inoculation, when zygophores first begin to differentiate but before they take on the aerial characteristic.

The mating-type genes of Mucoromycotina may have transcription factor activity and likely participate in regulating multiple gene expression cascades during sexual reproduction and vegetative development. The locus where these genes are encoded was thought to be syntenic across the entire subphylum. Using a combination of protein vs. nucleic acid searches, protein prediction, and Hidden Markov Models, I have increased the number of characterized mating-type loci of mucoromycetes. Amplicon sequencing should be performed to verify the presence of these genes in those particular loci, however. Contrary to the original hypothesis that all mucoromycetes would exhibit a great degree of conservation of gene content and organization, I found that not all mating-type loci harbor the same flanking genes. This variation in gene content of the locus, when mapped to a species tree, also reveals the stepwise assembly of the locus. As mucoromycetes evolved, each lineage recruited an additional

flank gene before diverging. This fits with the model of sex chromosome evolution and suggests that the mating-type loci may be on the trajectory towards becoming sex chromosomes. Indeed the recruitment of *glrA* to the *Rhizopus* loci, combined with the observation that this gene is differentially expressed during *P. blakesleeanus* mating, further supports the idea of mating-related genes becoming linked, as has been observed in some basidiomycetes. Besides the evolution of the locus, I also looked at the evolution of the individual mating-type genes and found that the SexP gene tree is congruent with the species tree, while the SexM gene tree is less congruent. This suggests that SexP resembles the ancestral cell identity gene in this lineage and that SexM may be species specific. Again, when considering that these two genes are differentially expressed during sexual reproduction and vegetative growth highlights the fact that they are each under distinct evolutionary constraints. Future work that characterizes the genes of mating-type loci should focus on identifying targets of the SexP and SexM transcription factors. Additionally, gene expression studies with *Rhizopus* grown on media with non-reducible sulfur sources, such as lanthionine thioether, could elucidate the significance of recruitment of glutathione reductase to the locus.

Figures

Summary of fungal lineages and their sexual reproduction

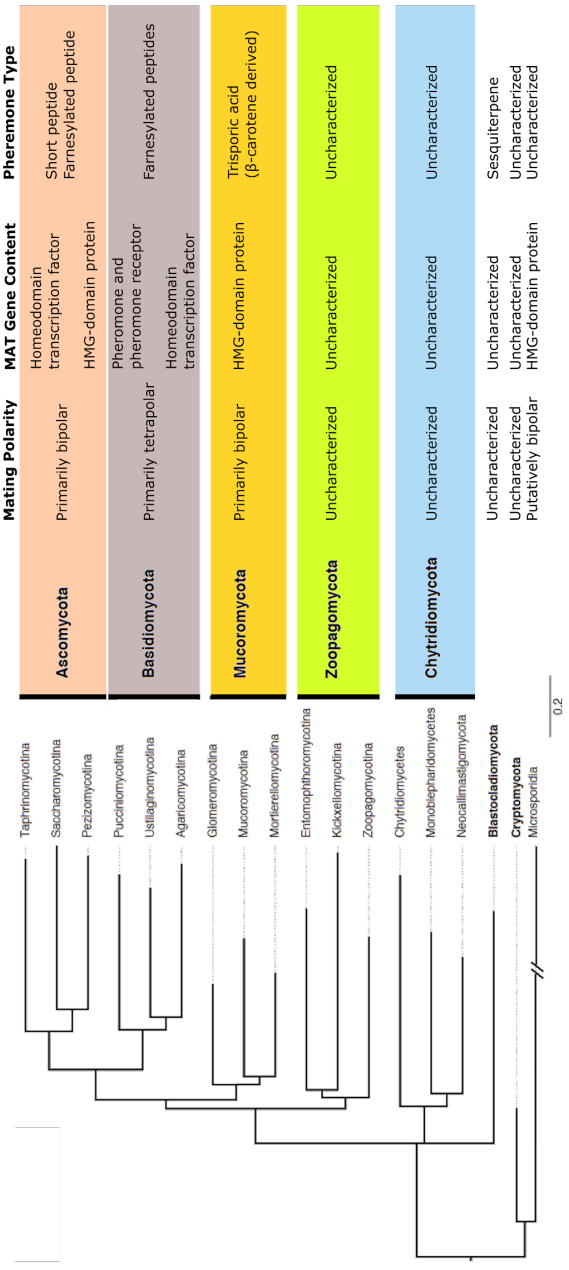

Figure 1.1. Summary of sexual reproduction strategies across king Phylogeny adapted from [232]] with permission.

Chapter 2: Mating-type Biased Gene Expression in *Phycomyces blakesleeanus*

A

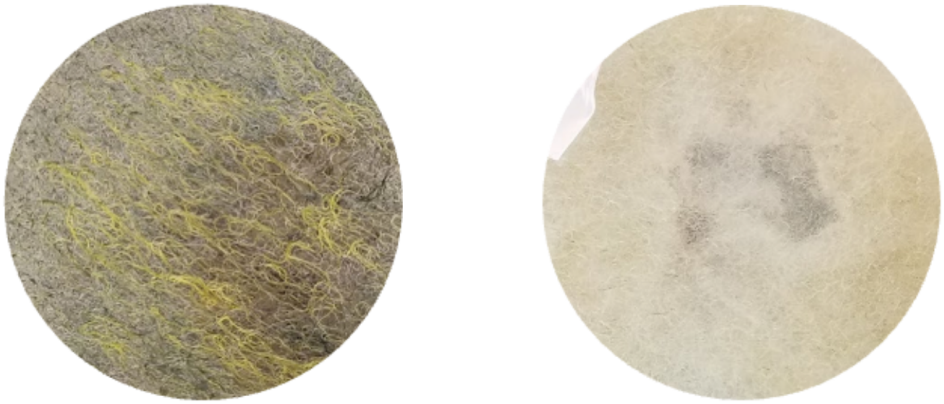

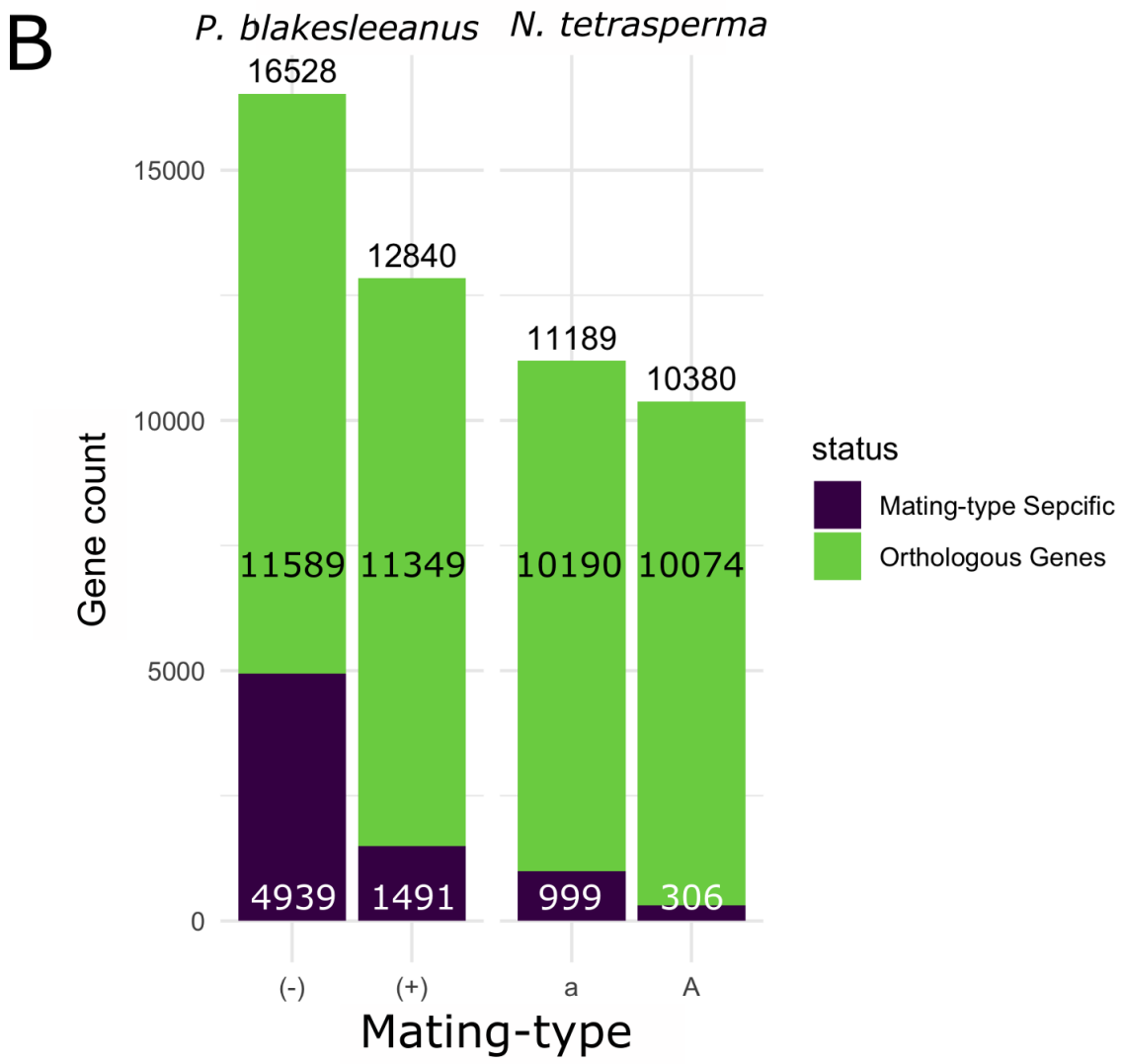
B
P. blakesleeanus
N. tetrasperma
16528
12840
11189
10380
15000
10000
5000
0
Gene count
11589
11349
10190
10074
4939
1491
999
306
(-)
(+)
a
A
Mating-type
status
Mating-type Sepcific
Orthologous Genes

C

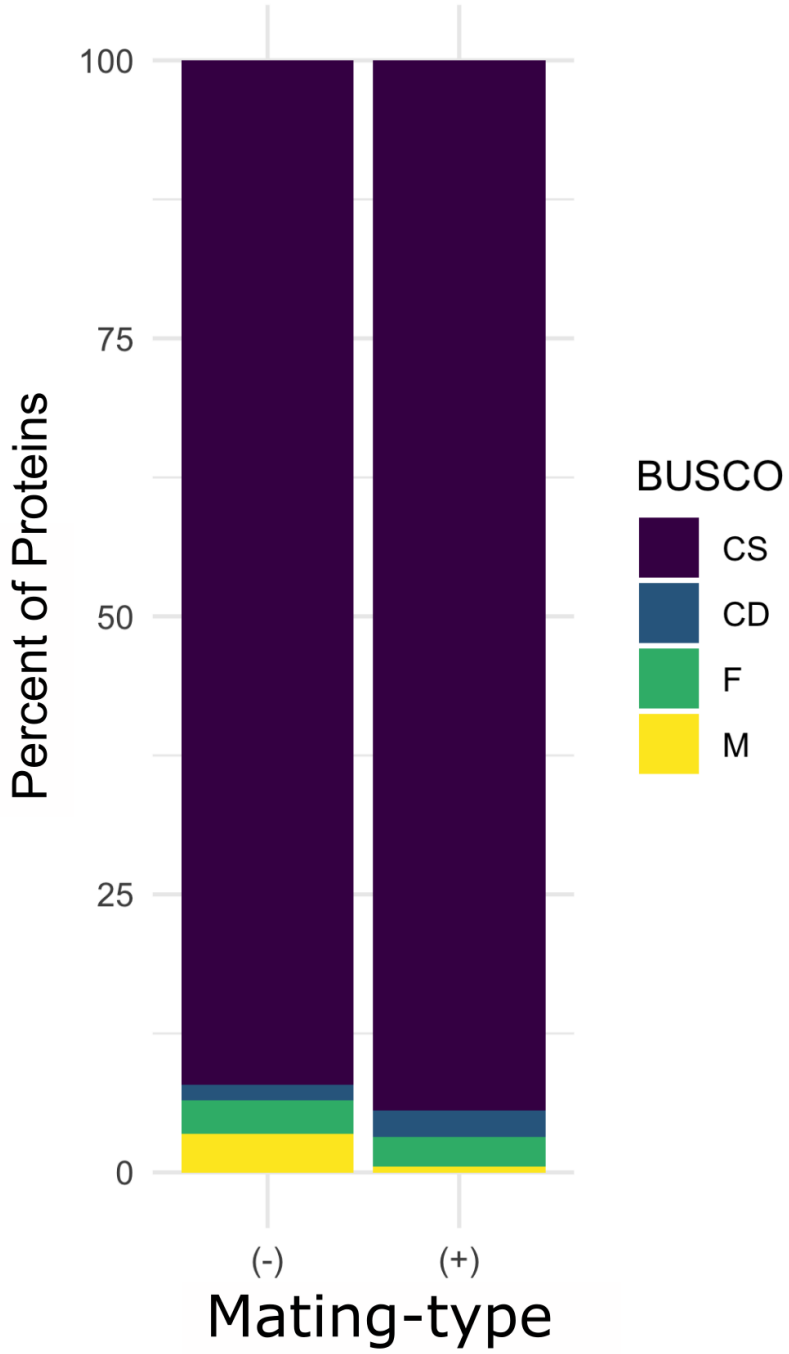

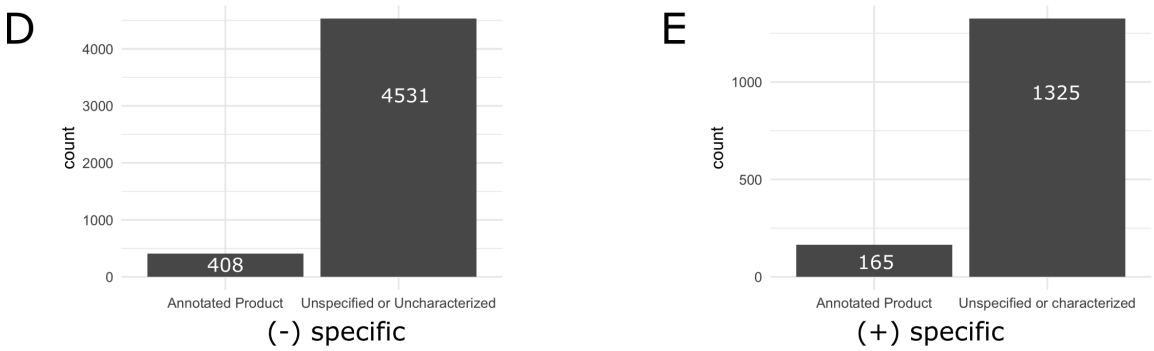

Figure 2.1. Comparison of (-) and (+) *P. blakesleeanus* mating-types. Phenotypic differences between the two mating types (A) were apparent despite all growing conditions being equal. A genetic basis for these differences could first be accounted for by a difference in genetic background, given that the number of orthologues between both mating-types is different (B). Despite orthology differences, BUSCO analysis indicates that both mating-types have comparable amounts of conserved genes (C). Genes for which an orthologue was not found in the opposite mating-type were largely uncharacterized, unspecified, or hypothetical proteins (D,E).

A

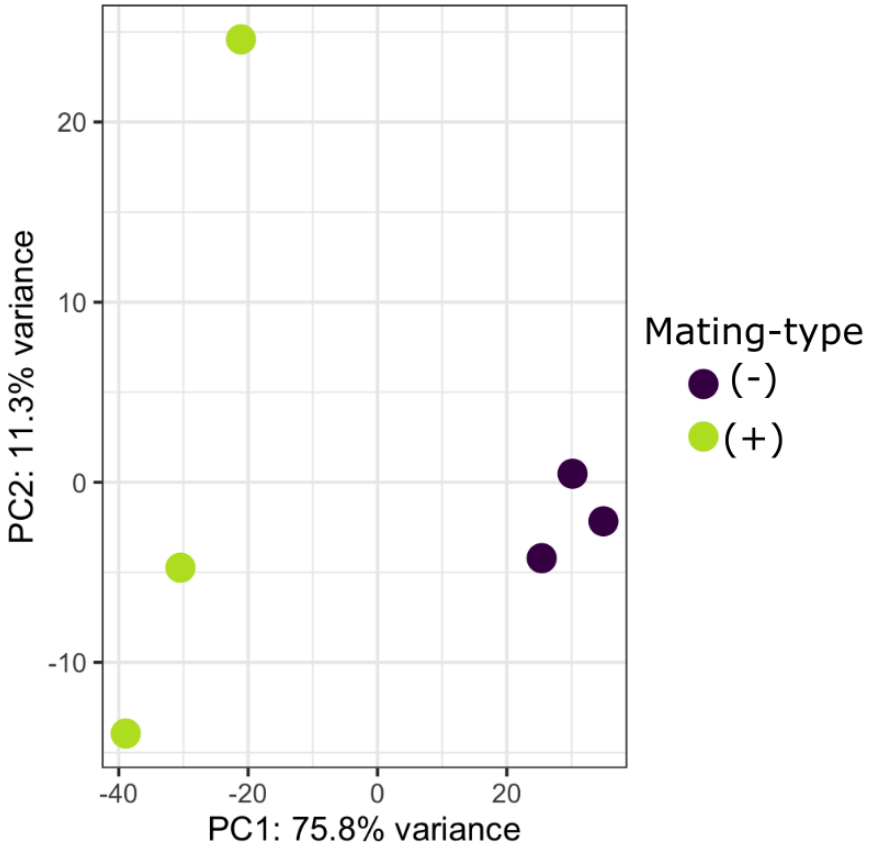
20
10
0
-10
PC2: 11.3% variance
-40
-20
0
20
PC1: 75.8% variance
Mating-type
(-)
(+)

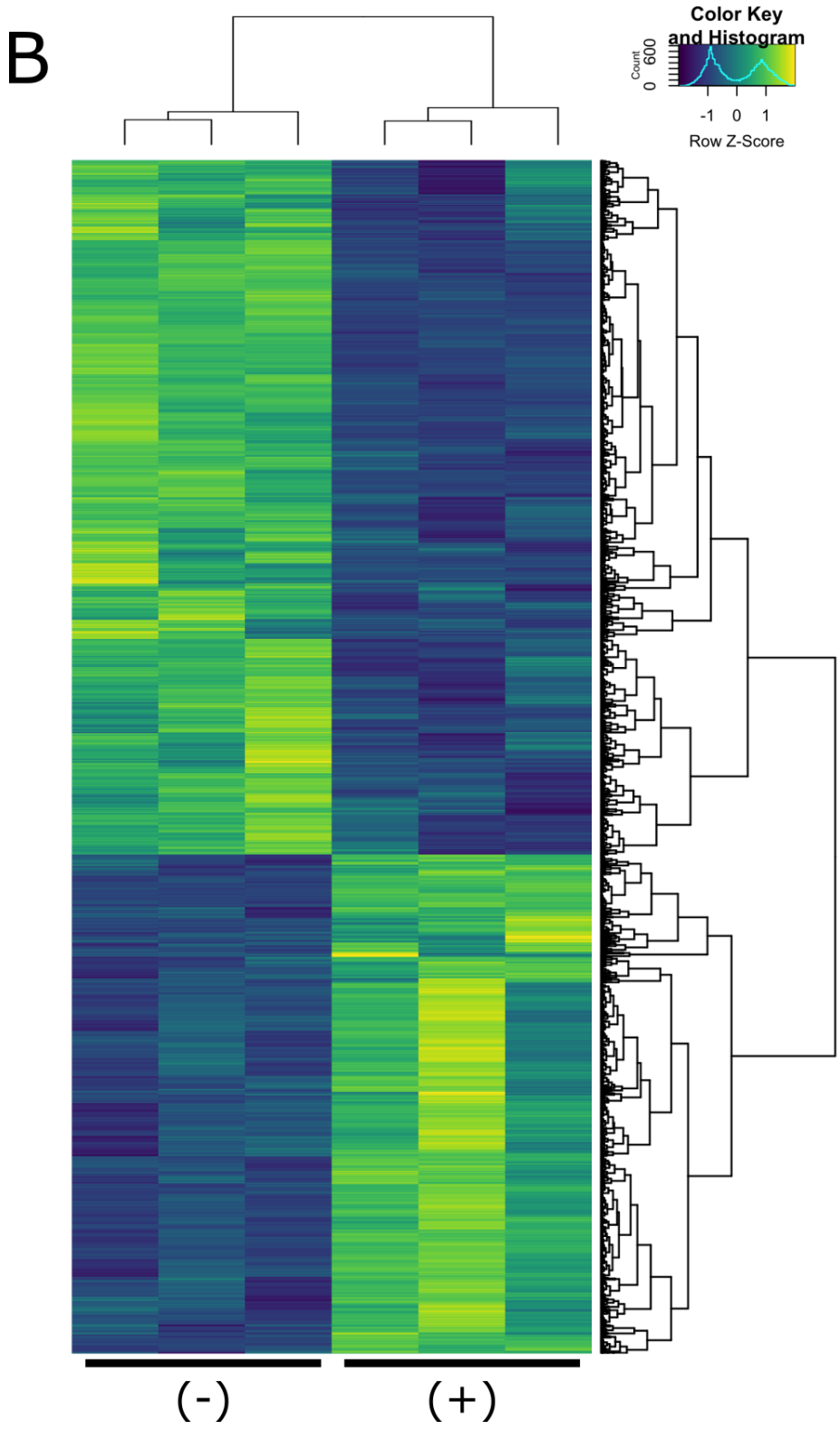
B
Color Key
and Histogram
Count
0
600
-1
0
1
Row Z-Score
(-)
(+)

C

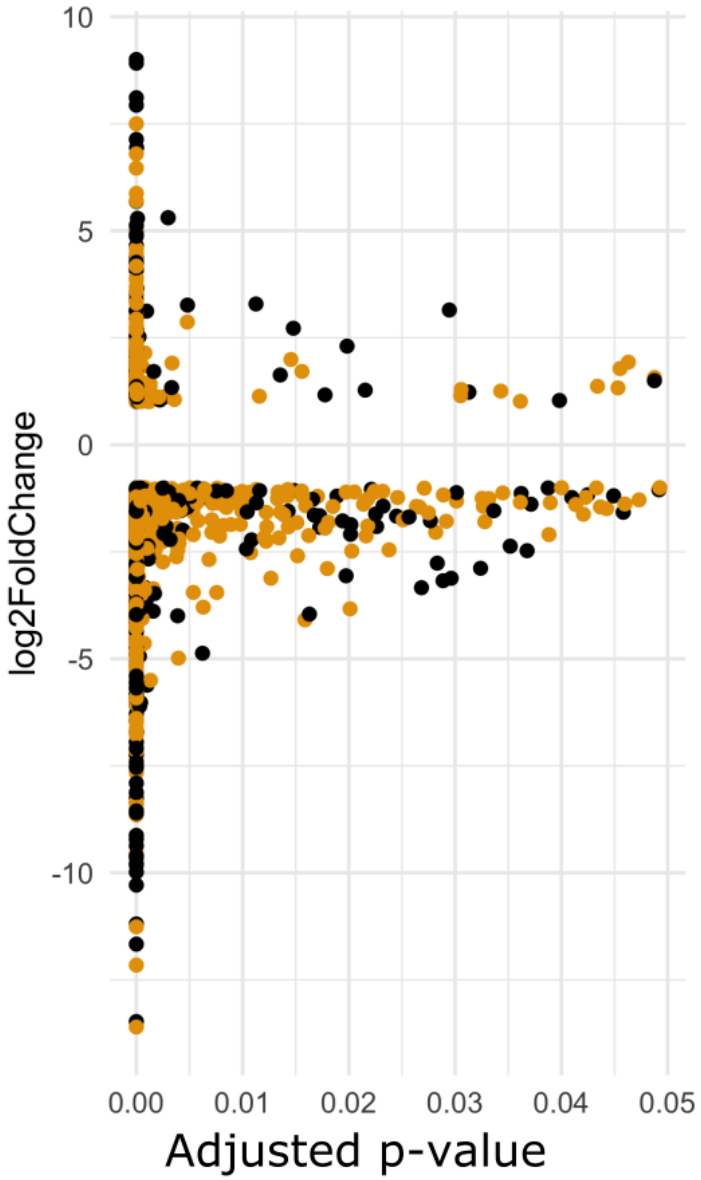

Figure 2.2. Summary of differential gene expression analysis. Replicates cluster by mating-type along PC1 (A). Despite one (+) mating-type not clustering tightly along PC2, Spearmann correlation hierarchical clustering places it with other replicates of the same mating type (B). Some variation in expression can be observed between replicates but may be accounted for by tissue heterogeneity. Genes identified as orthologues between the two mating types were observed among the differentially expressed genes (C) and a subset of these were single copy (orange). A majority of these orthologous genes were downregulated.

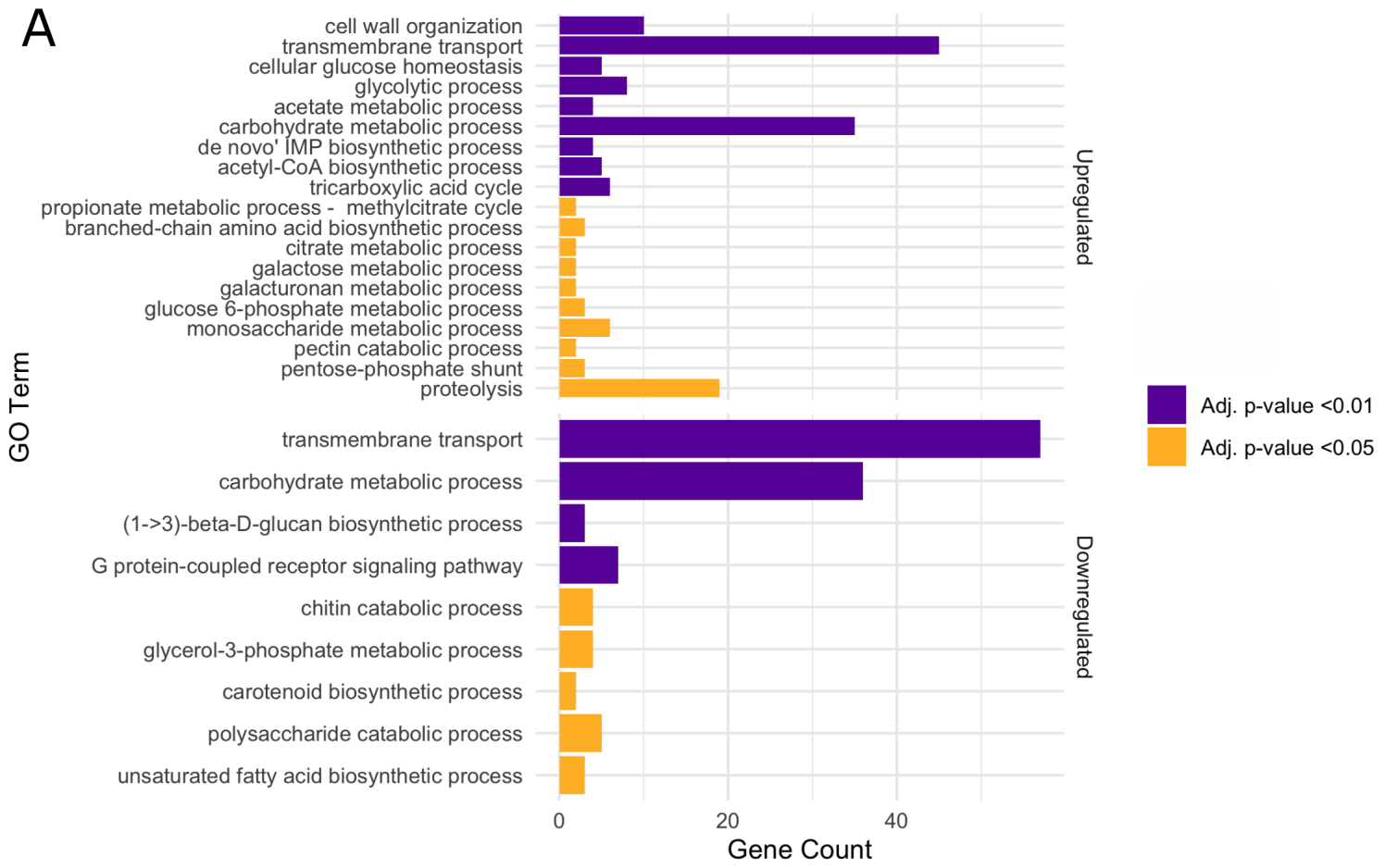
A
cell wall organization
transmembrane transport
cellular glucose homeostasis
glycolytic process
acetate metabolic process
carbohydrate metabolic process
de novo' IMP biosynthetic process
acetyl-CoA biosynthetic process
tricarboxylic acid cycle
propionate metabolic process - methylcitrate cycle
branched-chain amino acid biosynthetic process
citrate metabolic process
galactose metabolic process
galacturonan metabolic process
glucose 6-phosphate metabolic process
monosaccharide metabolic process
pectin catabolic process
pentose-phosphate shunt
proteolysis
transmembrane transport
carbohydrate metabolic process
(1->3)-beta-D-glucan biosynthetic process
G protein-coupled receptor signaling pathway
chitin catabolic process
glycerol-3-phosphate metabolic process
carotenoid biosynthetic process
polysaccharide catabolic process
unsaturated fatty acid biosynthetic process
GO Term
Upregulated
Downregulated
0
20
40
Gene Count
Adj. p-value <0.01
Adj. p-value <0.05

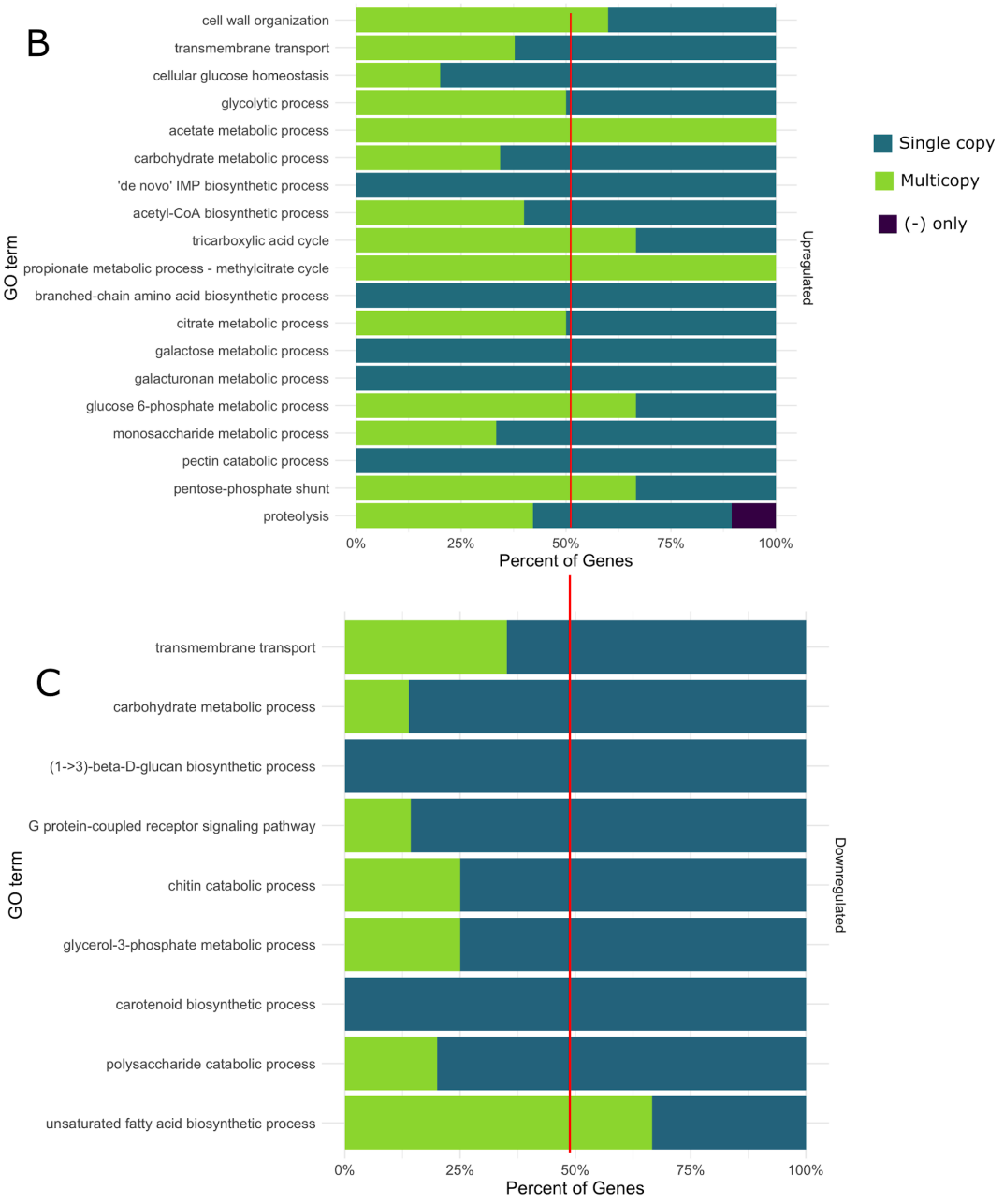

Figure 2.3. GO enrichment analysis of differentially expressed genes between mating-types of *P. blakesleeanus*. A total of 28 GO terms were significantly enriched (A) and were associated with a variable number of differentially expressed genes. The terms Transmembrane transport and Carbohydrate metabolic process were enriched in both upregulated and downregulated sets of genes. The enriched terms had varying numbers of multicopy and single-copy orthologues between the two mating-types (B, C). The ratio of multicopy to single copy orthologues varied more among the upregulated genes (B), whereas downregulated GO terms had much higher proportions of single-copy orthologues (C)

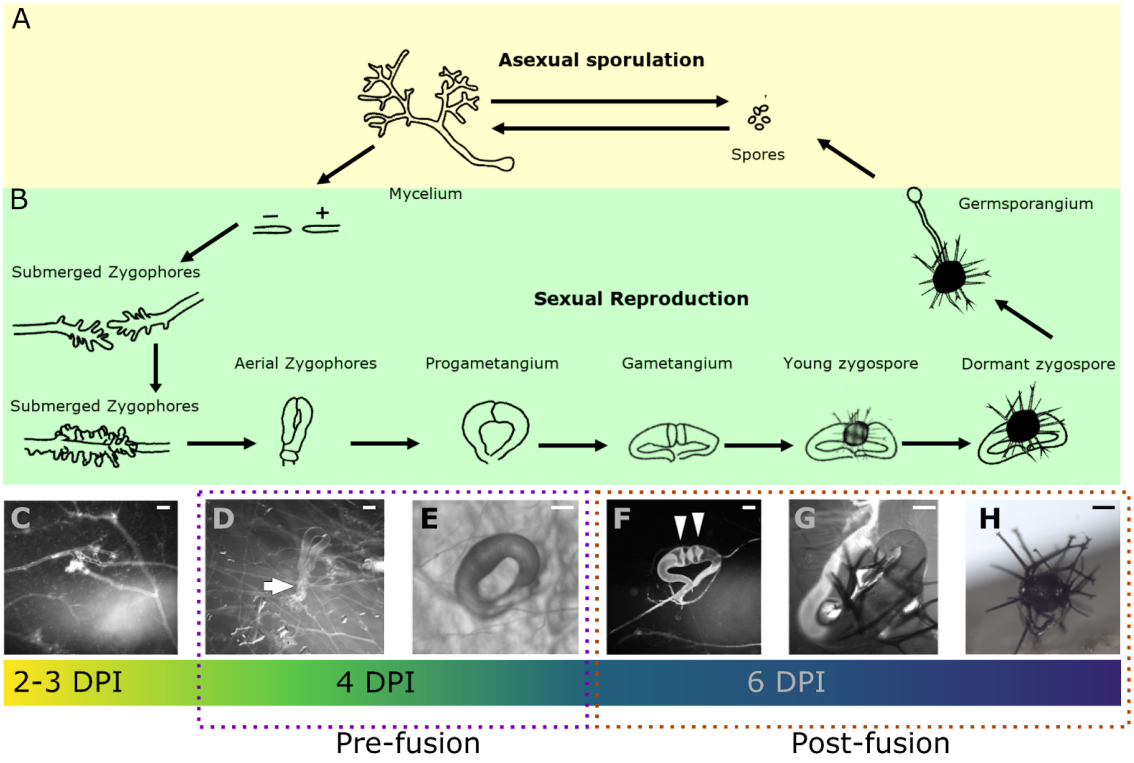

Figure 3.1. Reproductive cycles of *P. blakesleeanus* and associated structures. Cytology of asexual (A) and sexual (B) reproduction has been well-characterized in *P. blakesleeanus* (adapted from [33]. Sexual reproduction is semi-synchronous, in that no specific time point shows only one particular structure, rather certain structures are more prevalent at specific timepoints than others (gradient). Zygophores (C) are the earliest structure to differentiate and do so within the substrate. After zygophores make contact, they become aerial (D) and have coralloid swelling at the base (arrow); after this stage, the remaining structures occur above the substrate. The zygophores form ringlike progametangia prior to fusion at the tips (E). The presence of gametangia (F) indicates the onset of cell fusion. At this stage, adventitious septa can also be observed (arrowheads). As the zygospore develops, the apical cell walls dissolve. Thorn-like appendages develop on the suspensor cells. Sexual reproduction culminates in the production of a pigmented, dormant zygospore (H). The dotted boxes highlight the structures observed at the two stages of mating that were sampled. DPI= days post inoculation; Scale bars = 100 μm.

A

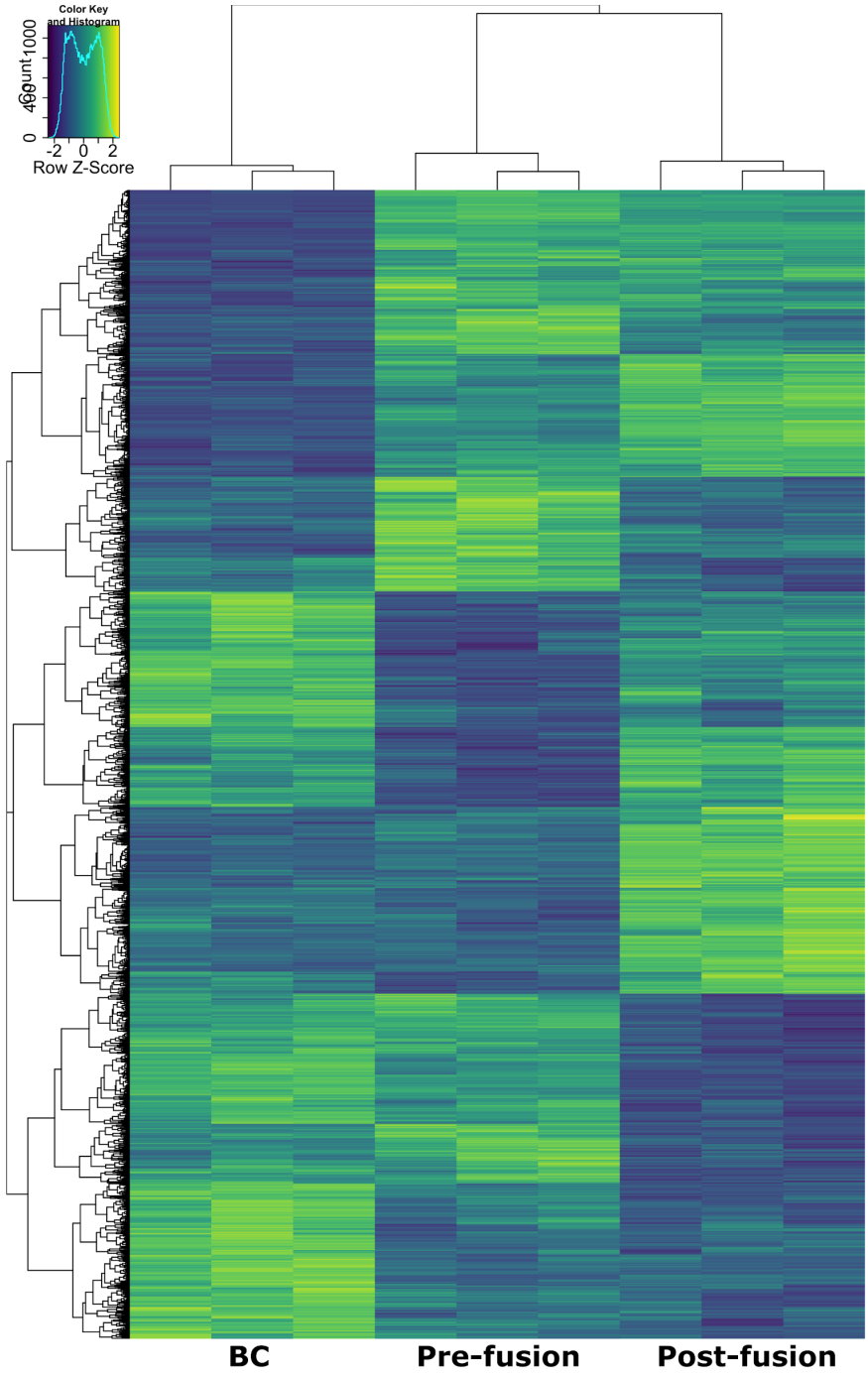
Color Key and Histogram
Count
0
500
1000
-2
0
2
Row Z-Score
BC
Pre-fusion
Post-fusion

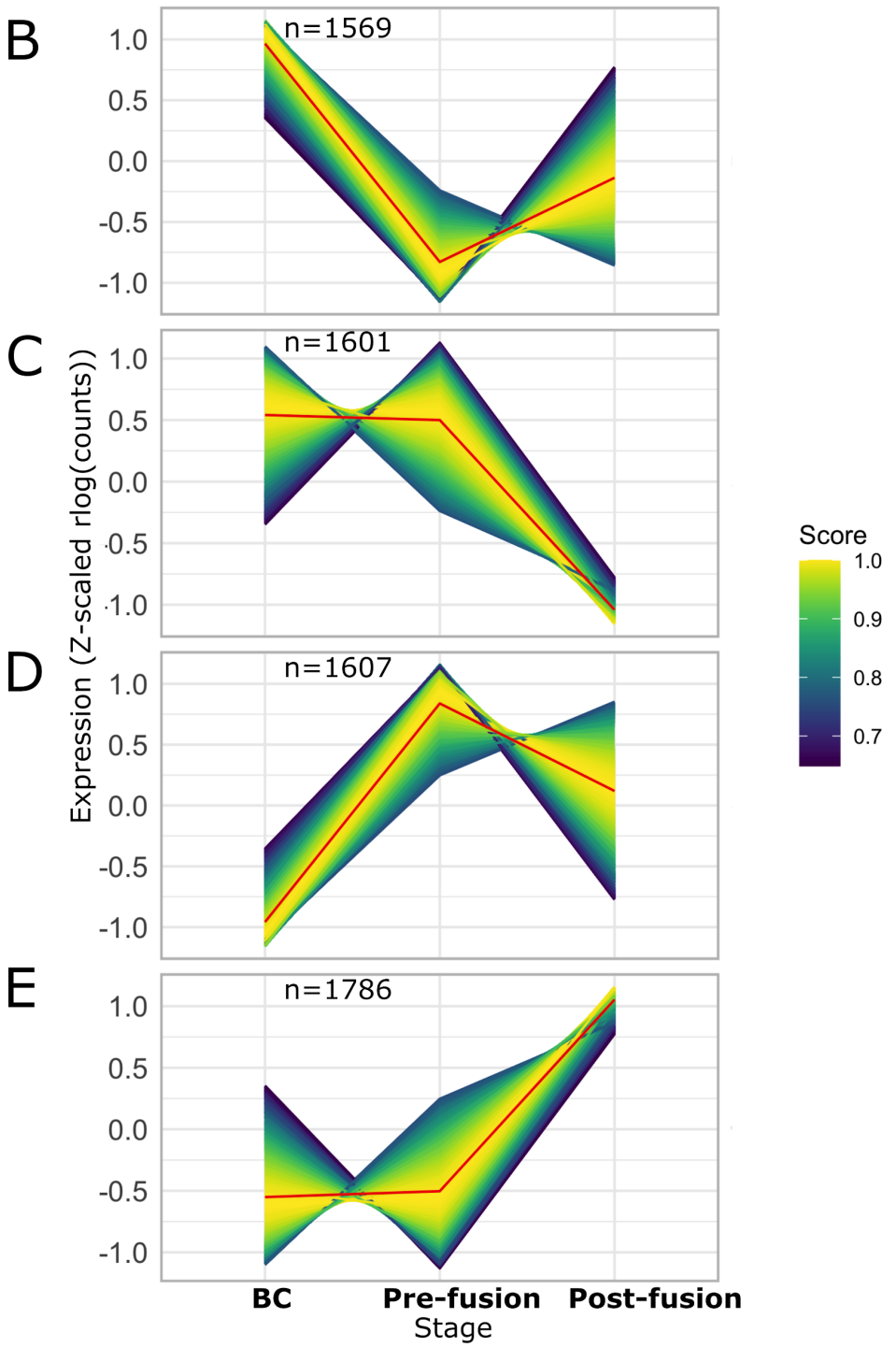
B
C
D
E
n=1569
n=1601
n=1607
n=1786
1.0
0.5
0.0
-0.5
-1.0
Expression (Z-scaled rlog(counts))
Score
1.0
0.9
0.8
0.7
BC
Pre-fusion
Post-fusion
Stage

Figure 3.2. Gene expression profiles of *Phycomyces blakesleeanus* during mating. (A) Hierarchical clustering of genes (rows) and samples (columns). K-means clustered expression profiles (B-E). Three of the expression profiles (B,D,E) show the highest expression at one of the sampled stages. The fourth profile (C) contains genes that have high expression in the first two stages, but downregulated at the onset of cell fusion. K-means cluster centroids are plotted in red. Genes in each cluster are plotted and colored based on their Pearson correlation to the centroid. The total number of genes within each cluster is shown at the top of each plot. Expression values are normalized and regularized log transformed counts which were then Z-scaled for visualization. BC: before crossing.

A

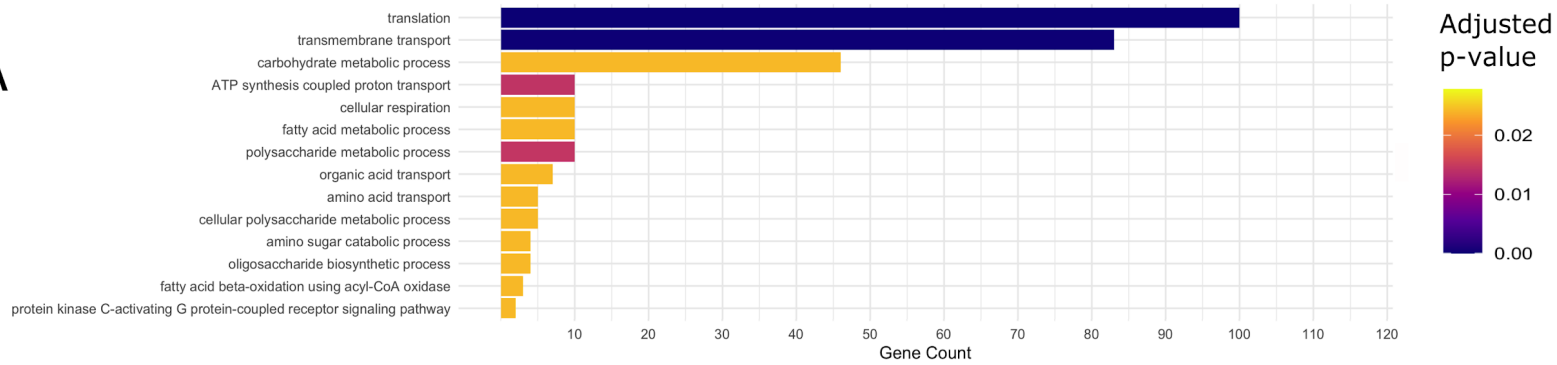
translation
transmembrane transport
carbohydrate metabolic process
ATP synthesis coupled proton transport
cellular respiration
fatty acid metabolic process
polysaccharide metabolic process
organic acid transport
amino acid transport
cellular polysaccharide metabolic process
amino sugar catabolic process
oligosaccharide biosynthetic process
fatty acid beta-oxidation using acyl-CoA oxidase
protein kinase C-activating G protein-coupled receptor signaling pathway
10
20
30
40
50
60
70
80
90
100
110
120
Gene Count
Adjusted p-value
0.02
0.01
0.00

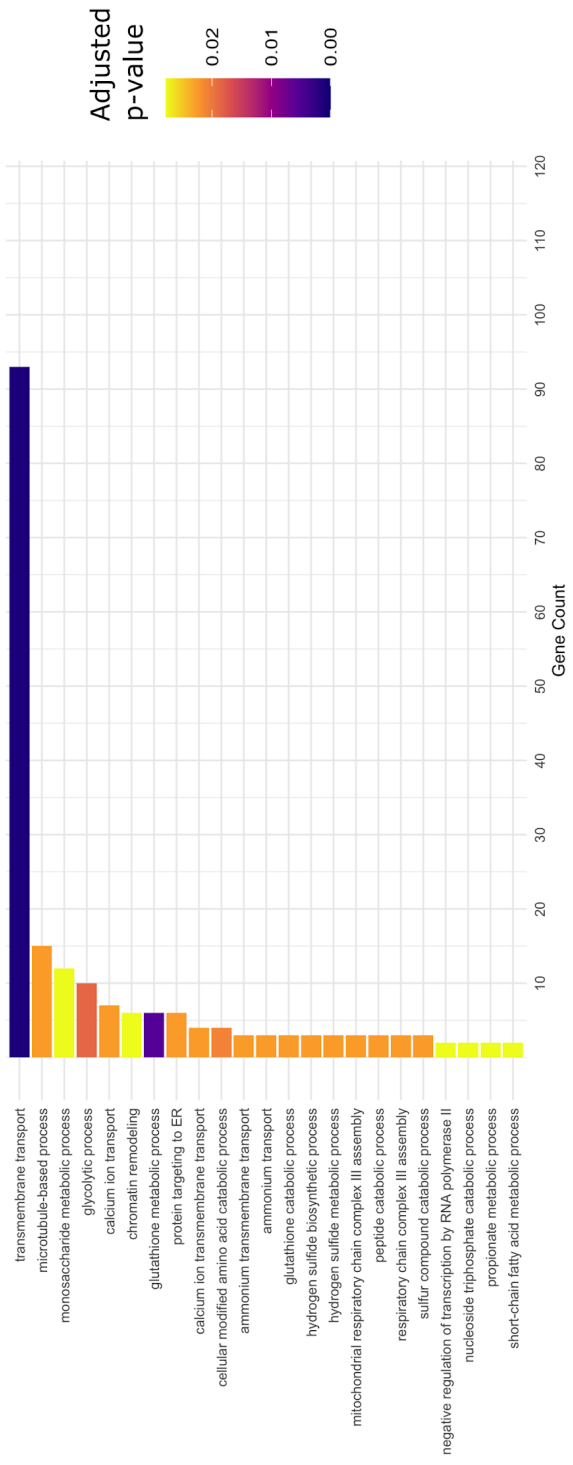
Adjusted
p-value
0.02
0.01
0.00
Gene Count
10
20
30
40
50
60
70
80
90
100
110
120
transmembrane transport
microtubule-based process
monosaccharide metabolic process
glycolytic process
calcium ion transport
chromatin remodeling
glutathione metabolic process
protein targeting to ER
calcium ion transmembrane transport
cellular modified amino acid catabolic process
ammonium transmembrane transport
ammonium transport
glutathione catabolic process
hydrogen sulfide biosynthetic process
hydrogen sulfide metabolic process
mitochondrial respiratory chain complex III assembly
peptide catabolic process
respiratory chain complex III assembly
sulfur compound catabolic process
negative regulation of transcription by RNA polymerase II
nucleoside triphosphate catabolic process
propionate metabolic process
short-chain fatty acid metabolic process

B

C

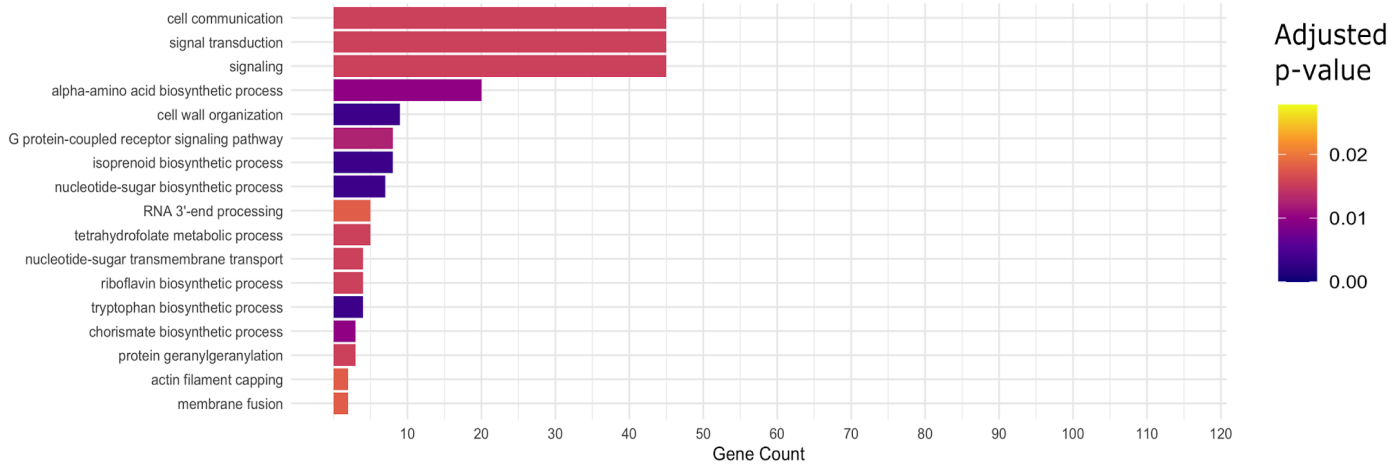
cell communication
signal transduction
signaling
alpha-amino acid biosynthetic process
cell wall organization
G protein-coupled receptor signaling pathway
isoprenoid biosynthetic process
nucleotide-sugar biosynthetic process
RNA 3'-end processing
tetrahydrofolate metabolic process
nucleotide-sugar transmembrane transport
riboflavin biosynthetic process
tryptophan biosynthetic process
chorismate biosynthetic process
protein geranylgeranylation
actin filament capping
membrane fusion
10
20
30
40
50
60
70
80
90
100
110
120
Gene Count
Adjusted p-value
0.02
0.01
0.00

D

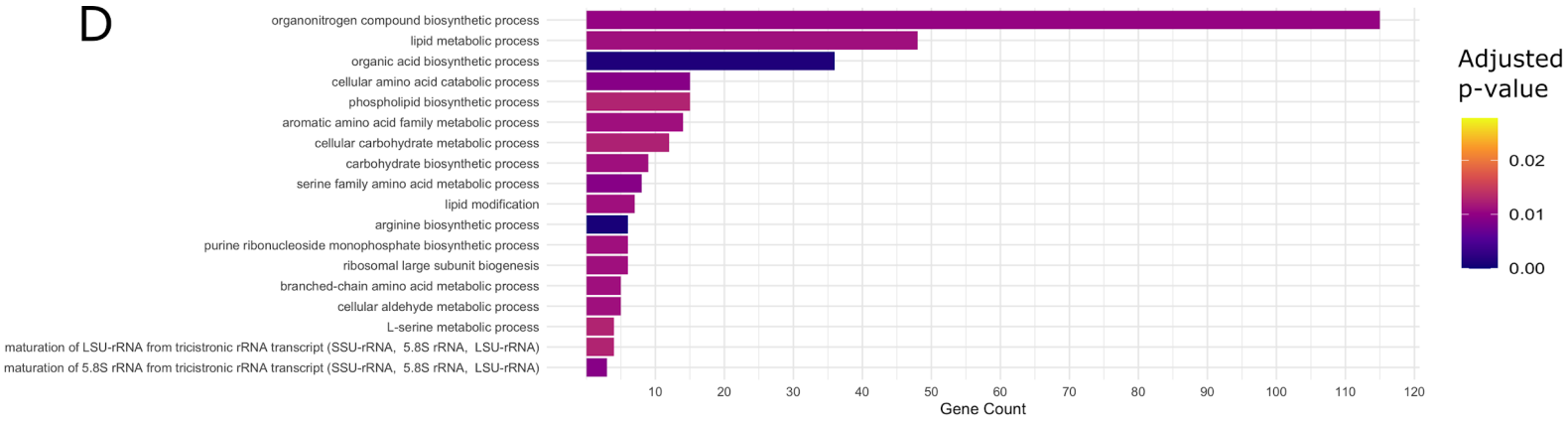
organonitrogen compound biosynthetic process
lipid metabolic process
organic acid biosynthetic process
cellular amino acid catabolic process
phospholipid biosynthetic process
aromatic amino acid family metabolic process
cellular carbohydrate metabolic process
carbohydrate biosynthetic process
serine family amino acid metabolic process
lipid modification
arginine biosynthetic process
purine ribonucleoside monophosphate biosynthetic process
ribosomal large subunit biogenesis
branched-chain amino acid metabolic process
cellular aldehyde metabolic process
L-serine metabolic process
maturation of LSU-rRNA from tricistronic rRNA transcript (SSU-rRNA, 5.8S rRNA, LSU-rRNA)
maturation of 5.8S rRNA from tricistronic rRNA transcript (SSU-rRNA, 5.8S rRNA, LSU-rRNA)
10
20
30
40
50
60
70
80
90
100
110
120
Gene Count
Adjusted p-value
0.02
0.01
0.00

Figure 3.3. Expression cluster GO enrichment results (FDR<5%). The Y-axis lists non-redundant enriched terms and the X-axis represents the number of genes associated with a term. Bars are colored by the adjusted p-value (FDR). The BCx cluster (A) is associated with 14 terms. The EAx cluster (B) has 23 enriched terms. The PEx cluster (C) has 17 enriched terms which are associated with mating-stimulated gene expression. The POx cluster (D) has 18 enriched terms.

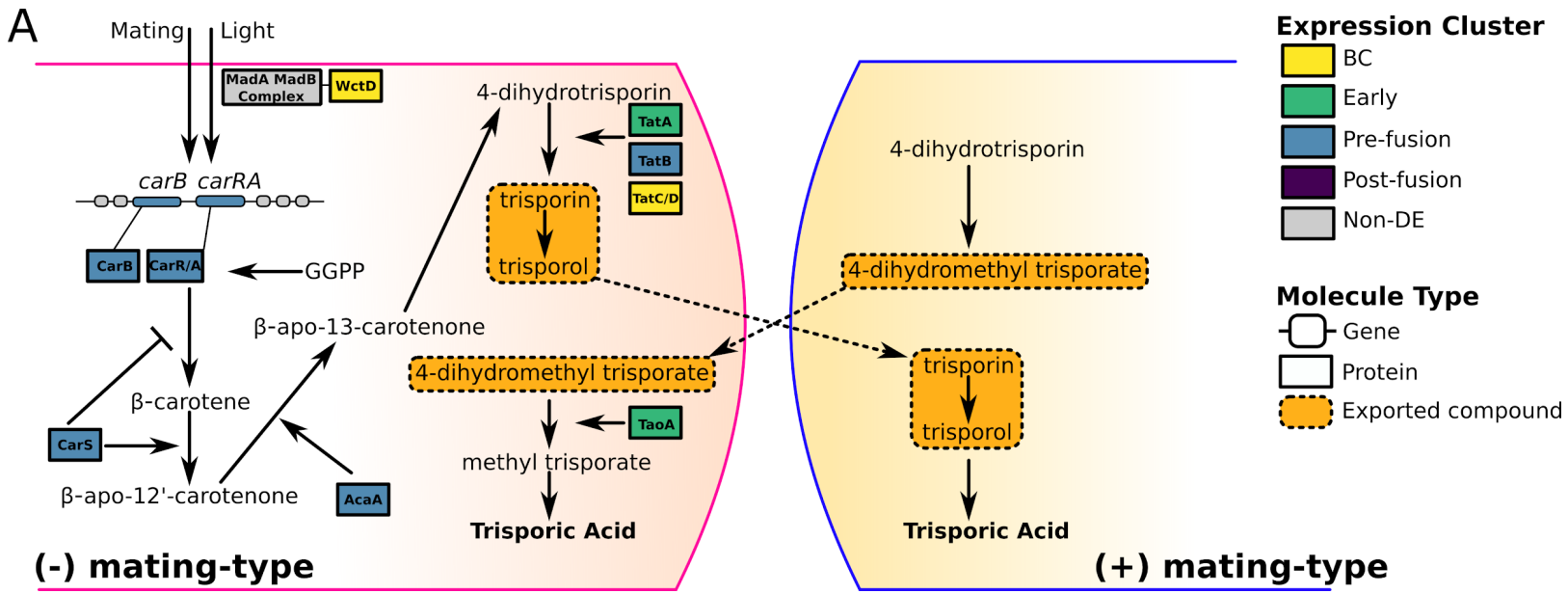
A
Mating
Light
MadA MadB Complex
WctD
carB carRA
CarB
CarR/A
GGPP
β-carotene
CarS
β-apo-12'-carotenone
AcaA
β-apo-13-carotenone
4-dihydrotrisporin
TatA
TatB
TatC/D
trisporin
trisporol
4-dihydromethyl trisporate
TaoA
methyl trisporate
Trisporic Acid
(-) mating-type
4-dihydrotrisporin
4-dihydromethyl trisporate
trisporin
trisporol
Trisporic Acid
(+) mating-type
Expression Cluster
BC
Early
Pre-fusion
Post-fusion
Non-DE
Molecule Type
Gene
Protein
Exported compound

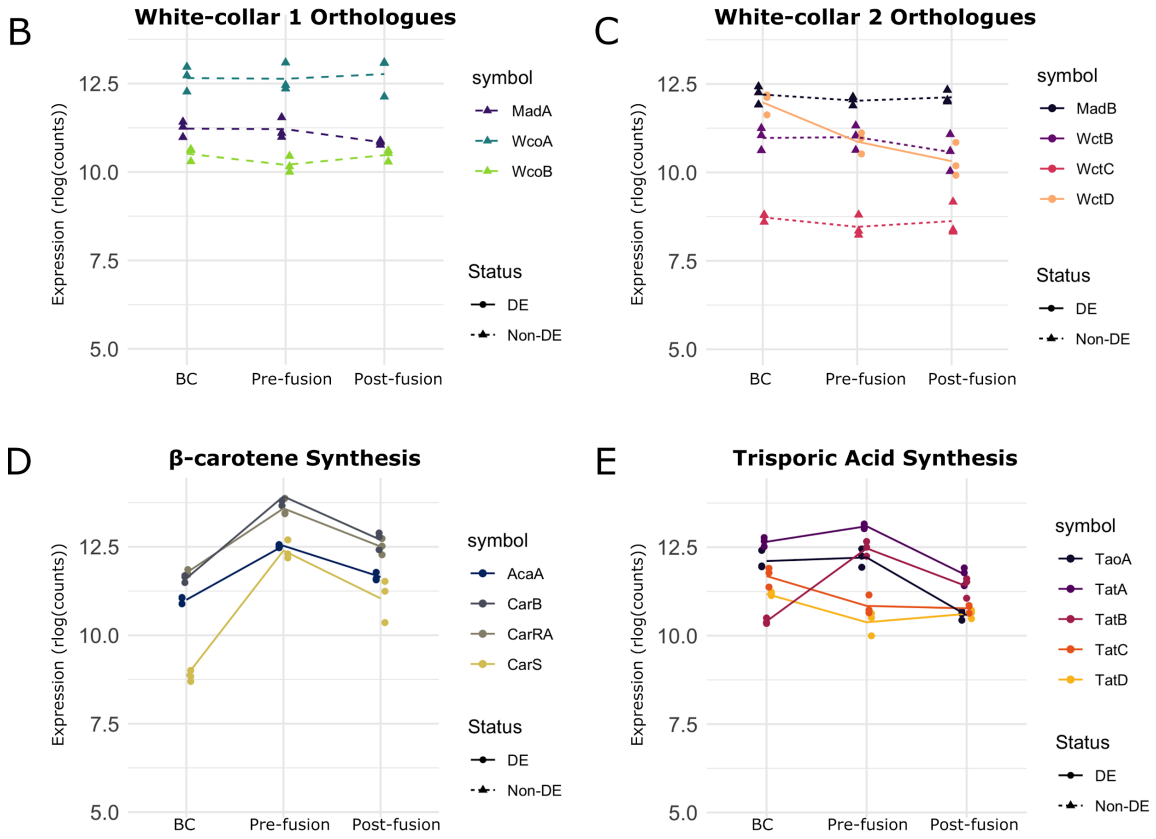

Figure 3.4. Schematic of carotenogenesis and trisporic acid synthesis pathways and expression of associated genes. Pathway diagram (A) adapted from Almeida & Cerdá-Olmedo 2008 (carotene synthesis) and Sutter et al. 1989 (trisporic acid synthesis). Solid arrows indicate a gene product's involvement at that step in the process. Gene expression plots (B-E) show average regularized log transformed counts as lines with individual values plotted as points. Light stimulates carotene synthesis via the MadA-MadB complex, though with one exception, these genes are not differentially expressed (B,C). The known β-carotene synthesis genes (D) are co-expressed and are part of the PEx cluster. The trisporic acid synthesis genes are also differentially expressed (E) and distributed between BCx, EAx, and PEx expression clusters.

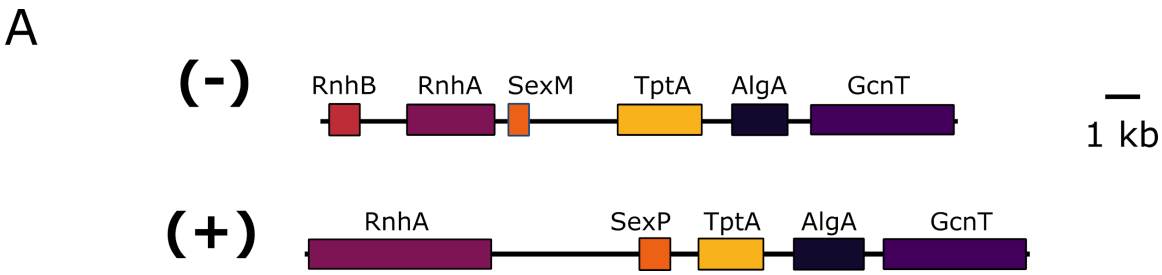
A
(-)
RnhB
RnhA
SexM
TptA
AlgA
GcnT
1 kb
(+)
RnhA
SexP
TptA
AlgA
GcnT

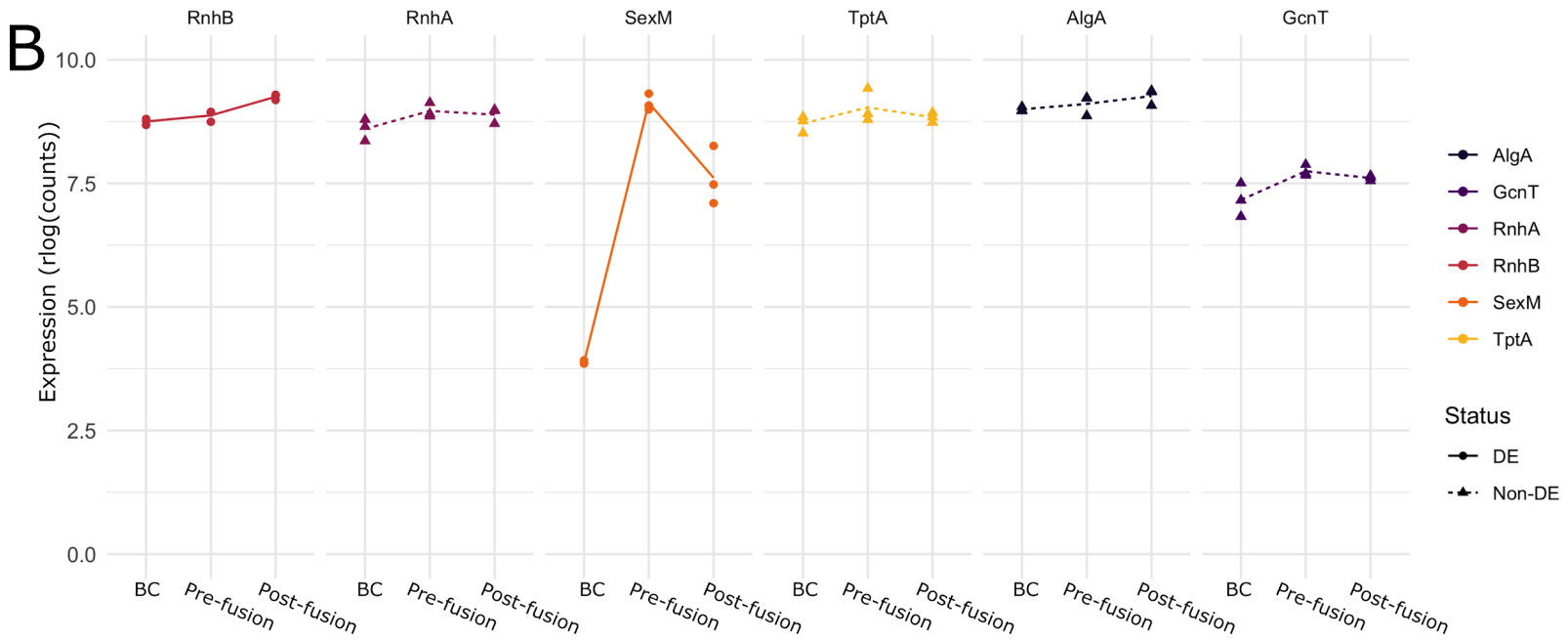
B
RnhB
RnhA
SexM
TptA
AlgA
GcnT
Expression (rlog(counts))
10.0
7.5
5.0
2.5
0.0
BC
Pre-fusion
Post-fusion
AlgA
GcnT
RnhA
RnhB
SexM
TptA
Status
DE
Non-DE

C

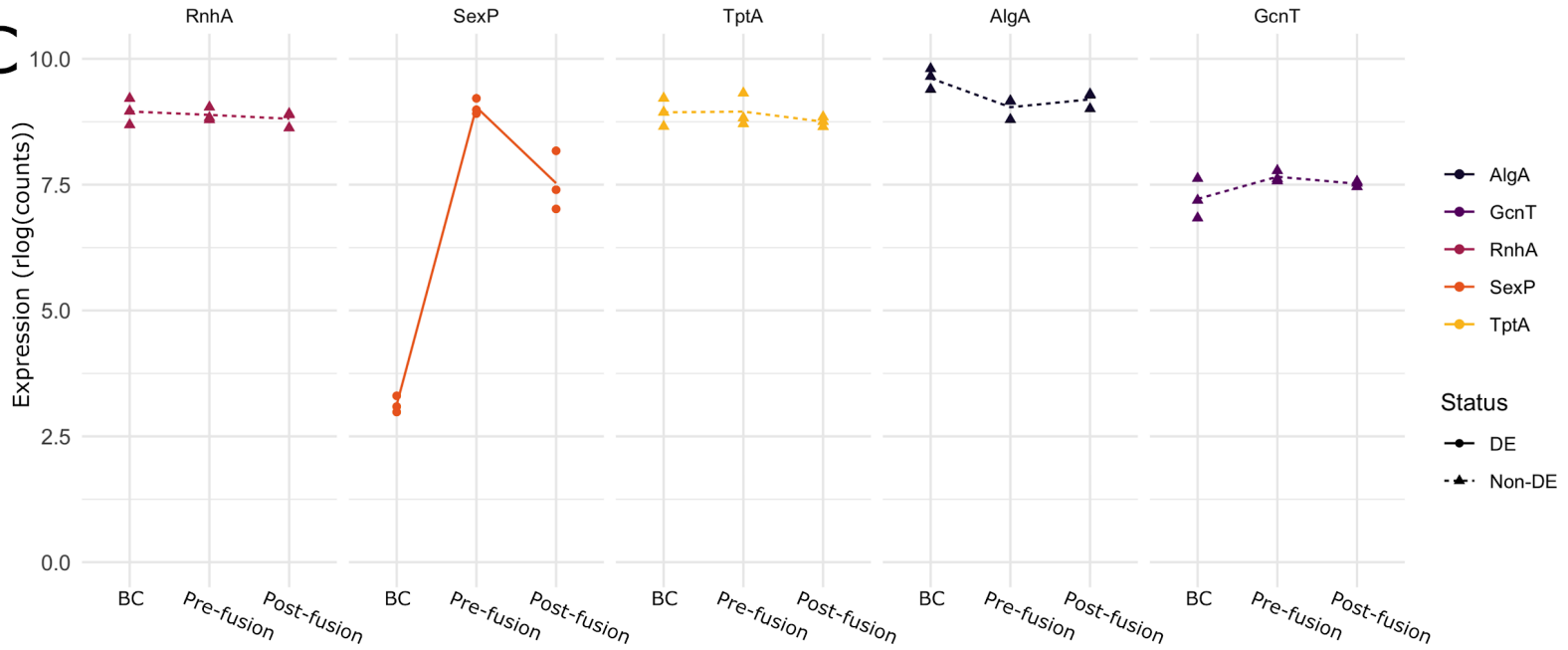
RnhA
SexP
TptA
AlgA
GcnT
Expression (rlog(counts))
10.0
7.5
5.0
2.5
0.0
BC
Pre-fusion
Post-fusion
AlgA
GcnT
RnhA
SexP
TptA
Status
DE
Non-DE

D

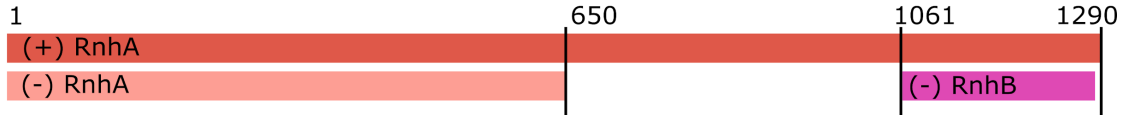

Figure 3.5. Mating-type locus gene expression. Gene order at the mating-type locus between the two strains is conserved (A), though the (-) mating-type has an additional predicted RNA helicase gene (RnhB; FungiDB). Gene expression plots (B,C) show average regularized log transformed counts as lines with individual values plotted as points. Genes of the (-) mating-type locus (B) are not differentially expressed with the exception of SexM and RnhB. Similarly, the genes of (+) mating-type locus are not differentially expressed except for SexP (C). Both RNA helicase genes from the (-) mating-type align to different regions of the (+)RnhA gene (D). Alignment source data in supplement.

Chapter 4: Characterization and Evolution of the Mucoromycotina Mating-type Locus

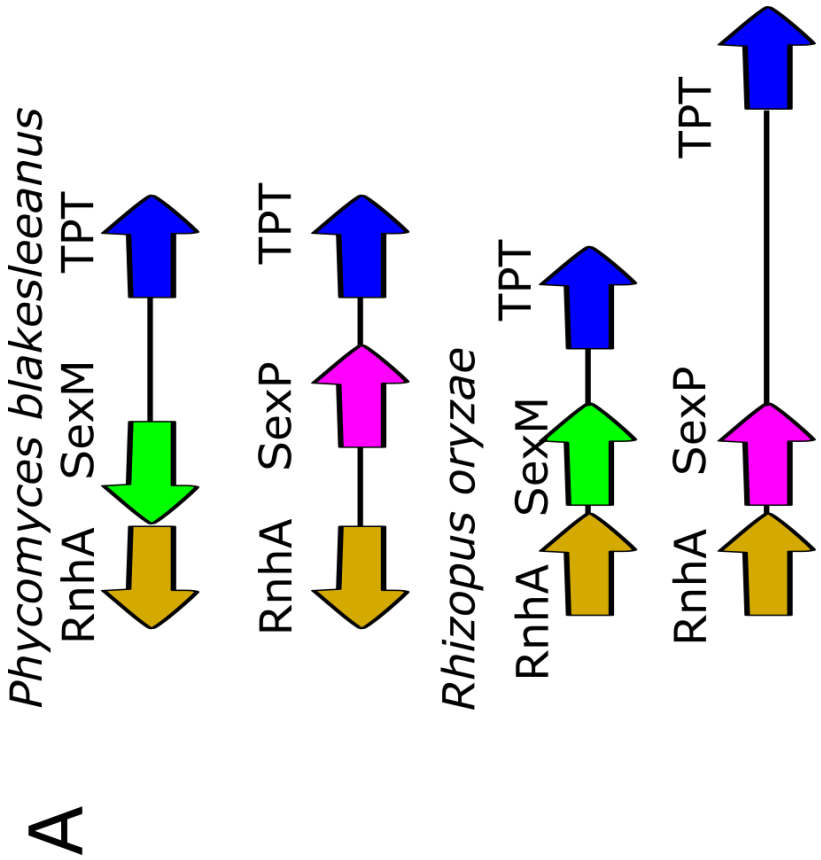

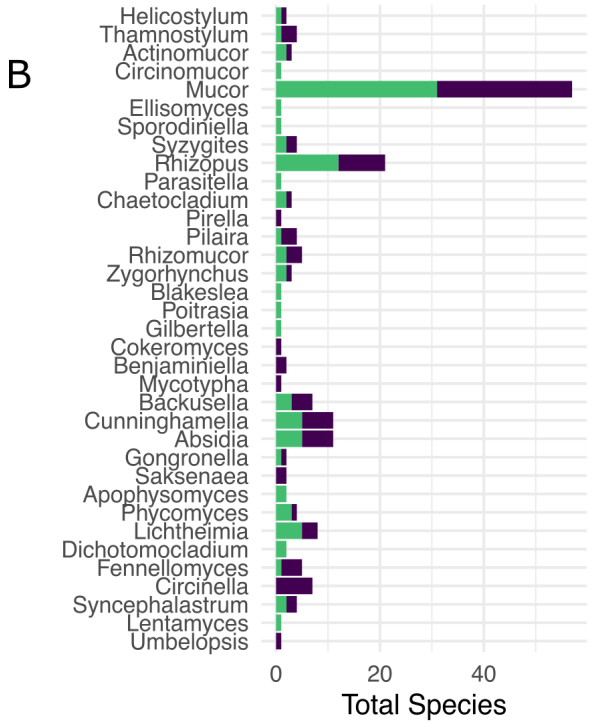
B
Helicostylum
Thamnostylum
Actinomucor
Circinomucor
Mucor
Ellisomyces
Sporodiniella
Syzygites
Rhizopus
Parasitella
Chaetocladium
Pirella
Pilaira
Rhizomucor
Zygorhynchus
Blakeslea
Poitrasia
Gilbertella
Cokeromyces
Benjaminiella
Mycotypha
Backusella
Cunninghamella
Absidia
Gongronella
Saksenaea
Apophysomyces
Phycomyces
Lichtheimia
Dichotomocladium
Fennellomyces
Circinella
Syncephalastrum
Lentamyces
Umbelopsis
0
20
40
Total Species

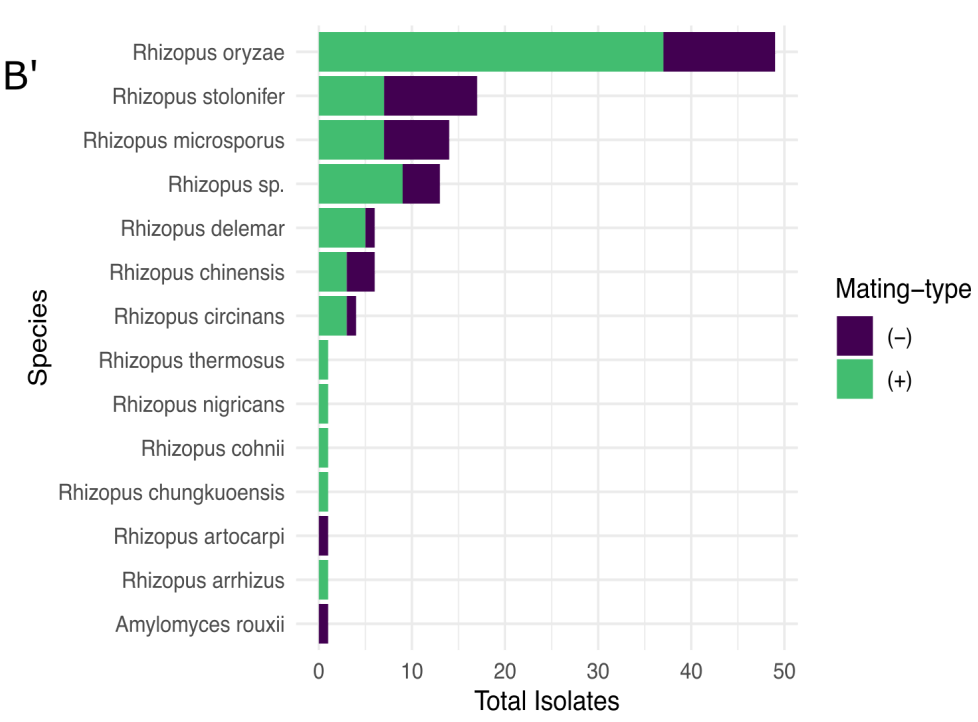
B'
Species
Rhizopus oryzae
Rhizopus stolonifer
Rhizopus microsporus
Rhizopus sp.
Rhizopus delemar
Rhizopus chinensis
Rhizopus circinans
Rhizopus thermosus
Rhizopus nigricans
Rhizopus cohnii
Rhizopus chungkuoensis
Rhizopus artocarpi
Rhizopus arrhizus
Amylomyces rouxii
0
10
20
30
40
50
Total Isolates
Mating−type
(−)
(+)

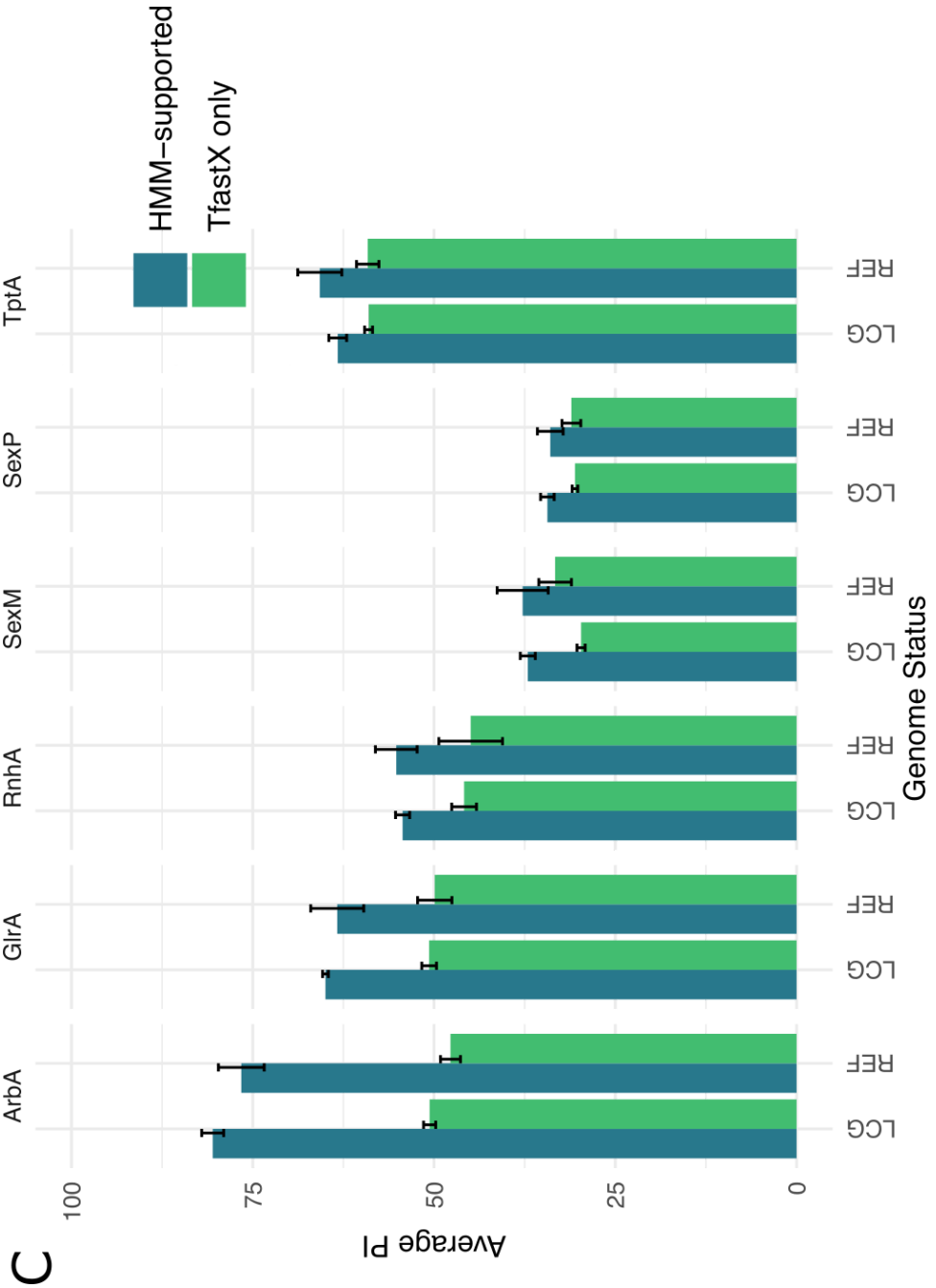
C
HMM−supported
TfastX only
ArbA
GlrA
RnhA
SexM
SexP
TptA
LCG
REF
Genome Status
Average PI
0
25
50
75
100

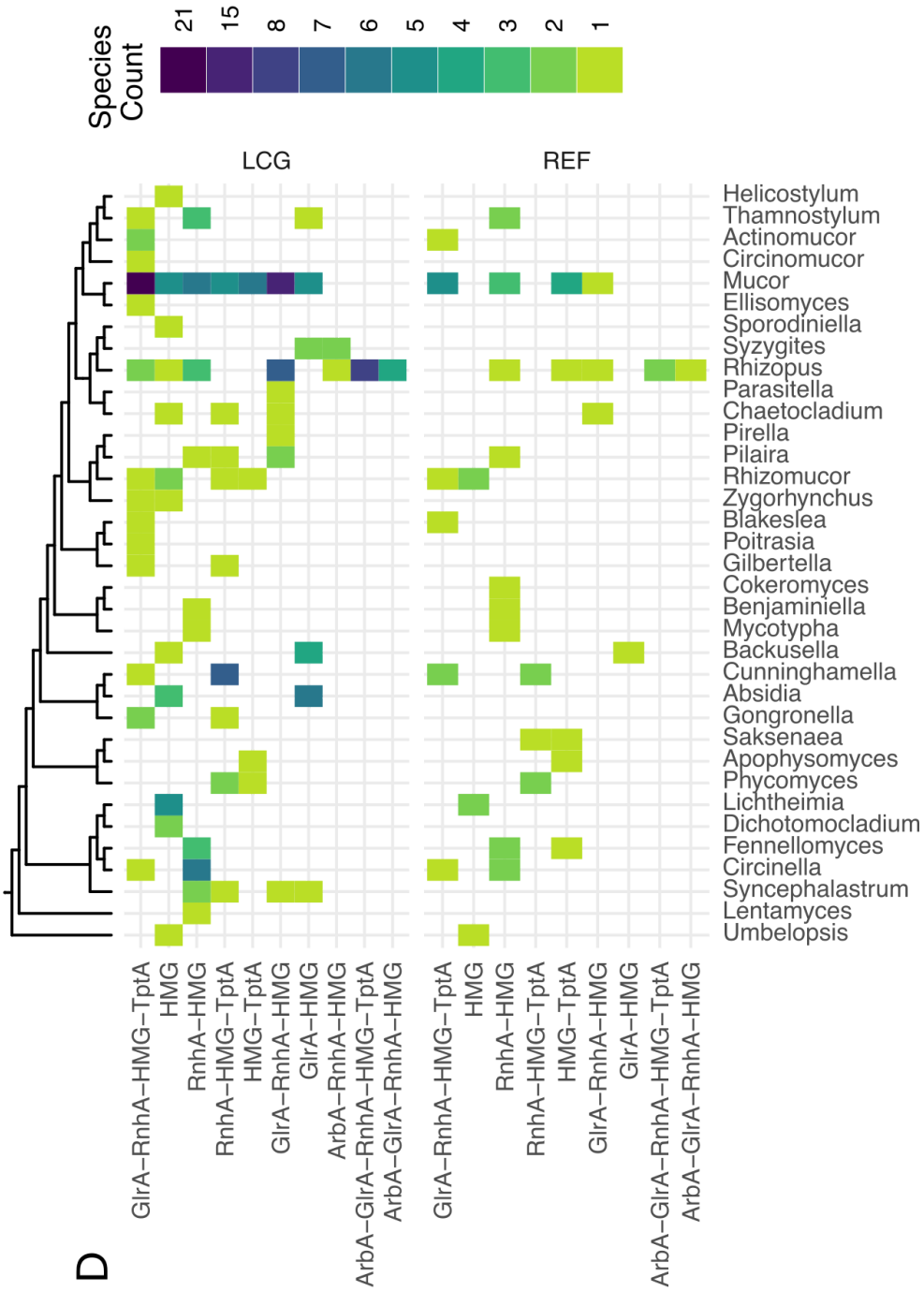
D
Species Count
21
15
8
7
6
5
4
3
2
1
LCG
REF
Helicostylum
Thamnostylum
Actinomucor
Circinomucor
Mucor
Ellisomyces
Sporodiniella
Syzygites
Rhizopus
Parasitella
Chaetocladium
Pirella
Pilaira
Rhizomucor
Zygorhynchus
Blakeslea
Poitrasia
Gilbertella
Cokeromyces
Benjaminiella
Mycotypha
Backusella
Cunninghamella
Absidia
Gongronella
Saksenaea
Apophysomyces
Phycomyces
Lichtheimia
Dichotomocladium
Fennellomyces
Circinella
Syncephalastrum
Lentamyces
Umbelopsis
GlrA–RnhA–HMG–TptA
HMG
RnhA–HMG
RnhA–HMG–TptA
HMG–TptA
GlrA–RnhA–HMG
GlrA–HMG
ArbA–RnhA–HMG
ArbA–GlrA–RnhA–HMG–TptA
ArbA–GlrA–RnhA–HMG

Figure 4.1 General characteristics of mating-type loci and overview of locus identification. The mating type loci of *P. blakesleeanus* and *R. oryzae* have been previously characterized and found to be syntenic (A). This analysis identified mating-type genes in a diverse set of species representing 36 genera (B). At the genus level, distribution of mating-type genes, sexM and sexP, appear nearly equal. (B') Increasing the resolution of this pattern revealed that (+) mating-types were generally overrepresented among individual species. HMMer was used to verify results of searches (C); error bars represent standard error. Mating-type loci were not varied in gene content across genera and species (D). REF: reference genome, LCG: light coverage genome

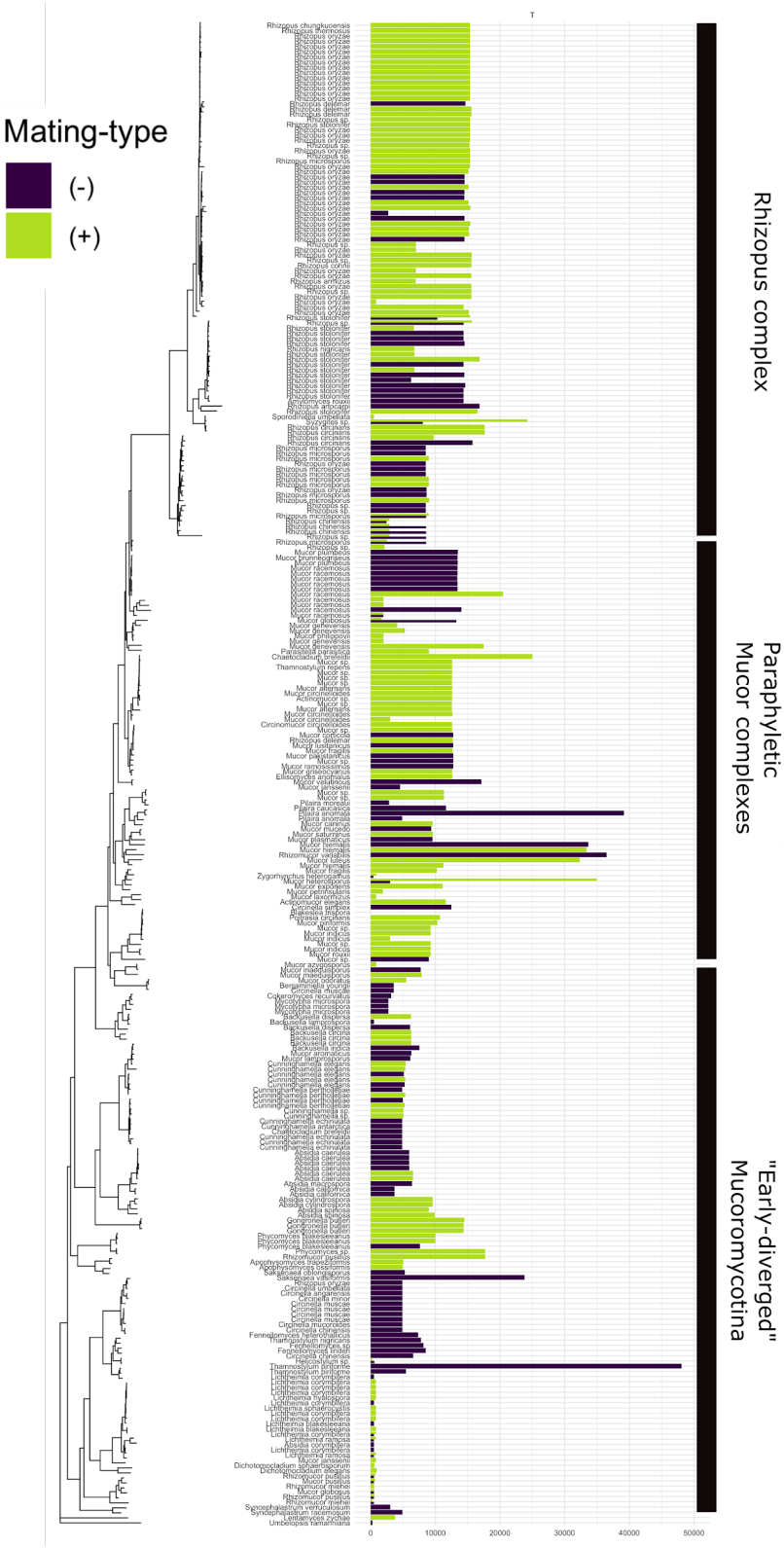
Mating-type
(-)
(+)
Rhizopus complex
Paraphyletic
Mucor complexes
"Early-diverged"
Mucoromycotina
0
10000
20000
30000
40000
50000

Figure 4.2 Locus length by mating-type across the species tree. Three broad phylogenetic categories were associated with distinct patterns in locus length, with the various paraphyletic *Mucor* spp. having the highest variation. Arrow-heads point to two isolates of *Rhizomucor pusillus.*

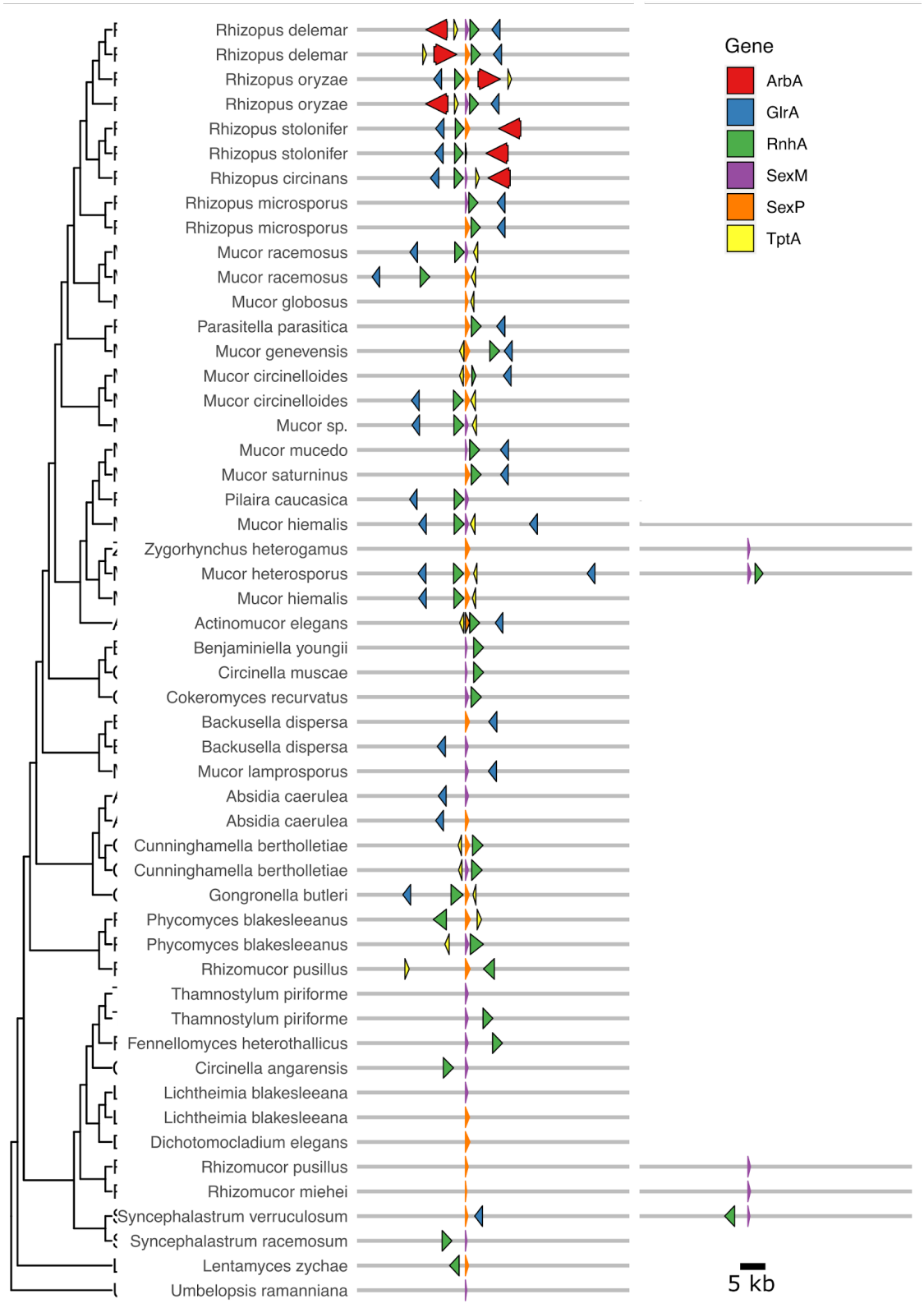
Rhizopus delemar
Rhizopus delemar
Rhizopus oryzae
Rhizopus oryzae
Rhizopus stolonifer
Rhizopus stolonifer
Rhizopus circinans
Rhizopus microsporus
Rhizopus microsporus
Mucor racemosus
Mucor racemosus
Mucor globosus
Parasitella parasitica
Mucor genevensis
Mucor circinelloides
Mucor circinelloides
Mucor sp.
Mucor mucedo
Mucor saturninus
Pilaira caucasica
Mucor hiemalis
Zygorhynchus heterogamus
Mucor heterosporus
Mucor hiemalis
Actinomucor elegans
Benjaminiella youngii
Circinella muscae
Cokeromyces recurvatus
Backusella dispersa
Backusella dispersa
Mucor lamprosporus
Absidia caerulea
Absidia caerulea
Cunninghamella bertholletiae
Cunninghamella bertholletiae
Gongronella butleri
Phycomyces blakesleeanus
Phycomyces blakesleeanus
Rhizomucor pusillus
Thamnostylum piriforme
Thamnostylum piriforme
Fennellomyces heterothallicus
Circinella angarensis
Lichtheimia blakesleeana
Lichtheimia blakesleeana
Dichotomocladium elegans
Rhizomucor pusillus
Rhizomucor miehei
Syncephalastrum verruculosum
Syncephalastrum racemosum
Lentamyces zychae
Umbelopsis ramanniana
Gene
ArbA
GlrA
RnhA
SexM
SexP
TptA
5 kb

Figure 4.3 Mating-type locus schematics mapped to a representative species tree. The mating-type genes (SexM or SexP) were aligned across all species. The second locus of candidate homothallic species are plotted on the right.

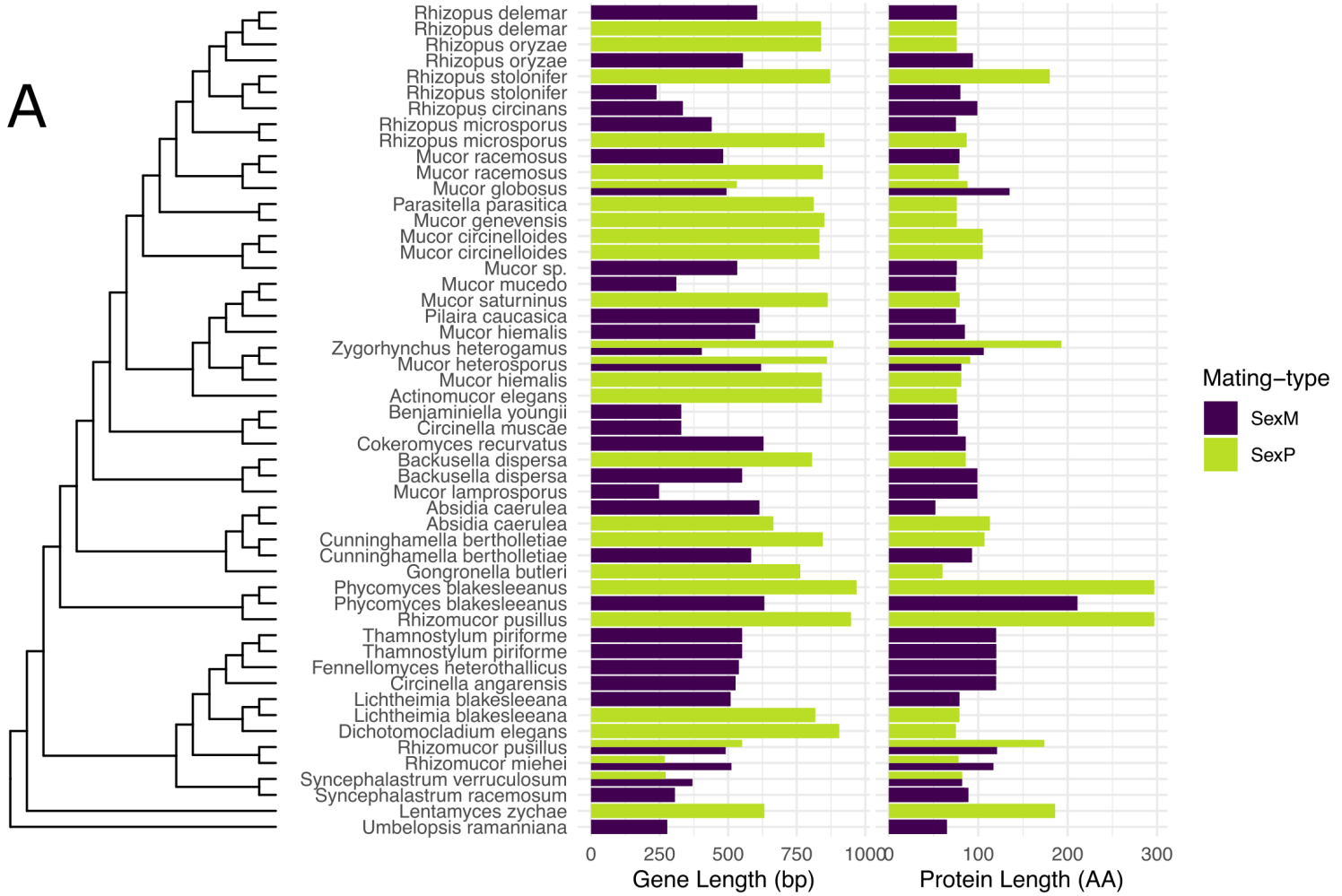
A
Rhizopus delemar
Rhizopus delemar
Rhizopus oryzae
Rhizopus oryzae
Rhizopus stolonifer
Rhizopus stolonifer
Rhizopus circinans
Rhizopus microsporus
Rhizopus microsporus
Mucor racemosus
Mucor racemosus
Mucor globosus
Parasitella parasitica
Mucor genevensis
Mucor circinelloides
Mucor circinelloides
Mucor sp.
Mucor mucedo
Mucor saturninus
Pilaira caucasica
Mucor hiemalis
Zygorhynchus heterogamus
Mucor heterosporus
Mucor hiemalis
Actinomucor elegans
Benjaminiella youngii
Circinella muscae
Cokeromyces recurvatus
Backusella dispersa
Backusella dispersa
Mucor lamprosporus
Absidia caerulea
Absidia caerulea
Cunninghamella bertholletiae
Cunninghamella bertholletiae
Gongronella butleri
Phycomyces blakesleeanus
Phycomyces blakesleeanus
Rhizomucor pusillus
Thamnostylum piriforme
Thamnostylum piriforme
Fennellomyces heterothallicus
Circinella angarensis
Lichtheimia blakesleeana
Lichtheimia blakesleeana
Dichotomocladium elegans
Rhizomucor pusillus
Rhizomucor miehei
Syncephalastrum verruculosum
Syncephalastrum racemosum
Lentamyces zychae
Umbelopsis ramanniana
0
250
500
750
1000
Gene Length (bp)
100
200
300
Protein Length (AA)
Mating−type
SexM
SexP

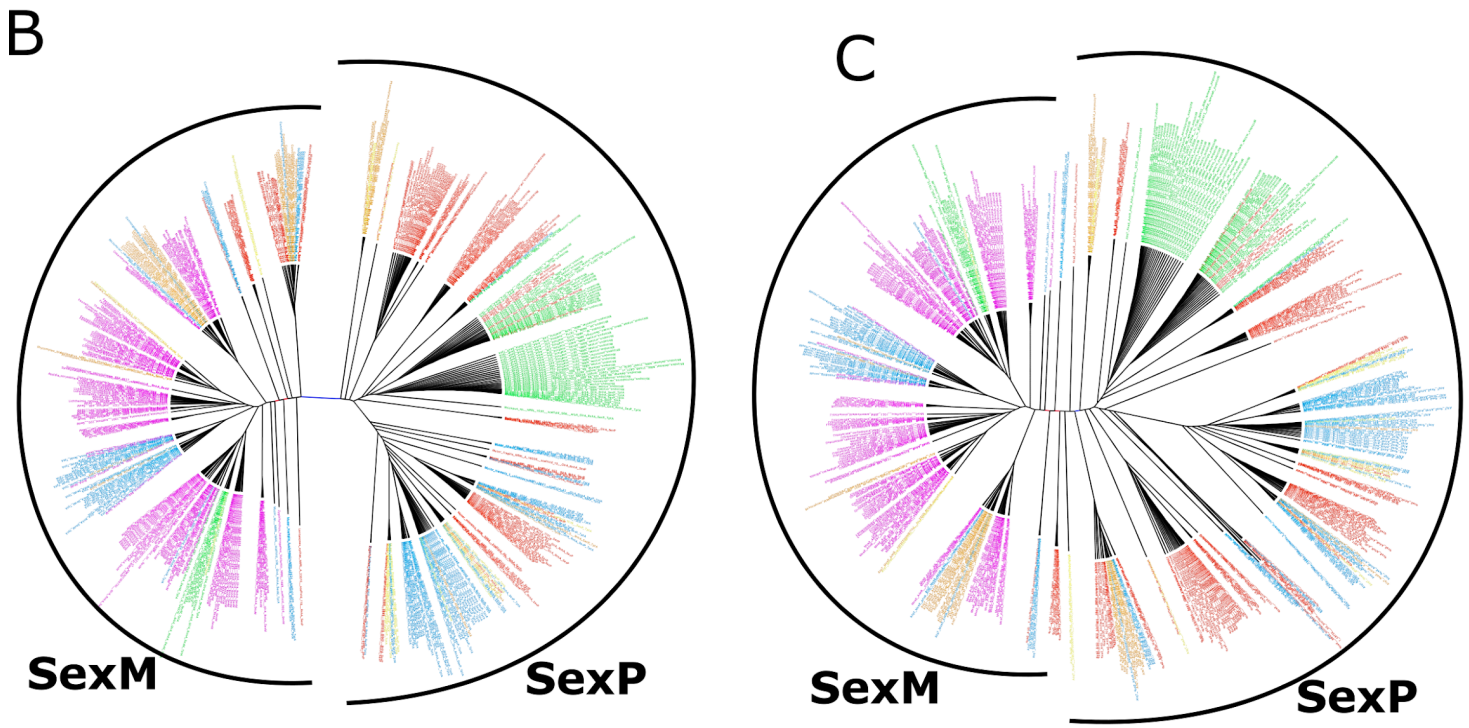
B
SexM
SexP
C
SexM
SexP
RnhA-GlrA-SexM
RnhA-SexM
GlrA-SexM
SexM
ArbA-GlrA-RnhA-HMG-TptA
GlrA-RnhA-HMG-TptA
RnhA-HMG-TptA
HMG-TptA
RnhA-GlrA-SexP
RnhA-SexP
GlrA-SexP
SexP

Figure 4.4 Comparison of SexM and SexP gene and protein sequences. The lengths of each mating-type gene and the corresponding protein length (A) did not vary widely among the representative species. Midpoint rooted (B) and unrooted (C) gene trees resolved evolutionary differences between the two genes.

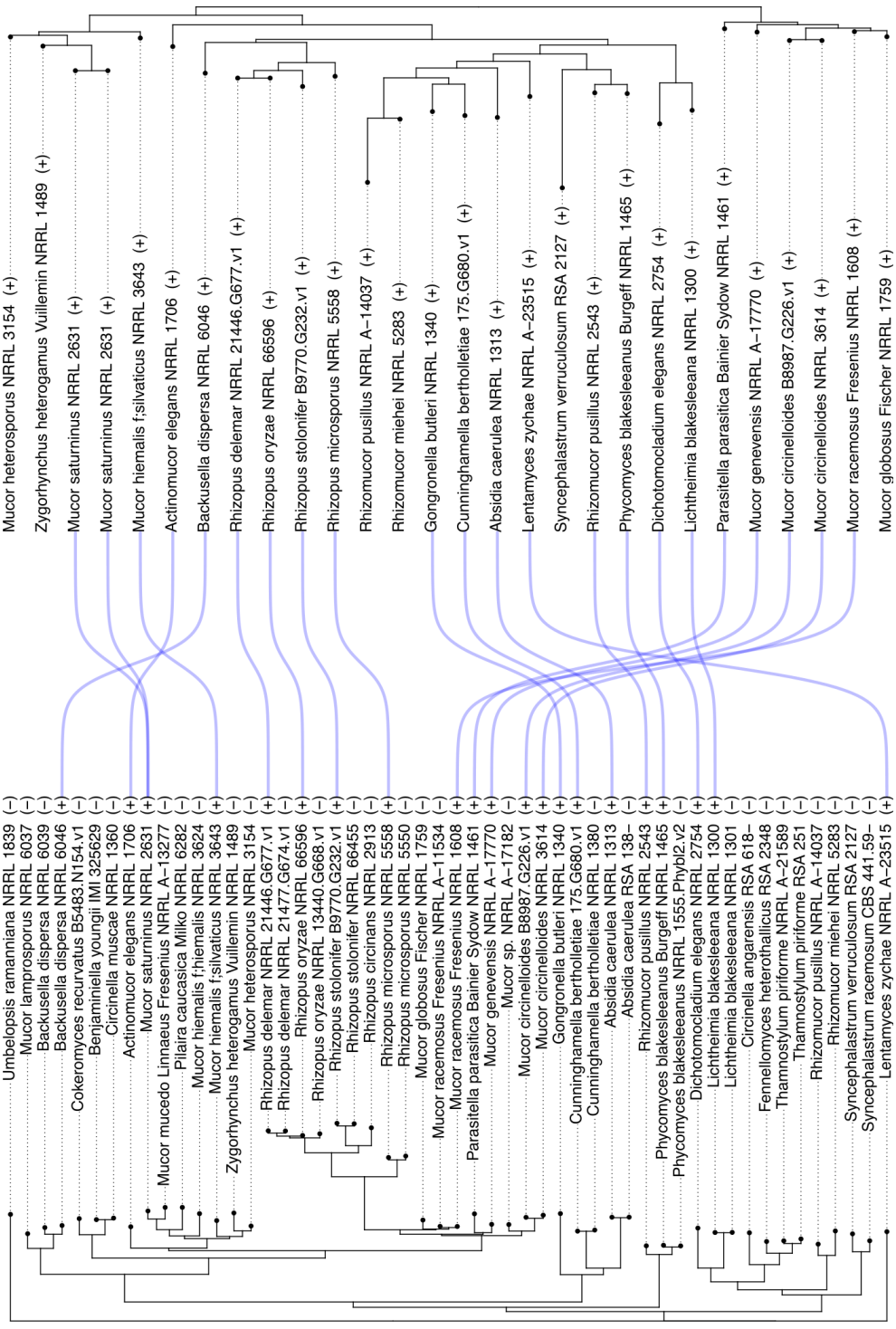
Mucor heterosporus NRRL 3154 (+)
Zygorhynchus heterogamus Vuillemin NRRL 1489 (+)
Mucor saturninus NRRL 2631 (+)
Mucor saturninus NRRL 2631 (+)
Mucor hiemalis f.silvaticus NRRL 3643 (+)
Actinomucor elegans NRRL 1706 (+)
Backusella dispersa NRRL 6046 (+)
Rhizopus delemar NRRL 21446.G677.v1 (+)
Rhizopus oryzae NRRL 66596 (+)
Rhizopus stolonifer B9770.G232.v1 (+)
Rhizopus microsporus NRRL 5558 (+)
Rhizomucor pusillus NRRL A–14037 (+)
Rhizomucor miehei NRRL 5283 (+)
Gongronella butleri NRRL 1340 (+)
Cunninghamella bertholletiae 175.G680.v1 (+)
Absidia caerulea NRRL 1313 (+)
Lentamyces zychae NRRL A–23515 (+)
Syncephalastrum verruculosum RSA 2127 (+)
Rhizomucor pusillus NRRL 2543 (+)
Phycomyces blakesleeanus Burgeff NRRL 1465 (+)
Dichotomocladium elegans NRRL 2754 (+)
Lichtheimia blakesleeana NRRL 1300 (+)
Parasitella parasitica Bainier Sydow NRRL 1461 (+)
Mucor genevensis NRRL A–17770 (+)
Mucor circinelloides B8987.G226.v1 (+)
Mucor circinelloides NRRL 3614 (+)
Mucor racemosus Fresenius NRRL 1608 (+)
Mucor globosus Fischer NRRL 1759 (+)
Umbelopsis ramanniana NRRL 1839 (–)
Mucor lamprosporus NRRL 6037 (–)
Backusella dispersa NRRL 6039 (–)
Backusella dispersa NRRL 6046 (+)
Cokeromyces recurvatus B5483.N154.v1 (–)
Benjaminiella yoongii IMI 325629 (–)
Circinella muscae NRRL 1360 (–)
Actinomucor elegans NRRL 1706 (+)
Mucor saturninus NRRL 2631 (+)
Mucor mucedo Linnaeus Fresenius NRRL A–13277 (–)
Pilaira caucasica Milko NRRL 6282 (–)
Mucor hiemalis f.hiemalis NRRL 3624 (–)
Mucor hiemalis f.silvaticus NRRL 3643 (+)
Zygorhynchus heterogamus Vuillemin NRRL 1489 (–)
Mucor heterosporus NRRL 3154 (–)
Rhizopus delemar NRRL 21446.G677.v1 (+)
Rhizopus delemar NRRL 21477.G674.v1 (–)
Rhizopus oryzae NRRL 66596 (+)
Rhizopus oryzae NRRL 13440.G668.v1 (–)
Rhizopus stolonifer B9770.G232.v1 (+)
Rhizopus stolonifer NRRL 66455 (–)
Rhizopus circinans NRRL 2913 (–)
Rhizopus microsporus NRRL 5558 (+)
Rhizopus microsporus NRRL 5550 (–)
Mucor globosus Fischer NRRL 1759 (–)
Mucor racemosus Fresenius NRRL A–11534 (–)
Mucor racemosus Fresenius NRRL 1608 (+)
Parasitella parasitica Bainier Sydow NRRL 1461 (+)
Mucor genevensis NRRL A–17770 (+)
Mucor sp. NRRL A–17182 (–)
Mucor circinelloides B8987.G226.v1 (+)
Mucor circinelloides NRRL 3614 (+)
Gongronella butleri NRRL 1340 (+)
Cunninghamella bertholletiae 175.G680.v1 (+)
Cunninghamella bertholletiae NRRL 1380 (–)
Absidia caerulea NRRL 1313 (+)
Absidia caerulea RSA 138– (–)
Rhizomucor pusillus NRRL 2543 (+)
Phycomyces blakesleeanus Burgeff NRRL 1465 (+)
Phycomyces blakesleeanus NRRL 1555.Phybl2.v2 (–)
Dichotomocladium elegans NRRL 2754 (+)
Lichtheimia blakesleeana NRRL 1300 (+)
Lichtheimia blakesleeana NRRL 1301 (–)
Circinella angarensis RSA 618– (–)
Fennellomyces heterothallicus RSA 2348 (–)
Thamnostylum piriforme NRRL A–21589 (–)
Thamnostylum piriforme RSA 251 (–)
Rhizomucor pusillus NRRL A–14037 (–)
Rhizomucor miehei NRRL 5283 (–)
Syncephalastrum verruculosum RSA 2127 (–)
Syncephalastrum racemosum CBS 441.59– (–)
Lentamyces zychae NRRL A–23515 (+)

A

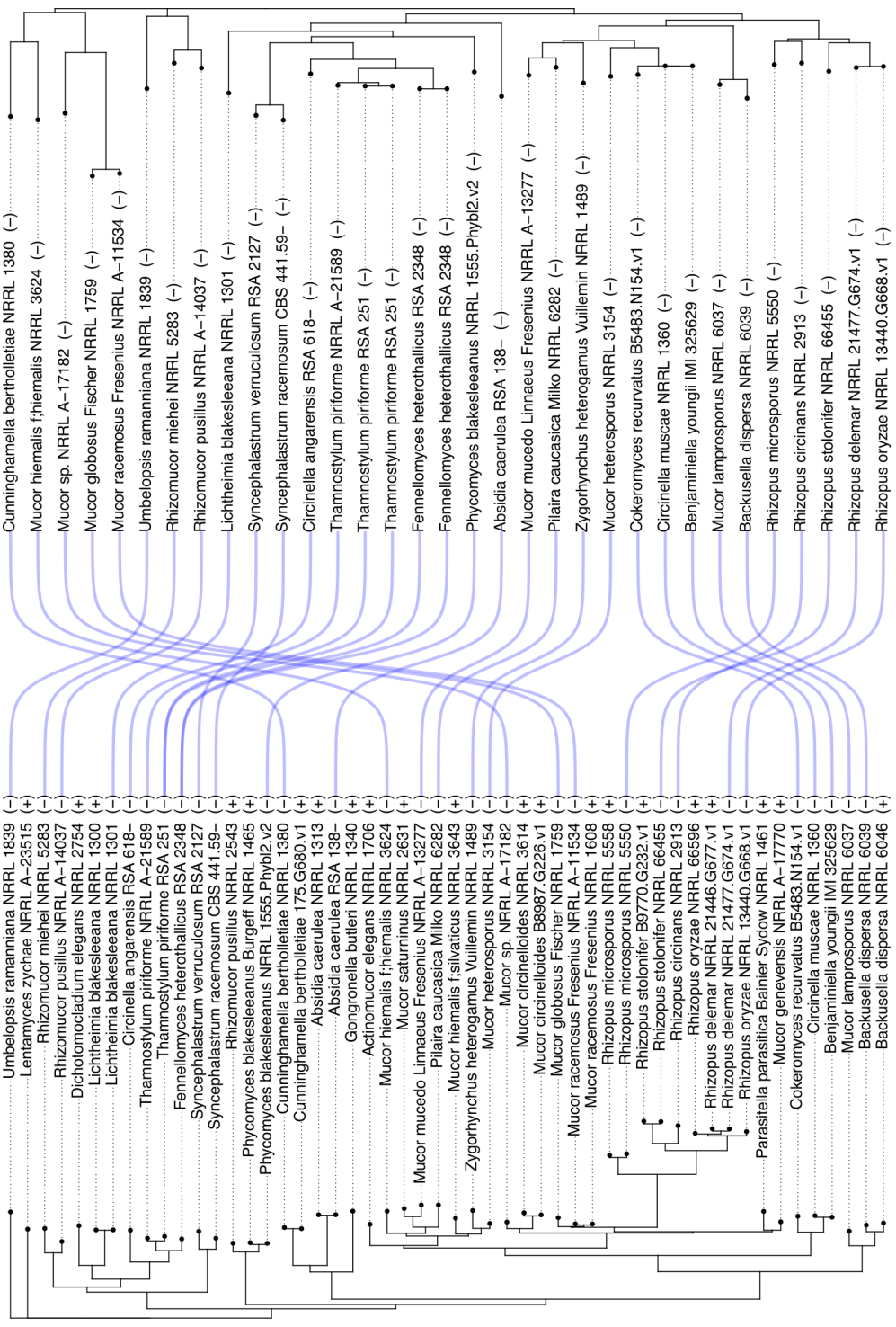
Cunninghamella bertholletiae NRRL 1380 (–)
Mucor hiemalis f;hiemalis NRRL 3624 (–)
Mucor sp. NRRL A–17182 (–)
Mucor globosus Fischer NRRL 1759 (–)
Mucor racemosus Fresenius NRRL A–11534 (–)
Umbelopsis ramanniana NRRL 1839 (–)
Rhizomucor miehei NRRL 5283 (–)
Rhizomucor pusillus NRRL A–14037 (–)
Lichtheimia blakesleeana NRRL 1301 (–)
Syncephalastrum verruculosum RSA 2127 (–)
Syncephalastrum racemosum CBS 441.59– (–)
Circinella angarensis RSA 618– (–)
Thamnostylum piriforme NRRL A–21589 (–)
Thamnostylum piriforme RSA 251 (–)
Thamnostylum piriforme RSA 251 (–)
Fennellomyces heterothallicus RSA 2348 (–)
Fennellomyces heterothallicus RSA 2348 (–)
Phycomyces blakesleeanus NRRL 1555.Phybl2.v2 (–)
Absidia caerulea RSA 138– (–)
Mucor mucedo Linnaeus Fresenius NRRL A–13277 (–)
Pilaira caucasica Milko NRRL 6282 (–)
Zygorhynchus heterogamus Vuillemin NRRL 1489 (–)
Mucor heterosporus NRRL 3154 (–)
Cokeromyces recurvatus B5483.N154.v1 (–)
Circinella muscae NRRL 1360 (–)
Benjaminiella yungii IMI 325629 (–)
Mucor lamprosporus NRRL 6037 (–)
Backusella dispersa NRRL 6039 (–)
Rhizopus microsporus NRRL 5550 (–)
Rhizopus circinans NRRL 2913 (–)
Rhizopus stolonifer NRRL 66455 (–)
Rhizopus delemar NRRL 21477.G674.v1 (–)
Rhizopus oryzae NRRL 13440.G668.v1 (–)
Umbelopsis ramanniana NRRL 1839 (–)
Lentamyces zychae NRRL A–23515 (+)
Rhizomucor miehei NRRL 5283 (–)
Rhizomucor pusillus NRRL A–14037 (–)
Dichotomocladium elegans NRRL 2754 (+)
Lichtheimia blakesleeana NRRL 1300 (+)
Lichtheimia blakesleeana NRRL 1301 (–)
Circinella angarensis RSA 618– (–)
Thamnostylum piriforme NRRL A–21589 (–)
Thamnostylum piriforme RSA 251 (–)
Fennellomyces heterothallicus RSA 2348 (–)
Syncephalastrum verruculosum RSA 2127 (–)
Syncephalastrum racemosum CBS 441.59– (–)
Rhizomucor pusillus NRRL 2543 (+)
Phycomyces blakesleeanus Burgeff NRRL 1465 (+)
Phycomyces blakesleeanus NRRL 1555.Phybl2.v2 (–)
Cunninghamella bertholletiae NRRL 1380 (–)
Cunninghamella bertholletiae 175.G680.v1 (+)
Absidia caerulea NRRL 1313 (+)
Absidia caerulea RSA 138– (–)
Gongronella butleri NRRL 1340 (+)
Actinomucor elegans NRRL 1706 (+)
Mucor hiemalis f;hiemalis NRRL 3624 (–)
Mucor saturninus NRRL 2631 (+)
Mucor mucedo Linnaeus Fresenius NRRL A–13277 (–)
Pilaira caucasica Milko NRRL 6282 (–)
Mucor hiemalis f;silvaticus NRRL 3643 (+)
Zygorhynchus heterogamus Vuillemin NRRL 1489 (–)
Mucor heterosporus NRRL 3154 (–)
Mucor sp. NRRL A–17182 (–)
Mucor circinelloides NRRL 3614 (+)
Mucor circinelloides B8987.G226.v1 (+)
Mucor globosus Fischer NRRL 1759 (–)
Mucor racemosus Fresenius NRRL A–11534 (–)
Mucor racemosus Fresenius NRRL 1608 (+)
Rhizopus microsporus NRRL 5558 (+)
Rhizopus microsporus NRRL 5550 (–)
Rhizopus stolonifer B9770.G232.v1 (+)
Rhizopus stolonifer NRRL 66455 (–)
Rhizopus circinans NRRL 2913 (–)
Rhizopus oryzae NRRL 66596 (+)
Rhizopus delemar NRRL 21446.G677.v1 (+)
Rhizopus delemar NRRL 21477.G674.v1 (–)
Rhizopus oryzae NRRL 13440.G668.v1 (–)
Parasitella parasitica Bainier Sydow NRRL 1461 (+)
Mucor genevensis NRRL A–17770 (+)
Cokeromyces recurvatus B5483.N154.v1 (–)
Circinella muscae NRRL 1360 (–)
Benjaminiella yungii IMI 325629 (–)
Mucor lamprosporus NRRL 6037 (–)
Backusella dispersa NRRL 6039 (–)
Backusella dispersa NRRL 6046 (+)

B

Figure 4.5 Tanglegrams comparing individual SexP (A) and SexM (B) gene trees to the representative species tree (left).

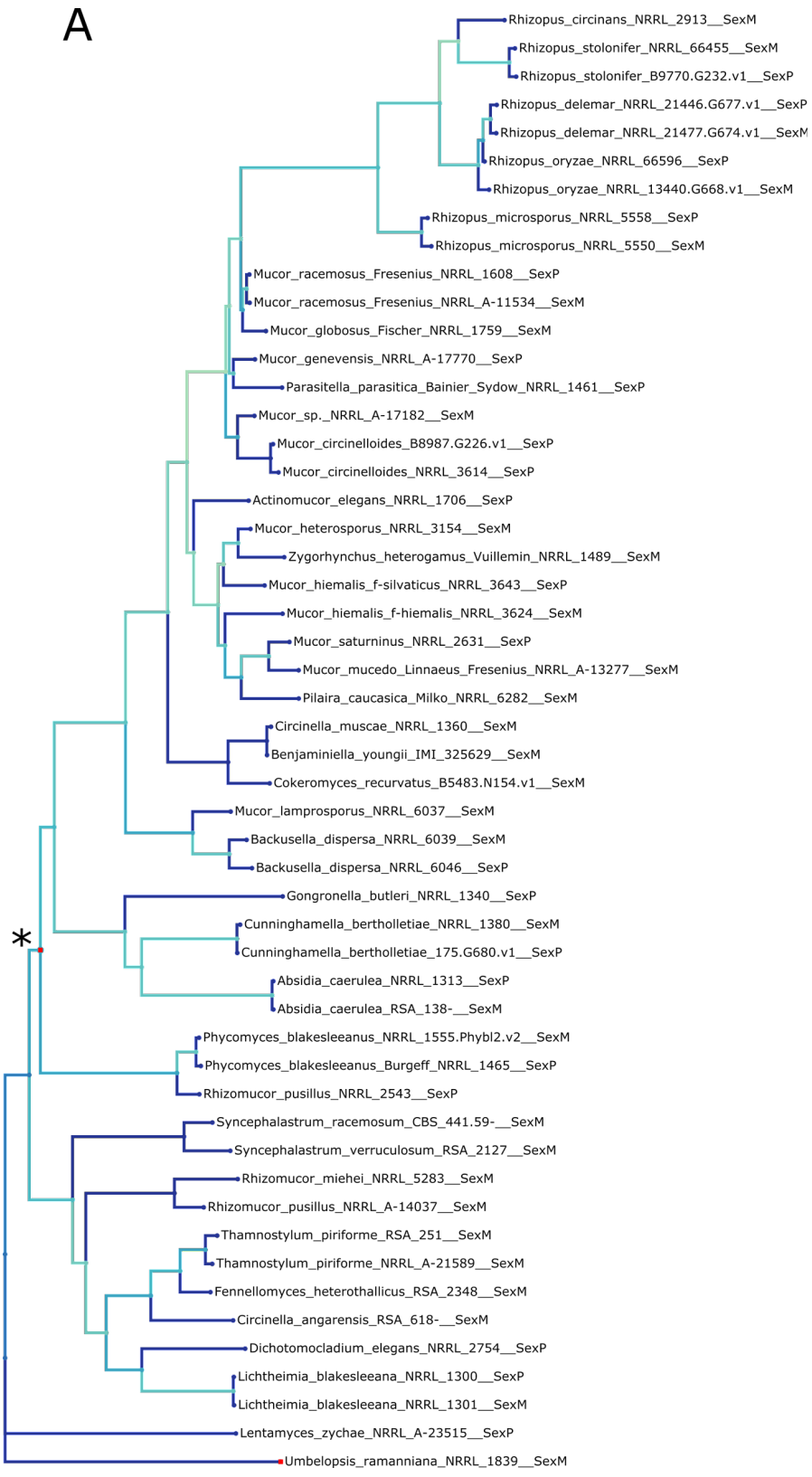
A
Rhizopus_circinans_NRRL_2913__SexM
Rhizopus_stolonifer_NRRL_66455__SexM
Rhizopus_stolonifer_B9770.G232.v1__SexP
Rhizopus_delemar_NRRL_21446.G677.v1__SexP
Rhizopus_delemar_NRRL_21477.G674.v1__SexM
Rhizopus_oryzae_NRRL_66596__SexP
Rhizopus_oryzae_NRRL_13440.G668.v1__SexM
Rhizopus_microsporus_NRRL_5558__SexP
Rhizopus_microsporus_NRRL_5550__SexM
Mucor_racemosus_Fresenius_NRRL_1608__SexP
Mucor_racemosus_Fresenius_NRRL_A-11534__SexM
Mucor_globosus_Fischer_NRRL_1759__SexM
Mucor_genevensis_NRRL_A-17770__SexP
Parasitella_parasitica_Bainier_Sydow_NRRL_1461__SexP
Mucor_sp._NRRL_A-17182__SexM
Mucor_circinelloides_B8987.G226.v1__SexP
Mucor_circinelloides_NRRL_3614__SexP
Actinomucor_elegans_NRRL_1706__SexP
Mucor_heterosporus_NRRL_3154__SexM
Zygorhynchus_heterogamus_Vuillemin_NRRL_1489__SexM
Mucor_hiemalis_f-silvaticus_NRRL_3643__SexP
Mucor_hiemalis_f-hiemalis_NRRL_3624__SexM
Mucor_saturninus_NRRL_2631__SexP
Mucor_mucedo_Linnaeus_Fresenius_NRRL_A-13277__SexM
Pilaira_caucasica_Milko_NRRL_6282__SexM
Circinella_muscae_NRRL_1360__SexM
Benjaminiella_youngii_IMI_325629__SexM
Cokeromyces_recurvatus_B5483.N154.v1__SexM
Mucor_lamprosporus_NRRL_6037__SexM
Backusella_dispersa_NRRL_6039__SexM
Backusella_dispersa_NRRL_6046__SexP
Gongronella_butleri_NRRL_1340__SexP
Cunninghamella_bertholletiae_NRRL_1380__SexM
Cunninghamella_bertholletiae_175.G680.v1__SexP
Absidia_caerulea_NRRL_1313__SexP
Absidia_caerulea_RSA_138-__SexM
Phycomyces_blakesleeanus_NRRL_1555.Phybl2.v2__SexM
Phycomyces_blakesleeanus_Burgeff_NRRL_1465__SexP
Rhizomucor_pusillus_NRRL_2543__SexP
Syncephalastrum_racemosum_CBS_441.59-__SexM
Syncephalastrum_verruculosum_RSA_2127__SexM
Rhizomucor_miehei_NRRL_5283__SexM
Rhizomucor_pusillus_NRRL_A-14037__SexM
Thamnostylum_piriforme_RSA_251__SexM
Thamnostylum_piriforme_NRRL_A-21589__SexM
Fennellomyces_heterothallicus_RSA_2348__SexM
Circinella_angarensis_RSA_618-__SexM
Dichotomocladium_elegans_NRRL_2754__SexP
Lichtheimia_blakesleeana_NRRL_1300__SexP
Lichtheimia_blakesleeana_NRRL_1301__SexM
Lentamyces_zychae_NRRL_A-23515__SexP
Umbelopsis_ramanniana_NRRL_1839__SexM
*

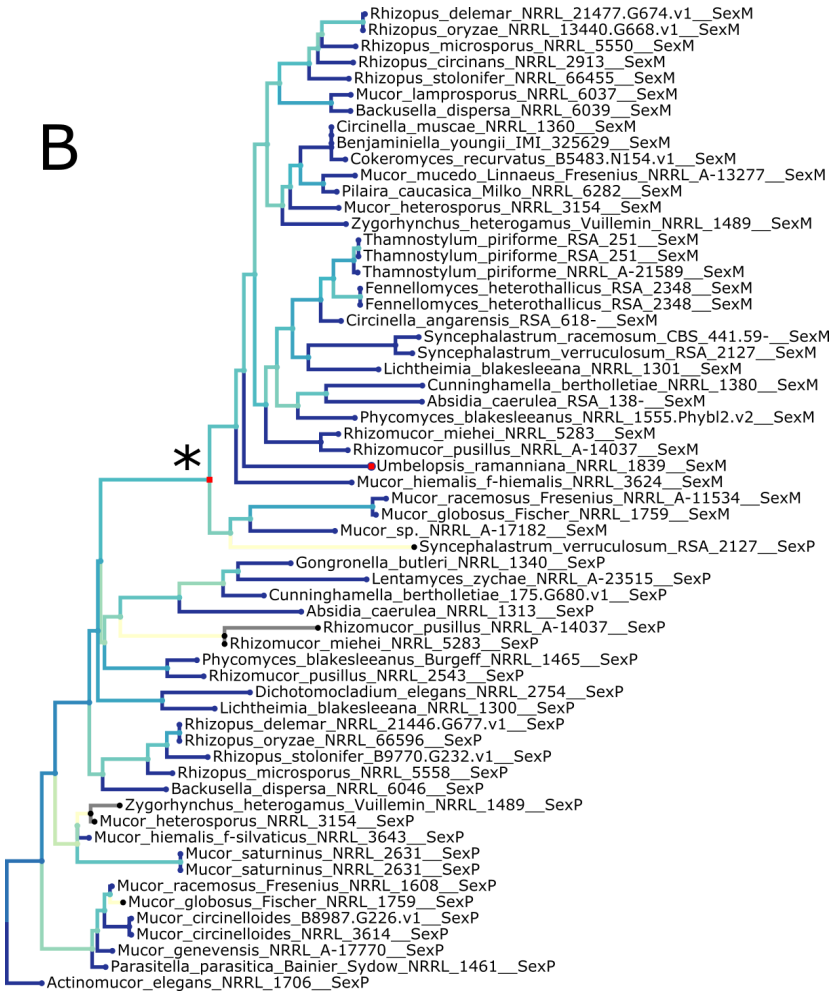
B
*
Rhizopus_delemar_NRRL_21477.G674.v1__SexM
Rhizopus_oryzae_NRRL_13440.G668.v1__SexM
Rhizopus_microsporus_NRRL_5550__SexM
Rhizopus_circinans_NRRL_2913__SexM
Rhizopus_stolonifer_NRRL_66455__SexM
Mucor_lamprosporus_NRRL_6037__SexM
Backusella_dispersa_NRRL_6039__SexM
Circinella_muscae_NRRL_1360__SexM
Benjaminiella_youngii_IMI_325629__SexM
Cokeromyces_recurvatus_B5483.N154.v1__SexM
Mucor_mucedo_Linnaeus_Fresenius_NRRL_A-13277__SexM
Pilaira_caucasica_Milko_NRRL_6282__SexM
Mucor_heterosporus_NRRL_3154__SexM
Zygorhynchus_heterogamus_Vuillemin_NRRL_1489__SexM
Thamnostylum_piriforme_RSA_251__SexM
Thamnostylum_piriforme_RSA_251__SexM
Thamnostylum_piriforme_NRRL_A-21589__SexM
Fennellomyces_heterothallicus_RSA_2348__SexM
Fennellomyces_heterothallicus_RSA_2348__SexM
Circinella_angarensis_RSA_618-__SexM
Syncephalastrum_racemosum_CBS_441.59-__SexM
Syncephalastrum_verruculosum_RSA_2127__SexM
Lichtheimia_blakesleeana_NRRL_1301__SexM
Cunninghamella_bertholletiae_NRRL_1380__SexM
Absidia_caerulea_RSA_138-__SexM
Phycomyces_blakesleeanus_NRRL_1555.Phybl2.v2__SexM
Rhizomucor_miehei_NRRL_5283__SexM
Rhizomucor_pusillus_NRRL_A-14037__SexM
Umbelopsis_ramanniana_NRRL_1839__SexM
Mucor_hiemalis_f-hiemalis_NRRL_3624__SexM
Mucor_racemosus_Fresenius_NRRL_A-11534__SexM
Mucor_globosus_Fischer_NRRL_1759__SexM
Mucor_sp._NRRL_A-17182__SexM
Syncephalastrum_verruculosum_RSA_2127__SexP
Gongronella_butleri_NRRL_1340__SexP
Lentamyces_zychae_NRRL_A-23515__SexP
Cunninghamella_bertholletiae_175.G680.v1__SexP
Absidia_caerulea_NRRL_1313__SexP
Rhizomucor_pusillus_NRRL_A-14037__SexP
Rhizomucor_miehei_NRRL_5283__SexP
Phycomyces_blakesleeanus_Burgeff_NRRL_1465__SexP
Rhizomucor_pusillus_NRRL_2543__SexP
Dichotomocladium_elegans_NRRL_2754__SexP
Lichtheimia_blakesleeana_NRRL_1300__SexP
Rhizopus_delemar_NRRL_21446.G677.v1__SexP
Rhizopus_oryzae_NRRL_66596__SexP
Rhizopus_stolonifer_B9770.G232.v1__SexP
Rhizopus_microsporus_NRRL_5558__SexP
Backusella_dispersa_NRRL_6046__SexP
Zygorhynchus_heterogamus_Vuillemin_NRRL_1489__SexP
Mucor_heterosporus_NRRL_3154__SexP
Mucor_hiemalis_f-silvaticus_NRRL_3643__SexP
Mucor_saturninus_NRRL_2631__SexP
Mucor_saturninus_NRRL_2631__SexP
Mucor_racemosus_Fresenius_NRRL_1608__SexP
Mucor_globosus_Fischer_NRRL_1759__SexP
Mucor_circinelloides_B8987.G226.v1__SexP
Mucor_circinelloides_NRRL_3614__SexP
Mucor_genevensis_NRRL_A-17770__SexP
Parasitella_parasitica_Bainier_Sydow_NRRL_1461__SexP
Actinomucor_elegans_NRRL_1706__SexP

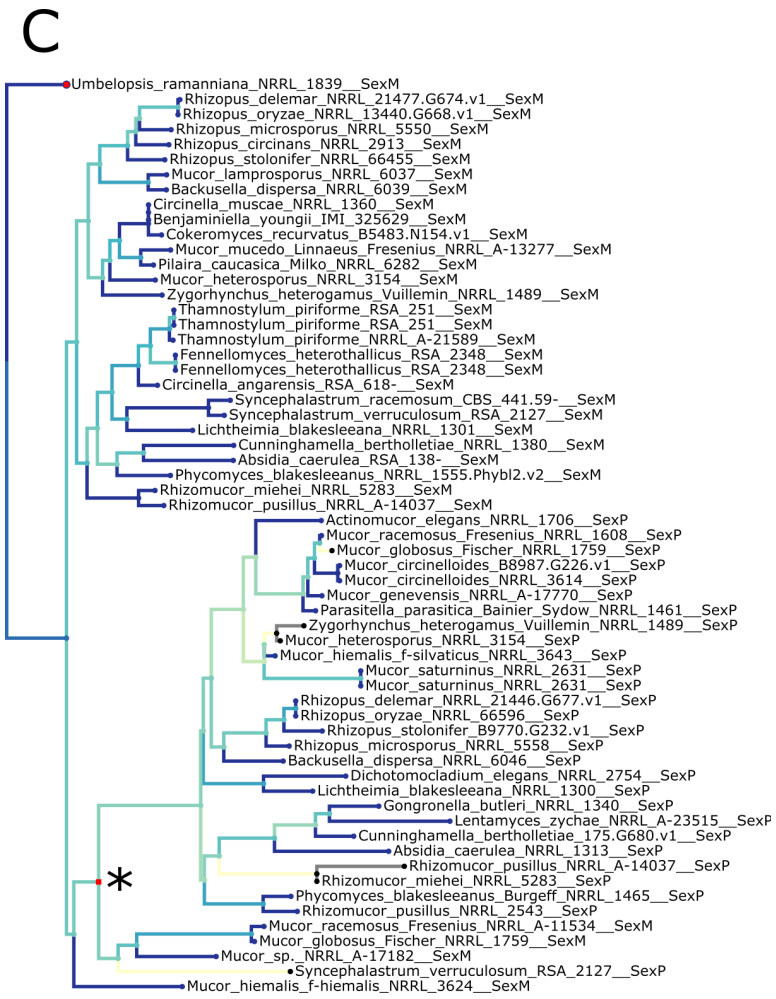

Figure 4.6 Comparison of branch similarity between the representative species tree (A) and combined SexP-SexM gene trees. Branches with high similarity as determined by phylo.io Jaccard index are shown in blue, while dissimilar branches are lighter in color or yellow. The species tree (A) was rooted by U. ramanniana. An unrooted tree (B) features paraphyletic clades of SexP while the SexM clade is more derived. When the SexP-SexM tree is rooted (C), two distinct sister clades form, each representing one of the mating-type genes. Asterisks denote nodes considered equivalent.

References

1. Thewissen JG, Hussain ST, Arif M. Fossil evidence for the origin of aquatic locomotion in archaeocete whales. Science. 1994;263:210–2.

2. Duzdevich D, Judson O, Judson O. Darwin's on the Origin of Species : A Modern Rendition. Bloomington, IN, UNITED STATES: Indiana University Press; 2014.

3. McGinnis W, Garber RL, Wirz J, Kuroiwa A, Gehring WJ. A homologous protein-coding sequence in Drosophila homeotic genes and its conservation in other metazoans. Cell. 1984;37:403–8.

4. Mark M, Rijli FM, Chambon P. Homeobox genes in embryogenesis and pathogenesis. Pediatr Res. 1997;42:421–9.

5. Ryan JF, Pang K, NISC Comparative Sequencing Program, Mullikin JC, Martindale MQ, Baxevanis AD. The homeodomain complement of the ctenophore Mnemiopsis leidyi suggests that Ctenophora and Porifera diverged prior to the ParaHoxozoa. Evodevo. 2010;1:9.

6. Simmons DK, Pang K, Martindale MQ. Lim homeobox genes in the Ctenophore Mnemiopsis leidyi: the evolution of neural cell type specification. Evodevo. 2012;3:2.

7. Fortunato SAV, Adamski M, Ramos OM, Leininger S, Liu J, Ferrier DEK, et al. Calcisponges have a ParaHox gene and dynamic expression of dispersed NK homeobox genes. Nature. 2014;514:620–3.

8. Fortunato SA, Leininger S, Adamska M. Evolution of the Pax-Six-Eya-Dach network: the calcisponge case study. Evodevo. 2014;5:23.

9. Carroll SB. Evo-devo and an expanding evolutionary synthesis: a genetic theory of morphological evolution. Cell. 2008;134:25–36.

10. Jenner RA, Wills MA. The choice of model organisms in evo-devo. Nat Rev Genet. 2007;8:311–9.

11. Barresi MJF, Gilbert SF. Developmental Biology. Oxford University Press; 2020.

12. Tomoyasu Y, Arakane Y, Kramer KJ, Denell RE. Repeated co-options of exoskeleton formation during wing-to-elytron evolution in beetles. Curr Biol. 2009;19:2057–65.

13. Booth DS, King N. Gene regulation in transition [Internet]. Nature Publishing Group UK. 2016 [cited 2022 May 26]. Available from: http://dx.doi.org/10.1038/nature18447

14. Friedrich M. Evo-Devo gene toolkit update: at least seven Pax transcription factor subfamilies in the last common ancestor of bilaterian animals. Evol Dev. 2015;17:255–7.

15. Chi N, Epstein JA. Getting your Pax straight: Pax proteins in development and disease. Trends Genet. 2002;18:41–7.

16. Shubin N, Tabin C, Carroll S. Fossils, genes and the evolution of animal limbs. Nature. 1997;388:639–48.

17. Shubin N, Tabin C, Carroll S. Deep homology and the origins of evolutionary novelty. Nature. 2009;457:818–23.

18. Drost H-G, Gabel A, Grosse I, Quint M. Evidence for active maintenance of phylotranscriptomic hourglass patterns in animal and plant embryogenesis. Mol Biol Evol. 2015;32:1221–31.

19. Irie N, Kuratani S. Comparative transcriptome analysis reveals vertebrate phylotypic period during organogenesis. Nat Commun. 2011;2:248.

20. Irie N, Kuratani S. The developmental hourglass model: a predictor of the basic body plan? Development. 2014;141:4649–55.

21. Wagner GP, Amemiya C, Ruddle F. Hox cluster duplications and the opportunity for evolutionary novelties. Proc Natl Acad Sci U S A. 2003;100:14603–6.

22. Ohno S. Evolution by Gene Duplication [Internet]. 1970. Available from: http://dx.doi.org/10.1007/978-3-642-86659-3

23. Ma L, Starr DA. Membrane fusion drives pronuclear meeting in the one-cell embryo [Internet]. J. Cell Biol. 2020. Available from: http://dx.doi.org/10.1083/jcb.202001048

24. Wendrich JR, Weijers D. The Arabidopsis embryo as a miniature morphogenesis model. New Phytol. 2013;199:14–25.

25. Goodenough U, Heitman J. Origins of eukaryotic sexual reproduction. Cold Spring Harb Perspect Biol [Internet]. 2014;6. Available from: http://dx.doi.org/10.1101/cshperspect.a016154

26. Wolpert L, Tickle C, Arias AM. Principles of Development. Oxford University Press; 2015.

27. Fournier D, Estoup A, Orivel J, Foucaud J, Jourdan H, Le Breton J, et al. Clonal reproduction by males and females in the little fire ant. Nature. 2005;435:1230–4.

28. Yang YY, Kim JG. The optimal balance between sexual and asexual reproduction in variable environments: a systematic review. Hangug hwangyeong saengtae haghoeji. BioMed Central; 2016;40:1–18.

29. Wei Y, Yang C-R, Zhao Z-A. Viable offspring derived from single unfertilized mammalian oocytes. Proc Natl Acad Sci U S A. 2022;119:e2115248119.

30. Booth W, Johnson DH, Moore S, Schal C, Vargo EL. Evidence for viable, non-clonal but fatherless Boa constrictors. Biol Lett. 2011;7:253–6.

31. Ryder OA, Thomas S, Judson JM, Romanov MN, Dandekar S, Papp JC, et al. Facultative Parthenogenesis in California Condors. J Hered. 2021;112:569–74.

32. Darwin E. Phytologia, or The philosophy of agriculture and gardening ... by Erasmus Darwin. 1800.

33. Heitman J, Kronstad JW, Taylor JW, Casselton LA, Others. Sex in fungi: molecular determination and evolutionary implications. ASM Press; 2007.

34. Smith JM, Maynard-Smith J. GRH volume 32 issue 3 Cover and Back matter. Genet Res . Hindawi Limited; 1978;32:b1–9.

35. Beukeboom LW, Perrin N. The Evolution of Sex Determination. Oxford University Press; 2014.

36. Hörandl E, Hadacek F. Oxygen, life forms, and the evolution of sexes in multicellular eukaryotes. Heredity [Internet]. 2020; Available from: http://dx.doi.org/10.1038/s41437-020-0317-9

37. Mirzaghaderi G, Hörandl E. The evolution of meiotic sex and its alternatives. Proc Biol Sci [Internet]. 2016;283. Available from: http://dx.doi.org/10.1098/rspb.2016.1221

38. Fraser JA, Heitman J. Fungal mating-type loci. Curr Biol. 2003;13:R792–5.

39. Wallen RM, Perlin MH. An Overview of the Function and Maintenance of Sexual Reproduction in Dikaryotic Fungi. Front Microbiol. 2018;9:503.

40. Lee SC, Ni M, Li W, Shertz C, Heitman J. The evolution of sex: a perspective from the fungal kingdom. Microbiol Mol Biol Rev. 2010;74:298–340.

41. Heitman J, Howlett BJ, Crous PW, Stukenbrock EH, James TY, Gow NAR. The Fungal Kingdom. ASM Press; 2017.

42. Wang Z, López-Giráldez F, Wang J, Trail F, Townsend JP. Integrative Activity of Mating Loci, Environmentally Responsive Genes, and Secondary Metabolism Pathways during Sexual Development of Chaetomium globosum. MBio [Internet]. 2019;10. Available from: http://dx.doi.org/10.1128/mBio.02119-19

43. Lehr NA, Wang Z, Li N, Hewitt DA, López-Giráldez F, Trail F, et al. Gene expression differences among three Neurospora species reveal genes required for sexual reproduction in Neurospora crassa. PLoS One. 2014;9:e110398.

44. Wang Z, Kin K, López-Giráldez F, Johannesson H, Townsend JP. Sex-specific gene expression during asexual development of Neurospora crassa. Fungal Genet Biol. 2012;49:533–43.

45. Cheng X, Hui JHL, Lee YY, Wan Law PT, Kwan HS. A “developmental hourglass” in fungi. Mol Biol Evol. 2015;32:1556–66.

46. Wang Z, Li N, Li J, Dunlap JC, Trail F, Townsend JP. The Fast-Evolving phy-2 Gene Modulates Sexual Development in Response to Light in the Model Fungus Neurospora crassa. MBio. 2016;7:e02148.

47. Galgoczy DJ, Cassidy-Stone A, Llinás M, O'Rourke SM, Herskowitz I, DeRisi JL, et al. Genomic dissection of the cell-type-specification circuit in Saccharomyces cerevisiae. Proc Natl Acad Sci U S A. 2004;101:18069–74.

48. Johnson AD. Molecular mechanisms of cell-type determination in budding yeast. Curr Opin Genet Dev. 1995;5:552–8.

49. Merlini L, Dudin O, Martin SG. Mate and fuse: how yeast cells do it. Open Biol. 2013;3:130008.

50. Herskowitz I. A regulatory hierarchy for cell specialization in yeast. Nature. 1989;342:749–57.

51. Sato S, Suzuki H, Widyastuti U, Hotta Y, Tabata S. Identification and characterization of genes induced during sexual differentiation in Schizosaccharomyces pombe. Curr Genet. 1994;26:31–7.

52. Barman A, Gohain D, Bora U, Tamuli R. Phospholipases play multiple cellular roles including growth, stress tolerance, sexual development, and virulence in fungi. Microbiol Res. 2018;209:55–69.

53. Hernández-Oñate MA, Herrera-Estrella A. Damage response involves mechanisms conserved across plants, animals and fungi. Curr Genet. 2015;61:359–72.

54. Aguirre J, Ríos-Momberg M, Hewitt D, Hansberg W. Reactive oxygen species and development in microbial eukaryotes. Trends Microbiol. 2005;13:111–8.

55. Dijksterhuis J. Fungal spores: Highly variable and stress-resistant vehicles for distribution and spoilage. Food Microbiol. 2019;81:2–11.

56. Mansfield JW, Galambos N, Saville R. The use of ascospores of the dieback fungus Hymenoscyphus fraxineus for infection assays reveals a significant period of biotrophic interaction in penetrated ash cells. Plant Pathol. Wiley; 2018;67:1354–61.

57. Wyatt TT, Wösten HAB, Dijksterhuis J. Chapter Two - Fungal Spores for Dispersion in Space and Time. In: Sariaslani S, Gadd GM, editors. Advances in Applied Microbiology. Academic Press; 2013. p. 43–91.

58. Schoustra S, Rundle HD, Dali R, Kassen R. Fitness-associated sexual reproduction in a filamentous fungus. Curr Biol. 2010;20:1350–5.

59. Cochrane VW. Dormancy in spores of fungi. Trans Am Microsc Soc. 1974;93:599–609.

60. Dyer PS, O'Gorman CM. Sexual development and cryptic sexuality in fungi: insights from Aspergillus species. FEMS Microbiol Rev. 2012;36:165–92.

61. Wang Z, Miguel-Rojas C, Lopez-Giraldez F, Yarden O, Trail F, Townsend JP. Metabolism and Development during Conidial Germination in Response to a Carbon-Nitrogen-Rich Synthetic or a Natural Source of Nutrition in Neurospora crassa.

MBio [Internet]. 2019;10. Available from: http://dx.doi.org/10.1128/mBio.00192-19

62. Nelson MA, Metzenberg RL. Sexual development genes of Neurospora crassa. Genetics. 1992;132:149–62.

63. Lubkowitz MA, Barnes D, Breslav M, Burchfield A, Naider F, Becker JM. Schizosaccharomyces pombe isp4 encodes a transporter representing a novel family of oligopeptide transporters. Mol Microbiol. 1998;28:729–41.

64. Wallen RM, Richardson K, Furnish M, Mendoza H, Dentinger A, Khanal S, et al. Hungry for Sex: Differential Roles for Ustilago maydisb Locus Components in Haploid Cells vis à vis Nutritional Availability. J Fungi (Basel) [Internet]. 2021;7. Available from: http://dx.doi.org/10.3390/jof7020135

65. Heistinger L, Moser J, Tatto NE, Valli M, Gasser B, Mattanovich D. Identification and characterization of the Komagataella phaffii mating pheromone genes. FEMS Yeast Res [Internet]. 2018;18. Available from: http://dx.doi.org/10.1093/femsyr/foy051

66. Merchán F, van den Ende H, Fernández E, Beck CF. Low-expression genes induced by nitrogen starvation and subsequent sexual differentiation in Chlamydomonas reinhardtii, isolated by the differential display technique. Planta. 2001;213:309–17.

67. Lee SC, Idnurm A. Fungal Sex: The Mucoromycota. Microbiol Spectr [Internet]. 2017;5. Available from: http://dx.doi.org/10.1128/microbiolspec.FUNK-0041-2017

68. She Z-Y, Yang W-X. Sry and SoxE genes: How they participate in mammalian sex determination and gonadal development? Semin Cell Dev Biol. 2017;63:13–22.

69. Martin T, Lu S-W, van Tilbeurgh H, Ripoll DR, Dixelius C, Turgeon BG, et al. Tracing the origin of the fungal α1 domain places its ancestor in the HMG-box superfamily: implication for fungal mating-type evolution. PLoS One. 2010;5:e15199.

70. Freihorst D, Fowler TJ, Bartholomew K, Raudaskoski M, Horton JS, Kothe E. 13 The Mating-Type Genes of the Basidiomycetes. In: Wendland J, editor. Growth, Differentiation and Sexuality. Cham: Springer International Publishing; 2016. p. 329–49.

71. Ait Benkhali J, Coppin E, Brun S, Peraza-Reyes L, Martin T, Dixelius C, et al. A network of HMG-box transcription factors regulates sexual cycle in the fungus Podospora anserina. PLoS Genet. 2013;9:e1003642.

72. Fujimura H, Yanagishima N. Mating-type-specific cell cycle arrest and shmoo formation by α pheromone of Saccharomyces cerevisiae in Hansenula wingei. Arch Microbiol. 1983;136:79–80.

73. Brun S, Kuo H-C, Jeffree CE, Thomson DD, Read N. Courtship Ritual of Male and Female Nuclei during Fertilization in Neurospora crassa. Microbiol Spectr. 2021;9:e0033521.

74. Glass NL, Grotelueschen J, Metzenberg RL. Neurospora crassa A mating-type region. Proc Natl Acad Sci U S A. 1990;87:4912–6.

75. Branco S, Carpentier F, Rodríguez de la Vega RC, Badouin H, Snirc A, Le Prieur S, et al. Multiple convergent supergene evolution events in mating-type chromosomes. Nat Commun. 2018;9:2000.

76. Branco S, Badouin H, Rodríguez de la Vega RC, Gouzy J, Carpentier F, Aguileta G, et al. Evolutionary strata on young mating-type chromosomes despite the lack of sexual antagonism. Proc Natl Acad Sci U S A. 2017;114:7067–72.

77. Samils N, Gioti A, Karlsson M, Sun Y, Kasuga T, Bastiaans E, et al. Sex-linked transcriptional divergence in the hermaphrodite fungus Neurospora tetrasperma. Proc Biol Sci. 2013;280:20130862.

78. Dranginis AM. Regulation of STA1 gene expression by MAT during the life cycle of Saccharomyces cerevisiae. Mol Cell Biol. 1989;9:3992–8.

79. Hartig A, Holly J, Saari G, MacKay VL. Multiple regulation of STE2, a mating-type-specific gene of Saccharomyces cerevisiae. Mol Cell Biol. 1986;6:2106–14.

80. Ma W-J, Carpentier F, Giraud T, Hood ME. Differential Gene Expression between Fungal Mating Types Is Associated with Sequence Degeneration. Genome Biol Evol. 2020;12:243–58.

81. Spatafora JW, Chang Y, Benny GL, Lazarus K, Smith ME, Berbee ML, et al. A phylum-level phylogenetic classification of zygomycete fungi based on genome-scale data. Mycologia. 2016;108:1028–46.

82. Hazard EI, Brookbank JW. Karyogamy and meiosis in an Amblyospora sp. (Microspora) in the mosquito Culex salinarius. J Invertebr Pathol. 1984;44:3–11.

83. Ehrenberg CG. Syzygites, eine neue Schimmelgattung: nebst Beobachtungen über sichtbare Bewegung in Schimmeln. 1829.

84. Naranjo-Ortiz MA, Gabaldón T. Fungal evolution: major ecological adaptations and evolutionary transitions. Biol Rev Camb Philos Soc. 2019;94:1443–76.

85. Moreau F. Les champignons, physiologie, morphologie développement ét systematique [Internet]. sidalc.net; 1952. Report No.: 589.222 M67 . Available from: http://www.sidalc.net/cgi-bin/wxis.exe/?IsisScript=UACHBC.xis&method=post&formato=2&cantidad=1&expresion=mfn=045263

86. Cerdá-Olmedo E. Phycomyces and the biology of light and color. FEMS Microbiol Rev. 2001;25:503–12.

87. Sanz C, Rodríguez-Romero J, Idnurm A, Christie JM, Heitman J, Corrochano LM, et al. Phycomyces MADB interacts with MADA to form the primary photoreceptor complex for fungal phototropism. Proc Natl Acad Sci U S A. 2009;106:7095–100.

88. Chaudhary S, Polaino S, Shakya VPS, Idnurm A. A new genetic linkage map of the zygomycete fungus Phycomyces blakesleeanus. PLoS One. 2013;8:e58931.

89. Silva F, Torres-Martínez S, Garre V. Distinct white collar-1 genes control specific light responses in Mucor circinelloides. Mol Microbiol. 2006;61:1023–37.

90. Göttig M, Galland P. Gravitropism in Phycomyces: violation of the so-called resultant law - evidence for two response components. Plant Biol . 2014;16 Suppl 1:158–66.

91. Puri SC, Verma V, Amna T, Qazi GN, Spiteller M. An endophytic fungus from Nothapodytes foetida that produces camptothecin. J Nat Prod. 2005;68:1717–9.

92. Tereshina VM, Memorskaya AS, Kochkina GA, Feofilova EP. Dormant Cells in the Developmental Cycle of Blakeslea trispora: Distinct Patterns of the Lipid and Carbohydrate Composition. Microbiology. 2002;71:684–9.

93. Wang H-B, He F, Lu M-B, Zhao C-F, Xiong L, Yu L-J. High-quality lycopene overaccumulation via inhibition of γ-carotene and ergosterol biosyntheses in Blakeslea trispora. J Funct Foods. 2014;7:435–42.

94. Hu W, Dai D, Li W. Anti-aging effect of Blakeslea trispora powder on adult mice. Biotechnol Lett. 2013;35:1309–15.

95. Ciegler A, Nelson GEN, Hall HH. Feed Additives, Microbiological Production of Carotenoids. Stabilization of β-Carotene in Dried Fermentation Solids. J Agric Food Chem. American Chemical Society; 1961;9:447–51.

96. Ciegler A. Microbial carotenogenesis. Adv Appl Microbiol. 1965;7:1–34.

97. Cohen Z, Ratledge C. Single Cell Oils: Microbial and Algal Oils. Elsevier Science; 2010.

98. Vinay K, Chandrasegaran A, Kanwar AJ, Saikia UN, Kaur H, Shivaprakash MR, et al. Primary cutaneous mucormycosis presenting as a giant plaque: uncommon presentation of a rare mycosis. Mycopathologia. 2014;178:97–101.

99. Xu W, Liang G, Peng J, Long Z, Li D, Fu M, et al. The influence of the mating type on virulence of Mucor irregularis. Sci Rep. 2017;7:10629.

100. Singh AK, Singh R, Joshi SR, Misra A. Mucormycosis in COVID-19: A systematic review of cases reported worldwide and in India. Diabetes Metab Syndr. 2021;15:102146.

101. Hoenigl M, Seidel D, Carvalho A, Rudramurthy SM, Arastehfar A, Gangneux J-P, et al. The emergence of COVID-19 associated mucormycosis: a review of cases from 18 countries. Lancet Microbe [Internet]. 2022; Available from: http://dx.doi.org/10.1016/S2666-5247(21)00237-8

102. Heitman J, Carter DA, Dyer PS, Soll DR. Sexual reproduction of human fungal pathogens. Cold Spring Harb Perspect Med [Internet]. 2014;4. Available from: http://dx.doi.org/10.1101/cshperspect.a019281

103. Hoffmann K, Pawłowska J, Walther G, Wrzosek M, de Hoog GS, Benny GL, et al.

The family structure of the Mucorales: a synoptic revision based on comprehensive multigene-genealogies. Persoonia. 2013;30:57–76.

104. Papp T, Csernetics Á, Nyilasi I, ÁBrÓk M, VÁgvÓlgyi C. Genetic Transformation of Zygomycetes Fungi. In: Rai M, Kövics G, editors. Progress in Mycology. Dordrecht: Springer Netherlands; 2010. p. 75–94.

105. Kellner M, Burmester A, Wöstemeyer A, Wöstemeyer J. Transfer of genetic information from the mycoparasite Parasitella parasitica to its host Absidia glauca. Curr Genet. 1993;23:334–7.

106. Schultze K, Schimek C, Wöstemeyer J, Burmester A. Sexuality and parasitism share common regulatory pathways in the fungus Parasitella parasitica. Gene. 2005;348:33–44.

107. Bergman K, Burke PV, Cerdá-Olmedo E, David CN, Delbrück M, Foster KW, et al. Phycomyces. Bacteriol Rev. 1969;33:99–157.

108. Idnurm A, Rodríguez-Romero J, Corrochano LM, Sanz C, Iturriaga EA, Eslava AP, et al. The Phycomyces madA gene encodes a blue-light photoreceptor for phototropism and other light responses. Proc Natl Acad Sci U S A. 2006;103:4546–51.

109. Corrochano LM, Kuo A, Marcet-Houben M, Polaino S, Salamov A, Villalobos-Escobedo JM, et al. Expansion of Signal Transduction Pathways in Fungi by Extensive Genome Duplication. Curr Biol. 2016;26:1577–84.

110. Nguyen TA, Greig J, Khan A, Goh C, Jedd G. Evolutionary novelty in gravity sensing through horizontal gene transfer and high-order protein assembly. PLoS Biol. 2018;16:e2004920.

111. Gutiérrez-Corona F, Cerdé-Olmedo E. Genetic determination of sporangiophore development inPhycomyces. Dev Genet. Wiley; 1988;9:733–41.

112. Mehta BJ, Cerdá-Olmedo E. Intersexual partial diploids of phycomyces. Genetics. 2001;158:635–41.

113. Idnurm A, Walton FJ, Floyd A, Heitman J. Identification of the sex genes in an early diverged fungus. Nature. 2008;451:193–6.

114. Li CH, Cervantes M, Springer DJ, Boekhout T, Ruiz-Vazquez RM, Torres-Martinez SR, et al. Sporangiospore size dimorphism is linked to virulence of Mucor circinelloides. PLoS Pathog. 2011;7:e1002086.

115. Gooday GW, Carlile MJ. The discovery of fungal sex hormones: III. Trisporic acid and its precursors. Mycologist. 1997;11:126–30.

116. Schachtschabel D, David A, Menzel K-D, Schimek C, Wöstemeyer J, Boland W. Cooperative biosynthesis of Trisporoids by the (+) and (-) mating types of the zygomycete Blakeslea trispora. Chembiochem. 2008;9:3004–12.

117. Satina S, Demerec M. MANOILOV'S REACTION FOR IDENTIFICATION OF THE SEXES. Science. 1925;62:225–6.

118. Feofilova EP. Heterothallism of mucoraceous fungi: A review of biological implications and uses in biotechnology. Appl Biochem Microbiol. 2006;42:439–54.

119. Feofilova EP, Tereshina VM, Memorskaya AS. Biochemical Mechanisms of Temperature Adaptation in the (+) and (-) Strains of Blakeslea trispora. Microbiology. 2005;74:650–4.

120. Shakya VPS, Idnurm A. Sex determination directs uniparental mitochondrial inheritance in Phycomyces. Eukaryot Cell. 2014;13:186–9.

121. Camino LP, Idnurm A, Cerdá-Olmedo E. Diversity, ecology, and evolution in Phycomyces. Fungal Biol. 2015;119:1007–21.

122. Lipson ED, Terasaka DT. Photogeotropism inPhycomyces double mutants. Exp Mycol. Elsevier; 1981;5:101–11.

123. Sanz C, Velayos A, Álvarez MI, Benito EP, Eslava AP. Functional analysis of the Phycomyces carRA gene encoding the enzymes phytoene synthase and lycopene cyclase. PLoS One. 2011;6:e23102.

124. Tagua VG, Navarro E, Gutiérrez G, Garre V, Corrochano LM. Light regulates a Phycomyces blakesleeanus gene family similar to the carotenogenic repressor gene of Mucor circinelloides. Fungal Biol. 2020;124:338–51.

125. Almeida ERA, Cerdá-Olmedo E. Gene expression in the regulation of carotene biosynthesis in Phycomyces. Curr Genet. 2008;53:129–37.

126. Lee SC, Heitman J. Sex in the Mucoralean fungi. Mycoses. 2014;57 Suppl 3:18–24.

127. Sutter RP, Whitaker JP. Zygophore-stimulating precursors (pheromones) of trisporic acids active in (-)-Phycomyces blakesleeanus. Acid-catalyzed anhydro derivatives of methyl 4-dihydrotrisporate-C and 4-dihydrotrisporate-C. J Biol Chem. 1981;256:2334–41.

128. Sarabia MJF, Eslava AP, Alvarez MI. Influence of parental strains on the germination of Phycomyces blakesleeanus zygospores. Genet Res . Cambridge University Press; 1988;52:91–5.

129. Ellegren H, Parsch J. The evolution of sex-biased genes and sex-biased gene expression. Nat Rev Genet. 2007;8:689–98.

130. Gryganskyi AP, Lee SC, Litvintseva AP, Smith ME, Bonito G, Porter TM, et al. Structure, function, and phylogeny of the mating locus in the Rhizopus oryzae complex. PLoS One. 2010;5:e15273.

131. Schulz E, Wetzel J, Burmester A, Ellenberger S, Siegmund L, Wöstemeyer J. Sex loci of homothallic and heterothallic Mucorales. Endocytobiosis Cell Res. 2016;27:39–57.

132. Gryganskyi AP, Golan J, Dolatabadi S, Mondo S, Robb S, Idnurm A, et al. Phylogenetic and Phylogenomic Definition of Rhizopus Species. G3 . 2018;8:2007–18.

133. Wetzel J, Scheibner O, Burmester A, Schimek C, Wöstemeyer J. 4-dihydrotrisporin-dehydrogenase, an enzyme of the sex hormone pathway of Mucor mucedo: purification, cloning of the corresponding gene, and developmental expression. Eukaryot Cell. 2009;8:88–95.

134. Mateus ID, Rojas EC, Savary R, Dupuis C, Masclaux FG, Aletti C, et al. Coexistence of genetically different Rhizophagus irregularis isolates induces genes involved in a putative fungal mating response. ISME J. 2020;14:2381–94.

135. Roukas T. The role of oxidative stress on carotene production by Blakeslea trispora in submerged fermentation. Crit Rev Biotechnol. 2016;36:424–33.

136. Alexa A, Rahnenfuhrer J. topGO: Enrichment Analysis for Gene Ontology. 2021.

137. Supek F, Bošnjak M, Škunca N, Šmuc T. REVIGO summarizes and visualizes long lists of gene ontology terms. PLoS One. 2011;6:e21800.

138. Kokina A, Kibilds J, Liepins J. Adenine auxotrophy--be aware: some effects of adenine auxotrophy in Saccharomyces cerevisiae strain W303-1A. FEMS Yeast Res. 2014;14:697–707.

139. Ruiz-Herrera J, Ortiz-Castellanos L. Cell wall glucans of fungi. A review. Cell Surf. 2019;5:100022.

140. Markov DA, Wojtas ID, Tessitore K, Henderson S, McAllister WT. Yeast DEAD box protein Mss116p is a transcription elongation factor that modulates the activity of mitochondrial RNA polymerase. Mol Cell Biol. 2014;34:2360–9.

141. Hamma T, Ferré-D'Amaré AR. Pseudouridine synthases. Chem Biol. 2006;13:1125–35.

142. Ackermann K, Waxmann A, Glover CV, Pyerin W. Genes targeted by protein kinase CK2: a genome-wide expression array analysis in yeast. Mol Cell Biochem. 2001;227:59–66.

143. Ding B-Y, Niu J, Shang F, Yang L, Chang T-Y, Wang J-J. Characterization of the Geranylgeranyl Diphosphate Synthase Gene in Acyrthosiphon pisum (Hemiptera: Aphididae) and Its Association With Carotenoid Biosynthesis. Front Physiol. 2019;10:1398.

144. Basenko EY, Pulman JA, Shanmugasundram A, Harb OS, Crouch K, Starns D, et al. FungiDB: An Integrated Bioinformatic Resource for Fungi and Oomycetes. J Fungi (Basel) [Internet]. 2018;4. Available from: http://dx.doi.org/10.3390/jof4010039

145. Kim Y-S, Oh D-K. Biotransformation of carotenoids to retinal by carotenoid 15,15'-oxygenase. Appl Microbiol Biotechnol. 2010;88:807–16.

146. Oh CS, Toke DA, Mandala S, Martin CE. ELO2 and ELO3, homologues of the Saccharomyces cerevisiae ELO1 gene, function in fatty acid elongation and are required for sphingolipid formation. J Biol Chem. 1997;272:17376–84.

147. Cowart LA, Obeid LM. Yeast sphingolipids: recent developments in understanding biosynthesis, regulation, and function. Biochim Biophys Acta. 2007;1771:421–31.

148. Lin R, Allis CD, Elledge SJ. PAT1, an evolutionarily conserved acetyltransferase homologue, is required for multiple steps in the cell cycle. Genes Cells. 1996;1:923–42.

149. Li Y, Yue X, Que Y, Yan X, Ma Z, Talbot NJ, et al. Characterisation of four LIM protein-encoding genes involved in infection-related development and pathogenicity by the rice blast fungus Magnaporthe oryzae. PLoS One. 2014;9:e88246.

150. Dietmeier K, Hönlinger A, Bömer U, Dekker PJ, Eckerskorn C, Lottspeich F, et al. Tom5 functionally links mitochondrial preprotein receptors to the general import pore. Nature. 1997;388:195–200.

151. Zheng W, Kathariou S. Differentiation of epidemic-associated strains of Listeria monocytogenes by restriction fragment length polymorphism in a gene region essential for growth at low temperatures (4 degrees C). Appl Environ Microbiol. 1995;61:4310–4.

152. Tsai R-T, Fu R-H, Yeh F-L, Tseng C-K, Lin Y-C, Huang Y-H, et al. Spliceosome disassembly catalyzed by Prp43 and its associated components Ntr1 and Ntr2. Genes Dev. 2005;19:2991–3003.

153. Boon K-L, Auchynnikava T, Edwalds-Gilbert G, Barrass JD, Droop AP, Dez C, et al. Yeast ntr1/spp382 mediates prp43 function in postspliceosomes. Mol Cell Biol. 2006;26:6016–23.

154. Medina HR, Cerdá-Olmedo E, Al-Babili S. Cleavage oxygenases for the biosynthesis of trisporoids and other apocarotenoids in Phycomyces. Mol Microbiol. 2011;82:199–208.

155. Doi M, Yamaoka I, Fukunaga T, Nakayama M. Isoleucine, a potent plasma glucose-lowering amino acid, stimulates glucose uptake in C2C12 myotubes. Biochem Biophys Res Commun. 2003;312:1111–7.

156. Xie X-L, Wei Y, Song Y-Y, Pan G-M, Chen L-N, Wang G, et al. Genetic Analysis of Four Sexual Differentiation Process Proteins (isp4/SDPs) in Chaetomium thermophilum and Thermomyces lanuginosus Reveals Their Distinct Roles in Development. Front Microbiol. 2019;10:2994.

157. Schmitt S, Ahting U, Eichacker L, Granvogl B, Go NE, Nargang FE, et al. Role of Tom5 in Maintaining the Structural Stability of the TOM Complex of Mitochondria*. J Biol Chem. 2005;280:14499–506.

158. Bornscheuer UT. Microbial carboxyl esterases: classification, properties and application in biocatalysis. FEMS Microbiol Rev. 2002;26:73–81.

159. Cavazzini D, Grossi G, Levati E, Vallese F, Montanini B, Bolchi A, et al. A family of archaea-like carboxylesterases preferentially expressed in the symbiotic phase of the mychorrizal fungus Tuber melanosporum. Sci Rep. 2017;7:7628.

160. Hipol RM, Broñola-Hipol RL. Carboxylesterase activity of fungi isolated from Marchantia polymorpha [Internet]. [cited 2022 Mar 27]. Available from: https://environmentaljournals.org/storage/models/article/eaNe9DtVqa34Ry1yUx3sNavUIRGj87LaIW1ybTEGKKrkGhRnEYTHnYziDwmx/carboxylesterase-activity-of-fungi-isolated-from-marchantia-polymorpha.pdf

161. Emms DM, Kelly S. OrthoFinder: phylogenetic orthology inference for comparative genomics. Genome Biol. 2019;20:238.

162. Ellison CE, Stajich JE, Jacobson DJ, Natvig DO, Lapidus A, Foster B, et al. Massive changes in genome architecture accompany the transition to self-fertility in the filamentous fungus Neurospora tetrasperma. Genetics. 2011;189:55–69.

163. Seppey M, Manni M, Zdobnov EM. BUSCO: Assessing Genome Assembly and Annotation Completeness. Methods Mol Biol. 2019;1962:227–45.

164. Jain C, Rodriguez-R LM, Phillippy AM, Konstantinidis KT, Aluru S. High throughput ANI analysis of 90K prokaryotic genomes reveals clear species boundaries. Nat Commun. 2018;9:5114.

165. Alonge M, Lebeigle L, Kirsche M, Aganezov S, Wang X, Lippman ZB, et al. Automated assembly scaffolding elevates a new tomato system for high-throughput genome editing [Internet]. bioRxiv. 2021 [cited 2022 Jun 9]. p. 2021.11.18.469135. Available from: https://www.biorxiv.org/content/10.1101/2021.11.18.469135v1

166. Bray NL, Pimentel H, Melsted P, Pachter L. Near-optimal probabilistic RNA-seq quantification. Nat Biotechnol. 2016;34:525–7.

167. Love MI, Huber W, Anders S. Moderated estimation of fold change and dispersion for RNA-seq data with DESeq2. Genome Biol. 2014;15:550.

168. Wickham H. ggplot2-Elegant Graphics for Data Analysis. Springer International Publishing. Cham, Switzerland. 2016;

169. Pheatmap: pretty heatmaps [Internet]. [cited 2022 Jun 10]. Available from: https://scholar.google.ca/scholar?cluster=14492249782051319874,10264989065414428931,16059388166350612695,4736603005197181311&hl=en&as_sdt=0,5&sciodt=0,5

170. Grolig F, Moch J, Schneider A, Galland P. Actin cytoskeleton and organelle movement in the sporangiophore of the zygomycete Phycomyces blakesleeanus. Plant Biol . 2014;16 Suppl 1:167–78.

171. Idnurm A. Sex determination in the first-described sexual fungus. Eukaryot Cell. 2011;10:1485–91.

172. De Cima S, Rúa J, Perdiguero E, del Valle P, Busto F, Baroja-Mazo A, et al. An

acetyl-CoA synthetase not encoded by the facA gene is expressed under carbon starvation in Phycomyces blakesleeanus. Res Microbiol. 2005;156:663–9.

173. Shakya VPS, Idnurm A. The inhibition of mating in Phycomyces blakesleeanus by light is dependent on the MadA-MadB complex that acts in a sex-specific manner. Fungal Genet Biol. 2017;101:20–30.

174. Murillo FJ, Cerdá-Olmedo E. Regulation of carotene synthesis in Phycomyces. Mol Gen Genet. 1976;148:19–24.

175. Schimek C, Petzold A, Schultze K, Wetzel J, Wolschendorf F, Burmester A, et al. 4-Dihydromethyltrisporate dehydrogenase, an enzyme of the sex hormone pathway in Mucor mucedo, is constitutively transcribed but its activity is differently regulated in (+) and (−) mating types. Fungal Genet Biol. 2005;42:804–12.

176. Kuzina V, Domenech C, Cerdá-Olmedo E. Relationships among the biosyntheses of ubiquinone, carotene, sterols, and triacylglycerols in Zygomycetes. Arch Microbiol. 2006;186:485–93.

177. Sahadevan Y, Richter-Fecken M, Kaerger K, Voigt K, Boland W. Early and late trisporoids differentially regulate β-carotene production and gene transcript Levels in the mucoralean fungi Blakeslea trispora and Mucor mucedo. Appl Environ Microbiol. 2013;79:7466–75.

178. Burmester A, Richter M, Schultze K, Voelz K, Schachtschabel D, Boland W, et al. Cleavage of beta-carotene as the first step in sexual hormone synthesis in zygomycetes is mediated by a trisporic acid regulated beta-carotene oxygenase. Fungal Genet Biol. 2007;44:1096–108.

179. Malika C, Ghazzali N, Boiteau V, Niknafs A. NbClust: an R package for determining the relevant number of clusters in a data Set. J Stat Softw. 2014;61:1–36.

180. Arrach N, Fernández-Martín R, Cerdá-Olmedo E, Avalos J. A single gene for lycopene cyclase, phytoene synthase, and regulation of carotene biosynthesis in Phycomyces. Proc Natl Acad Sci U S A. 2001;98:1687–92.

181. Demerec, M, Adelberg, E. A, Clark, A. J, Hartman, P. E. A proposal for a uniform nomenclature in bacterial genetics. Genetics. 1966;54:61–76.

182. Wetzel J, Burmester A, Kolbe M, Wöstemeyer J. The mating-related loci sexM and sexP of the zygomycetous fungus Mucor mucedo and their transcriptional regulation by trisporoid pheromones. Microbiology. 2012;158:1016–23.

183. Ries LNA, Beattie S, Cramer RA, Goldman GH. Overview of carbon and nitrogen catabolite metabolism in the virulence of human pathogenic fungi. Mol Microbiol. Wiley; 2018;107:277–97.

184. Vichido I, Mora Y, Quinto C, Palacios R, Mora J. Nitrogen regulation of glutamine synthetase in Neurospora crassa. J Gen Microbiol. 1978;106:251–9.

185. Fayyad-Kazan M, Feller A, Bodo E, Boeckstaens M, Marini AM, Dubois E, et al. Yeast nitrogen catabolite repression is sustained by signals distinct from glutamine and glutamate reservoirs. Mol Microbiol. 2016;99:360–79.

186. Wagner D, Wiemann P, Huß K, Brandt U, Fleißner A, Tudzynski B. A sensing role of the glutamine synthetase in the nitrogen regulation network in Fusarium fujikuroi. PLoS One. 2013;8:e80740.

187. Schwartz T, Kusnanj: MB, Fock HP. The involvement of glutamate dehydrogenase and glutamine synthetaselglutamate synthase in ammonia assimilation by the basidiomycete fungus Stropharia semiglobata [Internet]. 1991 [cited 2021 Apr 22]. Available from: https://www.microbiologyresearch.org/docserver/fulltext/micro/137/9/mic-137-9-2253.pdf?expires=1619127834&id=id&accname=sgid024313&checksum=A79C62FB56D4523CE2718AF8A95F0DC0

188. Fu YH, Marzluf GA. Characterization of nit-2, the major nitrogen regulatory gene of Neurospora crassa. Mol Cell Biol. 1987;7:1691–6.

189. Yuan GF, Fu YH, Marzluf GA. nit-4, a pathway-specific regulatory gene of Neurospora crassa, encodes a protein with a putative binuclear zinc DNA-binding domain. Mol Cell Biol. 1991;11:5735–45.

190. Marzluf GA. Genetics and molecular genetics of sulfur assimilation in the fungi. Adv Genet. 1994;31:187–206.

191. Breitenbach M, Weber M, Rinnerthaler M, Karl T, Breitenbach-Koller L. Oxidative stress in fungi: its function in signal transduction, interaction with plant hosts, and lignocellulose degradation. Biomolecules. 2015;5:318–42.

192. Kayano Y, Tanaka A, Akano F, Scott B, Takemoto D. Differential roles of NADPH oxidases and associated regulators in polarized growth, conidiation and hyphal fusion in the symbiotic fungus Epichloë festucae. Fungal Genet Biol. 2013;56:87–97.

193. Cano-Domínguez N, Alvarez-Delfín K, Hansberg W, Aguirre J. NADPH oxidases NOX-1 and NOX-2 require the regulatory subunit NOR-1 to control cell differentiation and growth in Neurospora crassa. Eukaryot Cell. 2008;7:1352–61.

194. Hassing B, Eaton CJ, Winter D, Green KA, Brandt U, Savoian MS, et al. Phosphatidic acid produced by phospholipase D is required for hyphal cell-cell fusion and fungal-plant symbiosis. Mol Microbiol. 2020;113:1101–21.

195. Araujo-Palomares CL, Richthammer C, Seiler S, Castro-Longoria E. Functional characterization and cellular dynamics of the CDC-42 - RAC - CDC-24 module in Neurospora crassa. PLoS One. 2011;6:e27148.

196. Chollet J, Dünkler A, Bäuerle A, Vivero-Pol L, Mulaw MA, Gronemeyer T, et al. Cdc24 interacts with septins to create a positive feedback loop during bud site assembly in yeast. J Cell Sci [Internet]. 2020;133. Available from:

http://dx.doi.org/10.1242/jcs.240283

197. Soulard A, Friant S, Fitterer C, Orange C, Kaneva G, Mirey G, et al. The WASP/Las17p-interacting protein Bzz1p functions with Myo5p in an early stage of endocytosis. Protoplasma. 2005;226:89–101.

198. Saengsawang W, Taylor KL, Lumbard DC, Mitok K, Price A, Pietila L, et al. CIP4 coordinates with phospholipids and actin-associated proteins to localize to the protruding edge and produce actin ribs and veils. J Cell Sci. 2013;126:2411–23.

199. Tonucci FM, Hidalgo F, Ferretti A, Almada E, Favre C, Goldenring JR, et al. Centrosomal AKAP350 and CIP4 act in concert to define the polarized localization of the centrosome and Golgi in migratory cells. J Cell Sci. 2015;128:3277–89.

200. Dietl A-M, Binder U, Bauer I, Shadkchan Y, Osherov N, Haas H. Arginine Auxotrophy Affects Siderophore Biosynthesis and Attenuates Virulence of Aspergillus fumigatus. Genes [Internet]. 2020;11. Available from: http://dx.doi.org/10.3390/genes11040423

201. Ghosh S, Navarathna DHMLP, Roberts DD, Cooper JT, Atkin AL, Petro TM, et al. Arginine-induced germ tube formation in Candida albicans is essential for escape from murine macrophage line RAW 264.7. Infect Immun. 2009;77:1596–605.

202. Serlupi-Crescenzi O, Kurtz MB, Champe SP. Developmental defects resulting from arginine auxotrophy in Aspergillus nidulans. J Gen Microbiol. 1983;129:3535–44.

203. Wilson AM, Wilken PM, van der Nest MA, Wingfield MJ, Wingfield BD. It's All in the Genes: The Regulatory Pathways of Sexual Reproduction in Filamentous Ascomycetes. Genes [Internet]. 2019;10. Available from: http://dx.doi.org/10.3390/genes10050330

204. Riquelme M, Aguirre J, Bartnicki-García S, Braus GH, Feldbrügge M, Fleig U, et al. Fungal Morphogenesis, from the Polarized Growth of Hyphae to Complex Reproduction and Infection Structures. Microbiol Mol Biol Rev [Internet]. 2018;82. Available from: http://dx.doi.org/10.1128/MMBR.00068-17

205. Fajardo-Somera RA, Jöhnk B, Bayram Ö, Valerius O, Braus GH, Riquelme M. Dissecting the function of the different chitin synthases in vegetative growth and sexual development in Neurospora crassa. Fungal Genet Biol. 2015;75:30–45.

206. Peraza-Reyes L, Berteaux-Lecellier V. Peroxisomes and sexual development in fungi. Front Physiol. 2013;4:244.

207. Van Assche JA, Van Laere AJ, Carlier AR. Trehalose metabolism in dormant and activated spores of Phycomyces blakesleeanus Burgeff. Planta. 1978;139:171–6.

208. Rossanese OW, Reinke CA, Bevis BJ, Hammond AT, Sears IB, O'Connor J, et al. A role for actin, Cdc1p, and Myo2p in the inheritance of late Golgi elements in Saccharomyces cerevisiae. J Cell Biol. 2001;153:47–62.

209. Halbrook J, Hoekstra MF. Mutations in the Saccharomyces cerevisiae CDC1 gene

affect double-strand-break-induced intrachromosomal recombination. Mol Cell Biol. 1994;14:8037–50.

210. Vazquez HM, Vionnet C, Roubaty C, Conzelmann A. Cdc1 removes the ethanolamine phosphate of the first mannose of GPI anchors and thereby facilitates the integration of GPI proteins into the yeast cell wall. Mol Biol Cell. 2014;25:3375–88.

211. Barraza A, Sánchez F. Trehalases: a neglected carbon metabolism regulator? Plant Signal Behav. 2013;8:e24778.

212. Sievers F, Wilm A, Dineen D, Gibson TJ, Karplus K, Li W, et al. Fast, scalable generation of high-quality protein multiple sequence alignments using Clustal Omega. Mol Syst Biol. 2011;7:539.

213. Lee SC, Corradi N, Doan S, Dietrich FS, Keeling PJ, Heitman J. Evolution of the sex-related locus and genomic features shared in microsporidia and fungi. PLoS One. 2010;5:e10539.

214. Ootaki T, Yamazaki Y, Noshita T, Takahashi S. Excess carotenoids disturb prospective cell-to-cell recognition system in mating responses ofPhycomyces blakesleeanus. Mycoscience. Springer-Verlag; 1996;37:427.

215. Kito H, Abe A, Sujaya I-N, Oda Y, Asano K, Sone T. Molecular characterization of the relationships among Amylomyces rouxii, Rhizopus oryzae, and Rhizopus delemar. Biosci Biotechnol Biochem. 2009;73:861–4.

216. Walther G, Pawłowska J, Alastruey-Izquierdo A, Wrzosek M, Rodriguez-Tudela JL, Dolatabadi S, et al. DNA barcoding in Mucorales: an inventory of biodiversity. Persoonia. 2013;30:11–47.

217. Robinson O, Dylus D, Dessimoz C. Phylo.io: Interactive Viewing and Comparison of Large Phylogenetic Trees on the Web. Mol Biol Evol. 2016;33:2163–6.

218. Younis IR, Elliott M, Peer CJ, Cooper AJL, Pinto JT, Konat GW, et al. Dehydroalanine analog of glutathione: an electrophilic busulfan metabolite that binds to human glutathione S-transferase A1-1. J Pharmacol Exp Ther. 2008;327:770–6.

219. Hawker LE, Beckett A. Fine Structure and Development of the Zygospore of Rhizopus sexualis (Smith) Callen. Philos Trans R Soc Lond B Biol Sci. The Royal Society; 1971;263:71–100.

220. Li J, Mahajan A, Tsai M-D. Ankyrin repeat: a unique motif mediating protein-protein interactions. Biochemistry. 2006;45:15168–78.

221. Wang J, Teves ME, Shen X, Nagarkatti-Gude DR, Hess RA, Henderson SC, et al. Mouse RC/BTB2, a member of the RCC1 superfamily, localizes to spermatid acrosomal vesicles. PLoS One. 2012;7:e39846.

222. Pearson WR, Wood T, Zhang Z, Miller W. Comparison of DNA sequences with protein sequences. Genomics. 1997;46:24–36.

223. Quinlan AR, Hall IM. BEDTools: a flexible suite of utilities for comparing genomic features. Bioinformatics. 2010;26:841–2.

224. Slater GSC, Birney E. Automated generation of heuristics for biological sequence comparison. BMC Bioinformatics. 2005;6:31.

225. Rice P, Longden I, Bleasby A. EMBOSS: the European Molecular Biology Open Software Suite. Trends Genet. 2000;16:276–7.

226. Edgar RC. MUSCLE: multiple sequence alignment with high accuracy and high throughput. Nucleic Acids Res. 2004;32:1792–7.

227. Price MN, Dehal PS, Arkin AP. FastTree 2--approximately maximum-likelihood trees for large alignments. PLoS One. 2010;5:e9490.

228. Revell LJ. phytools: an R package for phylogenetic comparative biology (and other things). Methods Ecol Evol. Wiley; 2012;3:217–23.

229. Yu G, Smith DK, Zhu H, Guan Y, Lam TT-Y. Ggtree : An r package for visualization and annotation of phylogenetic trees with their covariates and other associated data. Methods Ecol Evol. Wiley; 2017;8:28–36.

230. Paradis E, Claude J, Strimmer K. APE: Analyses of Phylogenetics and Evolution in R language. Bioinformatics. 2004;20:289–90.

231. Hopke A, Mela A, Ellett F, Carter-House D, Peña JF, Stajich JE, et al. Crowdsourced analysis of fungal growth and branching on microfluidic platforms. PLoS One. 2021;16:e0257823.

232. Stajich JE. Fungal Genomes and Insights into the Evolution of the Kingdom. Microbiol Spectr [Internet]. 2017;5. Available from: http://dx.doi.org/10.1128/microbiolspec.FUNK-0055-2016

233. Langfelder P, Horvath S. WGCNA: an R package for weighted correlation network analysis. BMC Bioinformatics. 2008;9:559.

234. Conway JR, Lex A, Gehlenborg N. UpSetR: an R package for the visualization of intersecting sets and their properties. Bioinformatics. 2017;33:2938–40.

Appendix

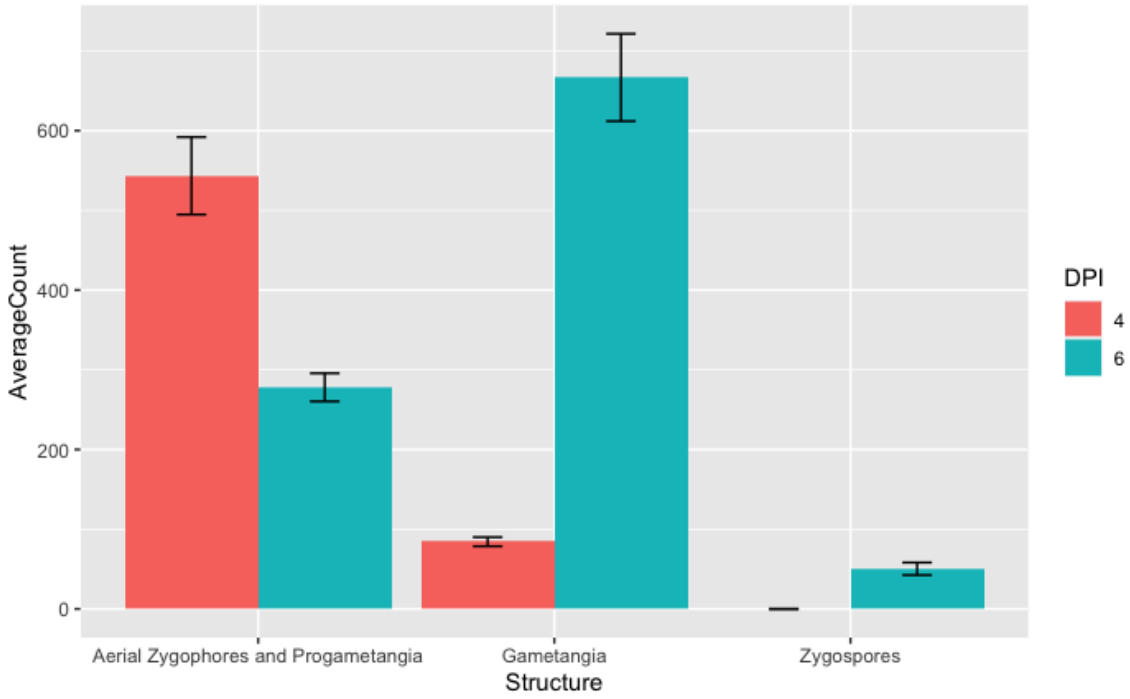

DPI	Structure	AverageCount	StdErr
4	Aerial Zygophores and Progametangia	543.3333333	48.5878357
6	Aerial Zygophores and Progametangia	278	17.61628035
4	Gametangia	84.33333333	5.696002497
6	Gametangia	666.6666667	54.83409321
4	Zygospores	0	0
6	Zygospores	50.33333333	7.838650678

Figure A.3.1 Quantification of sexual structures

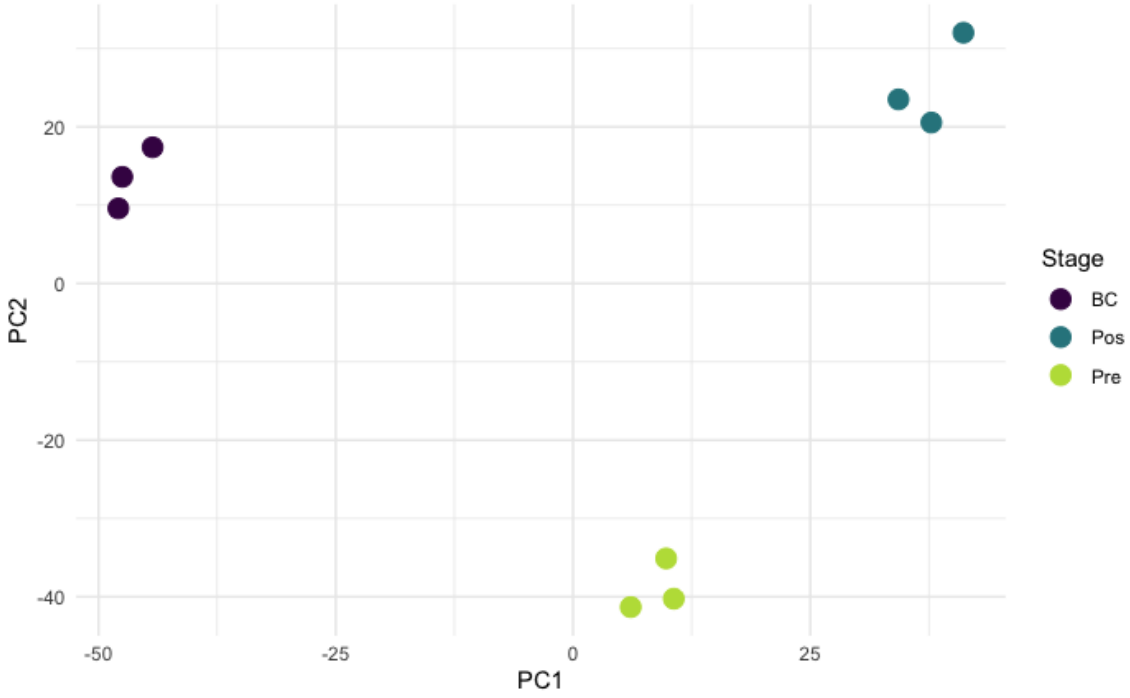

Figure A.3.1. PCA plot with three timepoints (BC-minus, pre-fusion, post-fusion)

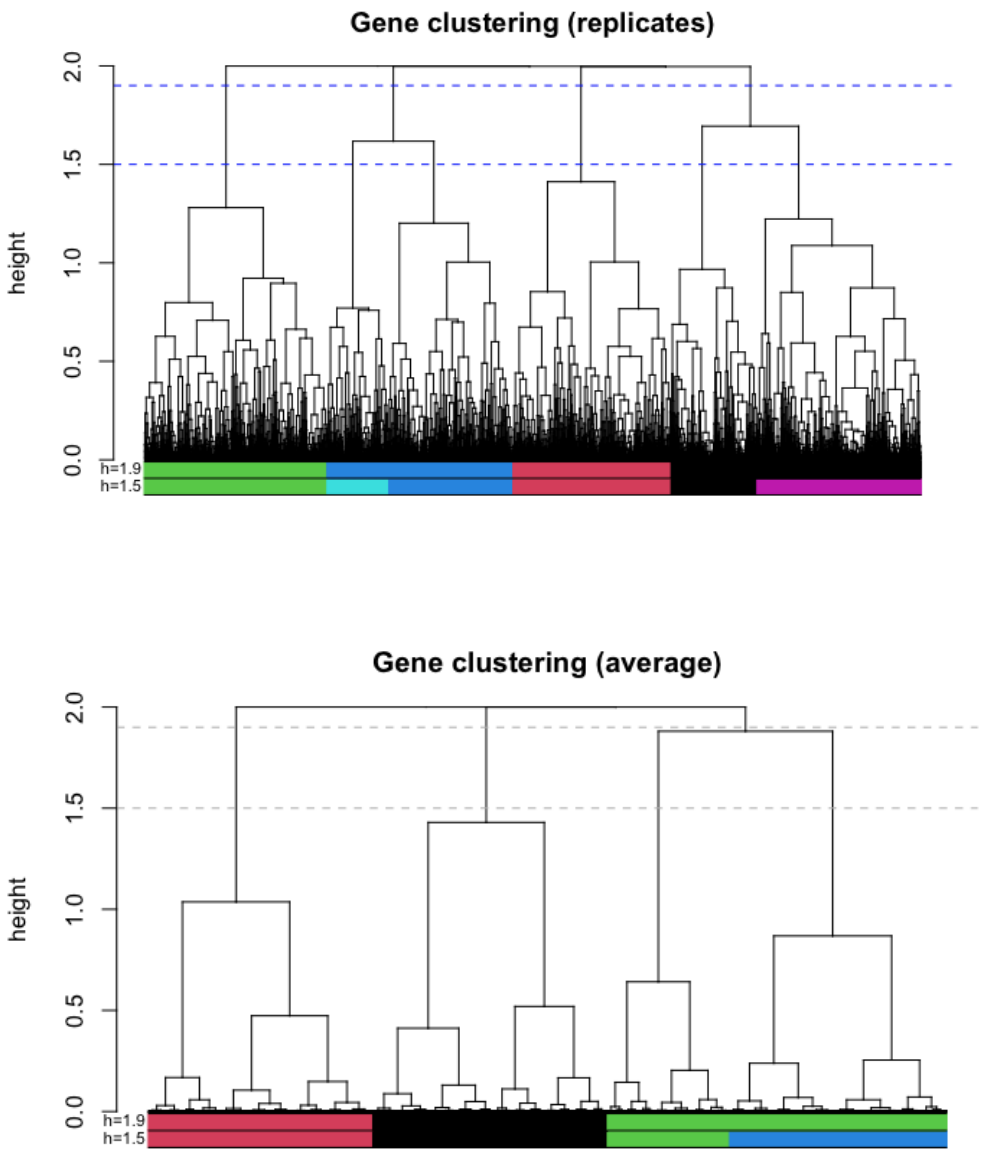

Figure A.3.2. Hierarchical clustering of genes recovers 4 top-level/broad expression clusters. genes clustered by average expression. Two different cut heights suggest different number of clusters, though still at a broader level. When looking at replicates, the cluster number changes at the same height. When clustering with replicates, there are 4 broad cluster

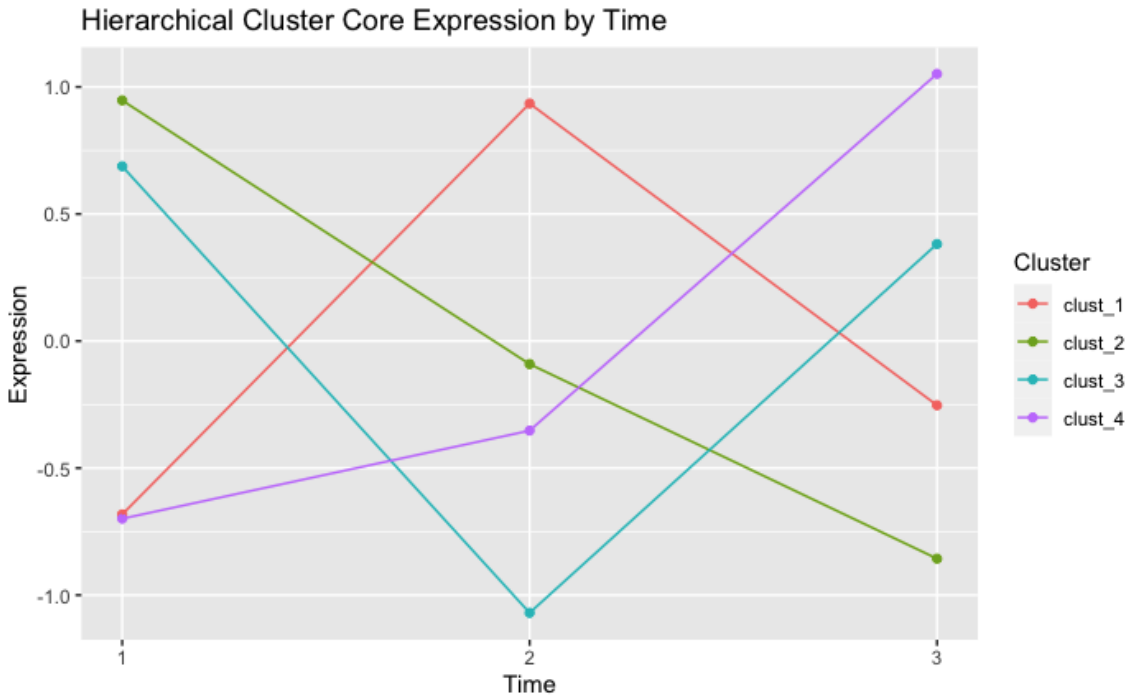

Figure A.3.3. Hierarchical Expression cluster medoids, h=1.5 using average expression

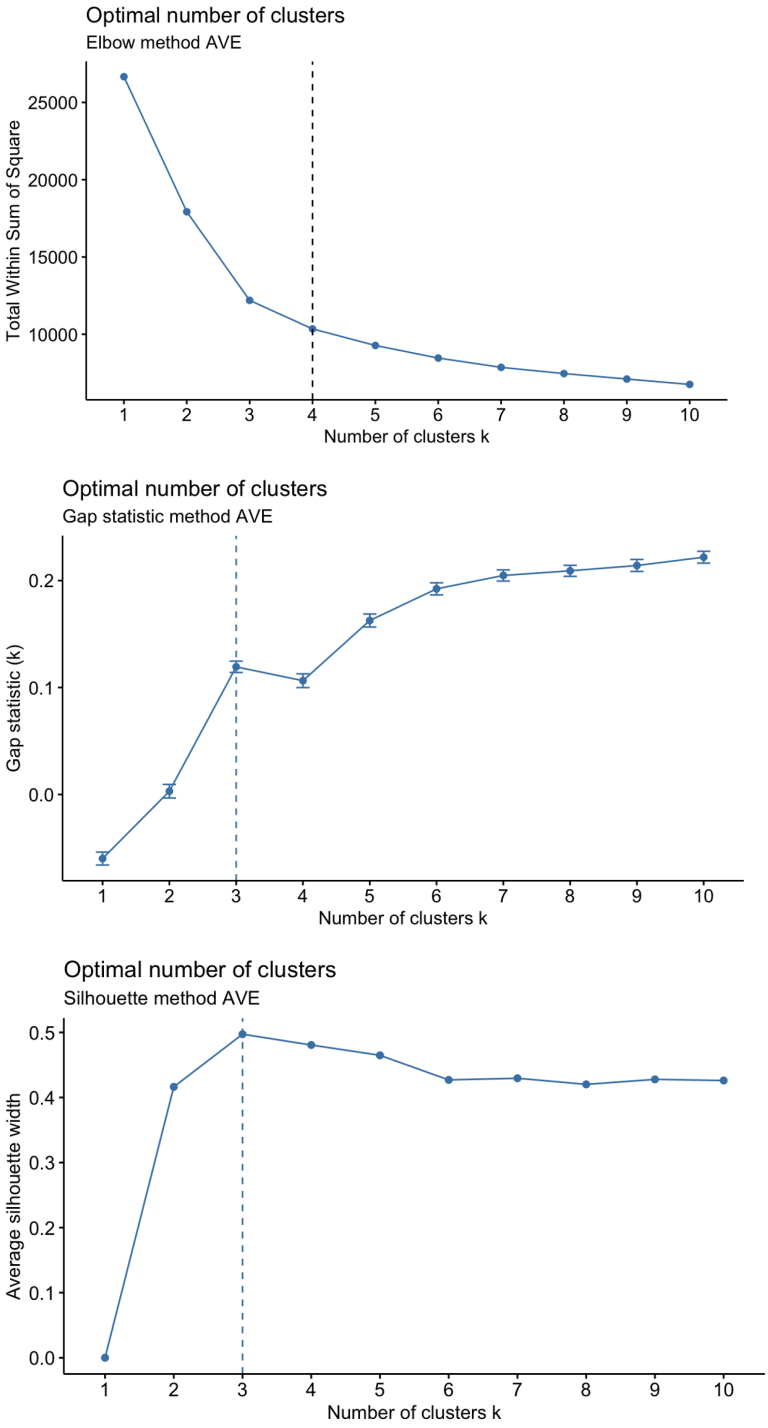

Figure A.3.4. Three plots for determining optimal K.

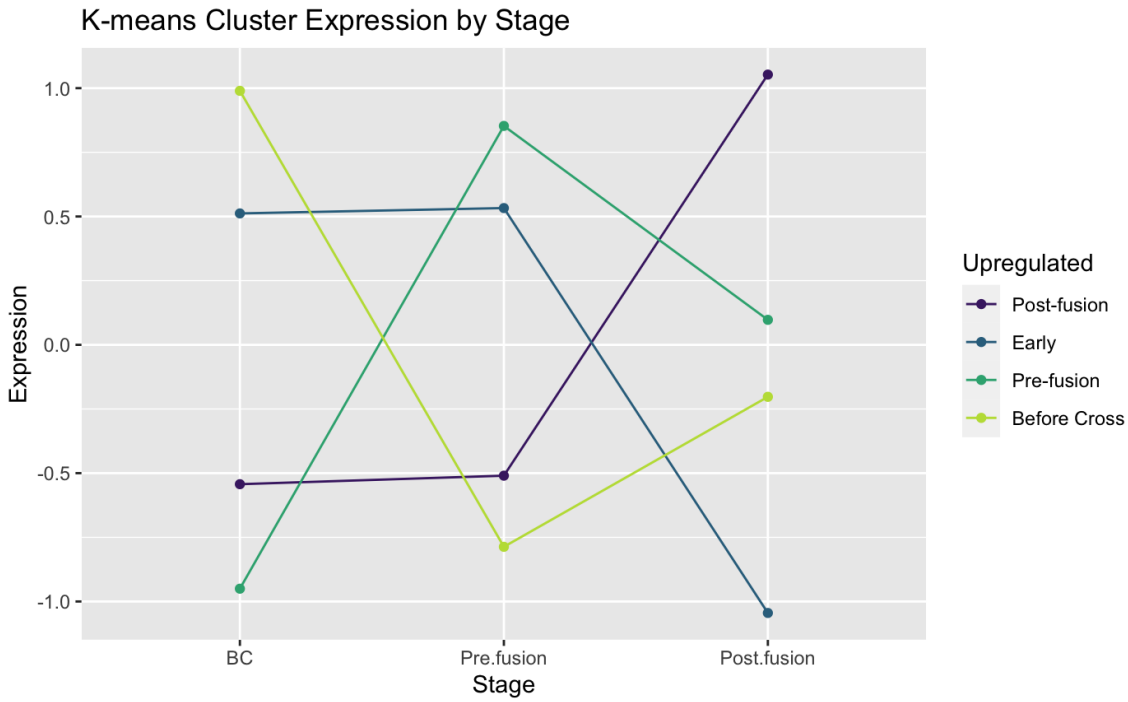

Figure A.3.5. Centroids of K-means clusters (K=4) plotted over time.

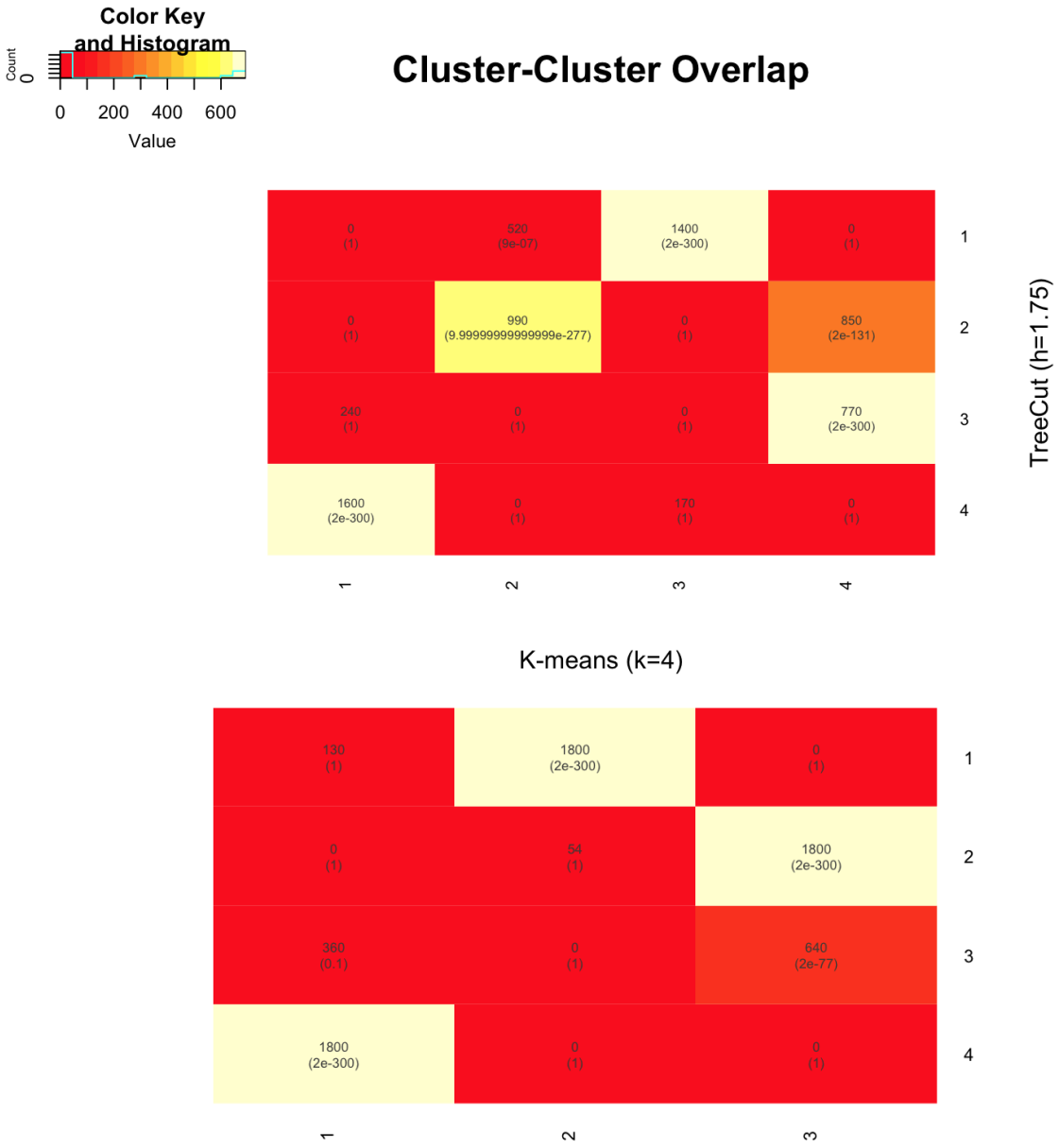

Figure A.3.6. 3/4 k-means and hierarchical clusters share member genes. Hierarchical cluster 2 shares members with two K-means clusters, Early and Post-fusion. Below is an additional view where K=3, but still using the 4 clusters from the hierarchical clustering analysis. Figures were produced with the WGCNA R package [233]

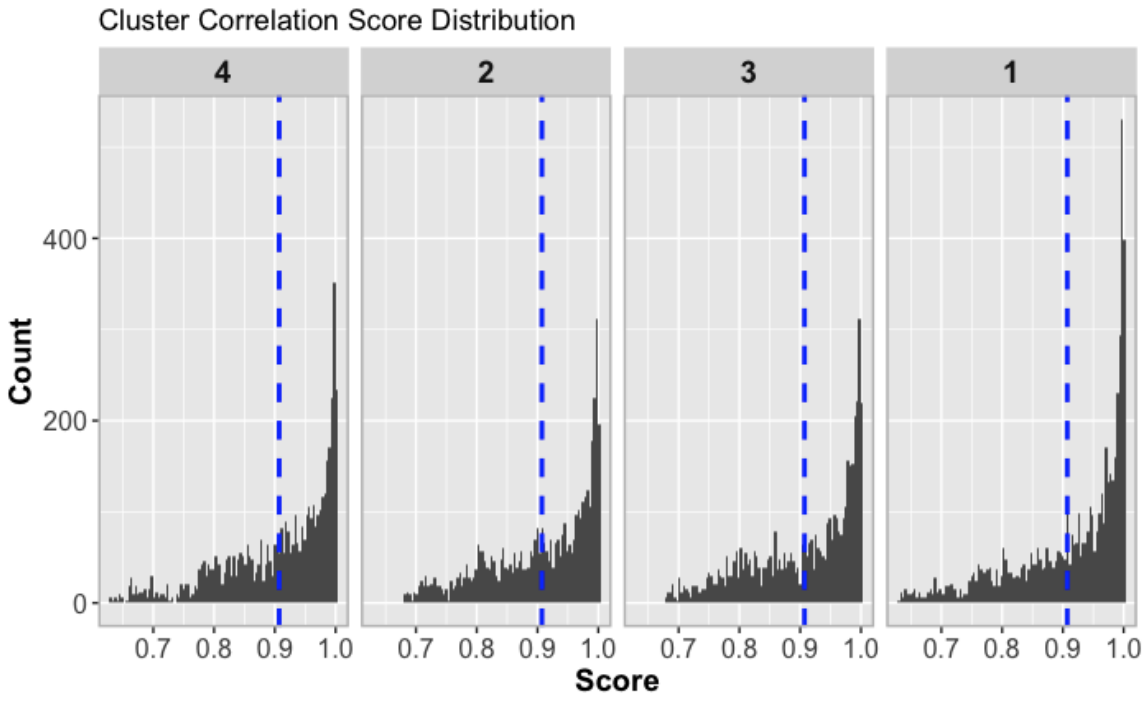

	BCx (4)	EAx (2)	PEx (3)	POx (1)
>= mean score	931 (57%)	827 (54%)	895 (56%)	1140 (61%)
< mean score	687	690	686	707
mean	**0.9054046**	**0.9047827**	**0.9054088**	**0.9119074**

Figure A.3.7. The histograms above show how the scores within the k-means clusters are distributed. The blue line represents the average score for that cluster. Generally, a little over half of the genes in the analysis have a correlation score higher than the average. Taking the average of scores within a cluster at a specific stage is no different than taking the average of scores across all three timepoints.

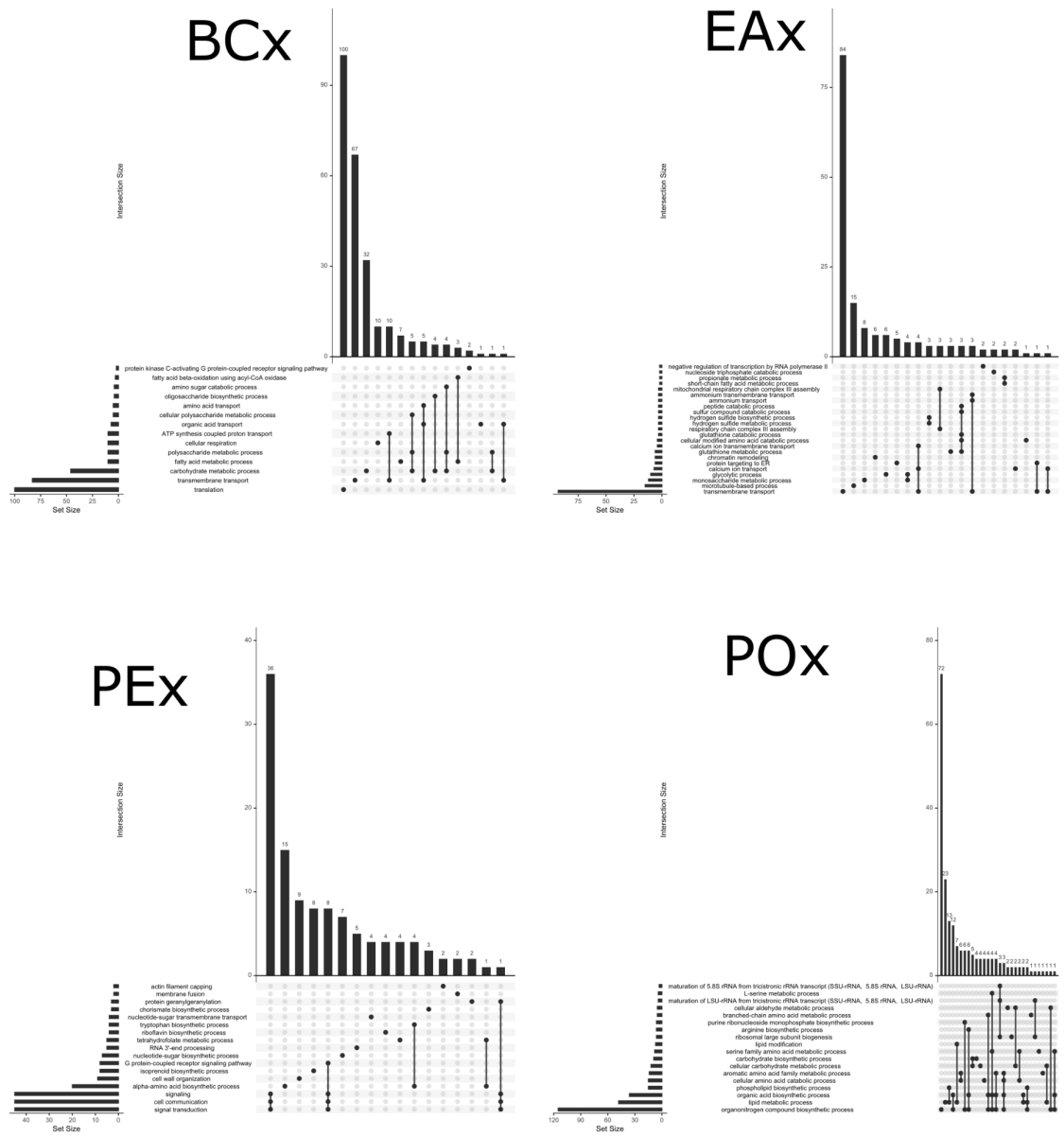

Figure A.3.8. GO enrichment terms overlap by cluster (upset plot). Upset plots produced with [234]

CLUSTAL Alignment of RNA helicse genes from UBC21 and NRRL1555

(+)RnhA_U21|1878835/1-1290
MSSRKSSRQRPPRGWDHSPRPQIDGPITVNANINFDTNEYQVSPAQPQVEYGYNQN
QDRS
(-)RnhA_NRRL1555|87354/1-649
MSSRKSSRQRPPRGWDHSPRPQIDGPITVNANINFDTNEYQVSPAQPQVEYGYNQN
QDCS
(-)RnhB_NRRL1555|157139/1-227 ----------

(+)RnhA_U21|1878835/1-1290
MRWAAEAQASWNTPFSTNTNFNTSSQPSSSQSSSAFNNSSGFQAWVEPTRSPERF
SHPDQ
(-)RnhA_NRRL1555|87354/1-649
MRWAAEAQASWNTPFSTNTNFNTSSQPSSSQSSSAFNNSSGFQAWVEPTRSPERF
SHPDQ
(-)RnhB_NRRL1555|157139/1-227 ----------

(+)RnhA_U21|1878835/1-1290
VVFKLNTEIPDRPIFVEKVDFASYRSKPIVPDPAEIMQGPPQVPVSNDRGRRDERILHI
P
(-)RnhA_NRRL1555|87354/1-649
VVFKLNTEIPDRPIFVEKVDFASYRSKPIVPDPAEIMQGPPQVPVSNDRGRRDERIPHI
P
(-)RnhB_NRRL1555|157139/1-227 ----------

(+)RnhA_U21|1878835/1-1290
VNHVRGPYESTDEYLYTHFELMRQDCLIPLQKAVQSYRLTADKPKDKLGLAMSDDQV
ETV
(-)RnhA_NRRL1555|87354/1-649
VNHVRGPYESTDEYLYTHFELMRQDCLIPLQKAVQSYRLTADKPKDKLGLAMSDDQV
ETV
(-)RnhB_NRRL1555|157139/1-227 ----------

(+)RnhA_U21|1878835/1-1290
ALSRDYRLYEHVRLNAIVFGSRQTLYRISFRLPYYCRVKWPQSKRLMEGSMVLLSKD
NFV
(-)RnhA_NRRL1555|87354/1-649
ALSRDYRLYEHVRLNAIVFGSRQTLYRISFRLPYYCRVKWPQSKRLMEGSMVLLSKD
NFV
(-)RnhB_NRRL1555|157139/1-227 ----------

(+)RnhA_U21|1878835/1-1290
SDIKIATVVNRGDEPMRGSSRFEYMINVKLECDNERDPLGFGDPSSADQDTYVMIEA
PTG

(-)RnhA_NRRL1555|87354/1-649
SDIKIATVVNRGDEPMRGSSRFEYMINVKLECDNERDPLGFGDPSSADQDTYVMIEA
PTG
(-)RnhB_NRRL1555|157139/1-227 ----------

(+)RnhA_U21|1878835/1-1290
YFEAYRHILSVLKNTQADELPLASYLVDISQDIRLPYYASRKQFYDIDPRKPTNSRDQQ
K
(-)RnhA_NRRL1555|87354/1-649
YFEAYRHILSVLKNTQADELPLASYLVDISQDIRLPYYASRKQFYDIDPRKPTNSRDQQ
K
(-)RnhB_NRRL1555|157139/1-227 ----------

(+)RnhA_U21|1878835/1-1290
NLVKADVEWPEKNTGMDRTQMDALQTMITNNIAIIQGPPGTGKTFVGTYGMKVLLKN
FDQ
(-)RnhA_NRRL1555|87354/1-649
NLVKADVEWPEKNTGMDRTQMDALQTMITNNIAIIQGPPGTGKTFVGTYGMKVLLKN
FDQ
(-)RnhB_NRRL1555|157139/1-227 ----------

(+)RnhA_U21|1878835/1-1290
GLGPIVCICQTNHALDQFLEHVLDFDPRVIRIGARSRSERLKDHILFEVRKEREAVRGL
G
(-)RnhA_NRRL1555|87354/1-649
GLGPIVCICQTNHALDQFLEHVLDFDPRVIRIGARSRSERLKDHILFEVRKEREAVRGL
G
(-)RnhB_NRRL1555|157139/1-227 ----------

(+)RnhA_U21|1878835/1-1290
RVYRKRDEISKKIREIIVTMYEEPCVTLDYLRKIKALRPRQLESLKRVGERGARNDALS
T
(-)RnhA_NRRL1555|87354/1-649
RVYRKRDEISKKIREIIVTMYEEPCVTLDYLRKIKALRPRQLESLKRVGERGARNDALS
T
(-)RnhB_NRRL1555|157139/1-227 ----------

(+)RnhA_U21|1878835/1-1290
AAVAAASAGGGGADEDSDDDWVIGSDITISKTRGAPTPAPSVWGGNRNQNQNQNPN
PNHR
(-)RnhA_NRRL1555|87354/1-649
AAVAAASAGGGGADEDSDDDWVIGSDITISKTRGAPTPAPSAWGGNRNQ----------
(-)RnhB_NRRL1555|157139/1-227 ----------

(+)RnhA_U21|1878835/1-1290
EEEKVPPVNPVEVWLKDAIEFVNESGAPFNLDDDEKADFLEQQKGLLFDEDEDEDEL
IEE

(-)RnhA_NRRL1555|87354/1-649 ----------
(-)RnhB_NRRL1555|157139/1-227 ----------

(+)RnhA_U21|1878835/1-1290
EELQEITQNFKEDLQDLKADKSPYINIGVAYRNQSESFSRRQTNRDETRKVINYKKTAA
R
(-)RnhA_NRRL1555|87354/1-649 ----------
(-)RnhB_NRRL1555|157139/1-227 ----------

(+)RnhA_U21|1878835/1-1290
GFDSSRFNFFDDSAAPLSYDEDDKEQDDEQHNVLERWMKDDDVSMWPLAVRLKAH
KKWAQ
(-)RnhA_NRRL1555|87354/1-649 ----------
(-)RnhB_NRRL1555|157139/1-227 ----------

(+)RnhA_U21|1878835/1-1290
QLQQEQGQTIRSLIVRYEECSKEIRKMQVKNDALICREARVVGLTSTAAAKYHDLLEE
MK
(-)RnhA_NRRL1555|87354/1-649 ----------
(-)RnhB_NRRL1555|157139/1-227 ----------

(+)RnhA_U21|1878835/1-1290
PKVMVVEEAAEMLEAHIVTALTQSLQHLILIGDHEQLRPSTAVHTLAKQHFLDVSLFER
L
(-)RnhA_NRRL1555|87354/1-649 ----------
(-)RnhB_NRRL1555|157139/1-227 ----------

(+)RnhA_U21|1878835/1-1290
VKNDMPYSRLSFQRRMRPEIRTLIDPIYFDPPLQDHPDVVKLPMVRGMDKSLFFLSHT
EP
(-)RnhA_NRRL1555|87354/1-649 ----------
(-)RnhB_NRRL1555|157139/1-227 ----------

(+)RnhA_U21|1878835/1-1290
ESHMEETASKSNEHEAEMAAKLSTYLLMQGYSPADITIITMYSGQRTTIKKALKKERKP
E
(-)RnhA_NRRL1555|87354/1-649 ----------
(-)RnhB_NRRL1555|157139/1-227
----------MYSGQRTTIKKALKKERKPE

(+)RnhA_U21|1878835/1-1290
VDTSLVQVSSVDGYQGEENKIIILSLVRSNNAGMIGFLSIANRVCVSLSRAKHGMYILG
N
(-)RnhA_NRRL1555|87354/1-649 ----------
(-)RnhB_NRRL1555|157139/1-227
VDTSLVQVSSVDGYQGEENKIIILSLVRSNNAGMIGFLSIANRVCVSLSRAKHGMYILG
N

(+)RnhA_U21|1878835/1-1290
AKLLCEKSDLWNEIVYNLEEKKAGNIGVRLALKCLRHNELTEVQWPVDFSDVEEGGC
TRP
(-)RnhA_NRRL1555|87354/1-649 ----------
(-)RnhB_NRRL1555|157139/1-227
AKLLCEKSDLWNEIVYNLEEKKAGNIGVRLALKCLRHNELTEVQWPVDFSDVEEGGC
TRP

(+)RnhA_U21|1878835/1-1290
CGTVLDCGHQCPLKCHVYEHDLVRCQLPCRKVFQPCGHACTRRCFEVCGSCLTPRV
LRLP
(-)RnhA_NRRL1555|87354/1-649 ----------
(-)RnhB_NRRL1555|157139/1-227
CGTVLDCGHQCPLKCHVYEHDLVRCQLPCRKVFQPCGHACTRRCFEVCGSCLTPRV
LRLP

(+)RnhA_U21|1878835/1-1290 CGHELKEECGKIKKLLEDPTSWRCKSCPKK
(-)RnhA_NRRL1555|87354/1-649 ----------
(-)RnhB_NRRL1555|157139/1-227 CGHELKEECGKIKKLLEDPTSWRCKSC---

Figure A.3.9 Alignment of RNA helicase genes from *P. blakesleeanus* (+) and (-)

```
#NEXUS
BEGIN TAXA;
	DIMENSIONS NTAX = 302;
	TAXLABELS
		Rhizopus_oryzae_NRRL_5896
		Rhizopus_oryzae_NRRL_6400
		NA
		Rhizopus_oryzae_NRRL_2871
		Rhizopus_oryzae_NRRL_A-13850
		Rhizopus_oryzae_NRRL_A-12745
		Rhizopus_oryzae_NRRL_A-13606
		Rhizopus_oryzae_NRRL_3613
		Rhizopus_oryzae_NRRL_66568
		Rhizopus_thermosus_Yamamoto_NRRL_2862
		Rhizopus_chungkuoensis_NRRL_2873
		Rhizopus_oryzae_NRRL_2625
		Rhizopus_oryzae_NRRL_2910
		Rhizopus_oryzae_NRRL_A-13738
		Rhizopus_oryzae_XY01909
		Rhizopus_oryzae_NRRL_A-21477
		Rhizopus_oryzae_NRRL_46180
		Rhizopus_delemar_NRRL_21447.G676.v1
		Rhizopus_delemar_NRRL_21446.G677.v1
		Rhizopus_delemar_NRRL_21477.G674.v1
		Rhizopus_sp._NRRL_3373
		Rhizopus_stolonifer_NRRL_1479
		Rhizopus_oryzae_NRRL_66596
		Rhizopus_oryzae_NRRL_2874
		Rhizopus_microsporus_var;chinensis_NRRL_2909
		Rhizopus_sp._NRRL_A-18714
		Rhizopus_oryzae_Went_Prinsen_Geerlings_NRRL_3563
		Rhizopus_oryzae_NRRL_2911
		Rhizopus_stolonifer_NRRL_3370
		Rhizopus_sp._NRRL_A-16766A
		Rhizopus_sp._NRRL_A-17388
		Rhizopus_chinensis_var._liquefaciens_NRRL_2870
		Rhizopus_chinensis_Saito_NRRL_2905
		Rhizopus_chinensis_Saito_NRRL_3671
		Rhizopus_microsporus_var;chinensis_NRRL_2906
		Rhizopus_microsporus_NRRL_5546
		Rhizopus_microsporus_NRRL_5552
		Rhizopus_oryzae_NRRL_1514
		Rhizopus_microsporus_NRRL_5558
		Rhizopus_microsporus_NRRL_5550
		Rhizopus_microsporus_NRRL_5548
		Rhizopus_microsporus_NRRL_5547
		Rhizopus_microsporus_NRRL_5551
		Rhizopus_sp._NRRL_2934
		Rhizopus_sp._NRRL_A-11791
		Rhizopus_microsporus_NRRL_13129
		Rhizopus_oryzae_NRRL_66564
		Rhizopus_microsporus_NRRL_5553
		Rhizopus_oryzae_NRRL_2344
		Rhizopus_sp._NRRL_A-10162
		Rhizopus_microsporus_var_chinensis_CCTCCM201021.CCTCCM201021.v1
		Mucor_plumbeus_NRRL_2353
		Mucor_brunneogriseus_NRRL_2351
		Mucor_plumbeus_JES_114
		Mucor_racemosus_Fresenius_NRRL_1622
		Mucor_racemosus_var._racemosus_NRRL_3641
		Mucor_racemosus_Fresenius_NRRL_A-19189
		Mucor_racemosus_Fresenius_NRRL_1608
```

Mucor_racemosus_Fresenius_NRRL_1504
Mucor_racemosus_Fresenius_NRRL_1688
Mucor_racemosus_NRRL_1627
Mucor_racemosus_Fresenius_NRRL_A-11534
Mucor_racemosus_Fresenius_NRRL_1994
Mucor_racemosus_Fresenius_NRRL_A-19185
Mucor_racemosus_f;sphaerosporus_NRRL_3645
Mucor_globosus_NRRL_1436
Mucor_globosus_Fischer_NRRL_1759
Mucor_philippovii_(nom;inval;)_NRRL_3036
Mucor_genevensis_NRRL_1756
Mucor_genevensis_NRRL_1821
Mucor_genevensis_NRRL_A-17770
Mucor_genevensis_NRRL_3101
Chaetocladium_brefeldii_NRRL_1350
Parasitella_parasitica_Bainier_Sydow_NRRL_1461
Mucor_janssenii_NRRL_2404
Mucor_velutinous_B5328.G224.v1
Ellisomyces_anomalus_RSA_581-
Mucor_ramosissimus_NRRL_3042
Mucor_pakistanicus_NRRL_6589
Mucor_fragilis_NRRL_2569
Mucor_lusitanicus_NRRL_3629
Rhizopus_delemar_NRRL_1472
Mucor_corticola_NRRL_A-16258
Mucor_sp._NRRL_A-17182
Mucor_griseocyanus_NRRL_3621
Mucor_sp._NRRL_A-21236
Circinomucor_circinelloides_NRRL_22899
Mucor_circinelloides_NRRL_A-25893
Mucor_circinelloides_B8987.G226.v1
Mucor_alternans_NRRL_A-16397
Mucor_sp._NRRL_A-17797
Actinomucor_sp._NRRL_A-23671
Mucor_sp._NRRL_A-21232
Mucor_sp._NRRL_A-25970
Thamnostylum_repens_Tieghem_Upadhyay_NRRL_6240
Mucor_sp._NRRL_A-21230
Mucor_sp._NRRL_A-14906
Mucor_circinelloides_NRRL_3614
Mucor_alternans_NRRL_A-15142
Mucor_sp._NRRL_A-25547
Mucor_sp._NRRL_A-25546
Circinella_simplex_CBS_142.35
Actinomucor_elegans_NRRL_1706
Mucor_laxorrhizus_NRRL_2814
Mucor_petrinsularis_var._echinosporus_NRRL_3141
Mucor_exponens_NRRL_1492
Mucor_heterosporus_NRRL_3154
Zygorhynchus_heterogamus_Vuillemin_NRRL_1489
Mucor_fragilis_NRRL_A-16026
Mucor_hiemalis_f;silvaticus_NRRL_3643
Mucor_luteus_NRRL_3633
Mucor_hiemalis_NRRL_2349
Mucor_hiemalis_f;hiemalis_NRRL_3624
Rhizomucor_variabilis_B7584.N167.v1
Mucor_plasmaticus_NRRL_2708
Mucor_saturninus_NRRL_2631
Mucor_mucedo_Linnaeus_Fresenius_NRRL_A-13277
Mucor_caninus_NRRL_A-12555
Pilaira_anomala_RSA_1997+
Pilaira_anomala_RSA_1998-
Pilaira_caucasica_Milko_NRRL_6282
Pilaira_moreaui_CBS_181.26
Syncephalastrum_racemosum_CBS_441.59-

Syncephalastrum_verruculosum_RSA_2127
Rhizomucor_miehei_NRRL_5283
Rhizomucor_pusillus_NRRL_A-14037
Mucor_globosus_NRRL_A-28295
Rhizomucor_miehei_NRRL_5902
Mucor_pusillus_Lindt_NRRL_3470
Rhizomucor_pusillus_NRRL_5893
Thamnostylum_piriforme_RSA_251
Thamnostylum_piriforme_NRRL_A-21589
Helicostylum_sp._NRRL_1397
Circinella_chinensis_CBS_150.53
NA
Fennellomyces_linderi_NRRL_2342T
Fennellomyces_sp_T-0311.Fenlin1.v1
Thamnostylum_nigricans_RSA_1406
Fennellomyces_heterothallicus_RSA_2348
Circinella_muscae_NRRL_1364
Circinella_muscae_NRRL_1356
Circinella_muscae_NRRL_1352
Circinella_muscae_CBS_107.13T
Circinella_chinensis_NRRL_2415
Circinella_mucoroides_NRRL_1354
Circinella_minor_CBS_143.56
NA
Circinella_angarensis_RSA_618-
Rhizopus_oryzae_NRRL_1470
NA
Circinella_umbellata_NRRL_1366
Dichotomocladium_elegans_NRRL_2754
Dichotomocladium_sphaerosporum_NRRL_22118
Mucor_janssenii_NRRL_A-23557
Lichtheimia_blakesleeana_NRRL_1300
Lichtheimia_blakesleeana_NRRL_1301
Lichtheimia_corymbifera_008-049.G678.v1
Lichtheimia_sphaerocystis_NRRL_6380
Lichtheimia_corymbifera_NRRL_1592
Lichtheimia_hyalospora_NRRL_1330
Lichtheimia_corymbifera_NRRL_2982
Lichtheimia_corymbifera_NRRL_6379
Lichtheimia_corymbifera_NRRL_A-11155
Lichtheimia_corymbifera_NRRL_2981
Lichtheimia_corymbifera_B2541.N169.v1
Lichtheimia_corymbifera_NRRL_2798
Absidia_corymbifera_Cohn_Saccardo_Trotter_NRRL_1334
Lichtheimia_ramosa_NRRL_3208
Lichtheimia_corymbifera_NRRL_1309
Lichtheimia_ramosa_B5399.G228.v1
Lentamyces_zychae_NRRL_A-23515
Umbelopsis_ramanniana_NRRL_1839
Saksenaea_vasiformis_B4078.G233.v1
Saksenaea_oblongisporus_B3353.N171.v1
Apophysomyces_ossiformis_NRRL_A-21654
Apophysomyces_trapeziformis_B9324.G229.v1
Phycomyces_blakesleeanus_NRRL_1555.Phybl2.v2
Phycomyces_blakesleeanus_Burgeff_NRRL_1465
Phycomyces_blakesleeanus_Burgeff_var._piloboloides_NRRL_2566
Rhizomucor_pusillus_NRRL_2543
Phycomyces_sp;JGI-2019a_NRRL_1467
Gongronella_butleri_NRRL_A-23795
Gongronella_butleri_NRRL_A-9978
Gongronella_butleri_NRRL_1340
Cunninghamella_elegans_B9769.G231.v1
Cunninghamella_bertholletiae_B7461.N158.v1
Cunninghamella_bertholletiae_NRRL_1380
Cunninghamella_bertholletiae_NRRL_1377

Cunninghamella_bertholletiae_175.G680.v1
Cunninghamella_bertholletiae_NRRL_1376
Cunninghamella_elegans_NRRL_1393
Cunninghamella_elegans_NRRL_1391
Cunninghamella_elegans_NRRL_1388
Cunninghamella_elegans_NRRL_1390
Cunninghamella_elegans_NRRL_1392
Cunninghamella_echinulata_RSA_2018-
NA
Cunninghamella_echinulata_NRRL_1384
Chaetocladium_brefeldii_RSA_1136-
Cunninghamella_antarctica_NRRL_6534
Cunninghamella_echinulata_NRRL_1387
Cunninghamella_sp._NRRL_A-21238
Cunninghamella_sp._NRRL_A-21271
NA
Cunninghamella_echinulata_NRRL_1385
Absidia_cylindrospora_NRRL_1343
Absidia_cylindrospora_NRRL_1345
Absidia_spinosa_var._azygospora_NRRL_2841
Absidia_spinosa_NRRL_A-13651
Absidia_californica_NRRL_2709
Absidia_californica_NRRL_2967
Absidia_macrospora_NRRL_5839
NA
Absidia_caerulea_NRRL_1314
Absidia_caerulea_NRRL_1313
Absidia_caerulea_RSA_138-
Absidia_caerulea_NRRL_5926
Absidia_caerulea_NRRL_A-26290
Absidia_caerulea_NRRL_1310
Mucor_lamprosporus_NRRL_6037
Mucor_aromaticus_NRRL_A-17745
Backusella_indica_NRRL_3247
Backusella_circina_FSU_941.Bacci1.v1
Backusella_circina_NRRL_2446
Backusella_circina_NRRL_A-17781
Backusella_dispersa_NRRL_6039
NA
Backusella_lamprospora_NRRL_1401
Backusella_dispersa_NRRL_6046
Mucor_odoratus_NRRL_3064
Mucor_maequisporus_var._kaki_NRRL_3295
Mucor_inaequisporus_NRRL_3626
Mucor_azygosporus_Benjamin_NRRL_3068
Mucor_indicus_NRRL_555
Mucor_sp._NRRL_A-25783
Mucor_indicus_Lendner_NRRL_13468
Mucor_indicus_Lendner_NRRL_13132
Mucor_sp._NRRL_A-25793
Mucor_rouxii_Calmette_Wehmer_NRRL_1894
Mucor_sp._NRRL_A-26212
Mycotypha_microspora_Fenner_NRRL_A-11005
Mycotypha_microspora_Fenner_NRRL_684
Mycotypha_microspora_IMI_282443
Circinella_muscae_NRRL_1360
Benjaminiella_youngii_IMI_325629
Cokeromyces_recurvatus_B5483.N154.v1
Mucor_piriformis_NRRL_3637
Poitrasia_circinans_NRRL_2546
Blakeslea_trispora_NRRL_2456.Blatri1.v1
Rhizopus_circinans_NRRL_2913
Rhizopus_circinans_NRRL_2917
Rhizopus_circinans_van_Tieghem_NRRL_13978
Rhizopus_circinans_NRRL_1475

```
                    Rhizopus_stolonifer_NRRL_66460
                    Rhizopus_artocarpi_NRRL_1799
                    Rhizopus_stolonifer_NRRL_66459
                    Rhizopus_stolonifer_NRRL_66454
                    Rhizopus_stolonifer_NRRL_66455
                    Rhizopus_stolonifer_NRRL_54667
                    Rhizopus_stolonifer_var;reflexus_NRRL_A-16792
                    Rhizopus_stolonifer_NRRL_1519
                    Rhizopus_stolonifer_var;reflexus_NRRL_A-18059
                    Rhizopus_stolonifer_NRRL_54333
                    Rhizopus_stolonifer_NRRL_66457
                    Rhizopus_stolonifer_NRRL_66456
                    Rhizopus_stolonifer_NRRL_66458
                    Rhizopus_stolonifer_NRRL_3372
                    Rhizopus_nigricans_Ehrenberg_NRRL_1477
                    Rhizopus_stolonifer_B9770.G232.v1
                    Amylomyces_rouxii_NRRL_A-25885
                    Syzygites_sp._MES_3091
                    Sporodiniella_umbellata_FLAS-F-62758
                    Rhizopus_oryzae_NRRL_62023
                    Rhizopus_oryzae_NRRL_A-11376
                    Rhizopus_arrhizus_IMI53173
                    Rhizopus_oryzae_NRRL_A-12998
                    Rhizopus_cohnii_NRRL_1517
                    Rhizopus_sp._NRRL_3368
                    Rhizopus_oryzae_NRRL_1522
                    Rhizopus_oryzae_NRRL_1512
                    Rhizopus_sp._NRRL_1524
                    Rhizopus_oryzae_NRRL_A-16827
                    Rhizopus_oryzae_NRRL_A-12997
                    Rhizopus_oryzae_NRRL_2004
                    Rhizopus_sp._NRRL_A-18472
                    Rhizopus_oryzae_NRRL_A-12134
                    Rhizopus_oryzae_CBS_330.53
                    Rhizopus_oryzae_NRRL_66592
                    Rhizopus_oryzae_NRRL_A-20824
                    Rhizopus_oryzae_NRRL_2286
                    Rhizopus_oryzae_NBRC_5318
                    Rhizopus_oryzae_99-892
                    Rhizopus_oryzae_HUMC_02.G673.v1
                    Rhizopus_oryzae_NRRL_A-12640
                    Rhizopus_oryzae_NRRL_13440.G668.v1
                    Rhizopus_oryzae_B7407.G225.v1
                    Rhizopus_oryzae_NRRL_21396.G670.v1
                    Rhizopus_oryzae_NRRL_A-21704
                    Rhizopus_oryzae_NRRL_A-10276
                    Rhizopus_oryzae_CBS_258.28
                    Rhizopus_delemar_99-880.IGS-99-880
                    Rhizopus_sp._NRRL_1530     ;
END;
BEGIN TREES;
        TRANSLATE
```

Figure A.4.1 Mucoromycete species tree

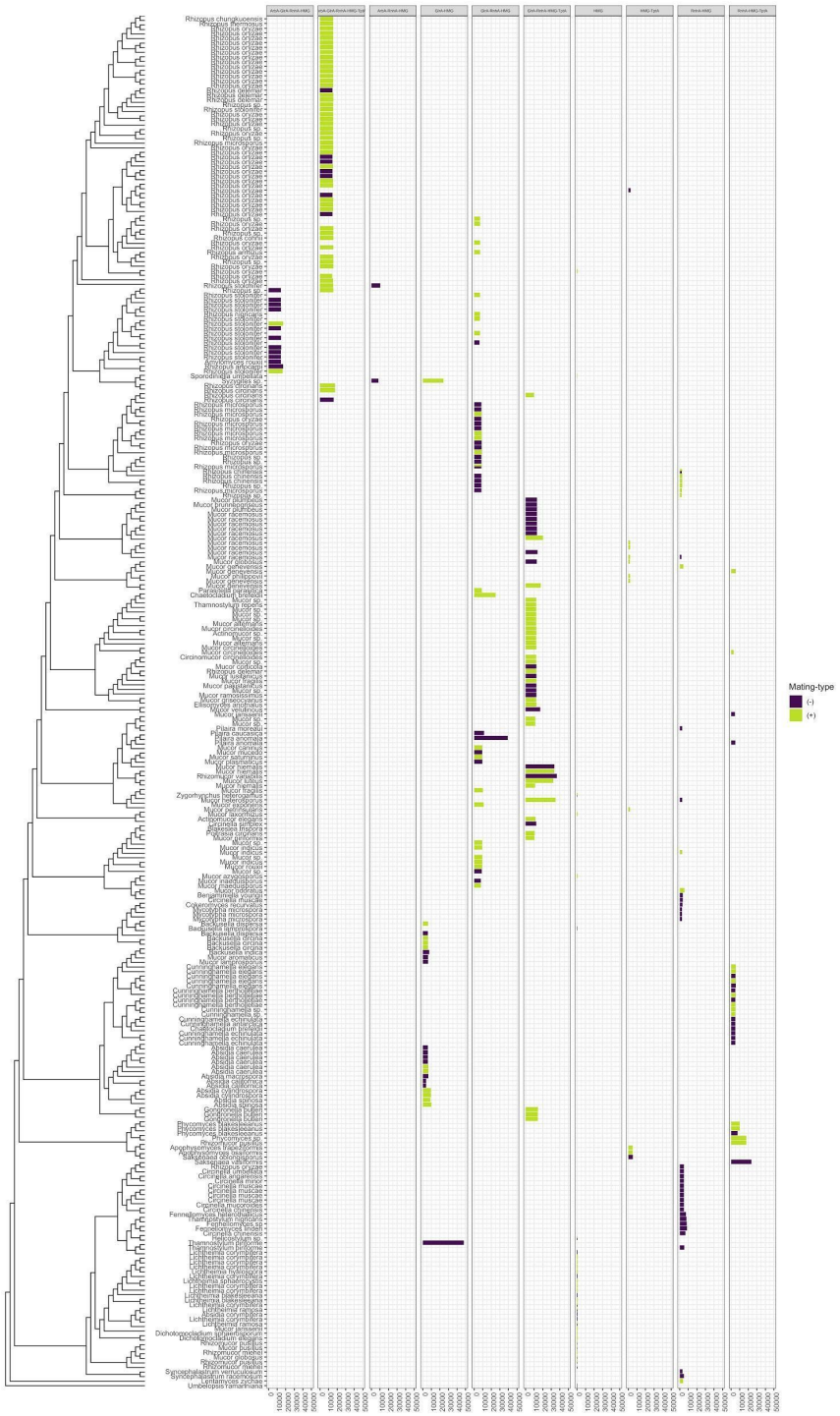

Figure A.4.2: locus size faceted by locus gene content

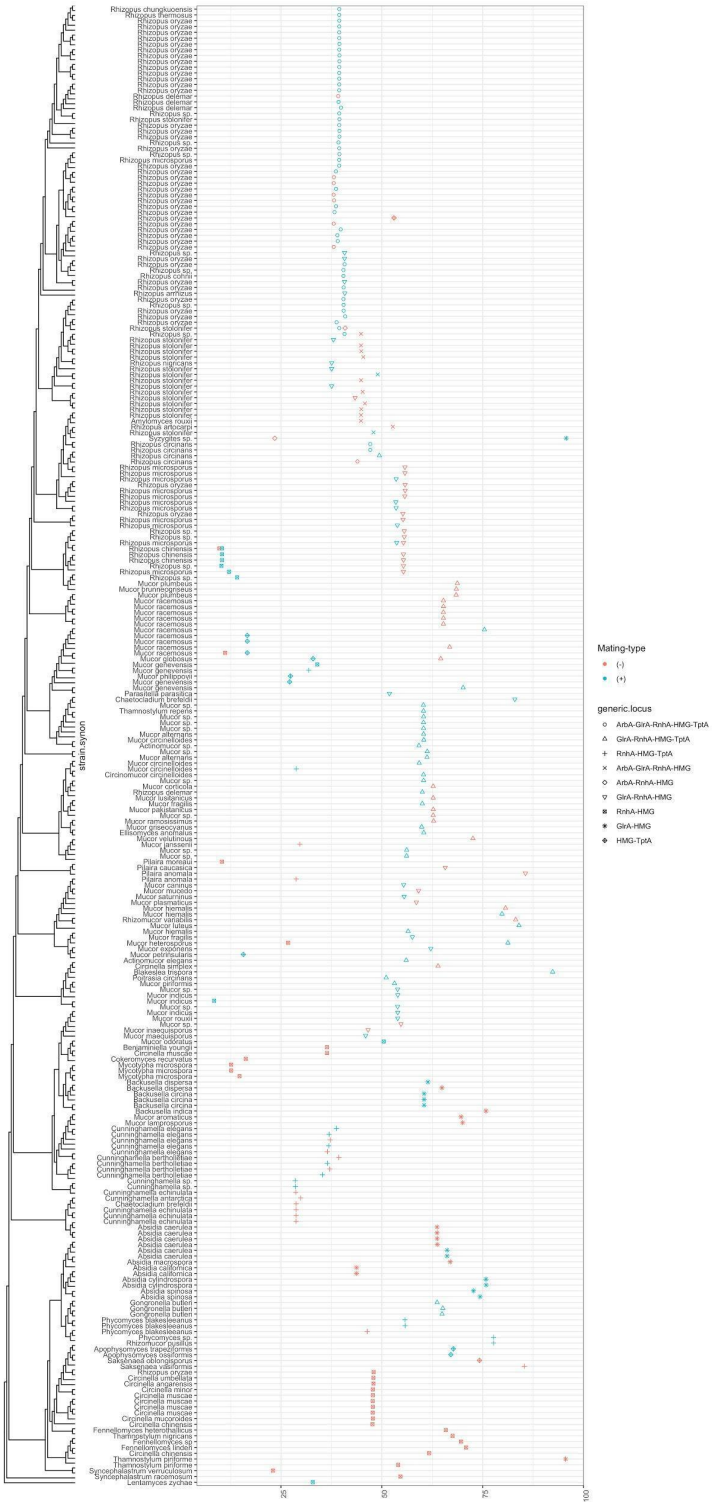

Figure A.4.3: percent of intergenic sequence by locus variant

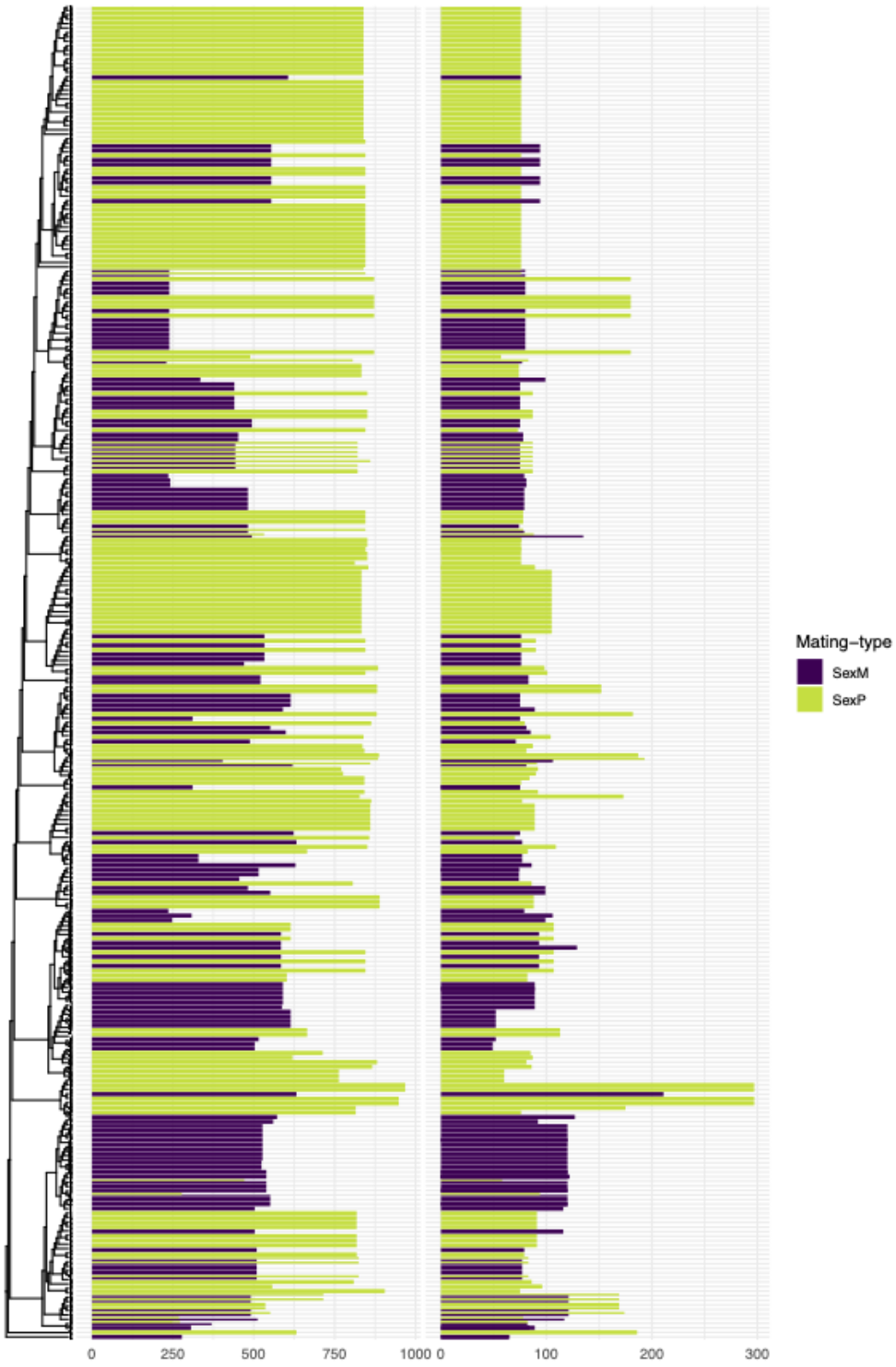

Figure A.4.4 sex gene and protein lengths across species tree

Tables A.2.2 - A.4.1 (hyperlink -- also included as supplemental files)
https://docs.google.com/spreadsheets/d/1GeH0UkMc7MyHDmL2j9y1cg8iU4Om5inwXRCCiu1HBG0/edit?usp=sharing

Scripts and pipelines used for the computational analyses can be found at
https://github.com/stajichlab/EvoDevo_of_Mucoromycotina